Partner control in arbuscular mycorrhizal symbiosis Peng Wang 2021

Partner control in arbuscular mycorrhizal symbiosis

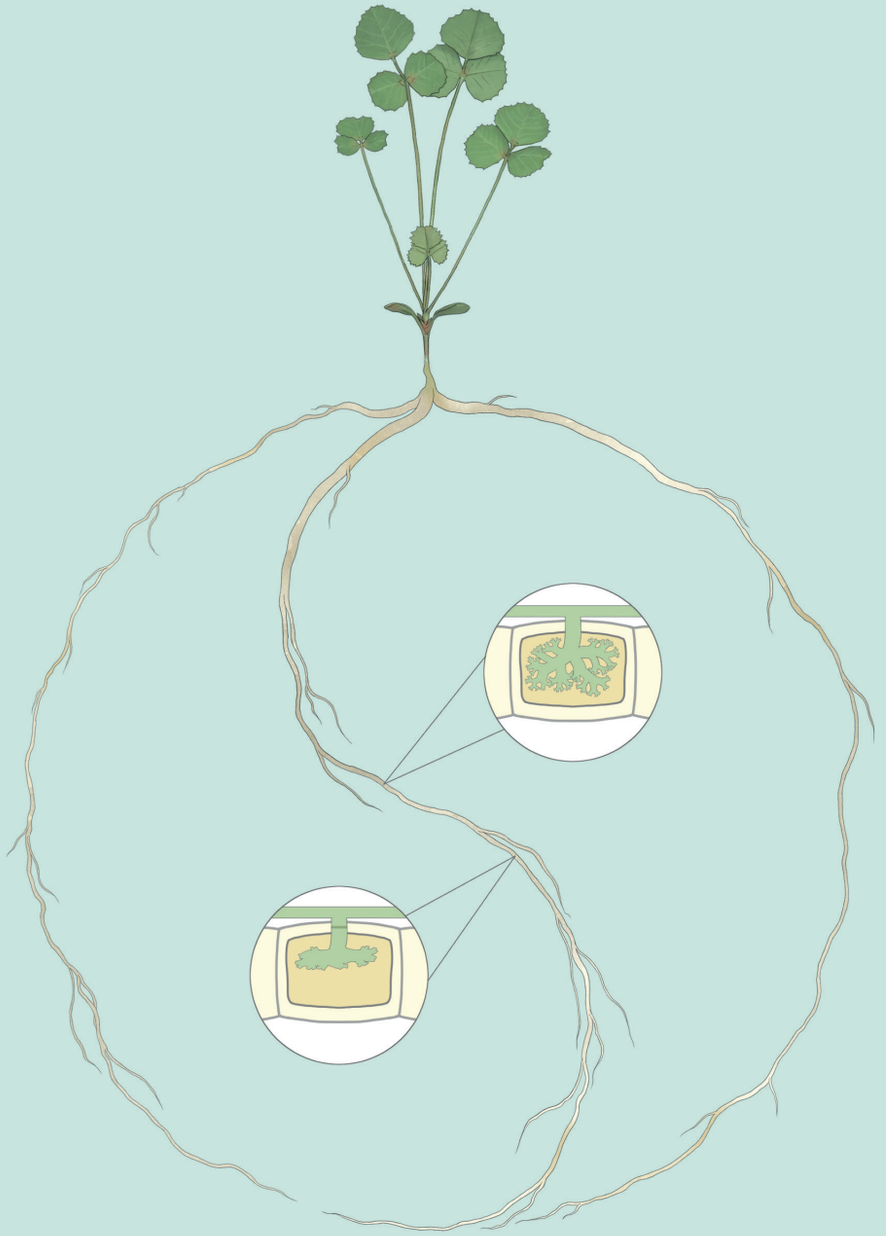

Peng Wang

Propositions

1. Plant Histone 2B is an overlooked target for fungi to overcome the plant's immune system.
   (this thesis)

2. Phosphate sensing SPX proteins are essential to keep the arbuscular mycorrhizal symbiosis beneficial.
   (this thesis)

3. A seed-propagated diploid hybrid potato designed by Zhang et al. (2021) will restructure the potato breeding market.

4. Advances in single cell proteomics will revolutionize our understanding of biological systems.

5. The earth does not need our protection, we are protecting ourselves.

6. Social media separate people more than that they bring people together.

Propositions belonging to the thesis, entitled

Partner control in arbuscular mycorrhizal symbiosis

Peng Wang
Wageningen, 30 August 2021

Partner control in arbuscular mycorrhizal symbiosis

Peng Wang

Thesis committee

Promotor
Prof. Dr A.H.J. Bisseling
Professor of Molecular Biology
Wageningen University & Research

Co-promotor
Dr E.H.M. Limpens
Assistant professor, Laboratory of Molecular Biology
Wageningen University & Research

Other members
Prof. Dr Francine Govers, Wageningen university & research
Prof. Dr Corné Pieterse, Utrecht University
Prof. Dr Natalia Requena, Karlsruhe Institute of Technology, Germany
Dr Andrea Genre, University of Turin, Italy

This research was conducted under the auspices of the Graduate School
Experimental Plant Sciences

Partner control in arbuscular mycorrhizal symbiosis

Peng Wang

Thesis
submitted in fulfilment of the requirements for the degree of doctor
at Wageningen University
by the authority of the Rector Magnificus,
Prof. Dr A.P.J. Mol,
in the presence of the
Thesis Committee appointed by the Academic Board
to be defended in public
on Monday 30 August 2021
at 1:30 p.m. in the Aula.

Peng Wang
Partner control in arbuscular mycorrhizal symbiosis
176 pages

PhD thesis, Wageningen University, Wageningen, the Netherlands (2021)
With references, with summary in English

ISBN: 978-94-6395-835-6
DOI: https://doi.org/10.18174/547713

Contents

Chapter 1 **7**

General introduction and thesis outline

Chapter 2 **19**

A nuclear-targeted effector of *Rhizophagus irregularis* interferes with Histone 2B mono-ubiquitination to promote arbuscular mycorrhization

Chapter 3 **45**

A host-dependent, potential glycan binding effector of *Rhizophagus irregularis* controls host immune responses

Chapter 4 **65**

Medicago SPX1 and SPX3 regulate phosphate homeostasis, mycorrhizal colonization and arbuscule degradation

Chapter 5 **103**

Medicago SPX1 and SPX3 interact with PIP2 plasma membrane aquaporins

Chapter 6 **119**

General discussion

Summary **135**

Reference **139**

List of publications **169**

About the author **170**

Acknowledgements **171**

Education statement **173**

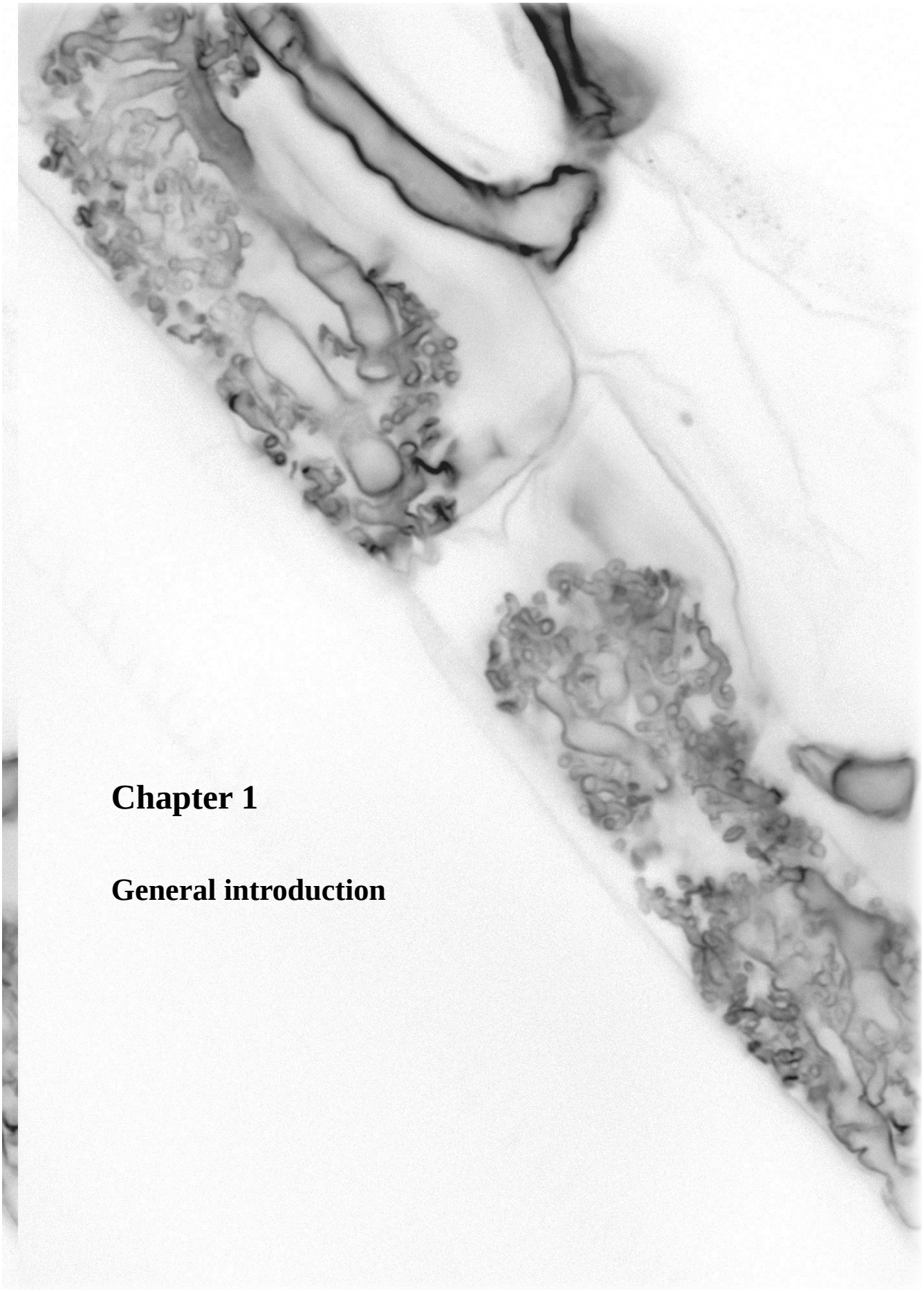

Chapter 1

General introduction

Arbuscular mycorrhiza (AM) is a widespread endosymbiotic association between AM fungi, belonging to the subphylum Glomeromycotina, and most land plants (Spatafora et al., 2016). This symbiosis originated ~450 million years ago and provides a number of benefits to plants such as improved uptake of scarce mineral nutrients, especially phosphate (Pi) and nitrogen (N), from the soil and protection against various biotic and abiotic stresses. In return, the biotrophic AM fungi receive fixed carbon from the host plant, which is essential for the fungi to fulfill their life cycle (Smith and Read, 2008; Luginbuehl and Oldroyd, 2017). As such, AM fungi play key roles in natural ecosystems and given their many potential benefits to plants they are widely recognized for their potential as sustainable biofertilizers (Madawala, 2021).

To form an evenly matched successful cooperation that stays mutualistic it is important that both partners have the ability to effectively control each other. Under natural conditions a single plant can be colonized by multiple AM fungi and a single AM fungus can colonize multiple host plants at the same time (Sanders and Croll, 2010). Since different fungi can differ in their symbiotic efficiency or compatibility, a plant needs to weigh the cost of the interaction to the benefits it receives. Different AM fungi are thought to provide different benefits (Streitwolf-engel et al., 1998). Although in general there appears to be little host specificity, so-called host preferences have been reported where different plant species growing at the same location appear to associate preferentially with different AM fungi (Martínez-García and Pugnaire, 2011; Torrecillas et al., 2012). However, the molecular mechanisms behind such partner selection, or variation in the plants growth response upon different AM fungal interactions, are far from understood. In this chapter I will introduce recent molecular insights into the communication between both partners that ultimately determines the outcome of the interaction. I will focus mainly on two aspects of control; first (pre-)contact communication to initiate the interaction and secondly, control of arbuscule development.

Root colonization by AM fungi

Under nutrient limiting conditions plants recruit AM fungi to enhance their nutrient foraging capability. Upon physical contact, the fungus forms a hyphopodium on a-trichoblasts of the root epidermis from where it penetrates the root (Fig. 1) (Gutjahr and Parniske, 2013). In response, the plant nucleus moves to a position underneath the hyphopodium and the plant cytoskeleton and endoplasmic reticulum get reorganized to form a tube-like structure, called the pre-penetration apparatus (PPA), which determines the entry path of the fungus (Genre et al., 2005). The PPA actively facilitates the local weakening of the plant cell wall and exocytosis-driven extension of the plasma membrane engulfs the penetrating fungal hypha (Genre et al., 2012). Once the fungus has passed the epidermis, the fungus can spread mainly via the intercellular spaces in the root cortex (Arum-type colonization), and/or it spreads in a cell-to-cell manner (Paris-type), depending on the plant species (Kubota et al., 2005; Bonfante and Genre, 2008). When the hyphae reach the inner root cortex cells they enter and form highly branched tree-like hyphal structures, called arbuscules (Parniske, 2008). First a trunk structure is formed, after which dichotomous branching generates the fine branches that fill the cell (Pumplin and Harrison, 2009). The entire arbuscule is surrounded by a specialized plant-derived membrane, called the peri-arbuscular membrane (PAM), which establishes a symbiotic interface for reciprocal nutrients exchange (Harrison and Ivanov, 2017). The exocytosis-related proteins VAMP721d/e, SYP132α, VAPYRIN and EXO70I were shown to be required for PAM formation (Ivanov et al., 2012; Huisman et al.,

2016; Zhang et al., 2015a). EXO70I is conserved in plants that can form AM symbiosis and as component of the exocyst complex is thought to tether exocytotic vesicles to the PAM (Zhang et al., 2015a). It was shown to interact with the VAPYRIN protein that accumulates on small mobile structures that are likely recycling endosomes (Zhang et al., 2015a; Bapaume et al., 2019). VAPYRIN has a N-terminal VAMP-associated protein (VAP)/major sperm protein (MSP) domain and a C-terminal ankyrin-repeat domain and is required for both epidermal penetration and arbuscule formation (Pumplin et al., 2010; Murray et al., 2011). The exact molecular function is not known. After tethering, the symbiosis-dedicated v- and t-SNAREsVAMP721d/e and SYP132α facilitate vesicle fusion at PAM (Ivanov et al., 2012; Huisman et al., 2016).

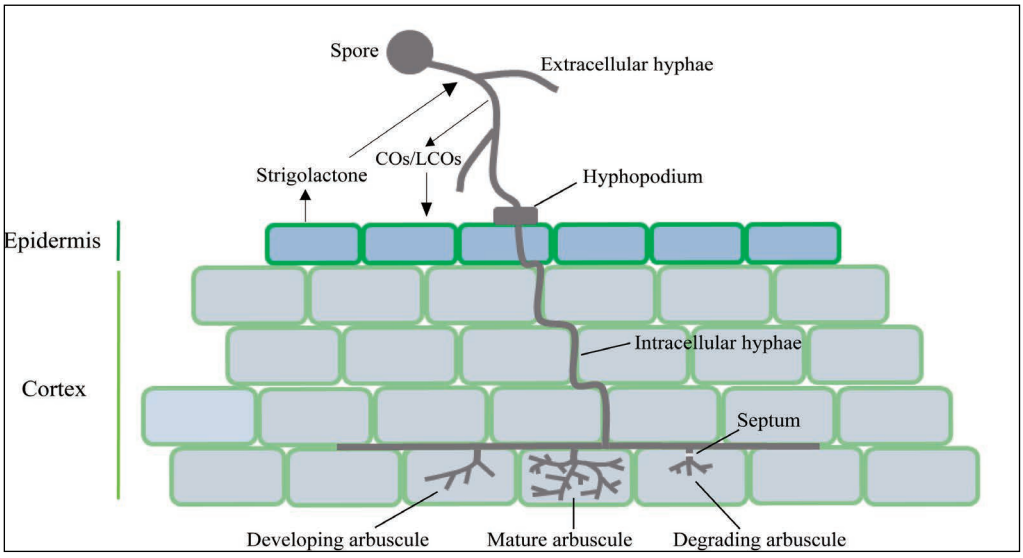

Fig. 1 Schematic image of arbuscular mycorrhizal developmental stages in Medicago. Root exudates including strigolactones induce spore germination and hyphal growth/branching; Branched extraradical hyphae secret Myc-COs/LCOs to activate the common symbiotic signaling pathway and form hyphopodia on atrichoblasts. After penetrating the epidermis, intraradical hyphae grow mostly in between root cortex cells to reach the inner cortical cells where they form highly branched arbuscules that represent a symbiotic interface where nutrient exchange takes place. Arbuscule development is not synchronized and follows different subsequent stages: bird's foot-like structures are formed that by dichotomous branching form fine branched mature arbuscules that fill the cells and eventually are degraded (degrading arbuscule characterized by septa) and removed from the cells.

Recently, the PAM interface was intensively investigated by using electron microscopy combined with tomography. Two types of extracellular membrane compartments, called intra-matrix compartment I (IMC-I) and IMC-II, were observed in the peri-arbuscular space (Ivanov et al., 2019; Roth et al., 2019). The vesicle- and dumbbell-shaped IMC-I compartments showed direct connections with the PAM, while the tubular IMC-II compartments appeared to form discrete units (Ivanov et al., 2019). Additionally, extensive membrane tubules (memtubs) were observed in the paramural space in between the fungal plasma membrane and fungal cell wall (Ivanov et al., 2019; Roth et al., 2019). The exact function of the observed membrane structures is not known, but they have been speculated to play a role in nutrient exchange and or exchange of signal molecules (Limpens, 2019).

The mature arbuscule almost completely occupies the whole cortical cell, whose central vacuole deflates and becomes fragmented. At this stage nutrients are actively exchanged by various transporter proteins localized on the PAM. For example, the symbiosis-specific phosphate transporter 4 (PT4) facilitates the uptake of Pi across the PAM (Javot et al., 2007). Mutation of MtPT4 leads to premature degradation of the arbuscules. PT4 mediated Pi uptake is energized by a proton gradient that is generated by the H+-ATPase HA1 (Krajinski et al., 2014; Wang et al., 2014a). In return for mineral nutrients such as phosphate and ammonium, the fungus obtains fixed carbon from the plant. In addition to sugars, especially glucose secreted by SWEET transporters (An et al., 2019), it has become clear that plant-derived fatty acids represent a major carbon source for the AM fungi (Jiang et al., 2017; Luginbuehl et al., 2017; Keymer et al., 2017). AM fungi were found lack a key enzyme to make fatty acids themselves which explains their obligate biotrophic dependency on the plant (Kirkpatrick et al., 2014; Wewer et al., 2014). Two half ABC-type lipid transporters, called STR and STR2, were found be required for the efficient transport of fatty acid precursors, likely β-monoacylglycerols, across the PAM (Zhang et al., 2010; Gutjahr et al., 2012; Bravo et al., 2017). Knock-out of these transporters severely impairs the development of the arbuscules.

Arbuscule development is a highly dynamic process with new arbuscules developing and degeneration of old arbuscules happening simultaneously and continuously. In planta time-lapse imaging of arbuscule in rice roots showed that arbuscules have a lifetime of only 2-5 days at maturity (Kobae and Hata, 2010). The degeneration starts at the arbuscular hyphal fine branches and eventually the collapsed arbuscule together with the surrounding matrix and PAM is disappear from the cell (Bonfante-Fasolo, 1984; Javot et al., 2011; Kobae and Hata, 2010), which subsequently can be colonized again. The reason why arbuscules degenerate is not really clear. It has been postulated to provide a means to abort underperforming arbuscules to prevent the interaction from becoming parasitic (Gutjahr and Parniske, 2017). After the first establishment of arbuscules, fungal hyphae continue to spread through the root and additionally (lipid filled) storage structures called vesicles are formed. Furthermore new spores are made that can establish new infection sites. As a result an underground mycelial network is formed (van der Heijden et al., 2015).

Pre-contact communication

From plant to fungus

Plant and microbes in the rhizosphere communicate with each other through the exchange of chemical molecules (De-la-Peña and Loyola-Vargas, 2014). Under Pi limiting conditions, plant roots secret a number of molecules to attract AM fungi. These molecules include for example flavonoids, 2-hydroxy fatty acids and strigolactones. Such molecules can induce AM fungal spore germination and hyphal branching, which promotes fungal–host encounters (Becard et al., 1992; Nagahashi and Douds, 2011; Akiyama et al., 2005; Besserer et al., 2006, 2008). Best studied is the function of strigolactones (SLs), which have been shown to trigger the activation of mitochondria and (oxidative) metabolism in the fungus (Akiyama et al., 2005; Besserer et al., 2006, 2008). Besides stimulants for AM fungi, strigolactones are also plant hormones that control plant architecture and productivity (Umehara, 2011; Yao et al., 2016; Waters et al., 2017). Their biosynthesis is regulated by both abiotic and biotic stresses. Especially Pi limitation has been shown to induce the production of strigo-

lactones in the roots of a number of plants as well as their exudation (Kohlen et al., 2011; Czarnecki et al., 2013). This helps to attract AM fungi plants to acquire more Pi from soil. Intriguingly, SL biosynthesis is also controlled by the GRAS transcription factors NSP1 and NSP2, which play a role in the common symbiotic signalling pathway (see below; (Catoira et al., 2000; Maillet et al., 2011; Schmitz and Harrison, 2014). Little is known about how SLs are perceived by AM fungi. Plant mutants impaired in strigolactone biosynthesis show reduced but still normal root colonization (Floss et al., 2008; Vogel et al., 2010; Maclean et al., 2017). This indicates that SLs are not the only limiting factor for mycorrhizal colonization. Recently, an N-acetylglucosamine (GlcNAc) transporter named NOPE1 was shown to be essential for the induction of transcriptome changes in AM fungi by rice root exudates (Nadal et al., 2017). Severely reduced AM colonization was observed in the nope1 mutant (Nadal et al., 2017). NGT1, a homolog of NOPE1 in Candida albicans, was shown to be required for the uptake of GlcNAc to control hyphal induction (Alvarez and Konopka, 2007). However, the application of GlcNAc did not complement the nope1 mutant phenotype. This suggests that NOPE1 can transport a yet-to-be identified molecule, which is perceived by AM fungi to prepare them for symbiosis (Nadal et al., 2017).

From fungus to plant

AM fungi also secrete diffusible chemicals in response to the plant signals. These signals trigger a set of changes in the plant root in preparation for fungal infection, such as calcium oscillations / spiking (Carotenuto et al., 2017), induction of lateral root formation (Gutjahr et al., 2009), formation of a pre-penetration structure (Maillet et al., 2011) and expression of symbiosis-specific genes (Camps et al., 2015a). The best studied fungal secreted signal molecules are GlcNAc-based signal molecules collectively called Myc-factors. These include lipo-chitooligosaccharides (Myc-LCOs) and short chain (tetra- and pentamers) chitooligosaccharides (Myc-COs) (Maillet et al., 2011; Genre et al., 2013). Myc-COs have been identified in germinated spore exudates at markedly higher concentrations than myc-LCO's, and their secretion was induced by the application of strigolactones (Genre et al., 2013). Myc-LCOs are very similar to the Nod factors produced by rhizobium bacteria that initiate a nitrogen-fixing nodule symbiosis with legume plants (Maillet et al., 2011). Both Nod factors and Myc-factors have been shown to activate a shared, so-called common symbiotic signaling pathway (Fig. 2) (Parniske, 2008; Gutjahr and Parniske, 2013). This is an ancient pathway that is conserved in intracellular symbioses-forming plants (Radhakrishnan et al., 2020).

Perception of LCOs and COs involves LysM domain containing receptor kinases (Kelly et al., 2017). In rice the LysM receptor kinase OsCERK1 was found to be required for AM symbiosis (Miyata et al., 2014; Zhang et al., 2014). The same receptor was previously identified as receptor for chitin-triggered immune responses, in line with its ortholog AtCERK1 from Arabidopsis (Shimizu et al., 2010; Willmann et al., 2011). Upon chitin perception OsCERK1 forms a complex with the co-receptor OsCEBiP to activate defense response (Akamatsu et al., 2013). To function in symbiotic signaling, OsCERK1 forms a different complex with OsMYR1/OsLYK2 as co-receptor (He et al., 2019). During evolution CERK1 homologs experienced duplication events that resulted in sub-functionalization of the various members in different plants. For example, in tomato the CERK1 homolog SlLYK12 is involved in mycorrhization while SlLYK1 is required for chitin-triggered immune responses (Liao et al., 2018). Similarly, in legumes like Medicago and Lotus the CERK1 homologs

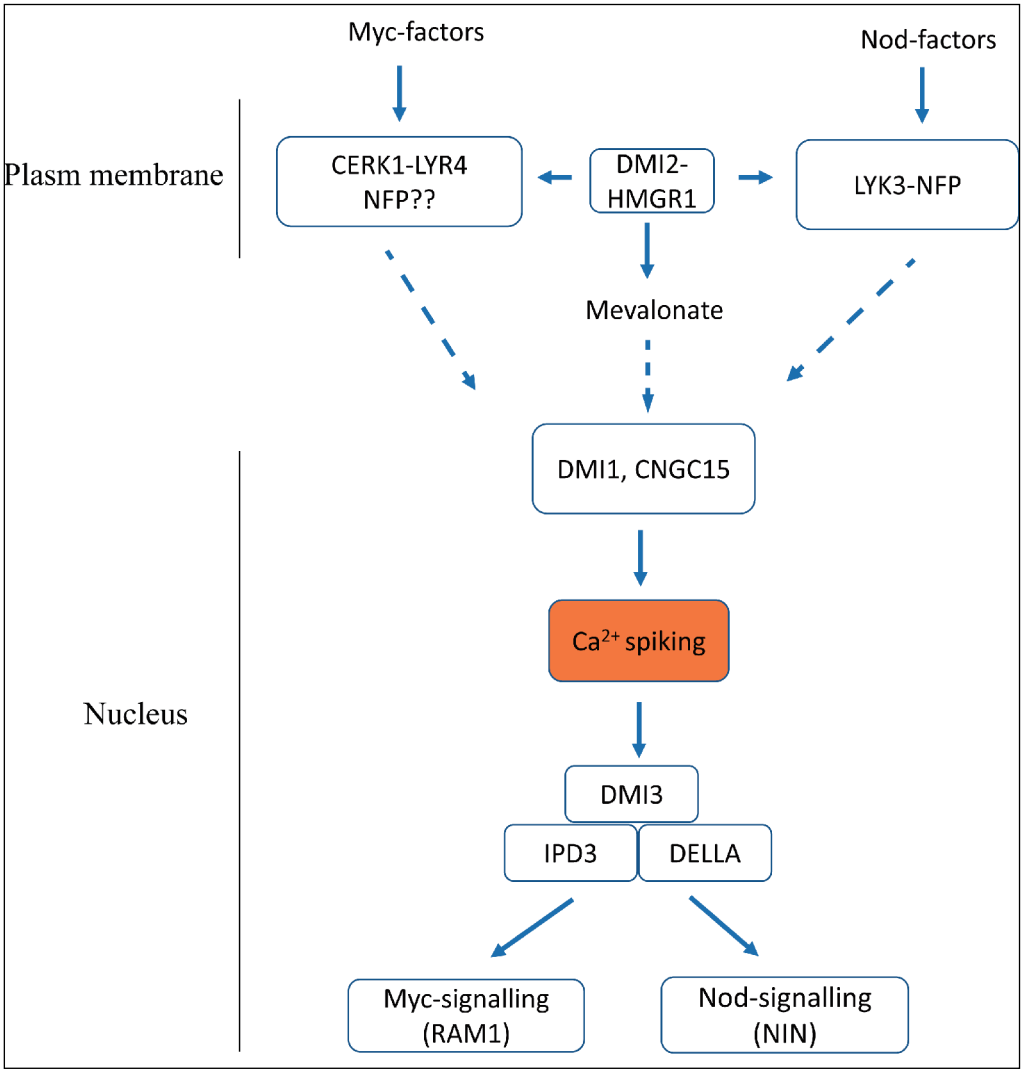

Fig. 2 Common symbiotic signaling pathway (CSSP) in Medicago. CSSP is essential for both AM symbiosis and rhizobium legume symbiosis. Myc-factors (Maillet et al., 2011; Genre et al., 2013) and Nod-factors (Lerouge et al., 1990) are recognized by plant LysM-domain containing receptor complexes (Bozsoki et al., 2017; Maillet et al., 2011; Limpens et al., 2003; Arrighi et al., 2006). The interaction between DMI2 co-receptor and the different receptors complex is required to activate CSSP (Endre et al., 2002). DMI2 also interacts with HMGR1 to produce mevalonate, which is suggested as a secondary messenger to nucleus (Venkateshwaran et al., 2015). Calcium spiking induced by the CSSP involves DMI1 and CNGC15 mediated channels (Ané et al., 2004; Charpentier et al., 2016). Calcium spiking triggers autophosphorylation of the calcium-camodulin-dependent kinase DMI3, which binds and phosphorylates IPD3 (Lévy et al., 2004; Messinese et al., 2007). DELLA transcription factor form a complex with MtDMI3/LjCCaMK and MtIPD3/LjCYCLOPS to initiate arbuscular mycorrhizal signaling or rhizobium signaling (Floss et al., 2013; Fonouni-Farde et al., 2016).

MtLYK3/LjNFR1 form a complex with MtNFR/LjNFR5 to perceive LCOs, while MtLYK9/MtCERK1 in complex with MtLYR4 and LjLys6/LjCERK6 are required for chitin / longer chain CO perception (Bozsoki et al., 2017). Mutations in the individual legume LysM receptor kinases showed either no or only slight effects on mycorrhization. Furthermore, it was recently shown that both short chain Myc-COs (CO4/CO5) and longer chain COs such as CO8 are able to trigger both symbiosis and immune responses in M. truncatula (Feng et al., 2019). This suggested that perception of mixes of both Myc-COs and Myc-LCOs may be required to distinguish AM fungi as symbionts from pathogens. Indeed, co-application of COs with LCOs promoted symbiotic signaling over immune signaling (Feng et al., 2019). Furthermore, knock-out of both MtCERK1 and MtNFP caused a severe reduction in fungal colonization, indicating that both CO and LCO perception contributes to mycorrhizal colonization (Feng et al., 2019). The fact that still some colonization occurred in the *Mtcerk1-Mtnfp* double mutant suggests that likely additional LysM receptors contribute. Also in Parasponia, the only non-legume able to establish a rhizobium symbiosis, two CERK1 homologs PanLYK1 and PanLYK3 are required for efficient colonization by AM fungi, of which PanLYK3 also acts a chitin receptor for immune responses (Rutten et al., 2020). To function in symbiotic signaling the LysM receptors interact further with the LRR-malectin domain containing co-receptor SYMRK. Knock-out of SYMRK severely impairs the ability to AM fungi to penetrate the epidermis and to activate the symbiotic signaling pathway (Endre et al., 2002; Stracke et al., 2002; Antolín-Llovera et al., 2014).

Interestingly, natural genetic variation in the second extracellular LysM domain of OsCERK1 was found to correlate with different colonization efficiencies of the AM fungus *Rhizophagus irregularis* DAOM197198 (Huang et al., 2020). Therefore, it would now be interesting to study whether variation in Myc-factor structure or ratios in different fungal species or strains may also play a role in host-preferences.

Besides Myc-factors, additional AM fungal signal molecules may also play a key role to initiate the symbiosis. In rice, a karrikin receptor called DWARF14-LIKE (D14L) was found to be required for perception of AM fungi (Gutjahr et al., 2015). Rice *d14l* mutants showed almost complete absence of hyphopodia and severely impaired root colonization. Furthermore, germinating spore extracts failed to induce transcriptional responses in *d14l* mutant roots. D14L is part of an intracellular receptor complex and is known to perceive smoke-compounds called karrikins (Kagiyama et al., 2013). In Arabidopsis D14L interacts with the E3 ligase More AXillary Growth2 (AtMAX2) which controls the degradation of the negative regulator Suppressor of MAX2-1 (AtSMAX1) (Nelson et al., 2011; Stanga et al., 2013). The MAX2 mutant in rice, Dwarf3 (D3), like D14L is also essential to establish an AM symbiosis (Yoshida et al., 2012) and OsSMAX1 was shown to negatively regulate AM symbiosis (Choi et al., 2020). However, karrikin application could not rescue the colonization defect in the d14l mutant, suggesting that other signaling molecules recognized by D14L still remain to be identified.

Effector proteins

In addition to the molecules described above AM fungi also secrete small proteins that can act as effector proteins. Effectors are defined as microbial secreted small proteins that dampen host plant immune responses and/or enable colonization of plant tissue (Hogenhout et al., 2009). Such effectors can function either in the apoplast or they can be translocated into

the host cells to execute their function (Lo Presti et al., 2015).

Like other fungi, the cell wall of AM fungi consists of chitin and β-glucans, which are major microbe-associated microbial pattern molecules (MAMPs) that are perceived by pattern recognition receptors to trigger immune responses in the plant (Zipfel, 2009; Fesel and Zuccaro, 2016; Rovenich et al., 2014; Gong et al., 2020). Plants secrete hydrolytic enzymes such as glucanases and chitinases that help to release MAMPs from the fungal cell walls and increase their detection (Kasprzewska, 2003; Ziegler et al., 2000; Jashni et al., 2015). Despite initial activation of defense responses during the AM symbiosis they appear to be rapidly quenched and AM fungi are able to intracellularly colonize over 75% of all land plants (Gianinazzi-Pearson et al., 1996; Harrison and Dixon, 1993; Kapulnik et al., 1996; Smith and Read, 2008; Genre et al., 2020). This indicates that AM fungi must have very efficient ways to subvert the immune system in such an extremely wide variety of hosts.

One of the first AM fungal effectors was identified from *Rhizophagus irregularis* DAOM197198 and named SP7 (Kloppholz et al., 2011). This secreted protein was shown to be able to translocate to the nucleus of Medicago root cells where it could interact with ERF19, a pathogenesis-related transcription factor, to interfere with ERF19-regulated defense gene expression (Kloppholz et al., 2011). Cell- and stage-specific transcriptome analyses showed that SP7 is highly expressed when the fungus is in close proximity to the root, but seems to be switched off as soon as the fungus enters the root (Zeng et al., 2018). Therefore, it is likely that SP7 only plays a significant role at the epidermis, when the fungus first contacts the root, and that other effectors take over its role once the fungus grows intraradically.

With the release of the *R. irregularis* DAOM197198 genome sequence, hundreds of additional potential effector proteins were predicted in the fungal genome (Tisserant et al., 2013; Lin et al., 2014). A comprehensive analysis of the transcriptome of *R. irregularis* was performed by using laser microdissection combined with RNA-seq. This included germinating spores, extracellular mycelium, intracellular mycelium and arbuscules, as well as whole mycorrhized root samples from three different host plants (*Allium schoenoprasum*, *Medicago truncatula* and *Nicotiana benthamiana*) (Zeng et al., 2018). This study revealed the expression of ~300 putative effectors and showed that the fungus adjusts its secretome in a host- and stage-dependent manner. A similar study of putative host-dependent expression of effectors was performed in *M. truncatula*, *Brachypodium distachyon* and *Lunularia cruciata* (Kamel et al., 2017). The occurrence of host-dependent effectors raises the hypothesis that they may be involved in regulating symbiotic efficiency and host preference. In Chapter 3, I studied the role of a chives-dependent effector and show that it can interfere with MAMP-triggered immune responses and that it can facilitate fungal colonization. This strongly supports the hypothesis that host immune responses may contribute to host preferential association with certain AM fungi. Variation in the effector repertoire of different AM fungi, even at the individual isolate level (Ropars et al., 2016); Chapter 3), may therefore help to determine the outcome of different plant-fungus combination.

Since the discovery of SP7, only a few effector proteins have been functionally studied. Such functional studies are hampered by the fact that AM fungi (currently) cannot be stably transformed due to their extreme coenocytic nature (Helber and Requena, 2008). One approach that can be used to knock-down the expression of genes in the fungus is host-in-

duced gene silencing (HIGS; (Nowara et al., 2010; Hartmann et al., 2020). Although it should be noted that the efficiency of this approach is extremely variable and only shown to work in a few cases. One of the effectors identified in this way is the strigolactone-induced putative secreted protein 1 (SIS1). Knock-down of SIS1 impaired AM colonization in Medicago and caused the formation of stunted arbuscules (Tsuzuki et al., 2016). The molecular mechanism by which SIS1 contributes to AM symbiosis is not known. In addition to SIS1, a Crinkler effector (RiCRN1) was also found to control AM colonization levels (Voß et al., 2018). Both suppression of expression via HIGS and overexpression of *RiCRN1* caused a reduction in fungal colonization, suggesting that it expression level needs tightly regulated for an efficient AM symbiosis. RiCRN was able to localize to nuclear bodies in plant nuclei, however its molecular role remains to be revealed. In Chapter 2 I studied another effector that is specifically expressed in arbuscule-containing cells and which can translocate to the host nucleus where it accumulates in the nucleolus and smaller nuclear bodies. This effector, called RiNLE1, was found to interact with host Histone 2B and can interfere with its mono-ubiquitination to dampen immune responses and can facilitate fungal colonization.

One of the best characterized AM effectors is the LysM domain containing effector RiSLM (Schmitz et al., 2019; Zeng et al., 2020). RiSLM was shown to bind both COs and LCOs in the (low) micromolar range and could efficiently interfere with chitin-triggered immune responses, but not symbiotic responses. It is most strongly expressed in intraradical fungal hyphae that grow inside the roots of a wide range of host plants. Knock-down of RiSLM expression greatly reduced fungal colonization levels. Homologs of RiSLM have so far been found in all sequenced AM fungal genomes/transcriptomes suggesting that they may be a conserved strategy of AM fungi to deal with the host immune system. In fact LysM domain containing effectors are also used by a wide range of pathogenic fungi to interfere with chitin-triggered immune responses (Jonge et al., 2010; Sánchez-Vallet et al., 2013), revealing a common strategy used by symbiotic and pathogenic fungi to interact with plants.

Arbuscule development

Arbuscules represent the heart of the symbiosis as they form the symbiotic interface where nutrient exchange takes place (Luginbuehl and Oldroyd, 2017). Arbuscule formation requires the activation of the common SYM pathway, see Figure 2. Especially CCaMK is essential to allow the formation of arbuscules in the inner cortex cells. CCaMK phosphorylates the transcription factor CYCLOPS which subsequently activates a program that ultimately leads to the accommodation of the fungus (Horváth et al., 2011; Takeda et al., 2012; Pimprikar et al., 2016). Knock-out mutants of CYCLOPS in *L. japonicus* and rice are still able to allow root colonization but arbuscule formation is almost completely blocked (Kistner et al., 2005; Yano et al., 2008). Similarly, arbuscule formation also requires the action of DELLA GRAS transcription factors. DELLA proteins are best known for their role as negative regulators of gibberellic acid (GA) signaling (Schwechheimer and Willige, 2009). They were found to form a complex with CCaMK and CYCLOPS, which activates the expression of the GRAS transcription factor RAM1 (Pimprikar et al., 2016). RAM1, possibly in combination with other GRAS transcription factors, subsequently induces a program that controls arbuscule branching (Park et al., 2015). The application of the gibberellin (GA) inhibitor paclobutrazol or overexpression a constitutive GA-repressing DELLA1-Δ18 isoform can complement RAM1 expression and arbuscule formation in cyclops mutants (Floss et al., 2013; Pimprikar et al., 2016). DELLA proteins seem to play an important role to inte-

grate arbuscule formation with nutritional needs and plant physiology. High Pi conditions correlate with increased GA levels that impair the formation of arbuscules (Davière and Achard, 2013; Foo et al., 2013). This is likely important to prevent the high carbon costs of feeding the fungus, while already sufficient Pi is available to the plant.

Upon its induction RAM1 induces the expression of WRINKLED1-like (WRI) AP2 transcription factors (Jiang et al., 2018; Xue et al., 2018). These include LjCBX1 in Lotus and WRI5a-c in Medicago. These WRINKLED transcription factors may function partly redundant to induce an arbuscule-specific transcriptional program that controls the bidirectional exchange of phosphorus and fatty acids (Limpens and Geurts, 2018). Among the genes directly regulated by WRI's are for example the arbuscule-specific symbiotic phosphate transporter PT4 and proton pump HA1, which creates the proton gradient that fuels PT4 to transport Pi from the fungus into the plant cells (Krajinski et al., 2014). The WRI's also induce the expression of a fatty acid biosynthesis regulon in arbuscule forming cells. This includes two presumed fatty acid transporters, STR/STR2, that are required to transport fatty acids across the peri-arbuscular membrane to feed the fungus (Zhang et al., 2010; Gutjahr et al., 2012). The common transcriptional regulation might offer a mechanism to couple Pi uptake from the fungus with carbon supply to the fungus. Such a connection has been previously suggested by the work of Kiers et al. (2011). This study showed that Medicago can transfer more carbon to a cooperative fungus that gives more phosphate to its host, while a less-cooperative strain that keeps more Pi to itself receives less carbon. Vice-versa, if the cooperative fungal strain gets more carbon it will also give more Pi to the plant. How such reciprocal rewarding is regulated at the molecular level remains a key question to be answered.

Another intriguing aspect of arbuscule development is the fact that these structures are relatively short lived. Recently, first molecular insight into the regulation of arbuscule degradation was obtained with the identification of the MYB1 transcription factor (Floss et al., 2017). MYB1 was identified in an RNAi screen for factors that can suppress the premature degradation of arbuscules in the pt4 mutant, which is impaired in Pi uptake at the arbuscules. It was shown to control the expression of hydrolytic enzymes, such as cysteine proteases and chitinases, that degrade the arbuscules. MYB1 is already rapidly induced early during arbuscule formation. Therefore, it was suggested that post-translational regulation prevents it from becoming active too early. MYB1 required an interaction with NSP1 and DELLA transcription factors for efficient activity (Floss et al., 2017). Since these transcription factors already play a role in the early stages of arbuscule formation, complex formation with MYB1 might part of this post-tranlational regulation. Furthermore, arbuscule degradation still occurred in a myb1 mutant background suggesting that additional regulators remain to be identified.

Premature arbuscule degradation in the *pt4* mutant was also shown to be suppressed when the plants are simultaneously starved for nitrogen. This suppression required the ammonium transporter MtAMT2;3 located at the peri-arbuscular membrane (Breuillin-Sessoms et al., 2015). This suggests that the plant not only monitors Pi supply but also N supply by the fungus. Because MtAMT2;3 failed to complement a yeast mutant impaired in ammonium transport, it was suggested that it may have a N-sensing and signaling function. Because of its key role in the regulation of reciprocal nutrient exchange and arbuscule lifetime it will be of key importance to unravel how plants perceive the Pi/N status in arbuscule containing

cells. Therefore, in Chapters 4 and 5 I studied the role of symbiosis-induced SPX proteins, which are well known for their role as Pi sensors and regulators of Pi homeostasis and signaling in plants (Puga et al., 2014; Wang et al., 2014b; Wild et al., 2016). Based on the data obtained I propose a model where SPX proteins monitor the Pi status in arbuscule-containing cells and control the activity of plasma membrane aquaporins to control the timely degradation of arbuscules when sufficient Pi is obtained.

Thesis outline

The research presented in this thesis investigated molecular mechanisms by which AM fungi and plants control each other to ensure a mutualistic symbiosis. It especially focusses on two aspects: 1) the role of fungal effector proteins to facilitate colonization of the plant; and 2) the role of phosphate sensing SPX proteins in the regulation of arbuscule development.

In **chapter 1**, a general introduction to the communication between plants and AM fungi is given, with a focus on (pre-)contact communication to initiate the interaction and the control of arbuscule development.

In **chapter 2**, we studied the function of a secreted, host nucleus-targeted fungal effector, called RiNLE1, that is highly and specifically expressed in arbuscules in a wide variety of host plants. We show that RiNLE1 accumulates in the nucleolus and smaller nuclear bodies of the host nucleus and interacts with the core nucleosome component Histone 2B. These helped us to find that RiNLE1 interferes with host H2B monoubiquitination to subvert host defense response. RiNLE1-like proteins are found in several biotrophic fungal genomes suggesting that RiNLE1-like effectors may be more widely recruited to manipulate host defense responses.

In **Chapter 3**, we studied the role of an effector that is expressed in a host-dependent manner. This effector, called RiFGB1 from *R. irregularis* DAOM197198, is highly induced in the monocot host Allium schoenoprasum (Chives) but not in dicot hosts like Medicago and Nicotiana. It shows homology to the Fungal Glucan Binding 1 (FGB1) effector from the root endophyte *Piriformaspora indica*. Our data suggest that RiFGB1 can bind to a range of glycan molecules and can interfere with immune responses induced by a variety of microbe-associated molecular pattern (MAMP) molecules, which correlates with a positive effect on fungal colonization. Intriguingly, we found that the *R. irregularis* C3 isolate, in contrast to the DAOM197198 isolate, does not upregulate FGB1 homologs strongly in chives. This correlates with a reduced ability of C3 to colonize chives. These data give credibility to the suggestion that effectors may determine host preferences.

In **chapter 4**, the role of phosphate-sensing SPX proteins in AM symbiosis was studied. Plants are able to control arbuscule development in a phosphate-dependent manner. However, how a plant is able to sense how much nutrients it receives from its partner is largely unknown. We identified two SPX genes in Medicago that are strongly induced during the AM symbiosis, specifically in arbuscule-containing cells. SPX proteins are known for their role as phosphate sensors to control phosphate homeostasis in plants. In line with this, the SPX proteins controlled phosphate starvation responses under non-symbiotic conditions , in part through interaction with the key transcription factor Phosphate Starvation Response 2,

PHR2. During the AM interaction the SPX proteins were found to initially play a positive role to stimulate colonization, likely through their effect on the exudation of strigolactones, and possibly other factors. However, later during the interaction they redundantly control the timely degradation of arbuscules.

In **chapter 5**, we studied how the SPX protein identified in chapter 4 might control arbuscule degradation. No interactions between the SPX proteins and known transcriptional regulators of arbuscule degradation were found, suggesting that other unknown factors must be involved. To identify these, co-immunoprecipitation coupled with tandem mass spectroscopy was used. This identified PIP2 plasma membrane aquaporins as potential interacting proteins. Interestingly, overexpression of PIP2 reduced arbuscule abundance but at the same time reduced the ratio of degrading arbuscules. These results now offer a basis to investigate the possibility that SPX proteins regulate Pi transport and/or arbuscule degeneration through the regulation of PIP2 activity.

In **chapter 6**, I summarize and discuss the results described in this thesis in a broader perspective to illustrate how plant immune response and nutrient exchange may contribute to partner preference in AM symbiosis.

Chapter 2

A nuclear-targeted effector of *Rhizophagus irregularis* interferes with Histone 2B mono-ubiquitination to promote arbuscular mycorrhization

Peng Wang[1], Henan Jiang[1], Sjef Boeren[2], Harm Dings[1], Olga Kulikova[1], Ton Bisseling[1], Erik Limpens[1]

[1]Laboratory of Molecular Biology, Wageningen University & Research, 6708 PB Wageningen, the Netherlands; [2]Laboratory of Biochemistry, Wageningen University & Research, 6708 WE Wageningen, the Netherlands

Author for correspondence: Erik Limpens (erik.limpens@wur.nl)

This chapter has been published in ***New Phytologist***.

https://doi.org/10.1111/nph.17236

Abstract

·Arguably, symbiotic arbuscular mycorrhizal (AM) fungi have the broadest host range of all fungi, being able to intracellularly colonize root cells in the vast majority of all land plants. This raises the question how AM fungi effectively deal with the immune systems of such a widely diverse range of plants.

·Here, we studied the role of a nuclear-localization signal containing effector from *Rhizophagus irregularis*, called Nuclear Localized Effector1 (RiNLE1), that is highly and specifically expressed in arbuscules.

·We show that RiNLE1 is able to translocate to the host nucleus where it interacts with the plant core nucleosome protein Histone 2B (H2B). RiNLE1 is able to impair the mono-ubiquitination of H2B, which results in the suppression of defense-related gene expression and enhanced colonization levels.

·This study highlights a novel mechanism by which AM fungi can effectively control plant epigenetic modifications through direct interaction with a core nucleosome component. Homologs of RiNLE1 are found in a range of fungi that establish intimate interactions with plants, suggesting that this type of effector may be more widely recruited to manipulate host defense responses.

Key words: arbuscular mycorrhiza, effector, H2B mono-ubiquitination, plant defense, *Rhizophagus irregularis*, symbiosis

Introduction

Microbes that intimately interact with plants face the challenge of dealing with the plant's immune system. Conserved microbe-associated molecular patterns (MAMPs), such as chitin or beta-glucans present in the cell walls of such microbes are potent triggers of defense responses in the plant. Pathogens typically subvert host immunity by secreting a range of effector proteins that can act outside or inside the host cell (Lo Presti et al., 2015). Recent studies on several pathogenic effectors proteins that are translocated into plant cells have revealed that epigenetic modifications are a key target to suppress immunity genes (Ramirez-Prado et al., 2018). Indeed, transcriptional reprogramming plays a central role in plant immunity (Jenner and Young, 2005). Especially, various histone modifying enzymes have been found to be a target of oomycete or fungal effector proteins to suppress defense gene expression. For example, the *Phytophthora sojae* effectors Avr52 and PsAvh23 and the non-ribosomal HC Toxin peptide from the maize pathogen *Cochliobolus carbonum* were shown to target histone acetyltransferases to modify histone acetylation levels, causing the suppression of defense gene expression or the activation of susceptibility genes (Ransom and Walton, 1997; Kong et al., 2017; Walley et al., 2008; Li et al., 2018).

Similar to fungal pathogens, also mutualistic arbuscular mycorrhizal (AM) fungi, belonging to the Glomeromycotina subphylum, contain chitin and beta-glucans in their cell walls (Wawra et al., 2016; Zeng et al., 2020; Lo Presti et al., 2015). AM fungi form root symbiotic associations with the vast majority (> 75%) of land plant species (Smith and Read, 2008). In this intimate partnership, the biotrophic AMF form highly branched arbuscules inside

root cortex cells, where they provide the plant host with mineral nutrients such as phosphate and ammonium, in return for plant-derived photosynthates (Gutjahr and Parniske, 2013). The apparent lack of host specificity in this interaction indicates that AM fungi must have broadly effective mechanisms to subvert the host immune system in such a wide variety of plants (Volpin et al., 1994; García-Garrido and Ocampo, 2002). In comparison, most pathogenic fungi typically have a rather narrow host range. Like their pathogenic counterparts, also AM fungi make use of effector proteins to deal with the plant immune system (Kloppholz et al., 2011; Zeng et al., 2020). However, the various mechanisms by which AM fungal effector proteins manipulate plant responses and contribute to their broad host range are far from understood (Lin et al., 2014; Voß et al., 2018; Kamel et al., 2017; Zeng et al., 2018; Tisserant et al., 2013).

In previous work we showed that many putative effector proteins from *Rhizophagus irregularis* are expressed at distinct stages of the interaction (Zeng et al., 2018). Several effector candidates were shown to be specifically expressed in arbuscules, when the fungus intracellularly colonizes root cortex cells. One of the highest expressed putative effectors in arbuscules encodes a small secreted protein containing a nuclear-localization signal. Here we show that this effector, which we called NUCLEAR LOCALIZING EFFECTOR 1 (RiNLE1), can translocate to the host nucleus where it interacts with the core nucleosome protein Histone 2B. RiNLE1 impairs the mono-ubiquitination of H2B, resulting in reduced expression of a set of defense-related genes and enhanced mycorrhizal colonization levels. This reveals that epigenetic reprogramming is a common target of pathogenic and mutualistic fungal effectors and identifies the direct targeting of H2B as a novel mechanism for fungal effector proteins.

Materials and methods

Plant and fungal material

Medicago truncatula Jemalong A17 (Medicago) seedlings were grown and transformed as described previously (Limpens et al., 2004). *Nicotiana benthamiana* was used for Agrobacterium tumefaciens-mediated transient expression as described before (Zeng et al., 2018). *Rhizophagus irregularis* DAOM197198 spores were obtained from Agronutrion, France. Spores were thoroughly washed through three layers of filter mesh (220 µm, 120 µm, 38 µm) before use. Plants for mycorrhization were grown in SC10 RayLeach cone-tainers (Stuewe and Sons, Canada) with premixed sand:clay (1:1 V/V) mixture and inoculated by placing ~200 pores ~2 cm below the seedling roots. Plants were grown in a 16 h daylight chamber at 21°C and watered by 10 ml ½ Hoagland medium with 20 µM phosphate twice a week (Zeng et al., 2018).

Cloning

Unless indicated, all the constructs used in this work were made using the Golden gate cloning system (Engler et al., 2014). All primers used are listed in supplementary table 1. The vectors used for cloning of the different constructs are listed in supplementary table 2. All newly made level zero cloning vectors were confirmed by sequencing.

Phylogeny

For phylogenetic analyses, RiNLE1 homologs were collected using protein-protein BLAST from NCBI and JGI. To select the effector homologs, the following criteria were used: (1), Protein should be predicted to have a signal peptide using SignalP-5.0 Server (http://www.cbs.dtu.dk/services/SignalP/); (2), the proteins should be predicted to be a potential effector based on EffectorP 2.0 (http://effectorp.csiro.au/); (3), the proteins should be predicted to be nuclear localized based on LOCALIZER software (http://localizer.csiro.au/). Identified homologs were aligned using MAFFT built in Geneious R11.0 (https://www.geneious.com). An unrooted phylogenetic tree was generated using the neighbour-joining tree builder in Geneious R11.0.

RNA *In Situ* Hybridization

Medicago roots hosting the arbuscular mycorrhizal fungus were fixed with 4% paraformaldehyde mixed with 3% glutaraldehyde in 50 mM phosphate buffer (pH 7.4) overnight, dehydrated in serial dilution of ethanol and embedded in paraffin (Paraplast X-tra, McCormick Scientific) as described (Kulikova et al., 2018). 7 µm thick root sections were cut by RJ2035 microtome (Leica). RNA *in situ* hybridization was conducted using Invitrogen ViewRNA ISH Tissue 1-Plex Assay kits (Thermo Fisher Scientific) according to the user manual available at (shorturl.at/fuzPT).

RNA ISH probe sets were designed and synthesized by request at Thermo Fisher Scientific. A typical probe set consists of ~20 synthetic adjacent oligonucleotide pairs. Each of these pairs is composed of a 20 bp primary sequence designed to target specific regions across the target mRNA sequence and a secondary extended sequence serving as a template for the amplification and detection of hybridization signals. Probe set for *RiNLE1* (catalogue number VF1-6001202) covered mRNA sequence from 2 bp to 613 bp and probe set for *MtPT4* (VF1-19337) – from 390 bp to 1296 bp. Probe set for *MtPT4* was used as a positive control for *in situ* hybridization. As negative controls a *RiNLE1* sense probe set (VPEPR3M) was used and probe sets were omitted for hybridization.

Localization of RiNLE1

To check the subcellular localization of RiNLE1, a *PT4p::GFP-RiNLE1* (lacking the endogenous signal peptide) construct was transformed into Medicago by *Agrobacterium rhizogenes* MSU440 mediated hairy root transformation (Limpens et al., 2004). Five weeks after inoculation with 200 *R. irregularis* spores, transgenic mycorrhizal roots were harvested for confocal microscopy to check the localization of RiNLE1.

Yeast secretion trap

The yeast signal sequence trap (YSST) was done using *Saccharomyces cerevisiae* Y02321 strain (Euroscarf, Frankfurt, Germany), and following the protocol described before (Zeng et al., 2020). Briefly, the *RiNLE1* full coding sequence without stop codon was inserted into the EcoRI and NotI sites of the pYST0 plasmid (Lee et al., 2006). Positive colonies from SD/-LEU plate were plated on sucrose selection medium (2% sucrose, 0.025% glucose, 6.7 g/L yeast nitrogen base without amino acids, 1.85 g/L Drop-out mix minus leucine, 2% Agar) and incubated at 30°C for 3 to 5 days. pYST0 empty vector transformed Y02321 strain was used as control.

Agroinfiltration of *Nicotiana benthamiana*

To determine whether the RiNLE1 protein can cross the plant cell wall and enter the nucleus, a *UBp::BCP1sp-GFP-RiNLE1* construct was transiently expressed in *Nicotiana benthamiana* (Nicotiana) leaves. *UBp::BCP1sp-GFP* was used as control. Agrobacterium infiltration of 5 week old Nicotiana leaves was performed as described before (Zeng et al., 2018), using co-transformed P19 as silencing inhibitor. The infiltrated plants were grown for 2 days and samples were collected for confocal microscopy using a Leica SP8 confocal microscope.

Hypersensitive response

The effect of RiNLE1 on AVR4 and CF-4 induced hypersensitive response (HR) was done as described (Ma et al., 2012). Nicotiana leaves were infiltrated with different combination of Agrobacterium carrying constructs and grown for 4 days in greenhouse, after which the leaves were harvested for trypan blue staining. The leaves were boiled in 50 mL staining solution (10 mL lactic acid, 10 mL phenol, 10 mL glycerol, 10 mL H_2O and 10 mg trypan blue) mixed with 50 mL 96% ethanol for 5 min. Subsequently, the leaves were destained (250 g chloral hydrate in100 mL H_2O) overnight at room temperature.

Co-immunoprecipitation (Co-IP) and liquid chromatography tandem-mass spectrometry (LC-MS/MS)

For identification of RiNLE1 interactors, a *PT4p::FLAG-RiNLE1* construct was transformed into Medicago roots as described above. *PT4p::FLAG-GFP* transformed roots were used as negative control. Total proteins were extracted from well-mycorrhized transgenic roots using Co-IP buffer (10% glycerol, 50 mM Tris-Hcl pH=8.0, 150 mM NaCl, 1% Igepal CA 630, 1 mM PMSF, 20 µM MG132, 1 tablet protease inhibitor cocktail). Centrifuge the total protein mix at 18580 g for 10 min at 4 °C, transfer supernatant to fresh 15 ml tube; Centrifuge at max speed for 10 min at 4 °C, transfer supernatant to new 15 ml tube; FLAG-tagged protein was pulled down by using µMACS and MultiMACS DYKDDDDK Isolation Kits (Miltenyi Biotec). Immunoprecipitated protein samples were digested into peptides by trypsin (Sigma-Aldrich).

Peptide samples were measured by nLC-MS/MS with a Proxeon EASY nLC1000 and a LTQ-Orbitrap XL mass spectrometer as previously described (Lu et al., 2011; Wendrich et al., 2017). In short, 18 ul of peptide sample was injected over a 0.10 * 32 mm Magic C18AQ 200A 5 µm beads (Bruker Nederland B.V.) pre-concentration column (prepared in-house) and peptides were eluted onto a 0.10 * 250 mm ReproSil-Pur 120 C18-AQ 1.9 µm beads analytical column (prepared in-house) with an acetonitril gradient at a flow of 0.5 ul/min with a Thermo EASY nanoLC1000. A gradient from 9 to 34% acetonitril in water with 1 ml/l formic acid was applied in 50 minutes. An electrospray potential of 3.5 kV was applied directly to the eluent and full scan positive mode FTMS spectra were measured between m/z 380 and 1400 in the Orbitrap at high resolution (60000) and MSMS spectra were measured in the ion trap.

LC-MS data analysis (false discovery rates were set to 0.01 on peptide and protein levels) and additional result filtering (minimally 2 peptides are necessary for protein identification of which at least one is unique and at least one is unmodified) were performed as described

previously (Smaczniak et al., 2012; Wendrich et al., 2017). Peptide data were mapped to *Medicago truncatula* uniprot 2018 and *Rhizophagus irregularis* DAOM197198 Uniprot 2018 to identify proteins. To analyse the relative abundance of proteins, their normalized label-free quantification (LFQ) intensities were compared (Cox et al., 2014). nLC-MSMS system quality was checked with PTXQC (Bielow et al., 2016) using the MaxQuant result files.

Yeast Two-Hybrid

To confirm interactions, Yeast two-hybrid analyses were applied using the Matchmaker Gold Yeast Two-Hybrid System (Clontech, USA) according to manufacturer's instruction. *RiNLE1* was inserted in the pGBKT7 bait vector, *MtH2B.1* was inserted in the pGADT7 prey vector. Bait and prey constructs were transformed into Y2H Gold and Y187 strain as described in instruction of the Matchmaker system, respectively. Bait and prey strains were mated following the manufacturer's handbook (Clontech, USA). After mating, yeast was plated on DDO and QDO/X/A plate to check mating and protein-protein interaction results, respectively.

Dexamethasone inducible RiNLE1 expression

The Dexamethasone (DEX) inducible expression system (Borghi, 2010) was applied to induce RiNLE1 expression in Medicago hairy roots. First, construct *LjUB1::GVG—AtUB10::DsRed—UAS::RiNLE1—UAS::GFP* and control construct *LjUB1::GVG—AtUB10::DsRed—Dummy3 (GCAACATACGCTGGA) —UAS::GFP* were transformed in Medicago hairy roots as described previously (Limpens et al., 2004). Composite plants containing transgenic roots were transferred to Emergence medium plates (Limpens et al., 2004). Three plants were collected for one repetition. After 1 day, 2 mL of 10 μM DEX dissolved in DMSO was spread onto the roots by pipetting. After 20 hours, clear GFP signal was visible under a fluorescence macroscope. Transgenic roots were harvested and stored in -80°C for further analysis.

RNA isolation and qPCR

All RNA samples in this work were isolated using Qiagen plant RNA mini kit, following the manufacturer's instructions. cDNA was made from 200 ng RNA using the iScript cDNA Synthesis kit (Bio-Rad). iQ SYBR Green Supermix (Bio-Rad) was used for qPCR in a Bio-Rad CFX connect real-time system. Primers used are listed in supplementary table 1. Gene expression was normalized using Medicago *Elongation factor 1* (*EF1*). Relative expression levels were calculated as $2^{-\triangle\triangle ct}$. Three technical replicates were used for each sample.

RNA Sequencing

RNA was isolated as described above. 3 transformed plants grown on one emergence plate was used as one replicate. 3 replicates were used for RNA-seq. RNA samples were sequenced using the BGI SEQ-500 Transcriptome platform. RNA-seq data were mapped to *Medicago truncatula* genome V4.0 using CLC genomics workbench 10.0.1 (Qiagen). Settings for TPM (transcripts per million), PCA (Principal component analysis) and differential expression analyses were performed as described by Zeng et al (Zeng et al., 2018). RNA-seq data was deposited to the NCBI Gene Expression Omnibus, under the accession number GSE155682.

RiNLE1 constitutive overexpression

For constitutive *RiNLE1* overexpression, RiNLE1 was expressed in Medicago hairy roots under the control of the Lotus *Ubiquitin 1* promoter. An empty vector construct was used as control. Transgenic roots were harvested three weeks after inoculation for mycorrhizal quantification and RNA isolation. Roots for mycorrhizal quantification were stained with WGA-Alexafluor 488 (Thermo Fisher Scientific, USA) and scored using the gridline intersect method (McGONIGLE et al., 1990).

Host-induced gene silencing

RiNLE1 hairpin constructs were generated using the gateway system (Invitrogen, USA). *RiNLE1* mRNA sequences were amplified and cloned into the *pENTR/D-TOPO* entry vector. Primers used are listed in supplementary table 1. Next, the fragment of RiNLE1 was cloned into the modified *pK7GWIWG2(II)-AtEF1* RR vector using LR clonase II (Invitrogen) to get the final silencing construct. An empty vector was used as control. Medicago A17 transformation, spore inoculation and mycorrhizal quantification were done as described above.

HUB1 experiments

The Medicago *HUB1* CDS (Medtr7g046250) was amplified using primers listed in supplemental table 1. The HUB1 DEX-inducible construct and *PT4p::HUB1* overexpression construct were made as described above using golden gate cloning (Engler et al., 2014). DEX induction, Medicago transformation, spores inoculation and mycorrhizal quantification were performed using the same conditions as described above for RiNLE1 overexpression.

Isolation of nuclear proteins

Nuclear proteins of Medicago roots were isolated as described previously with minor changes (Gendrel et al., 2005). 1 gram of roots was ground to a fine powder in liquid nitrogen and put in 30 ml of extraction buffer 1 (0.4 M sucrose, 10 mM Tris-HCl pH=8, 10 mM $MgCl_2$, 1 tablet protease inhibitor cocktail) in a 50-ml tube for 5 min. The solution was filtered through a 70 µm cell strainer into a new 50-ml tube and centrifuged at 3,000 g at 4 °C for 20 min. The pellet was subsequently resuspended in 1 ml of precooled buffer 2 (0.25 M sucrose, 10 mM Tris-HCl pH=8, 10 mM $MgCl_2$, 1% Triton X-100, 1 tablet protease inhibitor cocktail) and transferred into a 1.5-ml microcentrifuge tube. After centrifuging at 12,000 g at 4 °C for 10 min. the resulting pellet was resuspended in 300 µl precooled buffer 3 (1.7 M sucrose, 10 mM Tris-HCl pH=8, 10 mM $MgCl_2$, 0.15% Triton X-100, 1 tablet protease inhibitor cocktail). To this, 300 µl of buffer 3 was added in a new microcentrifuge tube and centrifuged at 15,000 g at 4 °C for 1 h to pellet nuclei. The nuclear pellet was resuspended in 300 µl RIPA buffer (10 mM Tris-HCl pH 7.5, 150 mM NaCl, 0.1% SDS, 1% Triton X-100, 1% Deoxycholate, 0.5 mM EDTA, 20 µM MG132, 1 tablet protease inhibitor cocktail) by pipetting and vortexing. The supernatant containing nuclear proteins was harvested for further analysis after centrifugation at 12,000 g at 4 °C for 10 min..

Western blot

Anti-GFP-HRP and anti-FLAG-HRP antibodies were obtained from Miltenyi biotec, USA. Ubiquitinated H2B monoclonal antibody (NRO3) was obtained from Medimabs, Canada.

Western blots were performed by using the BIO-RAD trans-blot turbo system using PVDF membranes. The blots were blocked using TBS/2%BSA/0.3%Tween-20 for 1 h shaking at room temperature. 1:5000 dilutions of the antibodies were used for detection by chemiluminescence using the clarity western ECL substrate (BIO-RAD). For detection of H2Bub a secondary anti-rabbit-HRP antibody was used (1:5000 dilutions).

Results

RiNLE1 is specifically expressed in arbuscules and translocates to the plant nucleus

Our previous stage-specific transcriptome analysis of the *Rhizophagus irregularis* secretome, identified ~50 putative effector proteins that showed specific expression in arbuscules (Zeng et al., 2018). One of the highest expressed arbuscule-specific effector candidates, RiNLE1 (GenBank: EXX65927.1), was predicted to localize to the nucleus, suggesting that it may translocate to the host cell to exert its function there (Fig. S1a), making it an intriguing candidate effector potentially controlling arbuscule formation.

As a first step to unravel the role of this conserved effector we confirmed the arbuscule-specific expression of *RiNLE1* via RNA *in situ* hybridization on mycorrhized Medicago roots. This showed that *RiNLE1* is indeed specifically expressed in arbuscules, similar to the expression of the arbuscule-containing cell-specific phosphate transporter 4 (*PT4*; Javot et al., 2007) used as positive control (Fig. 1a, b). No signal was detected in arbuscules in the negative controls when a *RiNLE1* sense probe was used or when probe sets were omitted (Fig. 1c, d).

Next we confirmed that RiNLE1 is secreted by using a yeast signal sequence trap assay, since *R. irregularis* currently cannot be stably transformed (Forbes et al., 1998; Helber and Requena, 2008). Therefore, the *RiNLE1* full coding sequence was fused to a yeast invertase (SUC2) lacking its endogenous signal peptide and transformed into the *Saccharomyces cerevisiae* Y02321 strain (Lee et al., 2006). Expression of this construct allowed Y02321 to grow on sucrose selection medium, whereas the empty vector control could not (Fig. 2a), indicating the secretion of RiNLE1-fusion protein.

RiNLE1 contains a nuclear-localization signal (NLS) at its C-terminus (Fig. S1a). To determine whether RiNLE1 can localize to the plant nucleus in arbuscule-containing cells, we first expressed N-terminal GFP-tagged RiNLE1 (no signal peptide) by the arbuscule-containing cell-specific *MtPT4* promotor (*PT4p::GFP-RiNLE1*). This showed that GFP-RiNLE1 localized to the nucleus, and especially accumulated in nuclear bodies, including the nucleolus, of arbuscule-containing cells (Fig. 1e-h) similar to its localization in *Nicotiana benthamiana* (Nicotiana) leaves (Fig. S1b; Zeng et al., 2018).

Next, we studied whether RiNLE1 can translocate to the host nucleus. We first tried to localize RiNLE1 using specific antibodies. However, despite multiple efforts we were not able to obtain an antibody that was specific enough to reliably detect RiNLE1 *in situ*. Therefore, we used an alternative approach by expressing a GFP-tagged RiNLE1 (no endogenous signal peptide) construct containing a plant signal peptide sequence from MtBCP1 to target it to the apoplast (Ivanov and Harrison, 2019) under the control of the constitutive *Lotus*

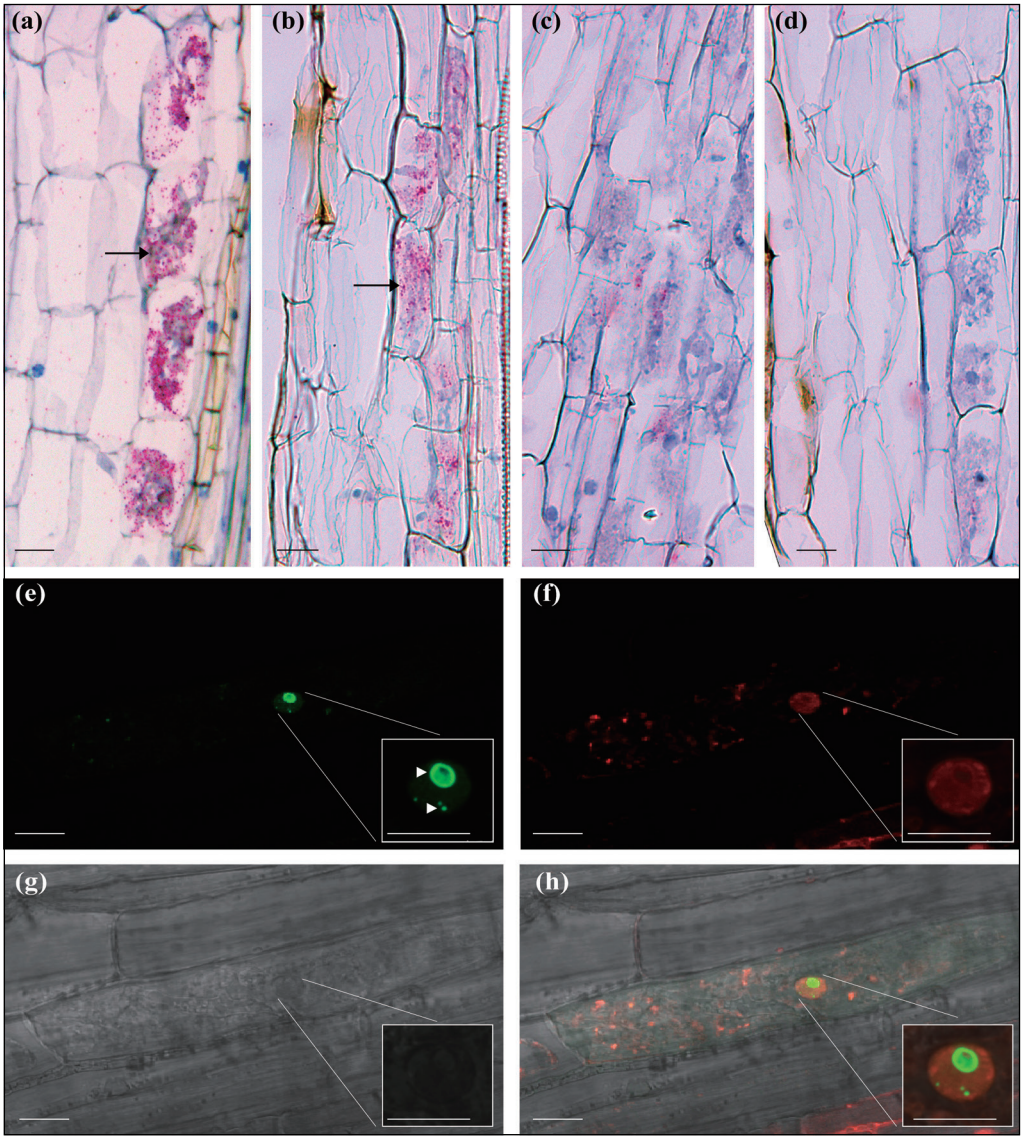

Fig. 1 RiNLE1 is specifically expressed in arbuscules and localizes in the plant nucleus. (a) RNA *in situ* hybridizations of the arbuscule-containing cell-specific *MtPT4* gene in mycorrhized *Medicago truncatula* roots. Arrow indicate in situ signal. (b) RNA *in situ* hybridizations of *RiNLE1* in mycorrhized *M. truncatula* roots. Arrow indicate in situ signal. (c) Negative control of RNA *in situ* hybridization where *RiNLE1* sense probe sets are used. (d) Negative control of RNA *in situ* hybridization where probe sets are omitted to reveal background signal. Scale bar (a-d) = 25 µm. (e-h) *PT4p::GFP-RiNLE1ΔSP* expressed in *M. truncatula* mycorrhizal roots. (e) GFP-RiNLE1 accumulates in the nucleolus and other nuclear bodies of the arbuscule containing cells, as indicated by arrowheads. (f) Corresponding red fluorescence resulting from co-expression of the DsRed1 protein under the control of the *Arabidopsis thaliana Ubiquitin10* promoter, used as marker for cytoplasm and nucleus. (g) Corresponding bright field image. (h) Corresponding overlay of GFP, DsRed and bright field image. Scale bar (d-g) = 10 µm.

japonicus Ubiquitin 1 promotor (*LjUB1p::BCPsp-GFP-RiNLE1*) in Nicotiana leaves. The MtBCP1 signal peptide was chosen because the endogenous signal peptide of RiNLE1 is not well processed in plants causing an accumulation of recombinant protein in the endoplasmic reticulum (Fig. S1c). *LjUB1::BCPsp-GFP* lacking *RiNLE1* was used as control. This showed that BCP1sp-GFP-RiNLE1 still accumulated in the nucleolus while the BCPsp-GFP control was only found in the apoplast, suggesting that RiNLE1 can translocate into plant cells even in the absence of the fungus (Fig. 2b). Western blot analyses confirmed the presence of the fusion proteins in Nicotiana leaves (Fig. S1d).

Collectively, these results indicate that RiNLE1 is specifically expressed in arbuscules from where it can translocate to the host nucleus.

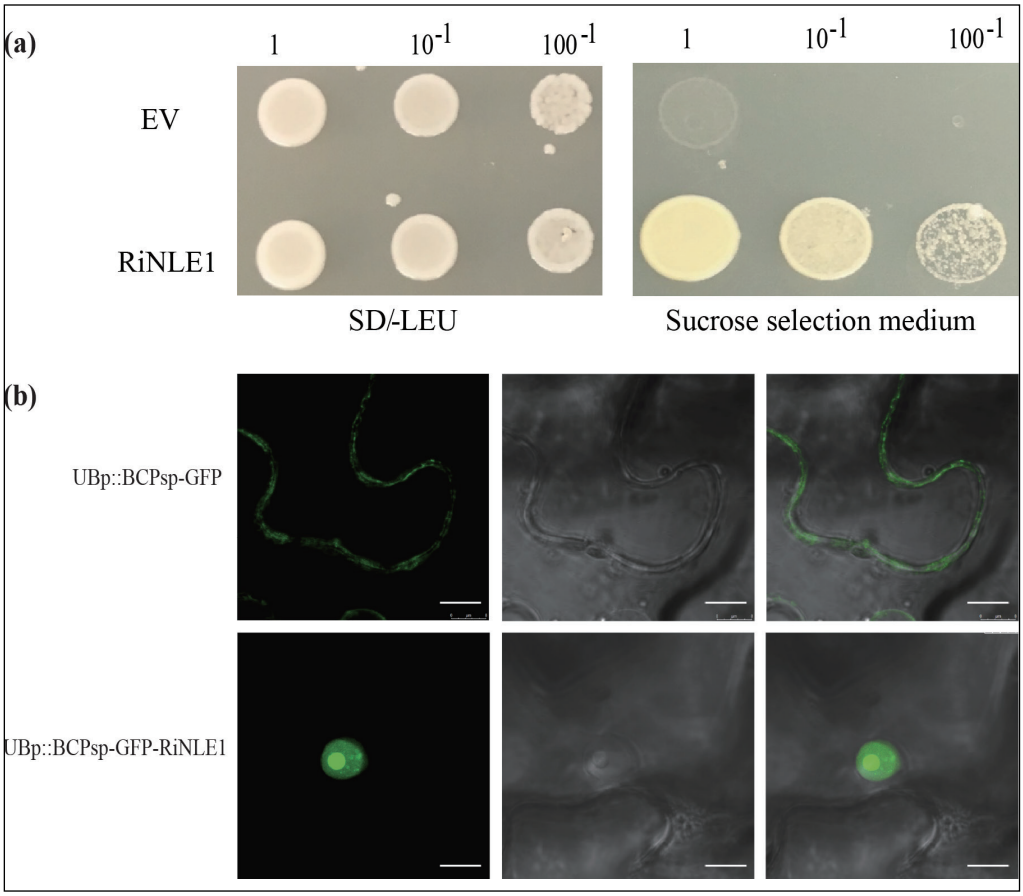

Fig. 2 RiNLE1 is secreted and translocates to the plant nucleus. (a) Yeast signal sequence trap showing that RiNLE1 is a secreted protein. *RiNLE1*, representing a fusion of full length *RiNLE1* with an invertase, and the empty pYST0 vector (EV) were transformed into *Saccharomyces cerevisiae* Y02321, and grown on SD/-Leu and sucrose selection medium at different dilutions for 3 days at 30 °C. (b) RiNLE1 can translocate to the plant nucleus. Expression of *UBp::BCP1sp-GFP* (upper row) and *UBp::MtBCP1sp-GFP-RiNLE1* (lower row), using the signal peptide of Medicago BLUE COPPER PROTEIN 1 (BCP1) to secrete GFP or GFP-tagged RiNLE1 to the apoplast, in *Nicotiana benthamiana* leaves. In contrast to the GFP control, the RiNLE1 fusion protein can be observed inside the plant nucleus indicating that NLE1 can translocate into the plant cell after been secreted to the apoplast. Scale bar = 10 μm.

RiNLE1-like proteins occur in various fungi

To determine whether RiNLE1 homologs can be found in other fungi, we searched for homologs via protein BLAST using NCBI and JGI MycoCosm databases. Numerous hypothetical proteins showing partial homology to part of RiNLE1 were initially identified. To select potential effector homologs among these hits, the following criteria were further applied: first, the proteins should have signal peptide predicted by SignalP-5.0 (http://www.cbs.dtu.dk/services/SignalP/); Second, the proteins should be predicted to be a potential effector based on EffectorP 2.0 (http://effectorp.csiro.au/); Last, the proteins should have a nuclear localization signal (NLS) predicted by LOCALIZER (http://localizer.csiro.au/). As a result, 19 homologs of RiNLE1 were identified (Table S3). These are all hypothetical proteins and lack any known protein domains (Fig. S2a). We could detect the presence of RiNLE1-like effectors, containing a signal peptide and a NLS at the C-terminus, in all AM fungal genomes available in NCBI and JGI (Fig. S2a, b). Interestingly, RiNLE1 homologs were also found in ectomycorrhizal fungi *Elaphomyces granulatus* (similarity 37.2%), the water mold parasite fungus *Rozella allomycis* (similarity 43.9%), the green algae parasitic fungus *Powellomyces hirtus* (similarity 41.6%), and the barley powdery mildew fungus *Blumeria graminis* (similarity 37.7%). These results indicate that RiNLE1-homologs exist in a wide range of fungi that intimately interact with plants or that intracellularly colonize other hosts.

Overexpression of RiNLE1 increases AM colonization

To explore the role of RiNLE1 in mycorrhization we first applied host induced gene silencing (HIGS) to knock down its expression (Nowara et al., 2010). However, despite several attempts using two different hairpin constructs, the expression of *RiNLE1* could not be successfully knocked down (data not shown). As an alternative approach we investigated the effect of overexpression of *RiNLE1* on mycorrhizal colonization. Therefore, *RiNLE1* (without signal peptide) was expressed in Medicago roots under the control of the constitutive *LjUbiquitin1* promoter and mycorrhization levels were quantified using the intersect method (McGONIGLE et al., 1990) three weeks after inoculation. Two independent repetitions with each 8 independently transformed roots both showed a significant increase in hyphal abundance compared to the empty vector control, while arbuscule abundance was not significantly changed (Fig. 3a, Fig. S3). The lack of effect on arbuscule numbers may be due to the fact that the fungal *RiNLE1* itself is already highly expressed specifically in arbuscule cells. qPCR analyses confirmed overexpression of *RiNLE1* and the phenotype, as the fungal *RiEF1* reference gene was significantly higher expressed in *UBQp::RiNLE1* roots compared to control roots, while *MtPT4* expression, a marker for arbuscule abundance, did not significantly change (Fig. 3b). These results indicate that RiNLE1 plays a positive role in AM colonization.

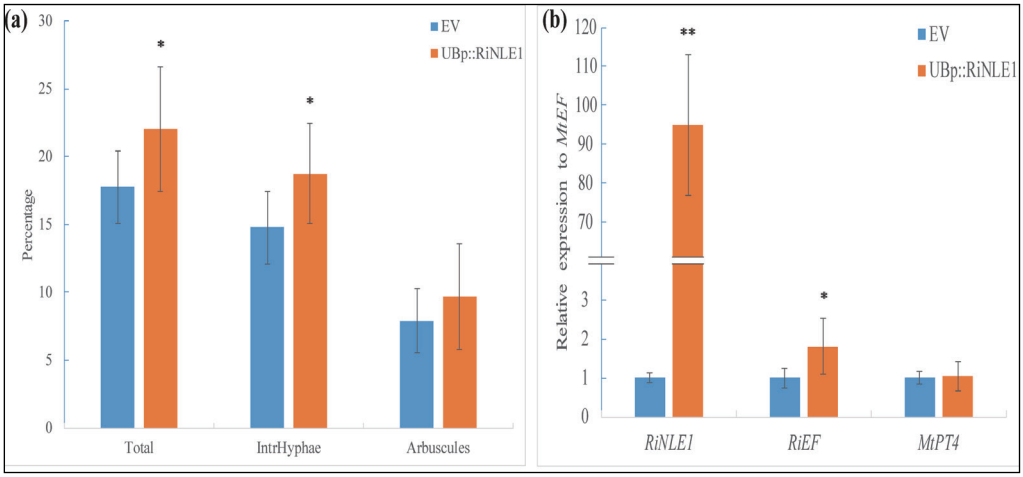

Fig. 3 Overexpression of RiNLE1 enhances mycorrhizal root colonization in *Medicago truncatula*. (a) Quantification of the level of mycorrhization in *UBp::RiNLE1* transgenic roots and empty vector control roots, 3 weeks post inoculation. Indicated are the percentage of intraradical hyphae (IntrHyphae), Arbuscules and overall level of colonization (Total). Data are represented as mean ± SD of 8 independently transformed plants per construct. Student's t test. *, $P < 0.05$. (b) qPCR analyses showing increased *RiEF* expression level as marker for fungal colonization in *RiNLE1* overexpression samples. No significant difference between EV and RiNLE1 samples is observed for arbuscular-specific *MtPT4* gene expression. Expression levels were normalized using *MtEF1* as reference. Data are represented as mean ± SD of 8 independently transformed plants per construct. Student's t test. *, $P < 0.05$. **, $P < 0.01$.

RiNLE1 suppresses host defense-related gene expression

Since we reasoned that RiNLE1 exerts its functions inside host nuclei, we explored the influence of RiNLE1 on plant gene expression. Therefore, we applied a dexamethasone (DEX) inducible promoter system (Borghi, 2010) to induce *RiNLE1* expression (lacking signal peptide) in Medicago roots. As a control we replaced the *RiNLE1* coding sequence by a short nonsense sequence (Dummy3 from the Golden Gate cloning kit; (Engler et al., 2014). DEX induction was confirmed 20 hours after treatment with 10 µM DEX by visualizing a co-transformed GFP marker that is under the control of the same DEX-inducible *cis*-regulatory element used to drive RiNLE1 (Fig. S4a, b). qPCR analysis further confirmed the induction of RiNLE1 (Fig. S4c). Therefore, this time point was chosen to monitor expression changes upon DEX-induction by RNA-sequencing. 3 replicates, representing pools of independently transformed roots, were used for both control and RiNLE1 samples.

RNA-seq data were analyzed using CLC genomics workbench 10.0.1 (Qiagen). Read mapping information is summarized in Table S4. Principal component analysis (PCA) of the RNA-seq data showed a clear separation of DEX-RiNLE1 samples and control DEX-EV samples in PC2 (27% variance) but not PC1 (49% variance) (Fig. S5a). This indicated that induction of RiNLE1 impacted gene expression levels, but that there was also a relative big variation between the different replicate samples. This is likely caused by the fact that different *A. rhizogenes* transformed roots (representing independent transformation events) were analysed for each replicate experiment and the level of *RiNLE1* expression in the dif-

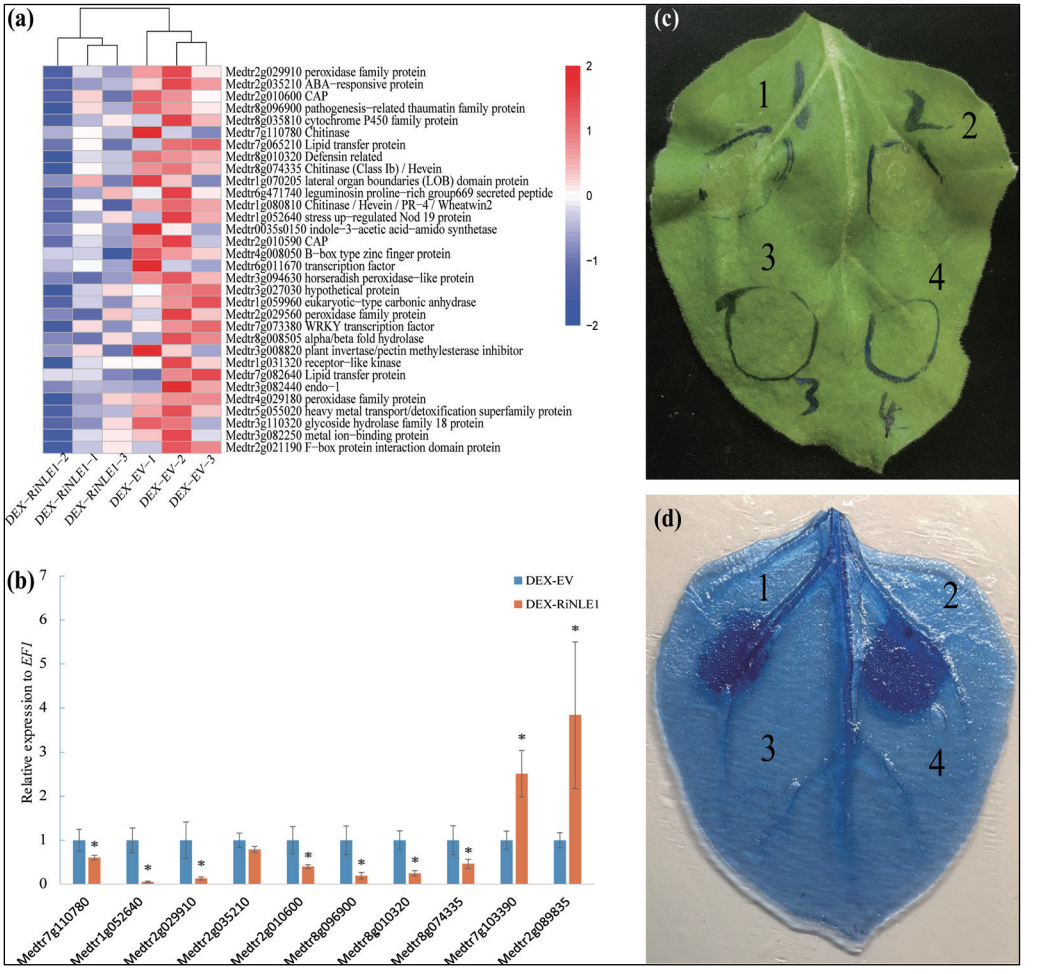

Fig. 4 Dexamethason (DEX) induced expression of *RiNLE1* suppresses defense gene expression in *Medicago truncatula* roots. (a) Induction of *RiNLE1* expression suppresses host defense gene expression based on RNAseq data. Heat map of DEGs that show significant (>2 fold, $P < 0.05$) downregulation upon 20 hours of DEX-treatment in *RiNLE1* expressing roots compared to empty vector controls. Expression values reflect log2 transformed transcripts per million (TPM). Columns were clustered using distance Euclidean, rows were ranged by fold change from high to low. (b) qRT-PCR analysis of selected defense-related genes (see also Table S6) based on the RNAseq analyses in independent DEX-induced RiNLE1 expressing and EV control roots. *MtEF1* was used as reference. Data are represented as mean ± SD of 3 biological replicates. Student's t test was used. *, $P < 0.05$. (c) RiNLE1 inhibits *Cladosporium fulvum* AVR4 effector and *Solanum lycopersicum* receptor-like protein Cf-4 induced hypersensitive response (HR). *Nicotiana benthamiana* leaves were infiltrated with the following combinations of Agrobacterium strains and grown for 4 days: 1 = 0.04 OD_{600} AVR4 + 0.04 OD_{600} Cf-4 (positive control), 2 = 0.04 OD_{600} AVR4 + 0.04 OD_{600} Cf-4 + 1 OD_{600} GFP (negative control), 3 = 0.04 OD_{600} AVR4 + 0.04 OD_{600} Cf-4 + 1 OD_{600} RiNLE1, 4 = 1 OD_{600} RiNLE1 (negative control). (d) Trypan blue staining of the leaves in (c) to visualise accumulation of HR.

ferent samples varied; TPM (transcripts per million) levels for RiNLE1: 5215, 1993, 3002 in the 3 replicates, respectively (bottom row in Table S5). Using a cut-off fold change > 2, and $P < 0.05$, we identified in total 76 differentially expressed genes (DEGs) in DEX-RiNLE1 samples relative to DEX-induced control samples (Table S5). Among the identified DEGs, 32 genes were downregulated upon *RiNLE1* induction (Fig. 4a, Table S6).

To determine whether the DEGs would be involved in a common biological process, we performed a gene-ontology (GO) enrichment analysis (Tian et al., 2017). This revealed a clear enrichment in genes associated with defense or stress-related processes among the 32 downregulated genes (Fig. S5b). In contrast, upregulated genes did not show enrichment in any biological process. Therefore, we especially focussed on the downregulated genes. The majority of these are encoding pathogenesis-related proteins, chitinases or peroxidases, related to plant response to biotic stress (Dodds and Rathjen, 2010) (Fig. 4a, Table S6).

To confirm the RNA-seq data, we selected 8 downregulated plant defense-related genes as well as 2 strongly upregulated genes and quantified their expressions via qPCR in an independent experiment. Except for one, all genes showed the expected differential regulation upon *RiNLE1* induction (Fig. 4b). Because *RiNLE1* is specifically expressed in arbuscules, we also analysed whether the expression of the 32 down-regulated genes was lower in arbuscule-containing cells compared to neighbouring non-colonized cortex cells, based on available cell-specific transcriptome data (Hogekamp and Küster, 2013; Zeng et al., 2018). This showed that the genes, whose expression could be reliably detected, were indeed significantly lower expressed in arbuscule-containing cells compared to neighbouring (non-colonized) cortex cells (Table S7).

To further assess the ability of RiNLE1 to suppress host defense responses, we tested the influence of RiNLE1 in a commonly used pathogenicity assay where co-expression of the plasma membrane localized *Solanum lycopersicum* immune receptor Cf4 with its avirulence target AVR4 from *Cladosporium fulvum* leads to a hypersensitive response (HR) in Nicotiana leaves (Liebrand et al., 2013; Ma et al., 2012). Co-expression of RiNLE1 together with AVR4 and Cf-4 in Nicotiana leaves did not lead to a strong HR, whereas co-expression of GFP as negative control did show a clear HR response (Fig.4c, d). This result supports a role for RiNLE1 in modulation of immune responses.

RiNLE1 interacts with Medicago Histone 2B

Because RiNLE1 can localize to the host nucleus and suppress defense-related gene expression, we reasoned that it does so by interacting with host proteins. To identify potential host targets we performed a co-immunoprecipitation (Co-IP) experiment coupled with liquid chromatography tandem-mass spectrometry (LC-MS/MS). Flag-tagged RiNLE1 was expressed from the arbuscule-containing cell specific MtPT4 promotor in Medicago hairy roots. Five weeks after inoculation with *R. irregularis*, we immuno-precipitated Flag-tagged RiNLE1 and its potential plant interactors using anti-Flag magnetic beads (Fig. S6). LC-MS/MS identified several proteins, including Histone 2B (H2B) to potentially interact with RiNLE1 (Table S8).

To confirm the mass-spectroscopy data, we performed an independent co-IP experiment by expressing Flag-tagged RiNLE1 together with the putative interactors in Nicotiana leaves. MtH2B.1 (H2B.1; Medtr4g064020) was chosen because it is highly expressed in arbus-

cule-containing cells. A nuclear-targeted *MtSPX3* (Medtr0262s0060 (Young et al., 2011)-Flag fusion protein and free GFP were used as negative controls. Western blot analyses confirmed the interaction of MtH2B.1 with RiNLE1 (Fig. 5a). Furthermore, GFP-RiNLE1 (no SP) and H2B-mCherry co-localized in the nucleus and nucleolus *N. benthamiana* leaves (Fig. S7b, c, d). Additionally, yeast-two hybrid analyses also confirmed the interaction of RiNLE1 with MtH2B.1 using RiNLE1 as bait, MtH2B.1 as prey (Fig. 5b). In subsequent independent co-IP experiments the interaction of RiNLE1 with the other 4 proteins (Med36a, H1, Dynamin1, API5; Table S8) enriched in the LC-MS/MS data could not be confirmed (data not shown).

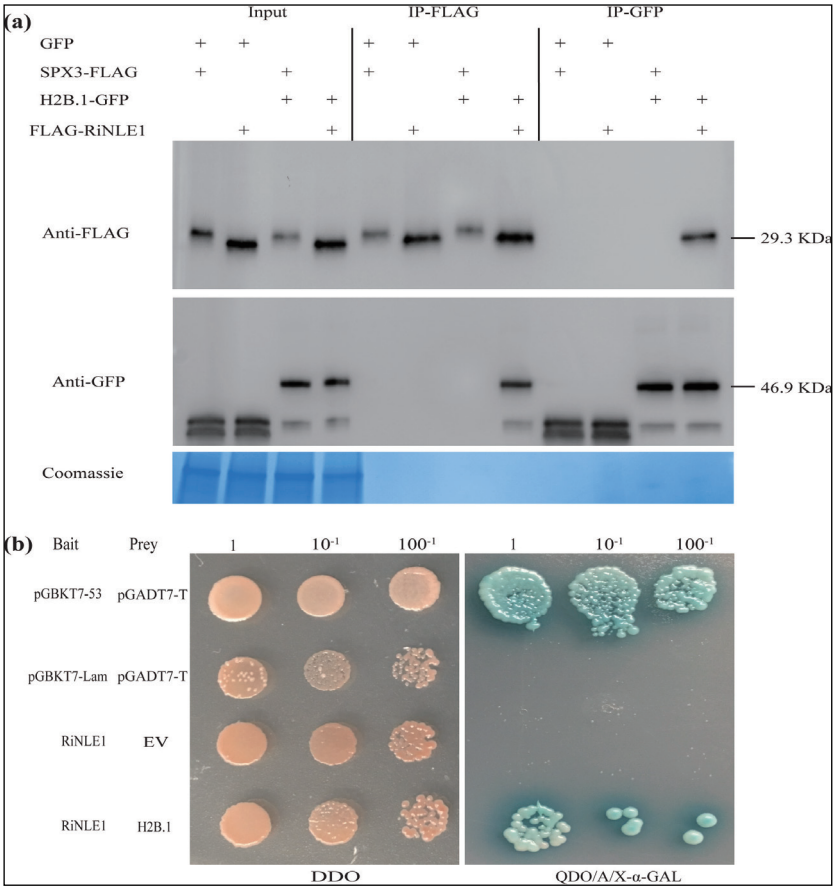

Fig. 5 RiNLE1 interacts with H2B. (a) Co-IP assay in transiently transformed *Nicotiana benthamiana* leaves confirmed the interaction between RiNLE1 and MtH2B.1 (Medtr4g064020). Free GFP and a Flag-tagged nuclear-localizing protein MtSPX3 (Medtr0262s0060) were included as controls. For the input blots, 0.2% input extract was loaded to detect FLAG- and GFP-tagged proteins using anti-Flag or anti-GFP antibodies respectively. After co-immunoprecipitation, 20% of the eluate was loaded for detection. Total protein levels were detected using Coomassie brilliant blue staining as loading control. (b) Y2H assay showing an interaction between RiNLE1 and MtH2B.1, using RiNLE1 as bait (pGBKT7) and H2B.1 as prey (pGADT7). Serial dilutions of overnight mated yeast cultures were plated on selective media. DDO was used as control plate to show mating was successful. Selection was done on QDO plates containing aureobasidin and LacZ staining as additional selection markers. The positive (pGBKT7_53 + pGADT7_T), negative (pGBKT7_lam + pGADT7_T), and EV (GBKT7_RiNLE1 + pGADT7) controls are shown.

RiNLE1 interferes with H2B mono-ubiquitination

The interaction studies raised the question how RiNLE1 can influence defense gene expression by interacting with H2B. H2B is a core component of nucleosomes and H2B modifications have been shown to regulate multiple processes from plant development to response to environmental stress (Zhao et al., 2019; Cao et al., 2015; Fleury et al., 2007). Most notably, several studies have reported a link between H2B mono-ubiquitination and plant immune responses (Dhawan et al., 2009; Zou et al., 2014; Zhang et al., 2015b). Therefore, we hypothesized that RiNLE1 may influence the mono-ubiquitination of H2B.

To assess the effect of RiNLE1 on H2B ubiquitination (H2Bub), we isolated nuclear proteins from DEX-induced *RiNLE1* overexpression roots and empty vector control roots. The levels of H2Bub were analysed by Western blot using an anti-H2Bub antibody, which detects a conserved mono-ubiquitinated lysine at the C-terminal domain of H2B. The specificity of this antibody has been well tested in Arabidopsis (Chen et al., 2017; Zou et al., 2014). As reference, an antibody against Histone 3 was used. Three independent experiments showed that the H2Bub levels were significantly reduced when RiNLE1 expression was induced (Fig. 6a). Quantification showed a ~40 % reduction in H2Bub levels in RiNLE1 induced samples (Fig. 6b). This indicates that RiNLE1 can inhibit H2B mono-ubiquitination in the plant.

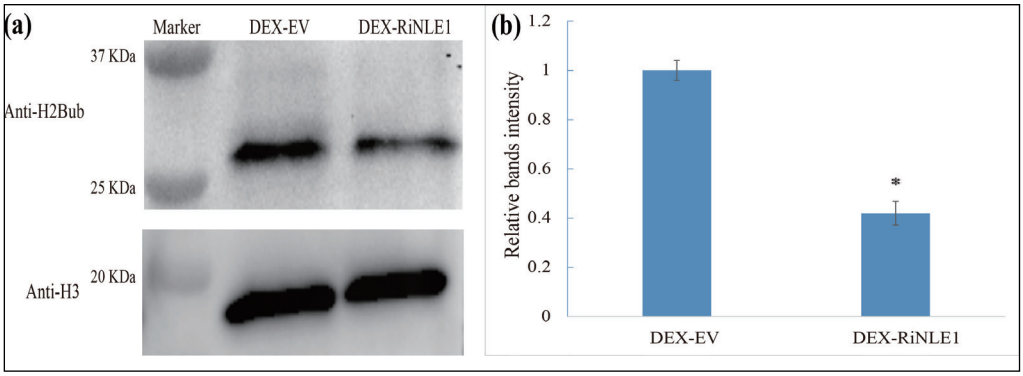

Fig. 6 RiNLE1 inhibits H2B mono-ubiquitination levels. (a) Western blot analysis of nuclear protein extracts from 20 h DEX-induced EV and *RiNLE1 Medicago truncatula* roots. Detection was using anti-H2Bub (top panel) or anti-H3 antibody (bottom panel). The expected sizes of H2Bub and H3 are 28 KDa and 17 KDa, respectively. Similar results were obtained in three independent experiments. (b) Quantification of the relative band intensities using imageJ based on the three independent experiments, including the one shown in (a), normalized to H3 levels. Error bars indicate SD from the three replicates. Student's t test was used. *P < 0.05.

H2Bub levels influence defense gene expression and arbuscular mycorrhization

To further establish that the downregulation of defense-related genes is associated with H2Bub levels, we replaced the H2B predicted mono-ubiquitination site K144 (Lysine) to A (alanine), to prevent it from becoming ubiquitinated. We then applied the DEX-inducible system to induce the expression of this modified *H2BK144A* in Medicago hairy roots and monitored if its overexpression would affect RiNLE1-responsive defense gene expression. DEX-induced wild type H2B expressing roots were used as control. *H2BK144A* expression

was significantly induced 20 hours after treatment with 10 µM DEX (Fig. S7a). Western blot analyses of nuclear protein extracts showed that the H2BK144A samples had significantly lower H2Bub levels compared to the empty vector control (Fig. 7a). Next, we determined the expression level of RiNLE1-responsive genes upon suppression of H2Bub levels. 5 of them showed significantly lower expression (Fig. 7b). The others are not different. This showed that the expression of the genes was suppressed upon inducible overexpression of *H2BK144A* (Fig. 7b). These data indicate that RiNLE1 can inhibit H2B mono-ubiquitination which in turn hampers the induction of a set of defense-associated genes in arbuscule-containing cells.

To determine whether increased H2Bub levels negatively affect mycorrhization, we overexpressed the RING E3 ligase H2B monoubiquitination1 (HUB1) enzyme responsible for H2B ubiquitination (Liu et al., 2007). First, we confirmed that DEX-inducible overexpression of the Medicago *MtHUB1* (Medtr7g046250) ortholog indeed leads to higher H2Bub levels in Medicago roots (Fig. 7a). Next, we monitored the expression of 10 selected defense genes in response to MtHUB1 overexpression by qPCR. The expression of 4 defense genes significantly increased in DEX-induced MtHUB1 roots compared to empty vector (EV) controls. The expression of 2 showed more complex regulation (Fig. 7e). These data indicate that increased H2Bub levels do affect the expression of RiNLE1-responsive defense-related genes.

To study the effect of *MtHUB1* overexpression on mycorrhization, we expressed *MtHUB1* under the control of the arbuscule-containing cell-specific *MtPT4* promoter in Medicago roots. Three weeks after inoculation the level of mycorrhizal colonization was scored using the intersect method (McGONIGLE et al., 1990). Compared to EV control samples, both colonization level and arbuscule abundance were significantly ($N=8$, $P<0.05$) reduced in *PT4p::MtHUB1* overexpression samples. Similar phenotypes were observed in two independent experiments (Fig. 7c). qPCR analyses confirmed the phenotype, using *RiEF* as a marker to represent fungal colonization level and *MtPT4* as marker for arbuscule abundance (Fig. 7d).

Discussion

Here we show that the arbuscule-specific effector RiNLE1 can translocate to the host nucleus where it interacts with H2B and can prevent H2B mono-ubiquitination to suppress defense gene activation and promote arbuscular mycorrhizal colonization.

Our results suggest that GFP-tagged RiNLE1 can translocate to the plant nucleus without the help of other fungal proteins. How effectors in general can translocate into host cells is still an unresolved issue and remains an interesting yet challenging topic to study (Petre and Kamoun, 2014). Irrefutable evidence will require the availability of a specific antibody against RiNLE1, which we unfortunately were not able to generate. In the host nucleus RiNLE1 accumulated in nuclear bodies, especially the nucleolus (Fig. 1e-h, Fig. S1b). Nuclear bodies are related to the formation of ribonucleoprotein complexes, processing of RNA and epigenetic regulation of gene expression (Shaw and Brown, 2004; Mao et al., 2011). Although we cannot rule out that RiNLE1 exerts its function specifically in these nuclear bodies, the observed accumulation could also be an artifact of overexpression.

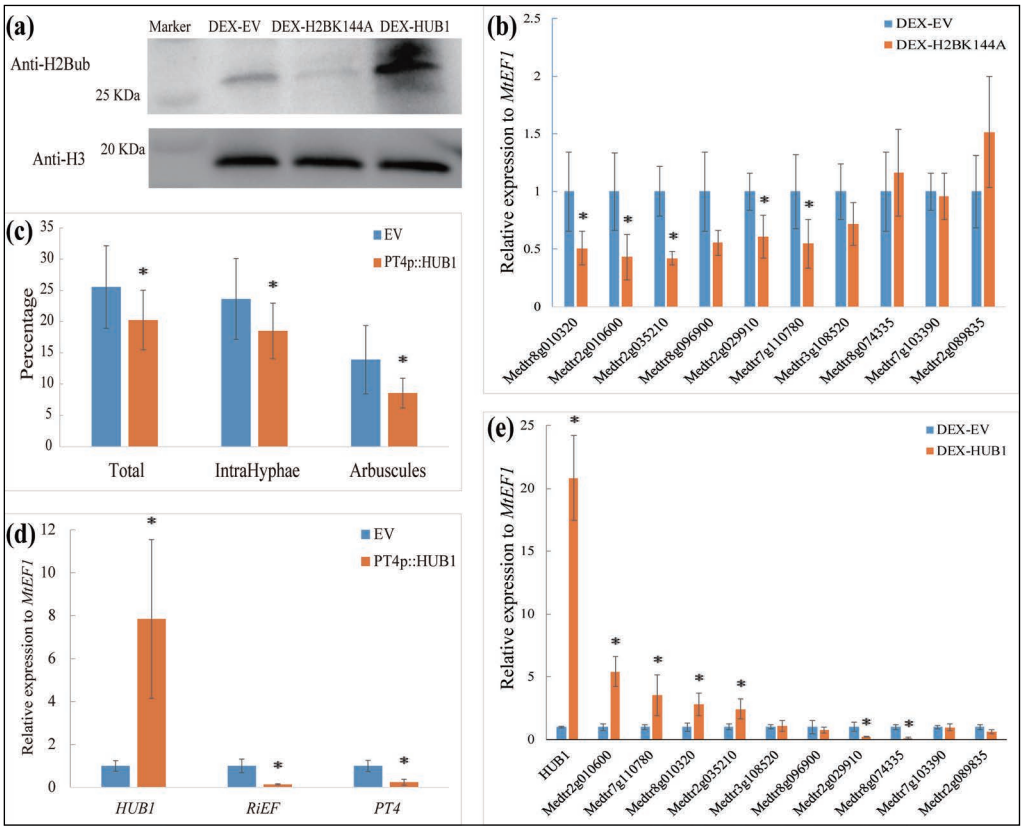

Fig. 7 H2Bub levels influence defense gene expression and arbuscular mycorrhization. (a) Western blot analysis of nuclear protein extracts from 20h DEX-induced EV, *MtH2BK144A* and *MtHUB1* expressing Medicago roots. Detection using anti-H2Bub (top panel) and anti-H3 antibody (bottom panel). (b) qPCR analysis of selected defense-related genes in DEX-induced *H2BK144A* roots compared to EV induced roots. *MtEF1* was used as reference gene. Medtr8g010320: Defensin related, Medtr2g010600: Catabolite activator protein (CAP), Medtr2g035210: ABA-responsive protein, Medtr8g096900: pathogenesis-related thaumatin family protein, Medtr2g029910: peroxidase family protein, Medtr7g110780: Chitinase, Medtr3g108520: gibberellin 2-beta-dioxygenase, Medtr8g074335: Chitinase (Class Ib) / Hevein, Medtr7g103390: Myb/SANT-like DNA-binding domain protein, Medtr2g089835: wound-responsive family protein. Error bars indicate SD from 3 replicates. (c) Quantification of mycorrhization in 8 independently transformed *M. truncatula* roots expressing *PT4p::MtHUB1* and 8 EV transformed roots as control 3 weeks post inoculation with *Rhizophagus irregularis* using the intersect method. Student's t test was used. *P < 0.05. Data are represented as mean ± SD. (d) qPCR analyses of *MtHUB1*, *RiEF* and *MtPT4* in *PT4p::MtHUB1* expressing and EV. *MtEF1* was used as reference. Data are represented as mean ± SD of 8 biological replicates. Student's t test. *, P < 0.05. (e) qRT-PCR analysis of defense-related gene expression from DEX-induced *MtHUB1* samples compared to DEX-induced EV samples. *MtEF1* was used as reference. Data are represented as mean ± SD of 3 biological replicates. Student's t test was used. *P < 0.05.

Like GFP-RiNLE1, H2B-GFP also accumulated in the nucleolus when we expressed it in Nicotiana leaves under the control of a strong constitutive promoter (Fig. S7b, c). Similar observations have been made for GFP-tagged H2B in other systems. Musinova et al. (2011) identified a nucleolar localization/retention signal (NoRS) in the H2B protein, enabling it to exchange between the nucleolus and nucleoplasm in human cell lines. A potential NoRS enriched with basic amino acids can also be found in RiNLE1 (KKKGKKGKPKRKH), which may cause the non-specific retention in the nucleolus especially when expressed under a strong promoter (Musinova et al., 2011).

We observed a downregulation of a subset of defense-related genes upon overexpression of both *RiNLE1* and a non-mono-ubiquitinated *H2B* form in Medicago roots. Arbuscule abundance was not affected upon *RiNLE1* overexpression, which is likely due to the high endogenous expression levels of RiNLE1 specifically in the arbuscules. This may limit an effect of additional expression of *RiNLE1* in these cells by the *LjUbiquitin* promoter. Vice versa, overexpression of MtHUB1 caused increased H2Bub levels and increased expression of RiNLE1-regulated defense-related genes, which correlated with lower AM colonization levels. Similar observations linking H2B mono-ubiquitination to defense have been reported in relation to pathogenic interactions. For example, in Arabidopsis H2B mono-ubiquitination has been shown to be required for transcriptional activation of resistance (R) genes *SNC1* and *RPP4*, involved in the resistance to necrotrophic fungal pathogens (Zou et al., 2014). Overexpression of *HUB1* led to resistance, while *hub1* loss-of-function mutants showed increased susceptibility to these fungi (Dhawan et al., 2009; Zou et al., 2014). Increased H2Bub levels also caused increased resistance against *Botrytis cinerea* by balancing the SA- and JA/ET- mediated signalling pathways in tomato (Zhang et al., 2015b). How H2B mono-ubiquitination or RiNLE1 affect specific genes is currently not known. The binding of RiNLE1 to H2B may obstruct the accessibility of HUB1 to mono-ubiquitinate H2B.

H2Bub has also been shown to be involved in histone-crosstalk, mediating for example the methylation of H3 (Sun and Allis, 2002; Zhao et al., 2019). Arabidopsis *hub1* and *hub2* mutants show reduced H3 methylation levels at several gene loci that regulate plant flowering time, indicating that H2Bub can enhance H3 methylation (Cao et al., 2008). Interestingly, in *hub1* mutants the H3K4me2 levels were also reduced at the R gene *SNC1* locus, suggesting that H2Bub-mediated H3 methylation also regulates defense responses (Lee et al., 2016). Therefore it would be interesting to follow-up whether RiNLE1 similarly affects other histone modifications in arbuscule-containing cells and whether it affects other genes that may be important for the symbiosis. Furthermore, beside mono-ubiquitination various other post-translation H2B modifications have been reported to affect gene expression that could be influenced by RiNLE1, but most of these are not yet well studied in plants.

To our knowledge this is the first example of a fungal effector directly targeting a core nucleosome histone protein, H2B, to control epigenetic modifications. So far, pathogenic effectors that affect histone modifications have been found to operate through their interaction with histone modifying enzymes (Ramirez-Prado et al., 2018; Kong et al., 2017; Li et al., 2018; Ransom and Walton, 1997; Walley et al., 2008). Whether RiNLE1 can also affect other post-translational H2B modifications remains to be studied. The other known example of a pathogen directly targeting a histone protein is the 6b oncoprotein encoded in the T-DNA of *Agrobacterium tumefaciens*. This protein was shown to act as a histone chaperone, interacting specifically with Histone 3 to control cell divisions (Terakura et al., 2007).

Interestingly, we found that in addition to being conserved in AM fungi, RiNLE1-like effectors occur in a variety of (biotrophic) pathogenic and mutualistic fungal species. This suggests that H2B may be a common target for such fungal effector proteins. The occurrence of a RiNLE1-type effector in the water mold parasitic fungus *Rozella allomycis* (Fig. S2; Table S3), which intracellularly colonizes Allomyces species, suggests that NLE1-type effectors may even reflect a broader fungal strategy to colonize other hosts (James et al., 2013; Gan et al., 2019).

It has become clear that interference with the chromatin organization of plants is a common strategy used by pathogenic microbes to subvert the host immune system (Ramirez-Prado et al., 2018). Our finding that also mutualistic AM fungi use effector proteins to modify the plants epigenome further supports the idea that pathogenic and mutualistic microbes use comparable strategies to interact with their plant hosts. We envision that more studies on the epigenomic reprogramming that occurs during the AM symbiosis will be a promising avenue to understand this fundamental symbiosis in plants.

Acknowledgements

The authors declare no conflict of interest. P.W. is supported by the China Scholarship Council (CSC) grant: 201606310038. Agrobacterium strains containing expression constructs for *SlCf-4* and *CfAVR-4* were kindly provided by dr. Matthieu Joosten (Laboratory of Phytopathology, Wageningen University & Research).

Supplementary figures

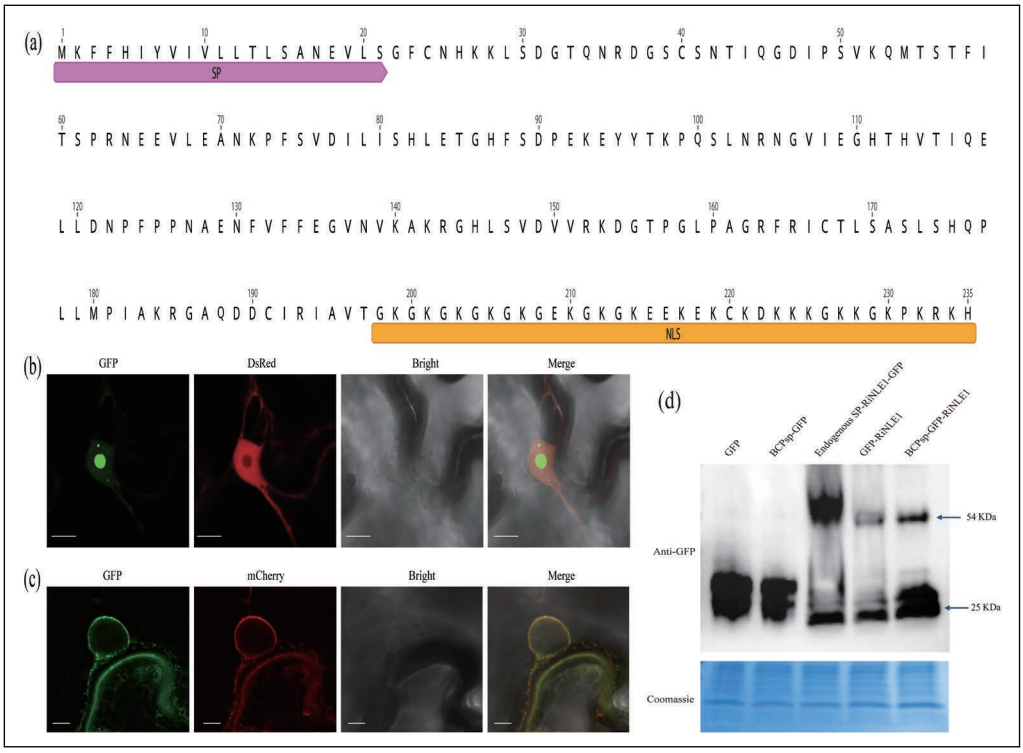

Fig. S1 RiNLE1 information. (a) RiNLE1 amino acid sequence. SP: signal peptide, NLS: nuclear localization signal. (b) Confocal images of GFP-RiNLE1(no SP) expressed from a constitutive Ubiquitin promoter in *Nicotiana benthamiana* leaves localizing to the nucleus and accumulating in the nucleolus and other nuclear bodies. A co-expressed *UBp::DsRed* as marker of nucleus (but not nucleolus) and cytoplasm. Scale bar = 10 μm. (c) Confocal image of RiNLE1-GFP with endogenous SP expressed from a constitutive Ubiquitin promoter in *N. benthamiana* leaves. Full length RiNLE1-GFP accumulates in the endoplasmic reticulum (ER). A co-expressed *Act2p::SP-mCherry-KDEL* as marker of ER. Scale bar = 5 μm. (d) Anti-GFP western blot confirming the expression of RiNLE1 fusion proteins in Nicotiana leaves. The slightly larger size of RiNLE1 expressed with endogenous SP indicates the failure of SP cleavage in *N. benthamiana* leaves. Total protein levels were detected using Coomassie brilliant blue staining as loading control.

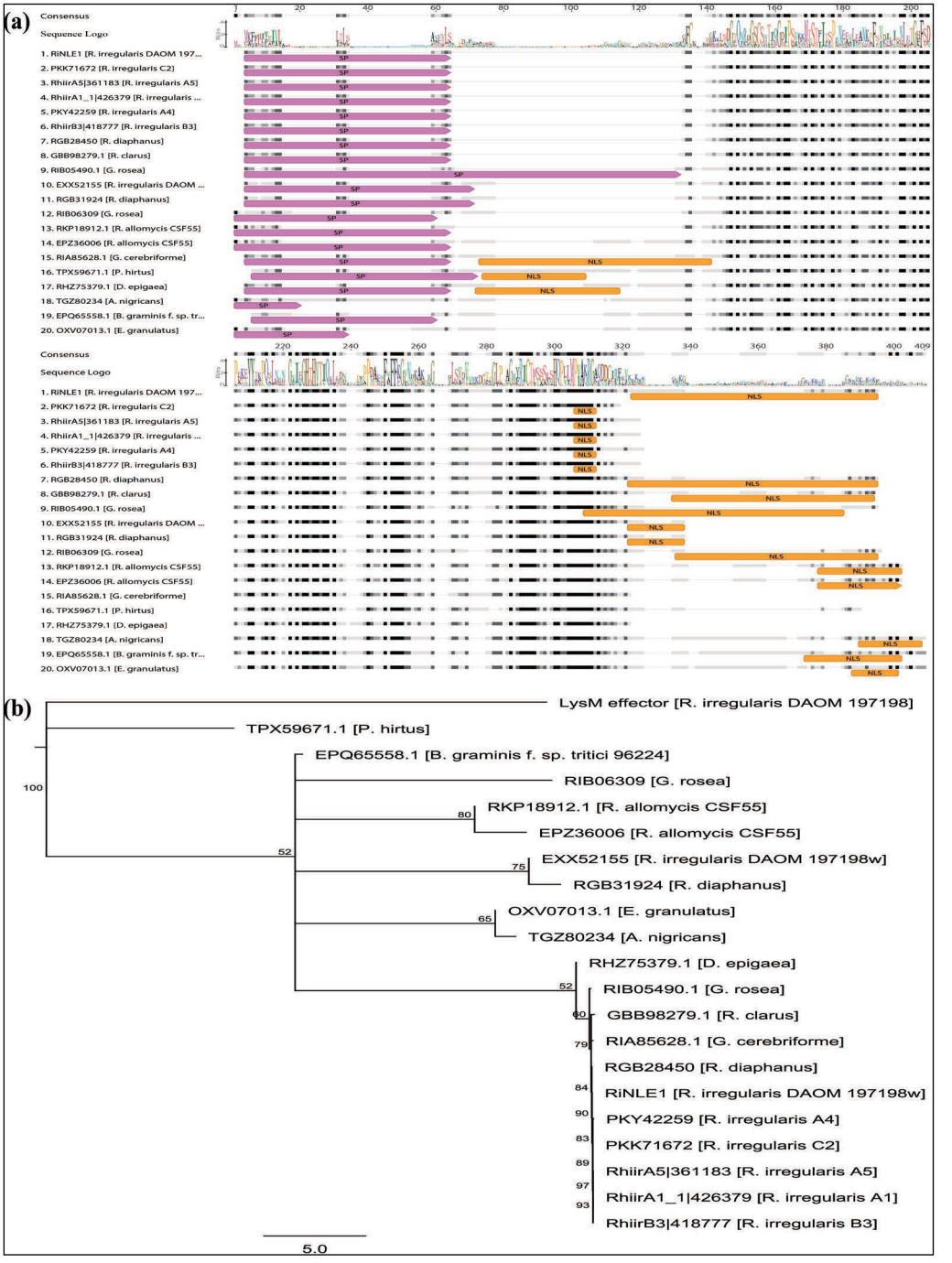

Fig. S2 RiNLE1-like proteins occur in a variety of fungal species. (a) RiNLE1-like effectors from different fungal species were aligned using MAFFT in Geneious R11.0 (https://www.geneious.com). SP (signal peptide) is annotated with a red bar. NLS (nuclear localization signal) is indicated by an orange bar. (B) Phylogenetic tree of RiNLE1-like proteins generated using the neighbour-joining tree builder in Geneious R11.0 (https://www.geneious.com). The *R. irregularis* LysM effector was used as outgroup, 1000 bootstraps were used.

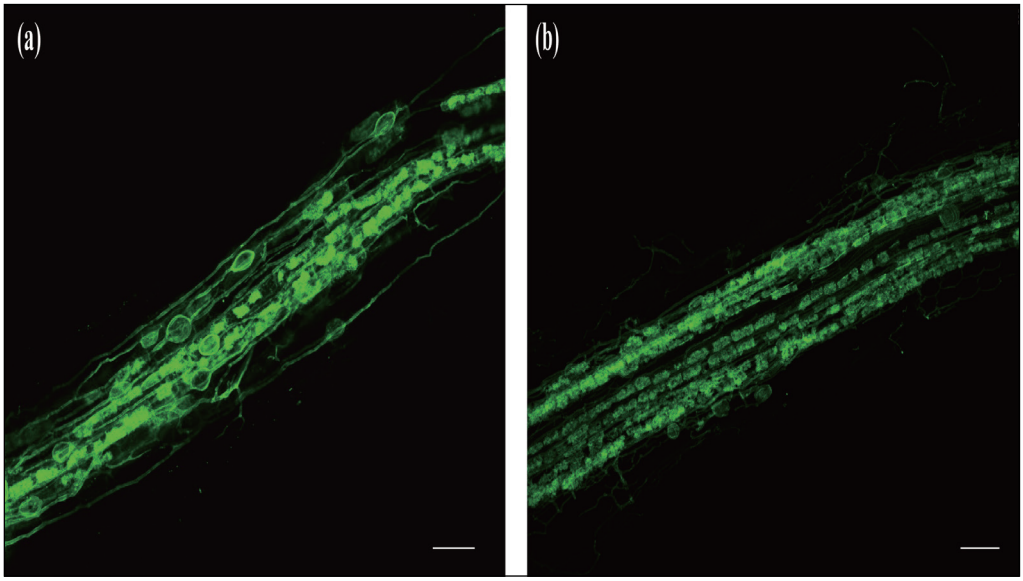

Fig. S3 Overexpression of RiNLE1 enhances AMF colonization. (a) Confocal picture of WGA-alexa488 stained empty vector transformed roots. Scale bar = 100 µm. (b) Confocal picture of WGA-alexa488 stained *UBp::RiNLE1* transgenic roots. Scale bar = 100 µm.

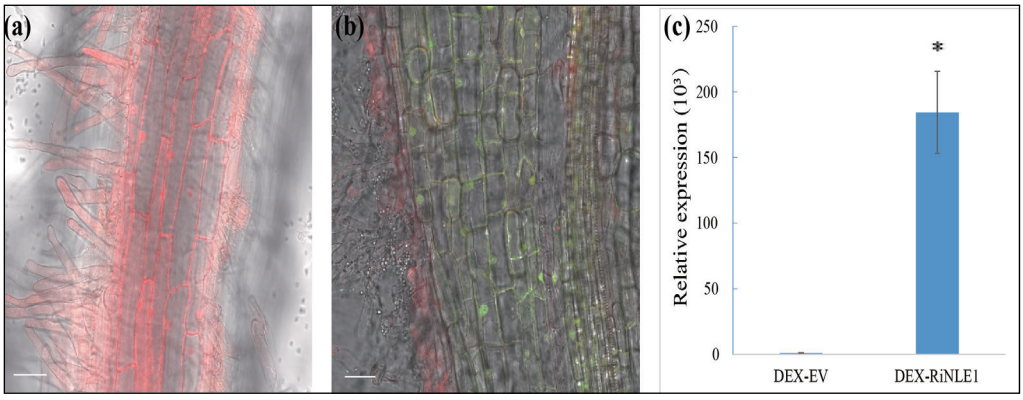

Fig. S4 Dexamethasone induction of RiNLE1 expression. (a) Confocal microscopy of *Medicago truncatula* transgenic roots containing the *UBp::GVG-UBp::DsRed-UASp::RiNLE1-UASp::GFP* construct 20 hours after treatment with DMSO. Picture is overlay of GFP, DsRed and bright field channels. Scale bar = 50µm. (b) Confocal microscopy of Medicago transgenic roots containing the *UBp::GVG-UBp::DsRed-UASp::RiNLE1-UASp::GFP* construct 20 hours after treatment with 10 µM DEX. Picture is overlay of GFP, DsRed and bright channels. Scale bar = 50 µm. (c) qRT-PCR analysis of RiNLE1 expression in DEX-induced roots compared to EV roots. MtEF1 was used as reference gene. Data are represented as mean ± SD of 3 biological replicates. Student's t test *P < 0.05.

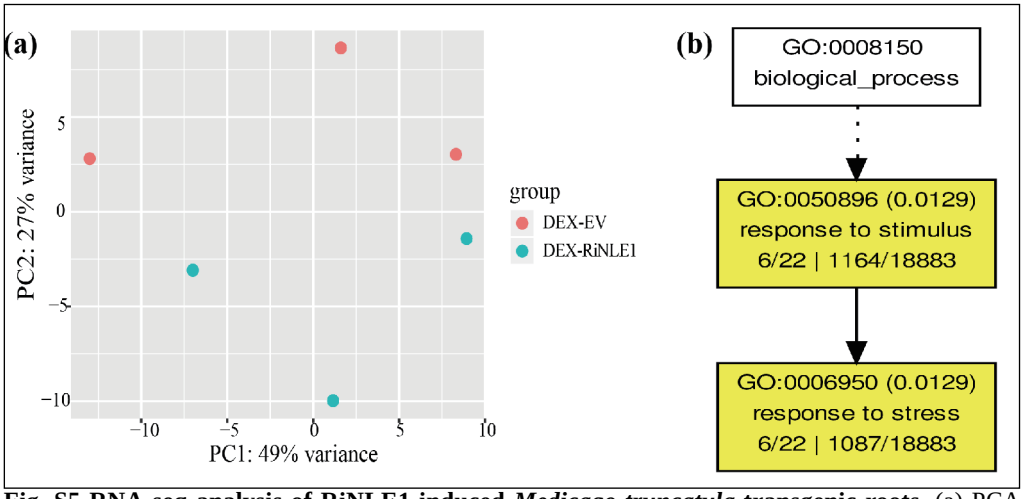

Fig. S5 RNA-seq analysis of RiNLE1 induced *Medicago truncatula* transgenic roots. (a) PCA plot analysis of the RNAseq data from 20h DEX-induced RiNLE1 and EV roots. Plot was generated using CLC genomics workbench 10.0.1 (Qiagen). (b) GO enrichment analysis for genes inhibited by RiNLE1 using agriGO v2.0. 6/22 means 6 of the 22 annotated genes are enriched for the GO term. 1164/18883 means 1164 genes associated with this GO term out of 18883 total annotated genes.

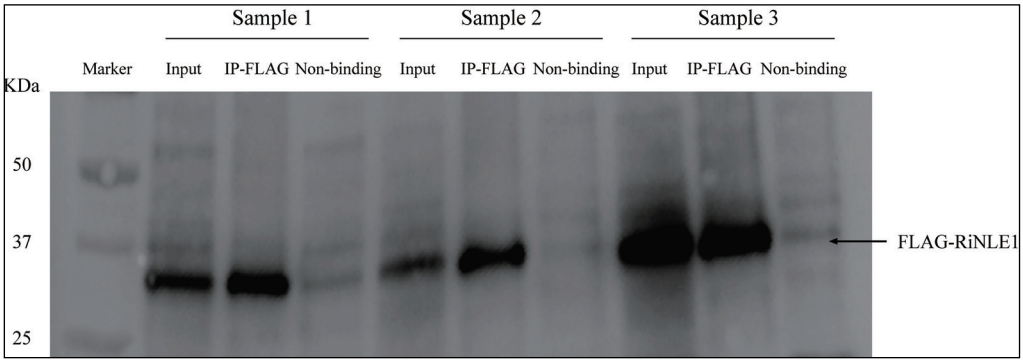

Fig. S6 Anti-FLAG western blot confirming the expression of FLAG-RiNLE1 fusion protein in *Medicago truncatula* roots and anti-FLAG immunoprecipitation. Equal amounts of input and non-bound protein fractions are loaded for each sample. For the IP-FLAG lanes 5 µl of each total 100 µl IP volume were loaded. The expected size of FLAG-RiNLE1 is ~30 KDa.

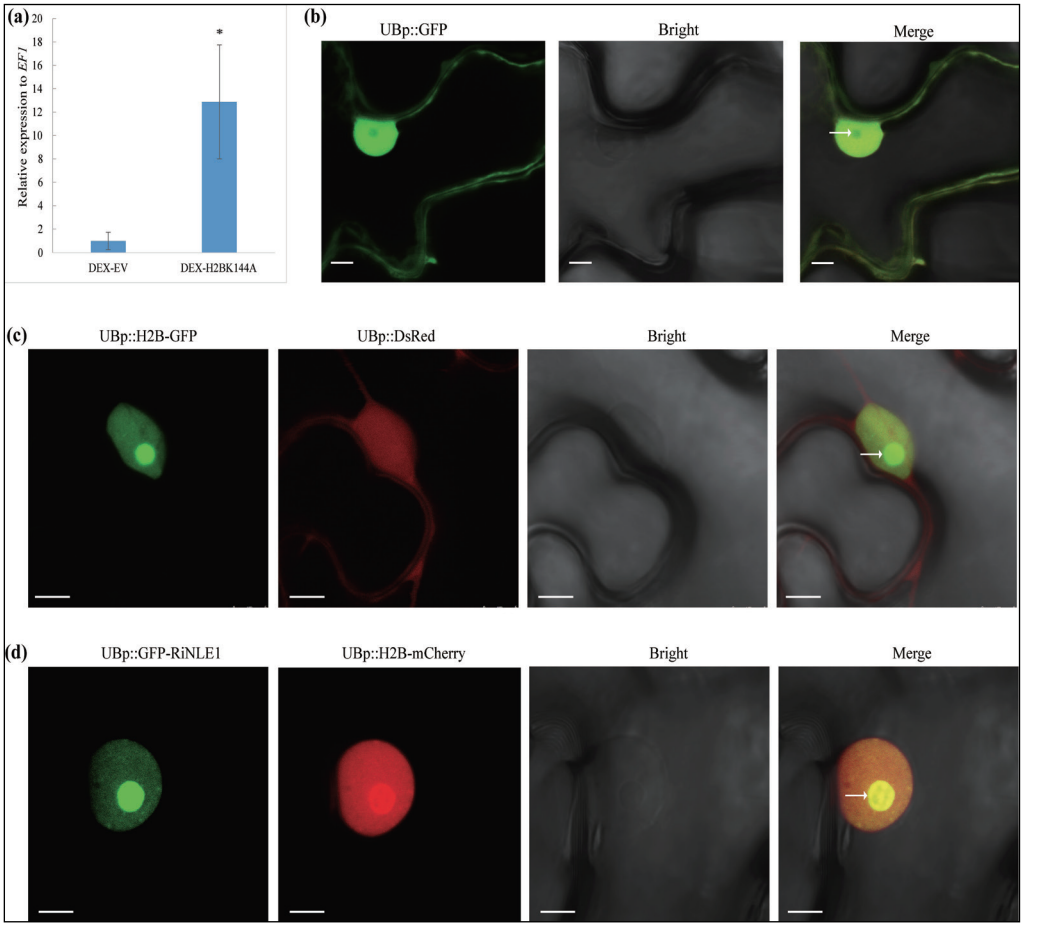

Fig. S7 Dexamethasone induction of modified H2B expression and H2B localization in *Nicotiana benthamiana* leaves. (a) qRT-PCR analysis of DEX-induced *H2BK144A* expression as compared to DEX-induced EV samples. Data are represented as mean ± SD of 3 biological replicates. Student's t test was used. *P < 0.05. (b) Confocal images of free GFP localizing to the nucleus and cytoplasm when expressed from a constitutive Ubiquitin promoter in *N. benthamiana* leaves as control. (c) Confocal images of H2B-GFP fusion protein localizing to the nucleus and accumulating in the nucleolus when expressed from a Ubiquitin promoter in *N. benthamiana* leaves. Co-expressed DsRed as marker of nucleus and cytoplasm. (d) Confocal images of GFP-RiNLE1 and H2B-mCherry colocalizing to the nucleus and accumulating in the nucleolus when expressed from a Ubiquitin promoter in *N. benthamiana* leaves. (b, c, d) Arrow points to nucleolus, scale bar = 5 μm.

Supplementary tables

Supplementary tables listed below can be downloaded from the ***New Phytologist*** website: https://doi.org/10.1111/nph.17236

Table S1 Primers list used in this work.

Table S2 Constructs made using golden gate system.

Table S3 RiNLE1 homologs from fungal species based on protein BLAST using NCBI and JGI MycoCosm databases.

Table S4 RNA-seq data Mapping statistics generated using CLC genomics workbench 10.0.1 (Qiagen).

Table S5 Expression browser of DEX-EV and DEX-RiNLE1 RNA-seq data. TPM = transcripts per million.

Table S6 RNA-seq expression data of gene down-regulated upon *RiNLE1* induction. Expression levels are the average of 3 replicates, each representing a pool of 2-3 independently transformed roots. A cut-off fold change > 2, and $P < 0.05$ was used. TPM= transcripts per million.

Table S7 Expression of RiNLE1-regulated defense-related gene in arbuscules (ARB) and neighbouring non-colonized cortex cells (HYP) based on Zeng et al. (2018). TPM = transcripts per million.

Table S8 LC-MS/MS identified peptides intensity information for FLAG-RiNLE1 Co-immunoprecipitation. LFQ (label-free quantification).

Chapter 3

A host-dependent, potential glycan binding effector of *Rhizophagus irregularis* controls host immune responses

Peng Wang[a], Jelle van Creij[a], Nick Snelders[b], Stephan Wawra[c], Willy van den Berg[d], Ton Bisseling[a], Erik Limpens[a] *

[a] Laboratory of Molecular Biology, Wageningen University & Research, 6708 PB Wageningen, the Netherlands

[b] Laboratory of Phytopathology, Wageningen University and Research, Wageningen, the Netherlands

[c] Botanical Institute, Cluster of Excellence on Plant Sciences (CEPLAS), Cologne Biocenter, University of Cologne, Cologne 50674, Germany

[d] Laboratory of Biochemistry, Wageningen University & Research, Wageningen 6708 WE, the Netherlands

* To whom correspondence should be addressed. Email: erik.limpens@wur.nl

Abstract

Arbuscular mycorrhizal (AM) fungi can form an endosymbiotic association with almost all land plants. Although there is very little host-specificity in this interaction, host preferences for distinct fungi have been reported under natural conditions and substantial variation in the mycorrhizal growth response of different hos-fungus combination has been found. The molecular basis for such host-dependent effects are still largely unknown. It has been hypothesized that variation in host immune responses may play an important role. Here we characterized a host-dependent effector from *Rhizophagus irregularis* DAOM197198 that is specifically highly induced upon symbiosis with *Allium schoenoprasum* (chives) The effector is part of a small gene family that show homology to the *Piriformospora indica* fungal β-glucan-binding lectin FGB1, and was therefore named RiFGB1. We show that RiFGB1 can bind glycans such as β-glucan, chitin and xylan. It is also able to interfere with a wide range of microbe-associated molecular pattern (MAMP) induced defense responses and facilitates AM colonization. Intriguingly, variation in expression of RiFGB1 homologs in different *R. irregularis* isolates correlates a reduced ability of the C3 isolate to colonize chives. Our results support a role for fungal effectors in the regulation of host preference.

Introduction

AM fungi, belonging to the Glomeromycotina subphylum, are able to intracellularly colonize and establish a symbiotic association with the roots of most land plants (Smith and Read, 2008). Upon a molecular dialogue the plant facilitates the colonization process leading to the accommodation of highly branched fungal hyphae as arbuscules inside root inner cortex cells (Gutjahr and Parniske, 2013). There, the fungus provides the plant host with mineral nutrients, such as phosphate and ammonium, in return for plant-derived carbon sources (Luginbuehl and Oldroyd, 2017; Wang et al., 2017). In general it is thought that there is no, to very little, host-specificity in this interaction (van der Heijden et al., 2015; Zeng et al., 2018). However, under natural conditions plant species seem to associate preferentially with distinct AM fungi. For example, different grass species co-occurring in the same field were found to be colonized by distinct AM fungi and six plant species in semi-arid Mediterranean prairies were found to host different AM fungi communities (Vandenkoornhuyse et al., 2003; Torrecillas et al., 2012). Furthermore, different isolates of *Glomus intraradices* showed significant preferences to different plant species (*Glycine max, Helianthus annuus* and *Allium porrum*) (Croll et al., 2008). What determines these so-called host preferences is largely unknown.

To be able to intimately interact with such an extremely broad range of host plants AM fungi, like *Rhizophagus irregularis*, must have very efficient mechanisms to deal with the host immune system in such wide variety of hosts. Similar to pathogenic fungi, the cell walls of AM fungi consist for example of chitin and β-glucans, which are potent triggers of plant immune responses (Lo Presti et al., 2015; Wawra et al., 2016; Zeng et al., 2020). Although not common, host preferences have been reported (Vandenkoornhuyse et al., 2003; Torrecillas et al., 2012; van der Heijden et al., 2015). Variation in the ability to subvert the plant immune system may contribute to the observed host-preferential associations. Although it is not fully understood how AM fungi manage to subvert the host immune system in such a

wide variety of plants, it has become clear that small secreted effector proteins should play a key role (Lo Presti et al., 2015). Effector proteins are best studied in pathogenic plant-fungus interactions (Lo Presti et al., 2015). Effectors can for example bind microbe-associated molecular pattern (MAMP) molecules to prevent the fungus from being detected by plant immune receptors; manipulate immune receptor function or can reprogram host gene expression by translocating into plant cells (Walley et al., 2008; Kong et al., 2017; Li et al., 2018). In case of AM fungi, several effector proteins have been reported to influence the colonization efficiency (Kloppholz et al., 2011; Tsuzuki et al., 2016; Voß et al., 2018; van Creij et al., 2020; Zeng et al., 2020). However, for only a few of these insight into their molecular function has been obtained. One of these is RiSP7, which was the first effector from *R. irregularis* to be studied. RiSP7 was shown to translocate the host plant nucleus where it could interact with the pathogenesis-related transcription factor ERF19 to promote colonization (Kloppholz et al., 2011). In Chapter 2 we identified another translocated effector, RiNLE1, which is able to interact with host Histone 2B and interfere with its mono-ubiquitination to suppress defense responses. Furthermore, we recently identified an apoplastic lysin motif containing effector, RiSLM1, that is able to bind chitin molecules and subvert chitin-triggered immunity to facilitate AM symbiosis (Zeng et al., 2020).

Interestingly, genome-wide transcriptome analyses revealed that the model AM fungus *R. irregularis* DAOM197198 can adjust its secretome in a host- and stage-dependent manner (Kamel et al., 2017; Zeng et al., 2018). Although many putative effector-encoding genes are more or less equally expressed in different host plants, several putative effectors were identified to be much higher expressed in the interaction with one host plant species compared to others. Host-dependent expression of effector genes has also been reported for other fungi. For example, 16 effectors of the white mold fungus *Sclerotinia sclerotiorum* were differentially expressed in four host plants (Guyon et al., 2014). Also effector genes of the root endophyte *P. indica* showed differential expression patterns in the interaction with barley or Arabidopsis, which correlated with different colonization strategies (Lahrmann et al., 2013). This raises the hypothesis that effector proteins may play a role in determining AM host-preferences found in nature through their effect on the host immune system, host metabolism and/or nutrient exchange (Limpens and Geurts, 2014).

To start to investigate this we focused here on a host-dependent effector of *R. irregularis* that is much higher expressed in the interaction with the monocot *Allium schoenoprasum* (chives), compared to dicots like *Medicago truncatula* (Medicago), *Nicotiana benthamiana* (Zeng et al., 2018). We named this effector RiFGB1 because it show homology to the β-glucan-binding lectin FGB1 effector from the root endophyte *P. indica* which was found to inhibit β-glucan-triggered immunity in plants (Wawra et al., 2016). Our results suggest that RiFGB1 can not only bind β-glucans but also other glycan molecules, like chitin and xylan. Furthermore, we show that RiFGB1 can suppresses β-glucan, chitin and even flg22-triggered defense responses and that it facilitates AM fungal colonization. Intriguingly, we identified a *R. irregularis* C3 isolate that lacks the strong induction of *RiFGB1* homologs in chives, which correlates with a reduced ability of this isolate to efficiently colonize chives.

Materials and methods

Plant and fungal material

Medicago truncatula Jemalong A17 (Medicago) was grown and transformed as described previously (Limpens et al., 2004). Chives (*Allium schoenoprasum*) was grown as described (Zeng et al., 2018). *Rhizophagus irregularis* DAOM197198 spores were obtained from Agronutrion, France. Spores were thoroughly washed through three layers of filter mesh (220 µm, 120 µm, 38 µm) before use. *Rhizophagus irregularis* C3 spores maintained as monoxenic carrot (*Daucus carota*) root culture (Ehinger et al., 2012; Lin et al., 2014). For mycorrhization assays, plants were grown in SC10 RayLeach cone-tainers (Stuewe and Sons, Canada) with premixed sand:clay (1:1 V/V) mixture and spores were inoculated by placing ~200 pores ~2 cm below the seedling roots. Plants were grown in a 16 h daylight chamber at 21℃ and watered by 10 ml ½ Hoagland medium with 20 µM phosphate twice a week for three weeks.

RiFGB1 protein production and purification

The RiFGB1 protein (lacking signal peptide) was produced in *E. coli* ORIGAMI strain using the Champion™ pET SUMO Expression System and in *E. coli* Shuffle strain as described (Lobstein et al., 2012; Zeng et al., 2020). Both of these two strains are capable of forming disulfide bonds in their cytoplasm. Primers with EcoRI and HindIII restriction sites used to clone the *RiFGB1* CDS are listed in table S1. Bacteria containing the protein-producing vector were grown in 1 L of LB medium supplemented with 50 µg/mL kanamycin, 10 mM KH_2PO_4, 50 mM $MgSO_4$ and 1% glycerol until the OD_{600} reached 0.8 at 37 °C. 0.05 mM IPTG was added into the medium and incubated at 37 °C overnight. Bacteria were collected by centrifuging and store at -80 °C until further purification.

Protein purification was done as described (Snelders et al., 2020). The bacterial pellets were disrupted by resuspending in 40 ml lysis buffer (50 mM Tris, 150 mM NaCl, 10% glycerol, 6 mg ml^{-1} lysozyme, 2 mg ml–1 deoxycholic acid, 0.06 mg ml^{-1} DNase I, 1 protease inhibitor cocktail) at 4 °C for 1 h. The lysate was transferred to 50 mL tubes and centrifuged at 15000 g at 4 °C for 1 h. The supernatant was collected and the 6×HIS-SUMO-tagged RiFGB1 protein was purified by passing through a NTA superflow metal affinity chromatography column (Qiagen) packed with 50% His60 Ni^{2+} Superflow Resin (Clontech). The purified effector protein was dialyzed with 250 mM $(NH_4)_2SO_4$, 8.5% glycerol according to Hofmeister series (Zhang and Cremer, 2006) containing ULP-1 protease to remove the 6×HIS-SUMO tag overnight at 4 °C. Then the proteins were further purified by size exclusion chromatography using a Superdex 75PG 26 x 60 on a ÄKTA fast-performance liquid chromatographer (GE healthcare, The Netherlands) using 250 mM $(NH_4)_2SO_4$, 8.5% glycerol (pH 7.4) as elution buffer. The purified protein was concentrated using an Amicon Ultra-15 centrifugal tube (EMD Millipore, The Netherlands) and the concentration was measured using Qubit (Thermo Fisher Scientific).

Binding affinity precipitation assays

Polysaccharide pull-down assays were done as described (Zeng et al., 2020). 10 mg insoluble Curdlan, chitin, chitosan or xylan (Sigma-Aldrich, Houten, the Netherlands) was added to 500 µl 250 mM $(NH_4)_2SO_4$, 8.5% glycerol (pH 7.4) buffer in 1.5 ml Eppendorf tubes.

Subsequently, RiFGB1 was added to a final concentration of 1 µM and incubated at room temperature for 1 h while rotating. The mixture was then centrifuged at 5000 g for 5 min. The supernatant (non-bound fraction) was collected, concentrated to 100 µl and boiled with 100 µl 2x protein SDS loading buffer for 5 min. The polysaccharide pellet (bound fraction) was washed 3 times with 500 µl of the above $(NH_4)_2SO_4$ buffer, resuspended in 100 µl of protein SDS loading buffer and boiled for 5 min. Protein fractions were analyzed by polyacrylamide gel electrophoresis with Coomassie Brilliant Blue R-250 staining.

RiFGB1 overexpression and host-induced gene silencing

For *RiFGB1* overexpression, constructs were made by using the Golden Gate cloning system (Engler et al., 2014). Level 0 modules of the *LjUB1* promotor, *MtBCP1* signal peptide, *RiFGB1* CDS (no signal peptide), and *CaMV35S* terminator were assembled into level 1 position 1 acceptor pICH47732 (*UB1p::BCP1sp-RiFGB1*). The resulting expression construct was then assembled into the level 2 acceptor pAGM4723 together with a level 1 position 2 DsRed marker gene (Jach et al., 2001). The final level 2 construct was transformed into *Medicago truncatula* by hairy root transformation mediated by *Agrobacterium rhizogenes* MSU440 as described (Limpens et al., 2004). Plant growth conditions and spores inoculation were done as described before (Zeng et al., 2020). Transgenic roots were harvested 4 weeks after inoculation with 200 *R. irregularis* spores for quantification and RNA isolation.

For host-induced gene silencing (HIGS), a 261 bp *RiFGB1* CDS fragment was cloned into pENTR™/D-TOPO™. Primers used are listed in Table S1. Next the *RiFGB1* fragment was cloned into the modified pK7GWIWG2 (II)-AtEF1α RR vector (Zeng et al., 2020) using LR clonase II (Invitrogen). Hairy roots transformation and mycorrhizal experiments were done as described above.

Reactive oxygen species (ROS) assay

ROS assay was done as described (Zeng et al., 2020). In brief, Medicago 5 day-old seedlings roots were cut into ~0.5 mm pieces and incubated overnight in 150 µL sterile MQ water in the dark in a 96-well polystyrene plate. 5 root pieces were placed into each well per biological replicate. MQ water was replaced by 100 µL MQ water containing 0.5 mM L-012 and 10 µg/mL horse radish peroxidase (HRP) with 1 µM CO7 (IsoSep), 1 µM Flg22 (GenScript) or 500 µM laminarin (Sigma). To study the role of RiFGB1 on ROS accumulation, 1 µM RiFGB1 protein was mixed with the above chemicals and treated the roots. Chemiluminescence was measured using a microplate luminometer (CLARIOSTAR, USA) for 30 min. 6 biological replicates were used for each treatment.

Defense and symbiotic gene expression analyses

Germinated Medicago seedlings were grown in liquid M medium without sucrose for 5 days as described (Zeng et al., 2020). To test whether the RiFGB1 effector interferes with defense response, 20 µM laminarin in combination with 2 µM RiFGB1 or 100 nM CO7 in combination with 100 nM RiFGB1 were added into the medium. To study whether RiFGB1 interferes with symbiotic signaling, 100 nM CO4 (Megazyme) or 10 nM LCOs (Sigma-Aldrich) was used in combination with 100 nM RiFGB1. After 1 hour incubation, roots were harvested for RNA isolation. Defense response marker genes, *MtPAL* (phenylalanine ammonia lyase), *MtEPI* (NAD-dependent epimerase/dehydratase) and *MtTHA* (thaumatin) and

symbiotic marker genes *MtPUB1* (Vernié et al., 2016), *MtTUBB1* (Lohar et al., 2006) and *MtVAPYRIN* (Pumplin et al., 2010) were analyzed by qPCR to monitor defense or symbiotic responses respectively. For all the analyses, three seedlings were grown together as one replicate, and three replicates were used.

RNA isolation and qPCR

All RNA samples in this study were isolated using a Qiagen plant RNA mini kit following the manufacturer's instructions. cDNA was made using the iScript cDNA synthesis kit (Bio-Rad). qPCR was done using iQ SYBR Green Supermix (Bio-Rad) on a Bio-Rad CFX connect real-time system. Primers used are listed in supplementary table 1. Gene expression was normalized using Medicago *Elongation factor 1* (*EF1*). Relative normalized expression levels were calculated as $2^{-\triangle\triangle ct}$. Three technical replicates were used for each sample.

Mycorrhizal quantification and microscopy

For quantification of AM colonization levels, roots were boiled in 10% (w/v) KOH for 10 min. Then roots were washed three times with PBS buffer (150 mM NaCl, 10 mM Na_2HPO_4, 1.8 mM KH_2PO_4, pH 7.4), and incubated in 0.2 µg/mL WGA-Alexafluor 488 (Molecular Probes) in PBS overnight at 4 °C. The colonization levels and arbuscule abundance were scored and calculated as described (McGONIGLE et al., 1990) using a Leica DM5500 B microscope.

RNA-seq of *R. irregularis*

RNA of ***R. irregularis*** C3 or DAOM197198 colonized *Medicago truncatula* and *Allium schoenoprasum* root samples were isolated as described above. Three independent biological replicates were used per fungus/host combination. RNA samples were sequenced using the BGI SEQ-500 Transcriptome platform (Zhu et al., 2018). DAOM197198 reads were mapped to the Rir17 assembly (Maeda et al., 2018) while C3 reads were mapped to the RirC3 assembly (van Creij unpublished). Mapping was performed with Hisat2 using the --dta option, and transcriptomes were assembled using Stringtie (Pertea et al., 2015; Kim et al., 2019). Differential expression was analyzed with DeSeq2 (Kim et al., 2019), with genes being considered as host-specific if fold-change was at least 4x higher than in other hosts (Masclaux et al., 2019).

Results

RiFGB1 is a host-dependent effector

To investigate the role of host-dependent effector proteins, we focused here on the putative RirG091260 (RiFGB1, see below) effector from *R. irregularis* DAOM197198, which we previously found to be differentially expressed between chives and dicot hosts like *Medicago* or *Nicotiana benthamiana* (Fig. 1A) (Zeng et al., 2018). Independent qPCR analyses of 3 week inoculated Medicago and chives plants confirmed the chives-enriched expression of this putative effector encoding gene (Fig. 1B).

RirG091260 encodes a 86 aa protein, containing a 24 aa signal peptide at the N-terminus

and a cysteine-rich domain that shows homology to the β-glucan-binding lectin FGB1 effector from *Piriformaspora indica* (Fig. S1A) (Wawra et al., 2016). Therefore, we named this effector RiFGB1. To examine how conserved this effector is, we searched for homologs within the fungal kingdom. FGB1-like effectors are widely presence in the fungal kingdom ranging from biotrophic to necrotrophic fungi (Fig. S1B), and can be detected in all AM fungal genomes available in NCBI and JGI with varying number of paralogs (Fig. 2). Five FGB1-like homologs could be identified in the *R. irregulars* DAOM197198 genome (Lin

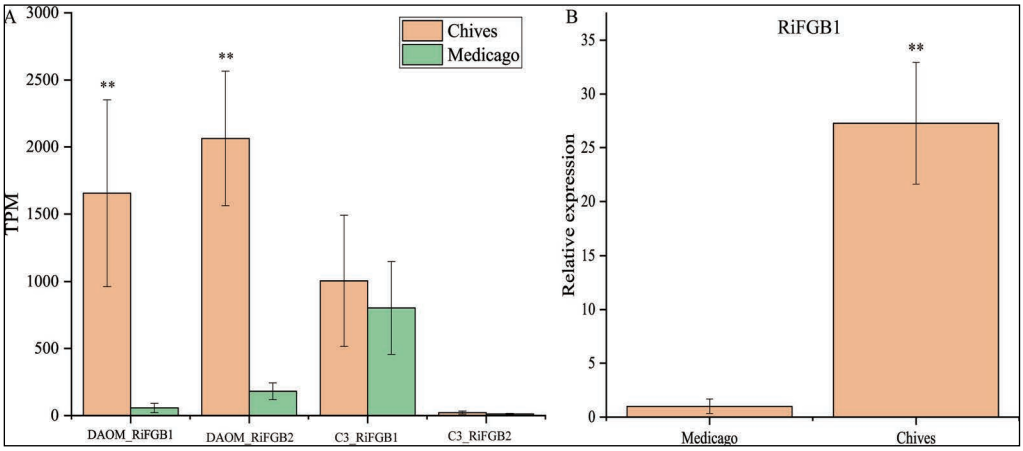

Fig. 1 *RiFGB1* from *Rhizophagus irregularis* DAOM197198 strain shows host-dependent expression. (A) *Rhizophagus irregularis* DAOM197198 *RiFGB1* and *RiFGB2* (RirG091270) is highly induced in chives. But *R. irregularis* C3 *RiFGB1* expression is not differentially expressed between chives and Medicago. Data for *R. irregularis* DAOM197198 were collected from (Zeng et al., 2018). Data for *R. irregularis* C3 were collected from (Van Creij, unpublished). TPM = Transcripts Per Million. Student's t test. **, $P < 0.01$. (B) qPCR analysis confirms the strong induction of *RiFGB1* (RirG091260) in the interaction with chives compared to Medicago. Both Medicago and chives were inoculated with 300 *R. irregularis* DAOM 197198 spores for 3 weeks. Error bars represent SD from 3 biological replicates. *RiEF* was used as reference gene. Student's t test. **, $P < 0.01$.

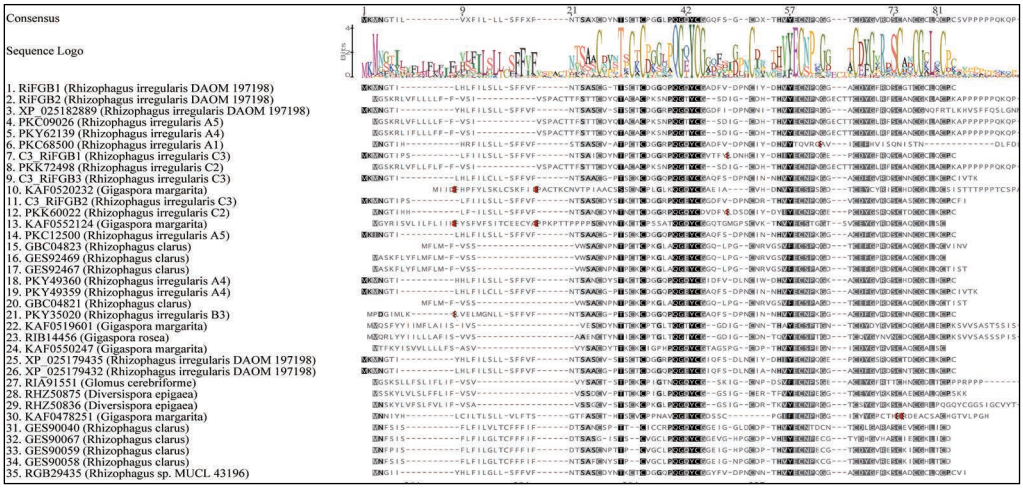

Fig. 2 Alignment of RiFGB1-like proteins in arbuscular mycorrhizal fungi. Data collected from NCBI and JGI MycoCosm. MAFFT built in Geneious R11.0 (https://www.geneious.com) was used for the alignment.

et al., 2014; Zeng et al., 2018). Two close homologs, RiFGB1 and RiFGB2 (RirG091270) located in tandem in the genome, showed similar host-dependent expression patterns, while the other 3 homologs were not, or very little, expressed during symbiosis with the plant species tested (Fig. 1A). The host-dependent expression of *RiFGB1* was confirmed by qPCR analysis (Fig. 1B).

To study if *RiFGB1* homologs in other *R. irregulars* strains are also expressed in a chives-dependent manner, we analyzed their expression in the *R. irregulars* C3 strain, which we recently sequenced (Van Creij, unpublished). *R. irregularis* C3 contains three RiFGB1 homologs (Fig. S2; table S2), two of them showed expression in AM symbiosis however none of them showed host-dependent expression pattern (Fig. 1A). These results suggest that the strong induction of RiFGB1-homologs upon symbiosis with chives varies between different isolates.

Ectopic overexpression of RiFGB1 increases AM colonization

To study the influence of RiFGB1 on arbuscular mycorrhization, we first applied host-induced gene silencing (HIGS) to knock down *RiFGB1* expression (Nowara et al., 2010). Unfortunately, the expression of *RiFGB1* could not be successfully knocked down (Fig. S3). As an alternative, we over-expressed *RiFGB1* in Medicago roots under the control of

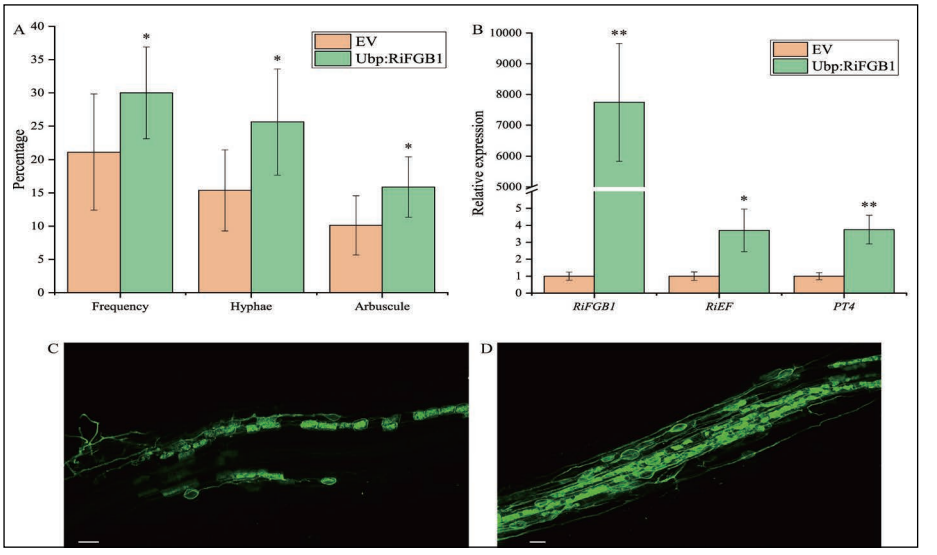

Fig. 3 Overexpression of RiFGB1 facilitates AM colonization in *Medicago truncatula*. (A) Quantification of mycorrhization levels in *UBp:BCPsp-RiFGB1* transgenic roots and empty vector control roots, 3 weeks post inoculation. Indicated are the percentage of intraradical hyphae (Hyphae), arbuscules and overall level of colonization (Frequency). Data are represented as mean ± SD of 8 independently transformed plants per construct. Student's t test. *, $P < 0.05$. (b) qPCR analyses showing increased *RiEF* expression level as marker for fungal colonization in *RiFGB1* overexpression samples. *MtPT4* gene expression as marker for arbuscule abundance. Expression levels were normalized using *MtEF1* as reference. Data are represented as mean ± SD of 8 independently transformed plants per construct. Student's t test. *, $P < 0.05$. **, $P < 0.01$. (C) Representing confocal picture of WGA-alexa488 stained empty vector transformed roots. Scale bar = 100 μm. (D) Representing confocal picture of WGA-alexa488 stained *UBp:BCPsp-RiNLE1* transgenic roots. Scale bar = 100 μm.

the Lotus *UBIQUITIN1* promotor (*UB1p::BCP1sp-RiFGB1*). To ensure proper processing in the secretory pathway we replaced its endogenous signal peptide with that the of Medicago BLUE COPPER PROTEIN 1 (*BCP1*) signal peptide (Ivanov and Harrison, 2019). Transgenic roots were selected based on a co-transformed DsRed marker. Mycorrhization levels were quantified three weeks post-inoculation with *R. irregularis* DAOM197198 spores using the objective gridline intersect method (McGONIGLE et al., 1990). Frequency of mycorrhization and abundance of arbuscules were both significantly higher in *RiFGB1* over-expression samples compared to empty vector control samples (Fig. 3A, C, D). This was further confirmed by the qPCR analyses. The expression level of the fungal housekeeping gene elongation factor (*RiEF*) and arbuscule-containing cell specific Phosphate Transporter 4 (*PT4*; Javot et al., 2007) were both significantly higher in *RiFGB1* over-expression roots compared to empty vector (EV) control roots (Fig. 3B). These results indicate that RiFGB1 has a positive effect on AM colonization.

Since RiFGB1 is much higher induced in the *R. irregularis* DAOM197198 isolate compared to the C3 isolate when interacting with chives, we asked whether this correlated with fungal colonization levels. To test this, chives plants were inoculated with 200 DAOM197198 or C3 spores and the mycorrhization levels were quantified after 5 weeks. Interestingly, colonization levels of the C3 isolate were significantly lower than those observed for the DAOM197198 isolate (Fig. 4). Although more repetitions are required to further substantiate the phenotype, this raises the intriguing possibility that the chives-enriched expression of RiFGB1 in the DAOM197198 isolate may contribute to the better colonization of chives.

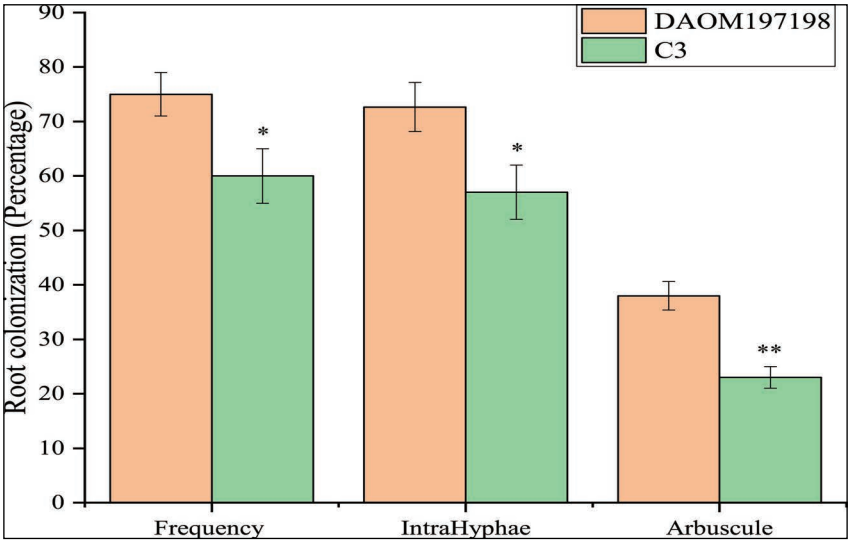

Fig. 4 *Rhizophagus irregularis* DAOM197198 isolate has a higher colonization efficiency in chives compared to the C3 isolate. Quantification of mycorrhization levels in chives roots 5 weeks post inoculation of DAOM197198 or C3 spores. Indicated are the percentage of intraradical hyphae (Hyphae), arbuscules and overall level of colonization (Frequency). Data are represented as mean ± SD of 3 independent plants. Student's t test. *, $P < 0.05$; **, $P < 0.01$.

RiFGB1 can bind to various glycans

Given the homology of RiFGB1 to the β-glucan binding FGB1 effector from *Piriformaspora indica*, we hypothesized that RiFGB1 may also bind β-glucans to interfere with their perception by the plant. To study this, we tried to purify RiFGB1 for use in binding studies and bioassays. Since RiFGB1 contains 12 cysteine residues that may form disulfide bridges, we used the Champion pET-SUMO expression system in combination with the *E. coli* ORIGAMI strain, which is modified to allow disulfide bridge formation. Initially we noticed that this protein is quite unstable leading to precipitation/gelling behavior upon cell lysis. To increase its stability we tried a range of protein buffer compositions according to the Hofmeister series (Zhang and Cremer, 2006), and found that the protein was most stable in a buffer containing 250 mM $(NH_4)_2SO_4$, 8.5% glycerol, pH=7.5. After NTA column purification and size-exclusion chromatography, a ~14 kDa RiFGB1 protein band was visible on

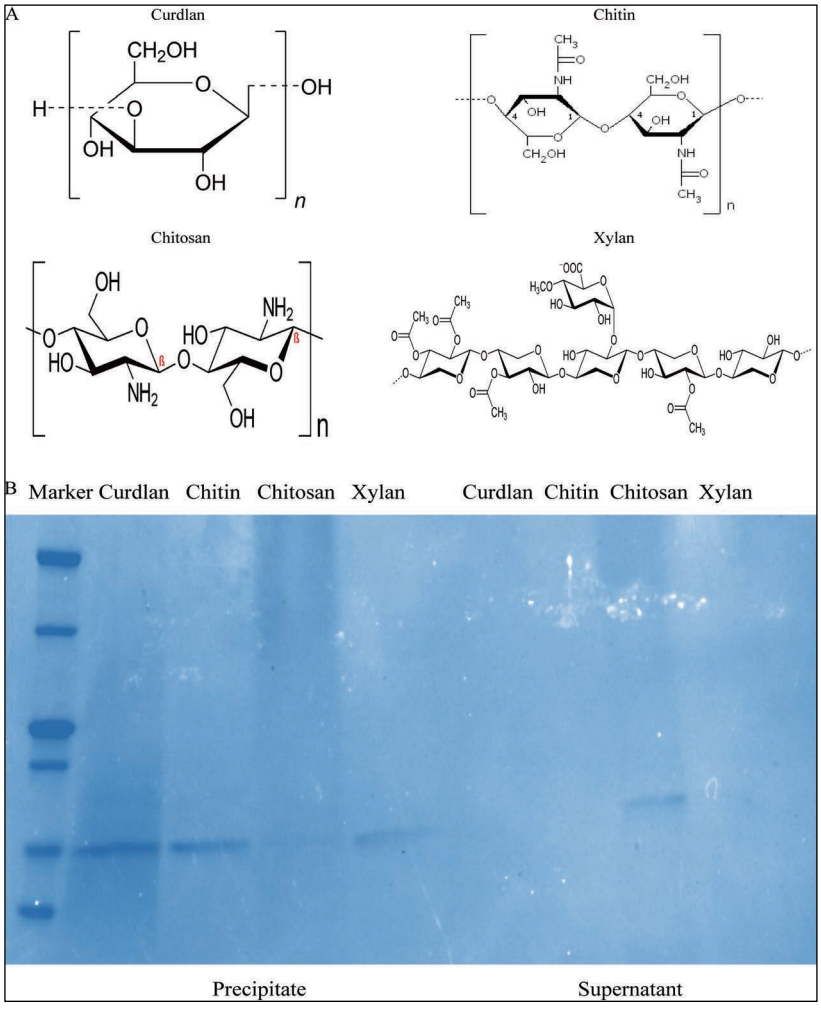

Fig. 5 RiFGB1 binds to various glycans. (A) structure of curdlan, chitin, chitosan and xylan. (B) Coomassie stained protein gel of affinity precipitation assays showing that RiFGB1 binds to insoluble curdlan (β-1,3-glucan), chitin and xylan, but not chitosan. The vast majority of the RiFGB1 protein incubated with chitosan is retained in the supernatant.

a Coomassie blue stained protein gel (Fig. S4).

Next, we first tested whether RiFGB1 can bind β-glucan-like molecules by using an affinity precipitation assay. Therefore, RiFGB1 was incubated with insoluble Curdlan (1,3-β-glucan), chitin, chitosan and xylan, respectively (Fig. 5A). After centrifugation, the supernatants and pellets of the different incubation were collected and analyzed by SDS-PAGE. This showed that the RiFGB1 protein could be precipitated with insoluble Curdlan, chitin and xylan, but not, or hardly, with chitosan (Fig. 5B). The potentially broad affinity of RiFGB1 for curdlan, chitin as well as the hemicellulose xylan was somewhat unexpected.

To further investigate the binding affinity of RiFGB1 for different glycan molecules, we attempted isothermal titration calorimetry (ITC) (Wawra et al., 2016). Unfortunately, our protein was not compatible with the ITC procedure, since protein buffer containing NH_4^+ interferes with the labelling reagent Lightning-Link® R-Phycoerythrin. As mentioned above, too low protein concentrations were obtained in other protein buffers suitable for ITC. In an attempt to produce more stable protein, we additionally expressed RiFGB1 in the *E. coli* Shuffle strain, which is reported to show enhanced capacity to correctly fold proteins with multiple disulfide bonds in the cytoplasm. However, this approach also failed to give satisfactory results. Which characteristics of the different glycan molecules determine the binding affinity of RiFGB1 therefore remains to be further investigated.

RiFGB1 suppresses defense responses by a wide range of MAMPs

To investigate whether RiFGB1 can interfere with β-glucan or chitin triggered immune responses we used two bioassays, measuring defense gene activation and reactive oxygen (ROS) production. For the defense gene assay we incubated freshly germinated Medicago

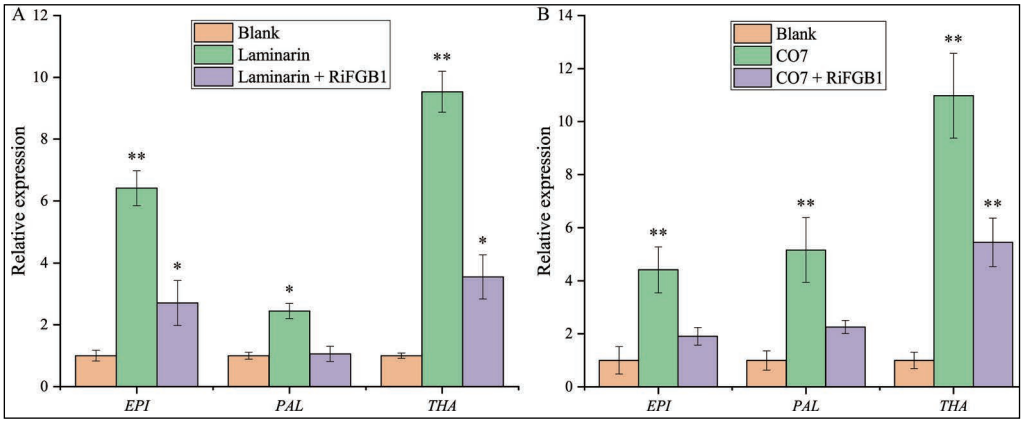

Fig. 6 RiFGB1 suppresses laminarin- and CO7-triggered Medicago defense gene expression. (A) RiFGB1 suppresses laminarin-triggered defense marker gene expression in *Medicago truncatula* seedling roots treated with 20 µM laminarin in combination with 2 µM RiFGB1 for 1 h. Three defense marker genes *EPI*, *PAL*, and *THA* were used to monitor defense responses by qPCR. (B) RiFGB1 suppresses CO7-triggered defense marker gene expression in *M. truncatula* seedling roots treated with 100 nM CO7 in combination with 100 nM RiFGB1 for 1 h. Three defense marker genes *EPI*, *PAL*, and *THA* were used to monitor defence responses by qPCR. All data in (A-B) are represented as mean ± SD of 3 biological replicates, and *MtEF* was used as reference. Student's t test. *, $P < 0.05$. **, $P < 0.01$.

seedlings in liquid ½ MS medium (no sugar) for 5 days at 21°C. Plants were then treated for 1 hour with 20 µM laminarin, a polysaccharide made up of made up of β(1→3)-glucan with β(1→6)-branches (Wawra et al., 2016), or 100 nM CO7 in the presence or absence of respectively 2 µM or 100 nM RiFGB1. Roots were harvested for RNA isolation and the expression of defense-related marker genes, *MtPAL* (phenylalanine ammonia lyase), *MtEPI* (NAD-dependent epimerase/dehydratase) and *MtTHA* (thaumatin) (Nars et al., 2013; Zeng et al., 2020), were determined by qPCR analysis. This showed that the induction by laminarin and CO7 of all three defense genes was markedly reduced upon co-treatment with RiFGB1 (Fig. 6A, B).

For the ROS assay 0.5–1 cm Medicago root fragments were treated with 500 µM laminarin or 1 µM CO7 in the presence or absence of RiFGB1. As an additional control to determine

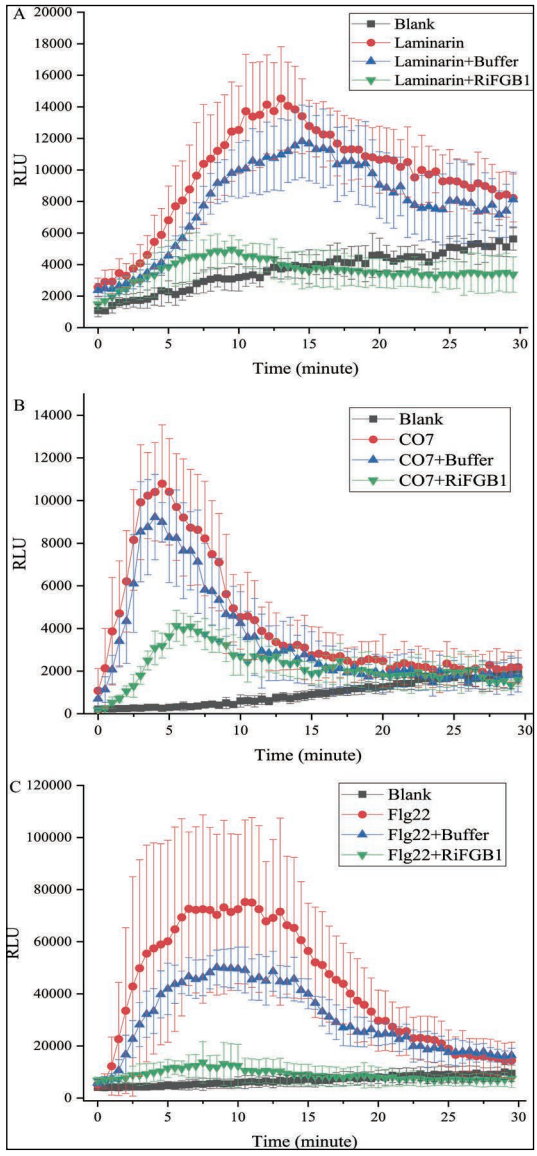

Fig. 7 RiFGB1 suppresses laminarin-, chitin- and Flg22-triggered reactive oxygen species burst in *Medicago truncatula* root pieces. (A) RLU (relative light unit) of *M. truncatula* root pieces treated with 300 µM laminarin with or without 5 µM RiFGB1 for 30 minutes. (B) RLU (relative light unit) of *M. truncatula* root pieces treated with 1 µM CO7 with or without 1 µM RiFGB1 for 30 minutes. (C) RLU (relative light unit) of *M. truncatula* root pieces treated with 1 µM Flg22 with or without 1 µM RiFGB1 for 30 minutes. In (A-C) error bars represent SD from 6 biological replicates.

the specificity of the RiFGB1 effect we now included the widely used Flg22 (a 22 amino acid peptide of Flagellin) peptide as trigger for MAMP-responses. All three MAMPs triggered a clear ROS burst in Medicago root fragments, although the timing and duration of the ROS burst varied for the different MAMPs (Fig. 7A-C). Interestingly the ROS bursts were greatly reduced upon co-treatment with RiFGB1 protein, not just for in the laminarin and CO7 treatments but also for the Flg22 treatment (Fig. 7A-C). These data suggest that RiFGB1 can broadly interfere with MAMP-triggered defense responses in Medicago roots. Using the same assay we were unable to detect a ROS burst upon CO7 or laminarin treatment in chives roots (Fig. S5). This prevented us from testing whether RiFGB1 also interferes with MAMP induced responses in chives.

RiFGB1 does not interfere with symbiotic signaling

AM fungi also use chitin-derived molecules to activate the symbiotic signaling pathway (Luginbuehl and Oldroyd, 2017). Such so-called Myc-factors consist of chitin-derived

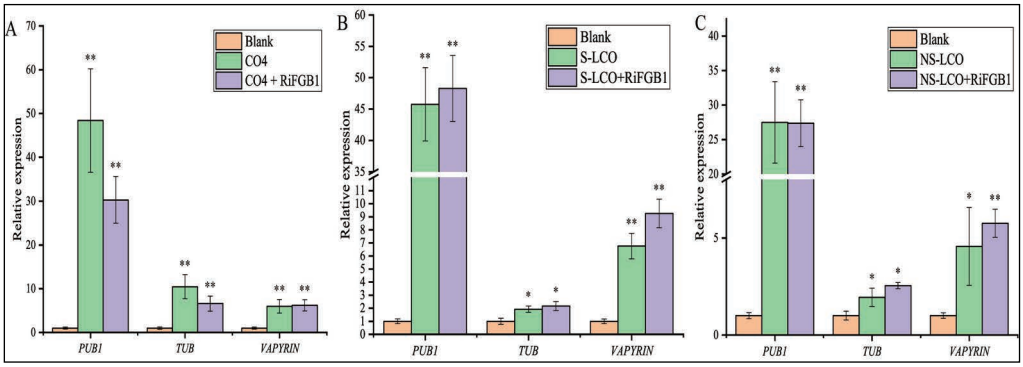

Fig. 8 RiFGB1 does not block symbiotic responses. Three symbiotic marker genes *PUB1*, *TUBB1*,and *Vapyrin* were used to monitor symbiotic responses. (A) qPCR analysis of *Medicago truncatula* roots treated with 100 nM CO4 in combination with 100 nM RiFGB1. (B) qPCR analysis of *M. truncatula* roots treated with 10 nM sulphated LCO in combination with 10 nM RiFGB1. (C) qPCR analysis of *M. truncatula* roots treated with 10 nM non-sulphated LCO in combination with 10 nM RiFGB1. In all data (A-C) MtEF was used as reference gene. Milli-Q treated blank sample was used as control. Error bars represent SD from 3 biological replicates. Student's t test. *, P< 0.05; **, P < 0.01.

lipo-chitooligosaccharides (Myc-LCOs) and short-chain chitooligosaccharides like CO4 or CO5 (Parniske, 2008; Maillet et al., 2011; Genre et al., 2013). To test whether RiFGB1 would also interfere with symbiotic signaling by these glycan based molecules, Medicago seedling roots were treated with sulphated Myc-LCO (10 nM), non-sulphated LCO (10 nM) and CO4 (100 nM) in the presence or absence of equal concentrations of RiFGB1 protein. In contrast to the inhibitory effect of RiFGB1 on MAMP-triggered responses, no significant effect of RiFGB1 was observed on symbiotic gene induction (MtPUB1, MtTUB1 and MtVAPYRIN) (Czaja et al., 2012; Camps et al., 2015b; Vernié et al., 2016) by any of the different Myc-factor molecules (Fig. 8). This indicates that RiFGB1 does not interfere with the symbiotic signaling by these glycan molecules.

Discussion

It has been hypothesized that fungal effector proteins might play a role in the preferential association of AM fungi with different hosts. In this study, we carried out a first characterization of the host-dependent effector, RiFGB1 from the AM fungus *R. irregularis* DAOM197198. We show that RiFGB1 can interfere with a wide range of PAMP-triggered immune responses and that it can increase root colonization when overexpressed. *RiFGB1* expression, as well as that of a close homolog called *RiFGB2*, is significantly induced when *R. irregularis* DAOM197198 colonizes chives compared to the dicot hosts Medicago and Nicotiana. The very close homology of RiFGB1 and RiFGB2 suggest a similar function, although this remains to be tested. Although homologs of RiFGB1 can be found in all currently sequenced AM fungi this host-dependent expression does not seem to be conserved. For example, the *R. irregularis* C3 isolate does not show the enriched expression compared to the other hosts (Fig. 1A). This correlates with a reduced colonization efficiency of C3 compared to the DAOM197198 strain. Therefore, although preliminary, our data suggest that host-dependent effectors may control host preferences through their effect on host immune signaling.

RiFGB1 shows homology to the β-glucan binding effector FGB1from *P. indica* (Wawra et al., 2016). Our affinity precipitation assays suggest that RiFGB1 can actually bind a range of glycan molecules, among which polymeric β-1,3-glucan (curdlan), chitin and even xylan. Strikingly chitosan, the deacetylated form of chitin, was not bound. What determines the binding affinity for the different glycan structures is currently unknown. The presence of multiple cysteine residues in the protein suggests that disulfide bridges may be important for its proper functioning. Using the *E. coli* ORIGAMI cell system, which facilitates disulfide bridge formation, stable RiFGB1 could only be obtained in a $(NH_4)_2SO_4$ buffer, which is thought to stabilize proteins by preferential solvation. However, this buffer impaired subsequent ITC binding assays. To study binding affinities more carefully, a different protein production system needs to be found that allows sufficient amounts of RiFGB1 to be isolated and which is compatible with ligand binding assays such as isothermal calorimetry or microscale thermophoresis. For example, insect cells, fungal production systems such as *Pichia pastoris* (Hitchman et al., 2009; Ahmad et al., 2014) or even production by P. indica (Wawra et al., 2016) could be tried.

In addition to chitin, the major part of the cell wall of fungi consists of glucans that are assembled into polymers with various chemical linkages of which β-1,3-glucan, with β-1,6 side branches, is thought to be the most abundant (Fesel and Zuccaro, 2016). The ability of RiFGB1 to bind to both chitin and β-1,3-glucan suggests that it might bind to the cell wall of *R. irregularis*. FGB1 from *P. indica* was shown to modulate fungal cell wall composition and was proposed to prevent β-glucans from being recognized by plant β-glucan receptor complexes (Wawra et al., 2016). In contrast to RiFGB1, PiFGB1 was reported to specific recognize fungal β-1,6 linked glucan side chains.

Interestingly, β-glucan and chitin perception in plants seem to be intertwined. It was shown that laminarihexaose-induced immune responses in Arabidopsis are dependent on the chitin receptor CERK1 (Mélida et al., 2018). This suggests that CERK1 may act as a co-receptor of β-glucan receptors, at least in Arabidopsis. Currently, only a single β-glucan receptor from soybean has been identified (Fliegmann et al., 2004). Recent work by Wanke et al

(2020) indicated that β-glucan perception mechanisms can differ between plant species, with varying responses being triggered in different plants by different β-glucan structures (Wanke et al., 2020). In addition to various linkages and side branches, especially the degree of polymerization of the glucan backbone appeared to be of importance. During AM symbiosis the expression and accumulation of specific β-glucanase proteins is induced during the early stage of AM symbiosis (Dumas-Gaudot et al., 1996; Pozo et al., 1999; García-Garrido and Ocampo, 2002). Such glucanases may release different glucan molecules that may be perceived by the host immune system.

Besides fungi, also plants cell walls contain various β-glucans. The most well-known β-1,3-glucan is callose, which reinforces cell walls upon attach by pathogenic microbes. Intriguingly, monocots, especially grasses contain unbranched glucose polysaccharides with alternating β-1,3 and β-1,4 linkages that are absent form dicots (Wanke et al., 2020). Furthermore, grasses evolved specific β-glucan endohydrolases (Bulone et al., 2019), which might affect fungal associations. Another difference between cell walls of dicots and grasses concerns the presence of xylan in the primary cell wall. In dicot plants xylan only occurs in the secondary cell wall (Mellerowicz and Gorshkova, 2011). It is therefore tempting to speculate that RiFGB1 may be upregulated in the monocot chives due to a difference in the β-glucan perception system compared to the dicot hosts, to avoid a strong defense response. Expression analyses in multiple monocot species could help to support this hypothesis.

Surprisingly, we found that RiFGB1 can not only interfere with immune responses triggered by laminarin or chitooligosaccharides but also by the bacterial flagellin peptide Flg22. Although we did not test the binding of Flg22 with RiFGB1, it seems unlikely that RiFGB1 will strongly interact with this unrelated peptide. In contrast to the MAMP responses no effect of RiFGB1 on symbiotic signaling by fungal LCO's was observed. This raises the question how RiFGB1 can then have such a broad effect on MAMP responses?

Two hypotheses could be envisioned for future study. RiFGB1 may broadly interfere with the activity of pattern recognition receptors on the plant cell surface by binding to the glycan moieties attached to these proteins in the process of glycosylation (Häweker et al., 2010). Glycosylation has been identified in the leucine-rich repeat (LRR)-ectodomains of pattern recognition receptors such as EFR, FLS2, CERK1 and BAK1 and such glycan additions were shown to be required for their activity in plant immune signaling (Van Der Hoorn et al., 2005; Zipfel et al., 2006; Häweker et al., 2010; Petutschnig et al., 2010). In contrast N-glycosylation of the LCO receptor NFP was found not to be essential for its activity (Lefebvre et al., 2012). The latter could potentially explain why RiFGB1 does not interfere with LCO signaling. Alternatively, the much higher affinity of Medicago LysM receptors for LCO's might overrule the effect of RiFGB1. Another possibility could be that RiFGB1 affects the plant cell wall composition which then indirectly interferes with the activity of pattern recognition receptors. It is becoming more and more clear that a dedicated cell wall integrity system is likely intertwined/integrated with host immune responses (Vaahtera et al., 2019).

In conclusion, the results in this chapter provide a first, though still preliminary, indication that host-dependent effectors may help to subvert the plant immune system and thereby influence host-preferential associations. Furthermore, it suggests a potential much broader role for glycan-binding FGB1-like effectors to interfere with PAMP-triggered immunity.

Supplementary figures

A

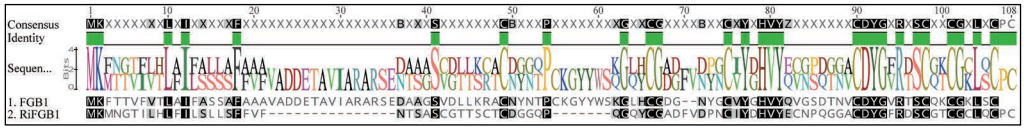

B

Fig. S1 RiFGB1-like effectors are widely exist in fungal kingdom. (A) Alignment of RiFGB1 with PiFGB1 from *Piriformaspora indica*. SP indicate signal peptide. (B) Alignment of RiFGB1-like effectors from different fungal species. MAFFT built in Geneious R11.0 (https://www.geneious.com) was used for the alignment.

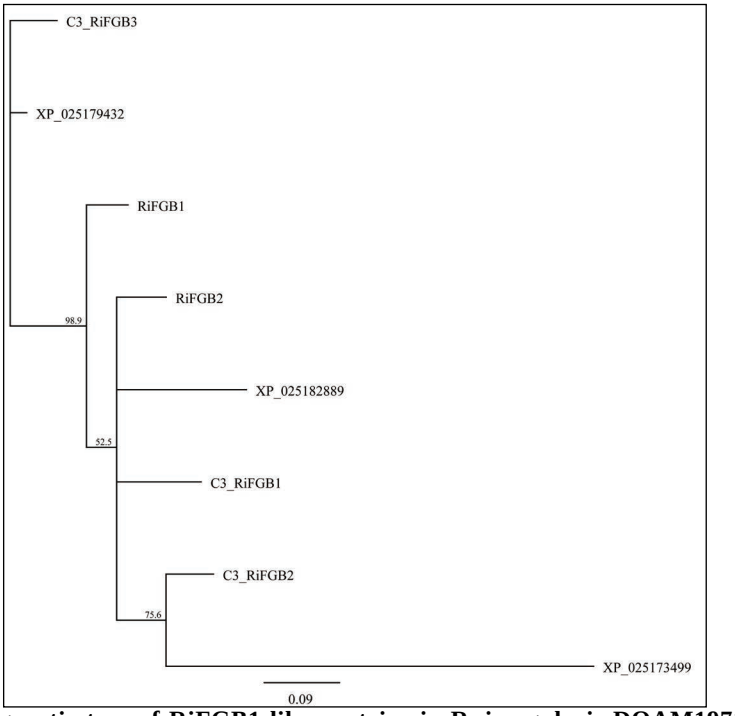

Fig. S2 Phylogenetic tree of RiFGB1-like proteins in R. irregularis DOAM197198 and C3 strains. The tree was generated using the neighbour-joining tree builder in Geneious R11.0 (https://www.geneious.com). 1000 bootstraps were used.

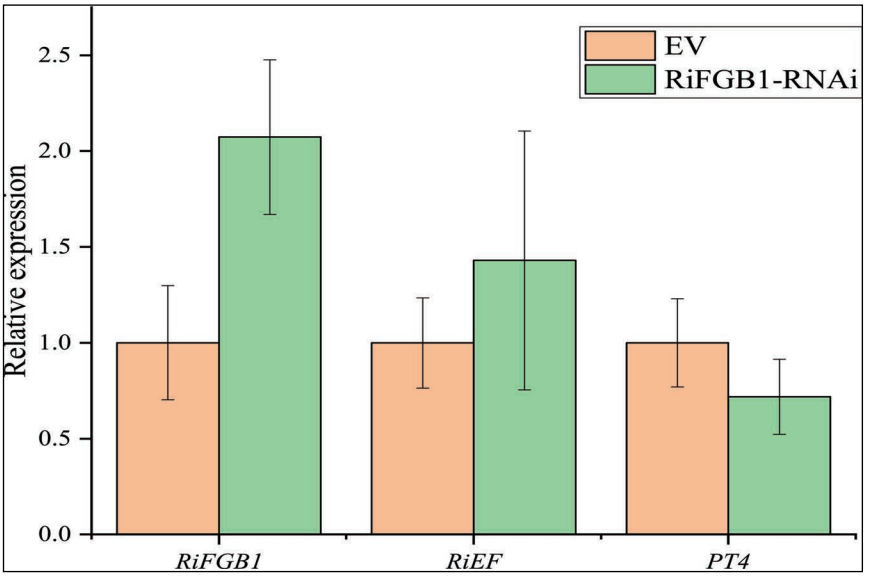

Fig. S3 Host-induced gene silencing failed to interfere with *RiFGB1* expression. qPCR analysis of EV control and *RiFGB1*-RNAi roots 3 weeks post-inoculation showing relative expression of *RiFGB1*, *RiEF* as marker for fungal abundance and *PT4* as marker for arbuscule abundance. Error bars represent SD from 6 biological replicates. *MtEF* was used as reference gene.

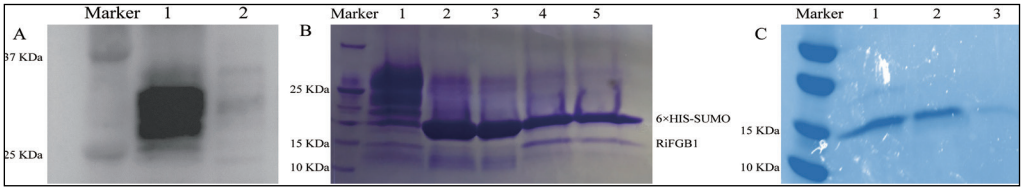

Fig. S4 RiFGB1 protein production and purification from ORIGAMI *E. coli*. (A) Anti-His blot showing 6×HIS-SUMO-RiFGB1: 1, protein eluted from Ni^{2+} column. 2, non-binding part. (B) Coomassie stained SDS-PAGE gel showing the removal of the 6×HIS-SUMO tag by ULP-1 protease. 1, Full 6×HIS-SUMO-RiFGB1 protein before digestion. 2 and 3, 6×HIS-SUMO after elution from the Ni^{2+} column. 4 and 5, flow-through of non-bound proteins after digestion by ULP-1 protease. The released RiFGB1 peptide is indicated. (C) Coomassie stained SDS-PAGE gel showing RiFGB1 after purification by size exclusion chromatography. Lanes 1, 2, and 3 represent different fractions from the size exclusion chromatography.

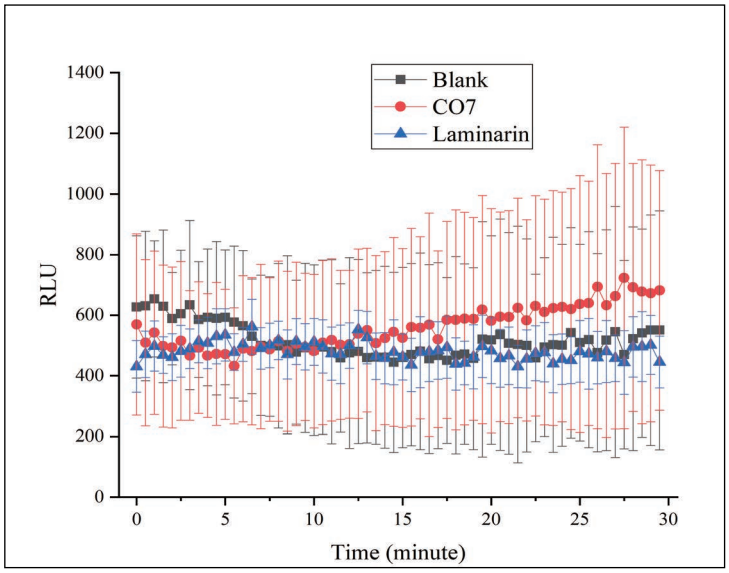

Fig. S5 ROS assay in Chives root pieces treated with laminarin and CO7. RLU (relative light unit) of chives root pieces treated with 1 μM CO7 or 300 μM laminarin for 30 minutes. Error bars represent SD from 6 biological replicates.

Supplementary tables

Table S1. Primers list used in this work

Experiment	Primer name	Primer sequence
Goldengate	F-RiFGB1-CDS1-no stop	AGAAGACTCAGGTAGTTGCGGTACTACTTCTTGT
Goldengate	R-RiFGB1-CDS1-no stop	GGAAGACAGCGAACAAGGACATTGCAAACAACC
Cloning	F-RiFGB1-xho I	TGCTCGAGAGTTGCGGTACTACTTCTTGT
Cloning	R-RiFGB1-BamH I	ACGGATCCTTAACAAGGACATTGCAAACAACC
Goldengate	F-BCPsp	AGAAGACTCAATGGCTTCTTCTCGTGTAGTT
Goldengate	R-BCPsp	GGAAGACAGACCTTGCAATTGCAACTGATGAAAG

Table S2 sequence of C3 RiFGB1 homologs

Name	Sequence
C3_RiFGB1	MKMNGTIPSLFIILSLLSFFVFNTSAICDYNTPCTCDGGRPQGQYCGVTFY-GLDNHCIYDHIYECNPQGEPCDYGFRQSCADCGCLQCPC
C3_RiFGB2	MKMNGTIPSLFIILSLLSFFVFNTSASCDYSTKCTCDGGRPQGEYCGGDFVD-PNCDRTHVYECNPQGGVCDYGVRGSCASCGCLQCPCFI
C3_RiFGB3	MKMNGTILHLFILCLLSFFVFNTSAACGPTSCKCDGGQPQGEYCGAQFSD-PNCINNHVYECNPKGGACDFGVRDSCNNCGCLKCPCIVTK

Chapter 4

Medicago SPX1 and SPX3 regulate phosphate homeostasis, mycorrhizal colonization and arbuscule degradation

Peng Wang[a], Roxane Snijders[a], Wouter Kohlen[a], Jieyu Liu[a], Sjef Boeren[b], Ton Bisseling[a], Erik Limpens[a,*]

[a] Laboratory of Molecular Biology, Wageningen University & Research, 6708 PB Wageningen, the Netherlands

[b] Laboratory of Biochemistry, Wageningen University & Research, Wageningen 6708 WE, the Netherlands

[*]To whom correspondence should be addressed. Email: erik.limpens@wur.nl

Key words: SPX, phosphate homeostasis, arbuscular mycorrhiza, arbuscule development, strigolactone

This chapter has been deposited in a slightly modified form at bioRxiv: https://doi.org/10.1101/2021.02.09.430431

Abstract

To acquire sufficient mineral nutrients such as phosphate (Pi) from the soil, most plants engage in a symbiosis with arbuscular mycorrhizal (AM) fungi. Attracted by plant-secreted strigolactones, the fungi colonize the roots and form highly-branched hyphal structures called arbuscules inside inner cortex cells. It is essential that the host plant controls the different steps of this interaction to maintain its symbiotic nature. However, how plants sense the amount of Pi obtained from the fungus and how this determines the arbuscule lifetime is far from understood. Here, we show that *Medicago truncatula* SPX-domain containing proteins SPX1 and SPX3 regulate root phosphate starvation responses as well as fungal colonization and arbuscule degradation. *SPX1* and *SPX3* are induced upon phosphate starvation but become restricted to arbuscule-containing cells upon establishment of the symbiosis. Under Pi-limiting conditions they facilitate the expression of the strigolactone biosynthesis gene *DWARF27*, which correlates with increased fungal branching by root exudates and increased root colonization. Later, in the arbuscule-containing cells SPX1 and SPX3 redundantly control the timely degradation of arbuscules. We propose a model where SPX1 and SPX3 control arbuscule degeneration in a Pi-dependent manner via a yet-to-identify negative regulator.

Introduction

In nature, plants usually face low mineral phosphate (Pi) availability in the soil, which limits their growth and development (Rouached et al., 2010). To deal with such phosphate limitation, plants typically induce a set of phosphate starvation induced (PSI) genes to acquire more Pi from the soil and to increase phosphate use efficiency (Bari et al., 2006; Zhou et al., 2008). In addition, most land plants engage in a symbiosis with arbuscular mycorrhizal (AM) fungi to increase their phosphate acquisition efficiency (Smith and Read, 2008). Under Pi starvation conditions, plant roots release strigolactones (SLs) that enhance spore germination and hyphal branching to initiate a symbiotic association (Akiyama et al., 2005; Besserer et al., 2006). Subsequently the fungus colonizes the roots and forms highly branched hyphal structures, called arbuscules, inside root cortex cells and its hyphae continue to form extensive networks in the soil. The hyphae can efficiently reach the scarcely available phosphate, which they deliver to the plant in return for carbon (fatty acids and sugars) (Luginbuehl and Oldroyd, 2017).

The maintenance of proper Pi homeostasis is important for plant growth and development, as either too low or too high Pi concentration in plant cells can be harmful to the plant (Wang et al., 2014b). Therefore plants continuously sense and signal the phosphate status in response to their environment. Also during the symbiosis the plant must integrate phosphate status with fungal colonization and arbuscule development to keep the interaction beneficial. However, how a plant determines how much Pi it gets locally at the arbuscules and regulates Pi homeostasis in relation to arbuscule development is still an open question (Ezawa and Saito, 2018; Müller and Harrison, 2019).

Arbuscules form a symbiotic interface where Pi is provided to the host plant (Ezawa and Saito, 2018). They are relatively short lived structures that are degraded and removed from the cortical cells after 2-7 days (Kobae and Hata, 2010). This transient characteristic is

thought to give the plant a means to locally abort arbuscules when these due to their age do not deliver sufficient nutrients (Lanfranco et al., 2018). In line with this, loss of the arbuscule-containing cell-specific PHOSPHATE TRANSPORTER 4 (PT4), responsible for transporting Pi across the peri-arbuscular membrane into the plant cell, leads to the premature degradation of the arbuscules in the model legume *Medicago truncatula* (Medicago) (Javot et al., 2007). This requires the activity of the MYB1 transcription factor, which induces the expression of hydrolytic enzymes such as cysteine proteases and chitinases to degrade the arbuscules (Floss et al., 2017). Intriguingly, it has been shown that Medicago can also adjust the amount of carbon that it delivers to the fungus depending on the amount of Pi obtained from the fungus (Kiers et al., 2011). AM fungal strains that deliver more Pi were shown to receive more carbon compared to less cooperative strains. This so-called reciprocal rewarding indicates that the plant is able to locally monitor the amount of Pi that it obtains from the fungus.

SPX domain containing proteins have emerged as key sensors and regulators of Pi homeostasis and signaling (Jung et al., 2018). The SPX domain is named after the Suppressor of Yeast gpa1 (Syg1), the cyclin-dependent kinase inhibitor in yeast PHO pathway (Pho81), and the human Xenotropic and Polytropic Retrovirus receptor 1 (Xpr1) (Barabote et al., 2006). This domain is able to sense the Pi status of a cell by binding with high affinity to inositol polyphosphates (PP-InsPs; (Wild et al., 2016; Jung et al., 2018). Changes in PP-InsPs levels in response to Pi deficiency are thought to modulate the activity of SPX-containing proteins and their interactors. The mode of action of single SPX domain containing proteins in the phosphate starvation response has been best studied in rice and Arabidopsis. The nuclear localized SPX1 and SPX2 proteins in Arabidopsis were shown to interact with PHOSPHATE STARVATION RESPONSE 1 (AtPHR1), a MYB transcription factor that together with its homologs controls phosphate starvation induced gene expression (Puga et al., 2014; Sun et al., 2016). Binding of AtSPX1/2 to AtPHR1 occurs at high Pi conditions and prevents the binding of AtPHR1 to the PHR1 binding site (P1BS) cis-regulatory element present in the promoters of many PSI genes. Similar regulation has been reported in rice where OsSPX1 and OsSPX2 control the activity of OsPHR2 in a phosphate dependent manner (Wang et al., 2014b). Other SPX members, such as OsSPX4 have been localized in the cytoplasm where they control the cytoplasm-to-nucleus shuttling of OsPHR2 in a Pi dependent manner (Hu et al., 2019). Furthermore, OsSPX4 was reported to regulate nitrate and phosphate balance in rice through interaction with the nitrate transceptor OsNRT1.1B, which triggers OsSPX4 degradation upon nitrate perception (Hu et al., 2019). OsSPX3 and OsSPX5 have been localized in both the cytoplasm and nucleus, and redundantly modulate Pi homeostasis as functional repressors of OsPHR2 (Shi et al., 2014).

Given their key role in sensing and signaling of phosphate status in cells, we studied the role of SPX proteins during AM symbiosis. We identified two SPX genes that are strongly upregulated upon AM symbiosis, most specifically in the arbuscule-containing cells of Medicago. We show that these genes regulate Pi homeostasis in non-mycorrhizal conditions, and during the symbiosis positively control mycorrhizal colonization, in part through the regulation of strigolactone levels, as well as the timely degradation of arbuscules.

Materials and methods

Plant and fungal material

Medicago truncatula A17 and R108 seedlings were grown and transformed as described (Limpens et al., 2004). The *spx1* (NF13203) and *spx3* (NF4752) Tnt1-insertion lines were obtained from the Noble Research Institute (https://medicago-mutant.noble.org/mutant/index.php). Homozygous *spx1* and *spx3* mutants were identified by PCR and crossed to obtain the *spx1/spx3* double mutant. Primers used are listed in Table S1. Plants were grown in SC10 RayLeach cone-tainers (Stuewe and Sons, Canada) with premixed sand:clay (1:1 V/V) mixture and watered with 10 ml ½ Hoagland medium with 20 μM (low Pi) or 500 μM H2PO4 (high Pi) twice a week in a 16 h daylight chamber at 21°C, as described previously (Zeng et al., 2018). *Rhizophagus irregularis* DAOM197198 spores (Agronutrion, France) were washed through three layers of filter mesh (220 μm, 120 μm, 38 μm) before inoculation. 200 pores were placed ~2 cm below seedling roots.

Phylogeny

SPX phylogenetic analysis was performed using the Geneious R11.0 software package (https://www.geneious.com). Medicago, Arabidopsis and rice SPX protein sequences were collected from PLAZA (https://bioinformatics.psb.ugent.be/plaza/) and aligned using MAFFT in Geneious R11.0. An unrooted SPX phylogenetic tree was generated using the neighbour-joining tree builder with 500 bootstraps.

Constructs

Most constructs were made using the Golden gate cloning system (Engler et al., 2014) Constructs for RNAi were made via Gateway cloning and constructs for Y2H experiments were made using in fusion cloning (Takara, Japan). Primers used are listed in Table S1. Vectors used for cloning are listed in table S2. All newly made vectors were confirmed by Sanger sequencing.

GUS histochemical analyses

To create the *MtSPX1p-GUS* and *MtSPX3p-GUS* constructs, a 1824 bp upstream of the *MtSPX1* (Medtr3g107393) ATG start codon and a 1260 bp upstream of the *MtSPX3* (Medtr0262s0060) ATG start codon was amplified by PCR from *M. truncatula* A17 genomic DNA as promoter, respectively. *MtSPX1p-GUS* and *MtSPX3p-GUS* constructs were introduced into Medicago plants using *Agrobacterium rhizogenes*-mediated root transformation (Limpens et al., 2004). GUS staining was done as described (An et al., 2019). Briefly, transgenic roots were harvested based on DsRed fluorescence (red fluorescent marker present in the constructs) and washed twice with PBS buffer for 10 min. Next, the roots were incubated in GUS reaction buffer (3% sucrose, 10mM EDTA, 2 mM potassium-ferrocyanide, 2 mM potassium-ferricyanide and 1 mg/ml X-Gluc in 100mM PBS, pH 7.0) for 30 min in vacuum, and then incubated at 37°C for 1 h. The stained roots were fixed in fixation buffer (5% glutaraldehyde in 100mM phosphate buffer, pH 7.2) for 2 h in vacuum at room temperature, followed by dehydrating with an ethanol series (20%, 30%, 50%, 70%, 90%, 100%) for 10 min each. Root segments were embedded in Technovit 7100 (Hereus-Kulzer, Germany) and cut into 8 μm longitudinal sections using a microtome (Leica RM2255) and

stained with 0.1% Ruthenium Red for 5 min. Images were taken using an Leica DM5500 B microscope.

Co-immunoprecipitation and western blotting

FLAG-tagged SPX1 and SPX3 and GFP-tagged PHR2 (Medtr1g080330) constructs were transiently expressed in Nicotiana leaves as described (Zeng et al., 2018). Total proteins were isolated using Co-IP buffer (10% glycerol, 50 mM Tris-Hcl pH=8.0, 150 mM NaCl, 1% Igepal CA 630, 1 mM PMSF, 20 μM MG132, 1 tablet protease inhibitor cocktail). GFP-Trap agarose beads (Chromotek) were used to immunoprecipitate GFP protein complexes. Western blot was performed as described (Bungard et al., 2010). 1:5000 diluted anti-GFP-HRP and anti-FLAG-HRP antibodies (Miltenyi biotec, USA) were used for detection.

RNA interference

A *SPX1SPX3* hairpin construct was generated targeting both *SPX1* and *SPX3* mRNA using the Gateway system (Invitrogen, USA). 534 bp of *SPX1* and 489 bp of *SPX3* mRNA sequence were combined together by overlap PCR and the resulting 1023 bp sequence was cloned into the pENTR/D-TOPO entry vector. Primers used are listed in table S1. Subsequently, the modified pK7GWIWG2(II)-AtEF1 RR vector (Zeng et al., 2020) was used for an LR reaction to get the final hairpin silencing construct.

Pi concentration measurement

Shoots inorganic Pi concentration was measured as described (Zhou et al., 2008). Briefly, Medicago shoots were crushed to a fine powder in liquid nitrogen, and rigorously vortexed for 1 min in 1 mL 10% (w/v) of perchloric acid. The homogenate was diluted 10 times by 5% (w/v) perchloric acid and then put on ice for 30 min, followed by centrifugation at 10,000 g for 10 min at 4°C to collect the supernatant. The molybdenum blue method was used to measure Pi content in the supernatant. To prepare the molybdenum blue solution, 6 mL solution A (0.4% ammonium molybdate dissolved in 0.5 M H_2SO_4) was mixed with 1 mL 10% ascorbic acid. 2 mL of molybdenum blue solution was added to 1 mL of the sample supernatant, and incubated in a water bath for 20 min at 42°C. Then the absorbance was measured at 820 nm , and Pi content was calculated by comparison to standard curve. The Pi concentration was normalized to the shoot fresh weight.

RNA isolation and qRT-PCR

RNA was isolated using the Qiagen plant RNA mini kit according to the manufacturer's instructions, including an on column DNAse treatment. cDNA was made using the iScript cDNA Synthesis kit (Bio-Rad) using 300 ng total RNA as template. qRT-PCR was performed using the iQ SYBR Green Supermix (Bio-Rad) in a Bio-Rad CFX connect real-time system. Primers used for qPCR are listed in Table S1. Medicago *Elongation factor 1* (*EF1*) was used as reference for normalization. Relative expression levels were calculated as $2^{-\triangle ct}$ with three technical replicates for each sample.

AM quantification

Mycorrhizal roots were stained using WGA-Alexafluor 488 (Thermo Fisher Scientific, USA). AM quantification was performed as described (McGONIGLE et al., 1990). In short,

a Leica DM5500 B microscope equipped with an eyepiece crosshair was used to inspect the intersections between the crosshair and roots at 200x magnification. The following categories were noted in each intersection: root only, hyphopodium, extraradical hyphae, intracellular hyphae (Intrahyphae), good arbuscule (equal or larger than 40 µm), degrading arbuscule (less than 40 µm, and presence of septa). In cases where at one intersection more than one category was observed, then each category was counted once at that position. 100 intersections were inspected for each sample (containing 30 cm root) and the percentage of each category was calculated.

Root exudate collection and quantification of strigolactones

Strigolactone analysis was done as described (van Zeijl et al., 2015; Liu et al., 2011). 6 seedlings of each genotype were grown in a X-stream 20 aeroponic system (Nutriculture) operating with 5 L of ½ Hoagland medium (Hoagland, 1950) containing 500 µM Pi in a greenhouse with natural light, 28 °C, 60% relative humidity. After 4 weeks, Pi starvation was initiated by replacing the high Pi medium with ½ Hoagland medium containing 20 µM Pi for one week. 24 hours before exudate collection, the medium was refreshed with new low Pi ½ Hoagland medium. The 5 liters containing 24-hour exudate were purified and concentrated by loading to a pre-equilibrated C18 column (Grace Pure C18-Fast 5000 mg/20 mL). Next, the column was washed with 50 mL of deionized water, followed by 50 mL of 30% acetone. Next, strigolactones were eluted with 50 mL 60% acetone and measured using a Quadcore as described (Kohlen et al., 2011).

***R. irregularis* branching assay**

R. irregularis spore germination and branching assays were performed as previously described (Besserer et al., 2006; Tsuzuki et al., 2016). 100 spores were grown on Solid M medium (BÉCARD and FORTIN, 1988) with 0.6% acetone, 0.01 µM GR24 or 100 times diluted root exudates (as collected above) in the dark at 22°C. 8 days after inoculation, hyphal branches were counted using a Leica M165 FC microscope.

***Phelipanche ramosa* germination assay**

Germination of *Phelipanche ramosa* seeds were performed as reported before (Kohlen et al., 2011). Previously cleaned seeds of *P. ramose* were preconditioned on wet filter paper for 10 days at 21°C. 50 µL of root exudates collected above were added to 1-cm discs containing approximately 50 preconditioned seeds. 10-7, 10-8 and 10-9 M of GR24 were used as positive control. Demineralized water were used as negative control. After 12 days, the germination rates were counted using a binocular microscope.

Confocal microscopy

The subcellular localization of fluorescently tagged proteins and detailed observation of the arbuscules using WGA-Alexafluor 488 stained roots were analysed using a Leica SP8 confocal microscope (For GFP/Alexafluor 488: excitation 488 nm, emission 500-540 nm; for DsRED/mCherry: excitation 552, emission 580-650 nm).

Statistical analyses

For pairwise comparisons, data were analyzed using T-Test built in EXCEL with tail 1, type

2. ANOVA built in Origin 2018 software was used to test difference over two groups of data with default settings. Replicates per experiment used are indicated in the corresponding figure legends.

Results

SPX1 and *SPX3* are strongly induced upon phosphate starvation and in arbuscule-containing cells

To identify *SPX* genes that might be important players during AM symbiosis, we first made a phylogenetic analysis of all single SPX domain proteins from Medicago, in relation to SPX proteins from arabidopsis and rice. This identified 6 members (Fig. 1A). We analyzed their expression in the roots of plants grown in high (500 µM) Pi, low (20 µM) Pi and 20 µM Pi plus *Rhizophagus irregularis* conditions for 3 weeks. qRT-PCR analyses showed that two *SPX* genes, *MtSPX1* (Medtr3g107393; hereafter *SPX1*) and *MtSPX3* (Medtr0262s0060; hereafter *SPX3*) were strongly induced by phosphate starvation as well as during the AM symbiosis (Fig. 1B). Transcriptome analyses of laser microdissected arbuscule-containing cells showed that these two *SPX* genes are dominantly expressed in arbuscule-containing cells (Fig. S1). To determine the spatial expression of *SPX1* and *SPX3* in more detail we analyzed promoter-GUS reporter constructs in transgenic roots grown for 3 weeks at 500 µM Pi, 20 µM Pi and 20 µM Pi with *R. irregularis* conditions. Plants grown at 500 µM Pi showed only weak GUS signal in the root tip, while under low Pi conditions strong GUS activity was detected throughout the root for both constructs (Fig. 1C-F). Sectioning of these roots showed that the SPX1 and SPX3 promoters were active in multiple cell types, including cortex and epidermis, of the root grown at low Pi, but not at high Pi (Fig. 1G, H). Upon AM symbiosis, the GUS signal became strongly restricted to the arbuscule-containing cells (Fig. 1I-L). No, or very low, GUS signal was observed in the non-colonized sections of the mycorrhizal roots. The arbuscule restricted expression was further confirmed by promoter:NLS-3×GFP analyses (Fig. S2). The same expression pattern of both SPX genes suggested that they may have similar functions, playing dual roles in the phosphate starvation response and AM symbiosis.

To study the subcellular localization of SPX1 and SPX3, C-terminal GFP-fusion constructs were expressed in Medicago roots and Nicotiana leaves using either the constitutive Lotus japonicus *Ubiquitin1* (*LjUB1*) promoter or their endogenous promoters. In all cases, including arbuscule-containing cells expressing SPX-GFP fusion under the control of their endogenous promoters, both fusion proteins localized to the cytoplasm as well as to the nucleus (Fig. S3A-E). The subcellular localization was not influenced by the Pi conditions (Fig. S3C, D).

To explain the transcriptional regulation of *SPX1* and *SPX3*, we examined their presumed promoter regions for known *cis*-regulatory elements involved in phosphate-starvation induced expression and arbuscule-specific regulation. This identified a P1BS (GNATATNC) binding site for the MYB transcription factor PHR (Bustos et al., 2010), a key regulator of PSI genes (Fig. S4A). The presence of this element suggests that both SPX genes are under the control of PHR-dependent transcriptional regulation upon phosphate stress. Furthermore, we identified *cis*-regulatory AW-boxes (CG(N)7CNANG) and CTTC-ele-

ments (CTTCTTGTTC) in the promoter regions of both genes, which are binding sites for WRINKLED1-like transcription factors that have recently been found to regulate arbuscule-specific expression (Fig. S4A). These elements can been found in the promoters of many arbuscule-enhanced genes, including genes involved in fatty acid synthesis and transport as well as genes required for phosphate uptake from the arbuscules (Xue et al., 2018; Jiang et al., 2018; Pimprikar et al., 2018). To study whether *SPX1* and *SPX3* are regulated by WRINKLED1-like transcription factors, we overexpressed *WRI5a* under the control of *LjUB1* promoter in Medicago roots at high Pi conditions. qPCR analyses showed that *SPX1*

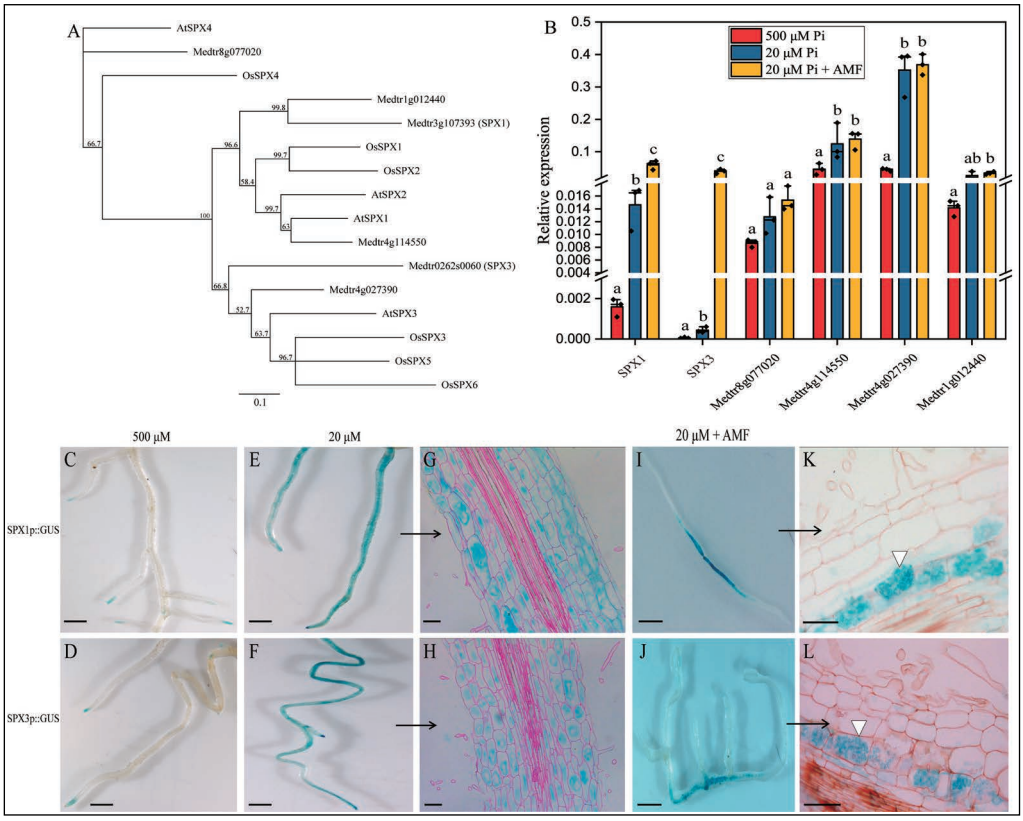

Fig. 1 Medicago SPX1 and SPX3 induced by phosphate starvation and arbuscular mycorrhizal fungi. (A) Phylogenetic relationship of SPX proteins in Medicago, Arabidopsis and Rice. Unrooted tree constructed using Geneious R11.0 by neighbour-joining method with bootstrap probabilities based on 500 replicates. The identifiers of Arabidopsis and rice SPX proteins are listed in Table S4. (B) qRT-PCR analyses of Medicago *SPX* expression at high Pi (500 μM), low Pi (20 μM) and arbuscular mycorrhizal (20 μM Pi plus AM fungi (AMF)) conditions. *SPX1* (Medtr3g107393) and *SPX3* (Medtr0262s0060) are induced at low Pi conditions, and even stronger upon symbiosis with AMF. Medicago *Elongation factor 1* (*MtEF1*) was used as internal reference. Data shown are the individual values of 3 biological replicates. Different letters indicate significant differences ($P < 0.05$) between treatments (ANOVA followed by Tukey's honestly significant difference). (C-D) *SPX1* and *SPX3* are expressed in root tips at 500 μM Pi. Scale bar =1 cm. (E-H) *SPX1* and *SPX3* at 20 μM Pi, (G) and (H) are longitudinal sections of (E) and (F). Sections are counterstained with 0.1% ruthenium red. Scale bar in (C-D), 1 cm, in (E-F), 100 μm. (I-L) SPX1 and SPX3 are highly and specifically induced in arbuscule-containing cortical cells (3 weeks post-inoculation). (K) and (L) are longitudinal sections of (I) and (J), white triangle points to arbuscule-containing cell. Scale bar in (I-J), 1 cm, in (K-L), 100 μm.

and *SPX3* expression are significantly induced by *WRI5a* overexpression (Fig. S4B). This suggests the arbuscule-specific expression of *SPX1* and *SPX3* may controlled by WRI5a. The presence of both P1BS and AW-box cis-regulatory elements may explain the observed expression patterns in the different conditions.

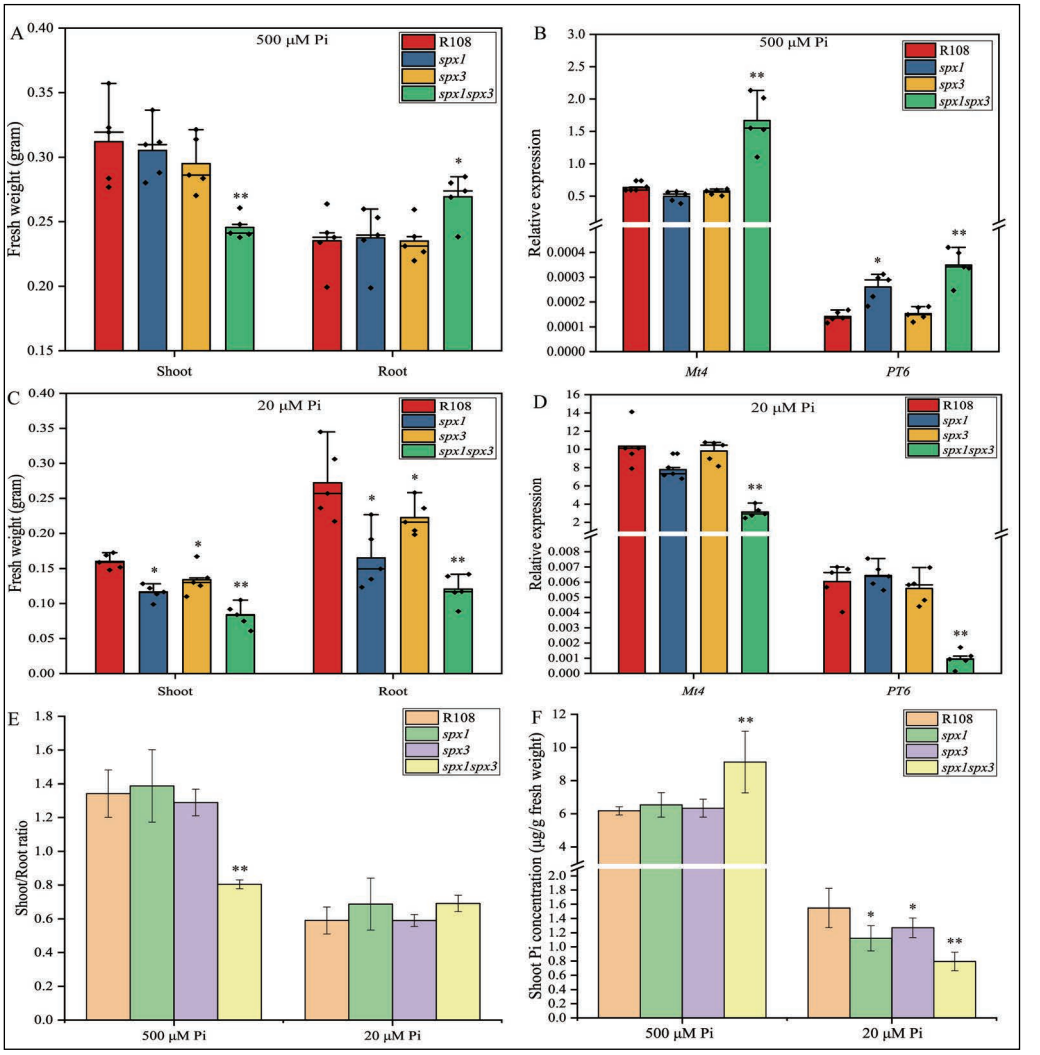

Fig. 2 SPX1 and SPX3 regulate Pi homeostasis. (A) Fresh weight of wild type R108, *spx1*, *spx3* and *spx1spx3* plants grown for 3 weeks at 500 µM Pi. (B) Relative expression of *Mt4* and *PT6* in root samples shown in (A) as determined by qPCR. *MtEF1* is used as reference gene. (C) Fresh weight of wild type R108, *spx1*, *spx3* and *spx1spx3* plants grown for 3 weeks at 20 µM Pi condition. (D) Relative expression of *Mt4* and *PT6* in the root samples shown in (C). Data shown are the individual values of 5 biological replicates. (E) Shoot-to-Root ratio of R108, *spx1*, *spx3* and *spx1spx3* plants shown in (A, C). (F) Shoot cellular Pi concentrations in R108, *spx1*, *spx3* and *spx1spx3* plants from (A, C). Values in (E-F) represent mean ± standard error of 5 replicate plants. All data significantly different from the corresponding R108 wild-type controls are indicated * $P < 0.05$; ** $P < 0.01$ (Student's t-test).

SPX1 and SPX3 regulate phosphate homeostasis

To study the function of SPX1 and SPX3, we identified *spx1* (NF13203_high_1) and *spx3* (NF4752_high_18) Tnt1-retrotransposon insertion mutants (Fig. S5A). Genotyping by PCR confirmed the Tnt1 insertion and a *spx1spx3* double mutant was developed by crossing *spx1* to *spx3* (Fig. S5B). RT-PCR confirmed the impairment of SPX1 and/or SPX3 expression in the respective mutant lines (Fig. S5C).

Since SPX proteins are thought to negatively regulate PHR activity at high Pi conditions to prevent the overaccumulation of phosphate, we first analysed the expression of PSI genes in the mutants and R108 wild-type under high and low Pi conditions. This showed a significantly higher expression of the PSI genes *Mt4* (U76742.1) (Burleigh and Harrison, 1999) and the phosphate transporter encoding gene *PT6* (Medtr1g069935) (Mbodj et al., 2018; Hu et al., 2019) in the *spx1spx3* double mutant under high Pi conditions (Fig. 2B). It correlated with a decreased shoot:root fresh weight ratio indicative of a phosphate starvation response in the double mutant (Fig. 2A, E). Furthermore, phosphate levels were increased in the shoots of the double mutant compared to wild-type plants grown at 500 µM Pi (Fig. 2F). Prolonged growth at 500 µM Pi further showed typical Pi toxicity effects (yellow colouring of the leaf margins) in the leaves of the double mutant (Fig. S6A). The single mutant lines did not show obvious phenotypes when grown at 500 µM Pi condition (Fig. 2A, E, F). These results suggest a negative role of SPX1 and SPX3 on phosphate starvation responses when ample Pi is available.

At low (20 µM) Pi conditions the fresh weight of the *spx1* and *spx3* single mutants was significantly lower than wild-type R108 plants, and the *spx1spx3* double mutant showed an additive effect (Fig. 2C-F, S6B). The leaves of the double mutant further showed accumulation of anthocyanins in the leaves indicative of Pi starvation stress (Fig. S6B). Consistently, the PSI genes *Mt4* and *PT6* were lower expressed in the double mutant compared to the wild type (Fig. 2D), while overexpression of *SPX1/3* enhanced the expression of *Mt4* and *PT6* at low Pi conditions (Fig. 4D). Shoot Pi concentration in single mutants and double mutant were all significantly lower compared to the wild type (Fig. 2F). These results suggest that SPX1 and SPX3 also play a positive role in the PSR response under limiting (20 µM) Pi conditions.

Overall, these results indicate that SPX1 and SPX3 are able to enhance the Pi starvation response at low Pi conditions and inhibit the Pi starvation response at high Pi conditions.

SPX1 and SPX3 interact with PHR2

In Arabidopsis and rice, SPX proteins have been reported to interact with PHR and inhibit its activity under high Pi conditions (Wang et al., 2014b; Puga et al., 2014). Therefore, we checked whether SPX1 and SPX3 could also interact with Medicago PHR homologs. Phylogenetic analyses indicated the presence of three PHR-like proteins in Medicago (Fig. S7). Co-immunoprecipitation analyses of GFP-tagged PHR with FLAG-tagged SPX1/3 proteins expressed in Nicotiana leaves revealed a clear interaction of both SPX1 and SPX3 with MtPHR2 (Medtr1g080330; hereafter PHR2 Fig. 3A). No significant interaction was found for the other two Medicago PHR-like proteins. To study the phosphate-dependency of the interaction we co-expressed GFP-tagged SPX1/3 together with Flag-tagged PHR2 in Medicago roots under high and low Pi conditions. Co-IP analyses showed that SPX1 and SPX3

interact with PHR2 under high Pi conditions, but no interaction were observed in low Pi conditions (Fig. 3B, C).

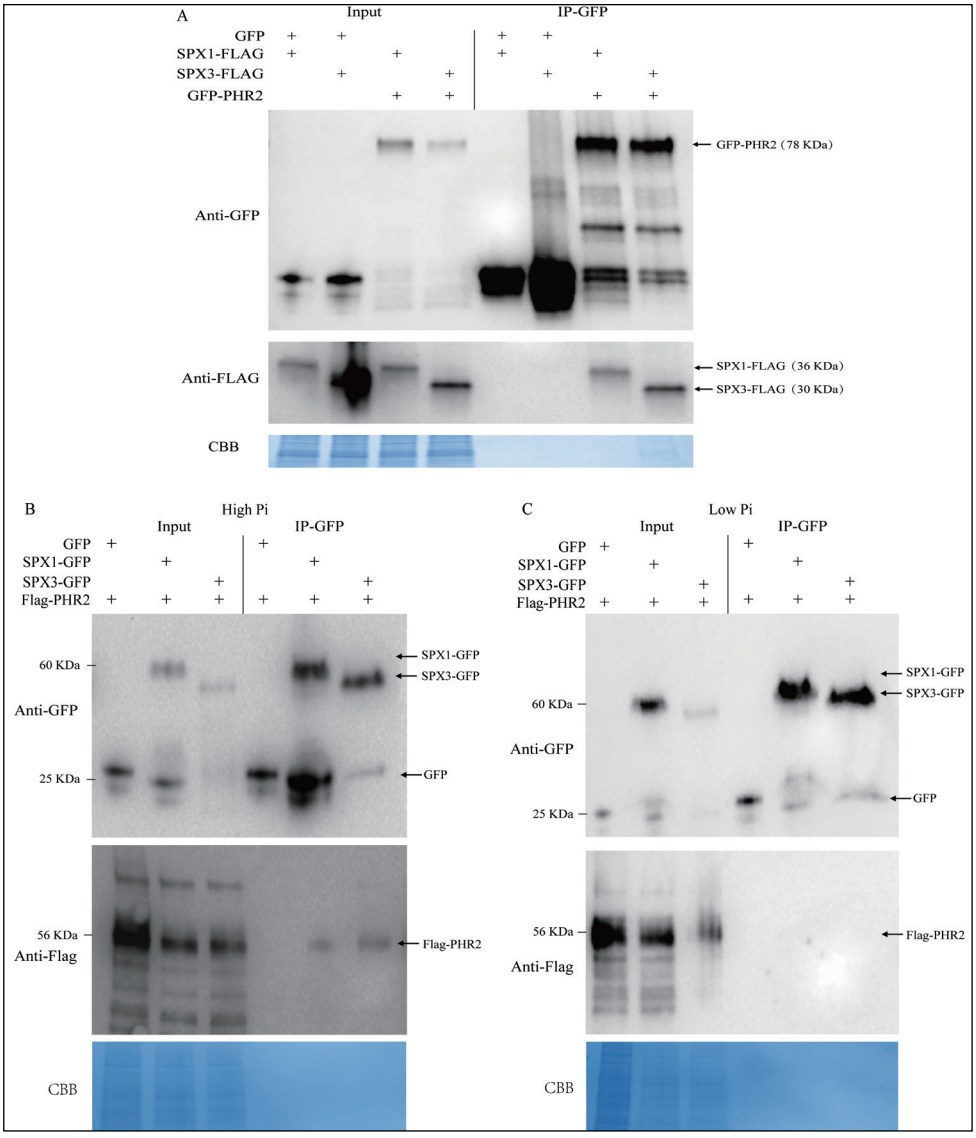

Fig. 3 SPX1 and SPX3 interact with PHR2 at high Pi conditions. (A) Western blot of co-immunoprecipitation samples showing SPX1 and SPX3 interaction with PHR2. FLAG-tagged SPX1 or SPX3 were co-expressed with free GFP or GFP-tagged PHR2 in Nicotiana leaves. Immunoprecipitation (IP) of GFP-tagged proteins shows the co-IP of the FLAG-tagged SPX proteins. (B) Western blot of co-IP samples showing SPX1 and SPX3 interaction with PHR2 in Medicago roots at high Pi conditions. Free GFP, GFP-tagged SPX1 or SPX3 were co-expressed with Flag-tagged PHR2 in Medicago roots on emergence medium with normal Pi concentration for two weeks. IP of GFP-tagged proteins shows the co-IP of the FLAG-tagged PHR2 proteins. (C) Western blot of co-IP samples showing SPX1 and SPX3 have no interaction with PHR2 in low Pi conditions. Medicago roots transformed with the same constructs in (B) grow on emergence medium for two weeks with 20 μM Pi. IP of GFP-tagged proteins shows no FLAG-tagged PHR2 proteins are co-immunoprecipitated. Coomassie brilliant blue (CBB) staining shows total protein levels as loading control.

To study whether PHR2 is indeed involved in the phosphate starvation response, we overexpressed *PHR2* using the *LjUB1* promoter in Medicago roots and analyzed the effect on the expression of PSI genes *Mt4* and *PT6* (Mbodj et al., 2018; Hu et al., 2019). Both *Mt4* and *PT6* are strongly induced under Pi limiting conditions and also show induced expression upon overexpression of *PHR2* (Fig. 4A, B). *PHR2* itself was not regulated in a Pi-dependent manner at the transcriptional level (Fig. 4A), in analogy to its homologs *AtPHR1* (Bustos et al., 2010) and *OsPHR2* (Zhou et al., 2008).

To determine whether the observed Pi related phenotypes are due to a negative regulation of PHR2 activity by SPX1 and SPX3 we overexpressed of *SPX1&3* together with *PHR2*

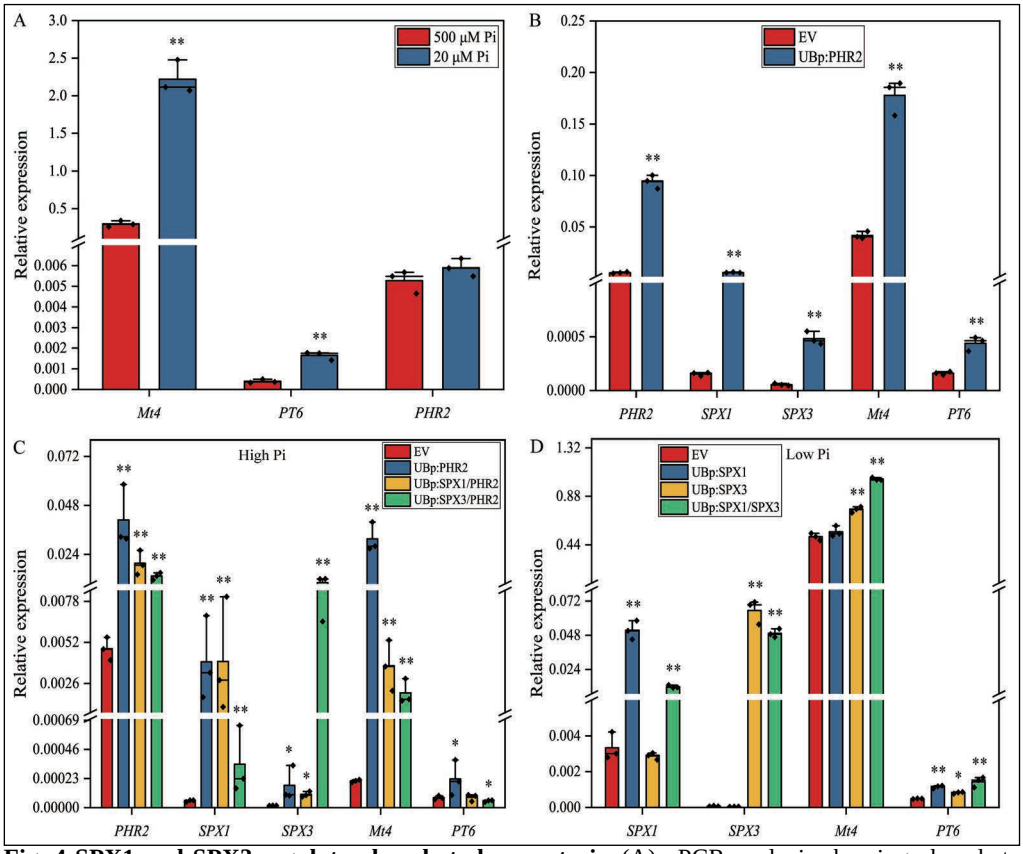

Fig. 4 SPX1 and SPX3 regulate phosphate homeostasis. (A) qPCR analysis showing phosphate starvation induced *Mt4* and *PT6* expression, but not of *MtPHR2* expression in Medicago A17 roots. Data shown are the individual values of 3 Medicago A17 plants. Data significantly different from 500 µM Pi conditions are indicated ** $P < 0.01$ (Student's t-test). (B) qPCR analysis showing that overexpression of *MtPHR2* (*LjUBp::PHR2*) induced *SPX1*, *SPX3*, *Mt4* and *PT6* expression in Medicago A17 transgenic roots grown for 4 days at low Pi conditions. (C) qPCR results showing that overexpression (using the *LjUB1* promoter) of *SPX1* or *SPX3* together with *PHR2* in high Pi conditions induced *Mt4* and *PT6* expression less than overexpression of *PHR2* alone in Medicago A17 transgenic roots. (D) qPCR results showing that overexpression of *SPX1/3* at low Pi conditions induced *Mt4* and *PT6* expression in Medicago A17 transgenic roots. Data shown in (B-D) are the individual values of 3 independently transformed roots. Data significantly different from the corresponding EV transformed controls are indicated * $P < 0.05$; ** $P < 0.01$ (Student's t-test). *MtEF1* was used as reference gene for normalization.

using the *LjUB1* promoter in Medicago roots. This showed that overexpression of *SPX1* or *SPX3* could indeed inhibit the induction of *Mt4* and *PT6* by PHR2 under high Pi conditions (Fig. 4C). We noticed that the (over)expression level of PHR2 was ~ 2x lower for the co-expression constructs containing *SPX1* and *SPX3* compared to overexpression of *PHR2* alone. This is likely a result of the expression construct rather than an effect of SPX1/3 on the activity of the *LjUB1* promoter. The much stronger reduced *Mt4* levels upon co-expression of *SPX1/3* support the inhibitory effect of SPX1/3 on the activity of PHR2 when sufficient Pi levels are reached.

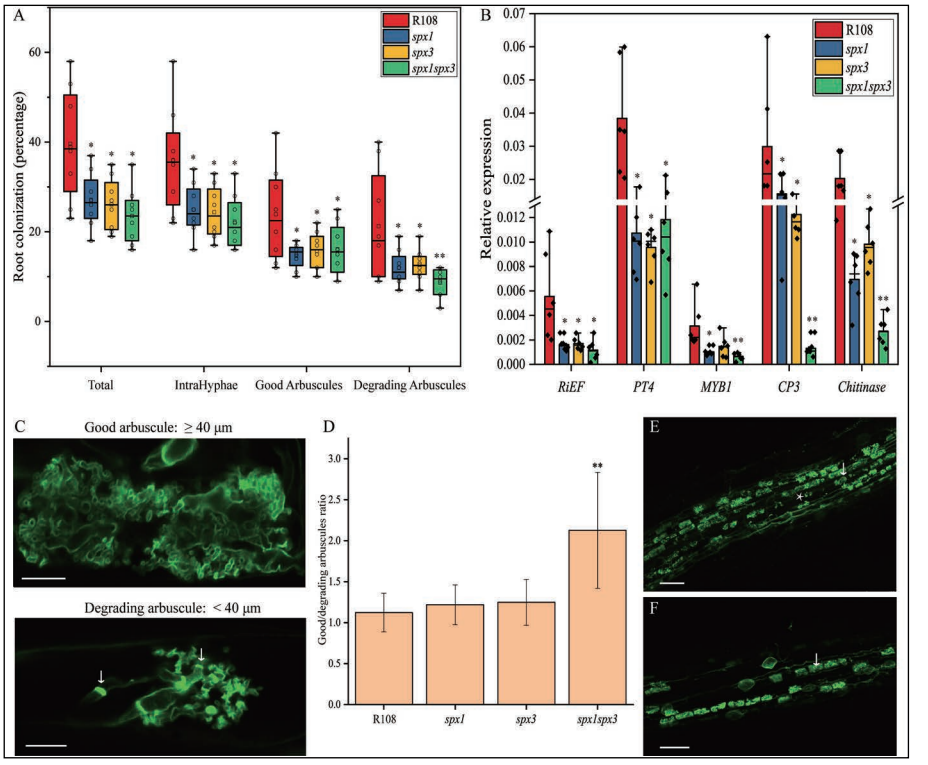

Fig. 5 SPX1 and SPX3 regulate AM colonization and arbuscule degeneration. (A) Quantification of mycorrhization levels in wild type R108, *spx1*, *spx3* and *spx1spx3* 3 weeks post inoculation with *R. irregularis*. 8 independently transformed roots were used as replicas for each sample. Quantification was performed using the magnified intersections method (McGONIGLE et al., 1990). Good arbuscule: larger or equal to 40 µm; Degrading arbuscules: smaller than 40 µm with septa (white arrow in C). Data significantly different from R108 wild-type controls are indicated * $P < 0.05$; ** $P < 0.01$ (Student's t-test). (B) Expression levels of *RiEF*, *PT4*, *CP3*, *Chitinase* and *MYB1* in root samples from (A) determined by qPCR analyses. *MtEF1* was used as internal reference. Data significantly different from R108 wild-type controls are indicated * $P < 0.05$; ** $P < 0.01$ (Student's t-test). (C) Representative images of good arbuscule and degrading arbuscules in WGA-Alexa488 stained roots 3 weeks post-inoculation. Arrow points to septa. Scale bar = 10 µm. (D) Good-to-degrading arbuscule ratio of R108, *spx1*, *spx3* and *spx1spx3* mycorrhizal samples from (A). Values represent mean ± standard error of 8 independently transformed roots. Data significantly different from R108 wild-type controls are indicated ** $P < 0.01$ (Student's t-test). (E) and (F) Representative images of WGA-Alexa488 stained *R. irregularis* in R108 and *spx1spx3*. White arrow marks a good arbuscule. Asterisk marks a degrading arbuscule. Scale bar = 100 µm.

SPX1 and SPX3 regulate AM colonization and arbuscule degeneration

Next, we examined the role of SPX1 and SPX3 in the interaction with AM fungi. Three weeks after inoculation with *R. irregularis* spores, mycorrhization was quantified in the *spx1* and *spx3* single mutants, the *spx1spx3* double mutant and R108 wild-type controls using the magnified intersect method (McGONIGLE et al., 1990). Eight plants were used as replicates for each line. Compared to R108, single mutant and double mutant plants all showed significantly lower root colonization levels and arbuscule abundance (Fig. 5A). Transcript levels of *RiEF* and *PT4*, molecular markers for respectively fungal colonization and arbuscule abundance, confirmed the lower colonization levels in the mutants (Fig. 5B).

Because SPX1 and SPX3 are specifically expressed in arbuscule-containing cells in mycorrhized roots, arbuscule morphology was quantified in more detail. We defined arbuscules larger or equal to 40 µm as "good" arbuscules, and arbuscules smaller than 40 µm with typical features of degradation, including visible septa, as "degrading" arbuscules (Fig. 5C). Interestingly, there were significantly fewer degrading arbuscules in the *spx1spx3* double mutant compared to R108 wild-type plants, resulting in a much higher good/degrading arbuscule ratio (Fig. 5A, E, F). spx1 and spx3 single mutant showed a similar good/degrading arbuscule ratio as wild-type R108 (Fig. 5A), suggesting a redundant role for SPX1 and SPX3 in the regulation of arbuscule degradation. To further determine the effects on arbuscule morphology, we checked *PT4*, *CP3* and *Chitinase* expression in Fig. 5B with normalization to the fungal *RiEF*. A significantly higher *PT4* expression and lower *CP3, Chitinase* were detected in *spx1spx3* double mutant (Fig. S8A). In line with this, arbuscule size (length) distribution also showed there are more 50-60, 60-70 and 70-80 µm of arbuscules in *spx1spx3* double mutant compared to R108 wild type, and less 20-30 and 30-40 µm of arbuscules were observed in *spx1spx3* double mutant. These results indicating SPX1 and SPX3 indeed regulate arbuscule degradation.

Arbuscule degradation in Medicago is regulated by the MYB1 transcription factor, which controls the expression of hydrolase genes such as *Cysteine Protease 3* (*CP3*) and *Chitinase* (Floss et al., 2017). qRT-PCR analyses showed a strongly impaired expression of these hydrolase genes in the *spx1spx3* double mutant (Fig. 5B). Similar phenotypes were observed upon knock-down of both *SPX1* and *SPX3* by RNA interference (Fig. S9A, B). To further confirm that the phenotype was indeed caused by a mutation in *SPX1* and *SPX3*, we complemented the *spx1spx3* double mutant by driving *SPX1* and *SPX3* expression from by their native promoters in *A. rhizogenes* transformed roots. This indeed complemented the mycorrhization levels, arbuscule abundance and marker gene expression to wild-type levels (Fig. S9C, D), showing that the phenotypes are not caused by background insertions/mutation in the mutant lines.

Overall, these results indicate that both SPX1 and SPX3 positively regulate AM colonization levels and redundantly regulate arbuscule degradation.

SPX1 and SPX3 likely control AM colonization by regulating strigolactone levels

To explain the positive role of SPX1 and SPX3 in mycorrhizal colonization, we found that the expression of a key gene required for strigolactone biosynthesis, *MtDWARF27* (*D27*; (Hao et al., 2009; Liu et al., 2011) was not (or much lower) induced upon Pi starvation in *spx1* and *spx3* single mutants compared to wild-type plants (Fig. 6A). No additive effect

on *D27* expression was observed in the *spx1spx3* double mutant. Under low phosphate conditions, strigolactone levels increase drastically in several species and this induction in strigolactone biosynthesis correlates with an increased *D27* expression under this condition (Liu et al., 2011) (Fig. 6A). *D27* expression was induced when SPX1 and SPX3 were overexpressed together at low Pi conditions using the *LjUB1* promoter in *A. rhizogenes* transformed roots (Fig. S10A). At high Pi conditions D27 expression did not appear to be affected (Fig. S10B). This revealed a positive effect of SPX1 and SPX3 on *D27* expression at low Pi conditions, and thereby possibly on strigolactone levels. Reduced strigolactone levels could explain the lower colonization levels observed in the mutants as these are key signal molecules that induce growth and branching in AM fungi (Besserer et al., 2006; Tsuzuki et al., 2016). Unfortunately, we were unable to detect known strigolactone levels in the R108 genetic background. This may be caused by sub-detection levels or as yet unknown strigolactone derivates in R108. As an alternative, we used an AM hyphal branching assay as proxy for strigolactone levels in root exudates (Besserer et al., 2006, 2008). This demonstrated that exudates collected from the *spx1/3* mutant roots, grown under Pi limiting condi-

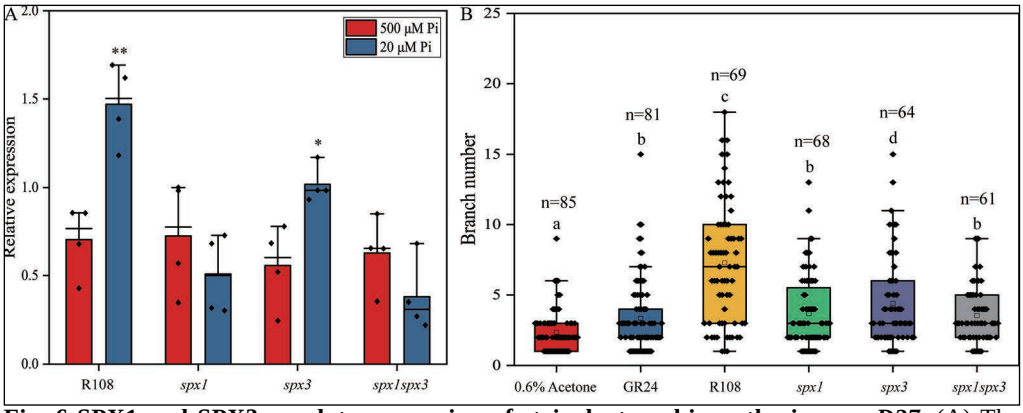

Fig. 6 SPX1 and SPX3 regulate expression of strigolactone biosynthesis gene *D27*. (A) The induction of D27 expression in low Pi conditions is impaired in *spx1*, *spx3*, and *spx1spx3* mutants. Data shown are the individual values of 3 plant replicates. Data significantly different from corresponding controls are indicated * $P < 0.05$; ** $P < 0.01$ (Student's t-test). (B) *R. irregularis* spores treated with root exudates of R108, *spx1*, *spx3* and *spx1spx3* for 8 days. 0.01 µM GR24 and 0.6% acetone were respectively used as positive and negative controls. Hyphal branch numbers in spores treated with root exudates of *spx1*, *spx3* and *spx1spx3* mutants are significantly lower compared to spores treated with R108 root exudates. n indicates the number of spores counted. Data shown are the individual values of the replicates, different letters indicate significant difference ($P < 0.05$) between treatments (ANOVA followed by Tukey's honestly significant difference).

tions, were much less able to induce *R. irregularis* branching compared to wild-type R108 root exudates (Fig. 6B, S10C). Furthermore, the root exudates were applied to the seeds of parasitic plant *Phelipanche ramosa*, germination rates were scored after 12 days. The exudates of R108 plants induced 21% germination, while no clearly germination was induced when apply the exudates of *spx1*, *spx3* and *spx1spx3* mutant (Fig. S10D, E). This suggests the strigolactones concentration in the mutants root exudates are much lower than in R108 root exudates. And thus failed to induce *P. ramosa* germination. Different concentration of GR24 was used as positive control and they all induced over 50% of germination (Fig. S10D). Together these data strongly suggests that strigolactone levels are reduced in the spx

mutants, although an additional effect on other root exudates cannot be ruled out.

Overexpression of SPX1 and SPX3 increases AM colonization and arbuscule degradation

The mutant analyses showed that SPX1 and SPX3 redundantly regulate arbuscule degradation. To further study this we overexpressed *SPX1*, *SPX3*, and *SPX1;SPX3* together under the control of the *LjUB1* promoter. This resulted in significantly increased colonization

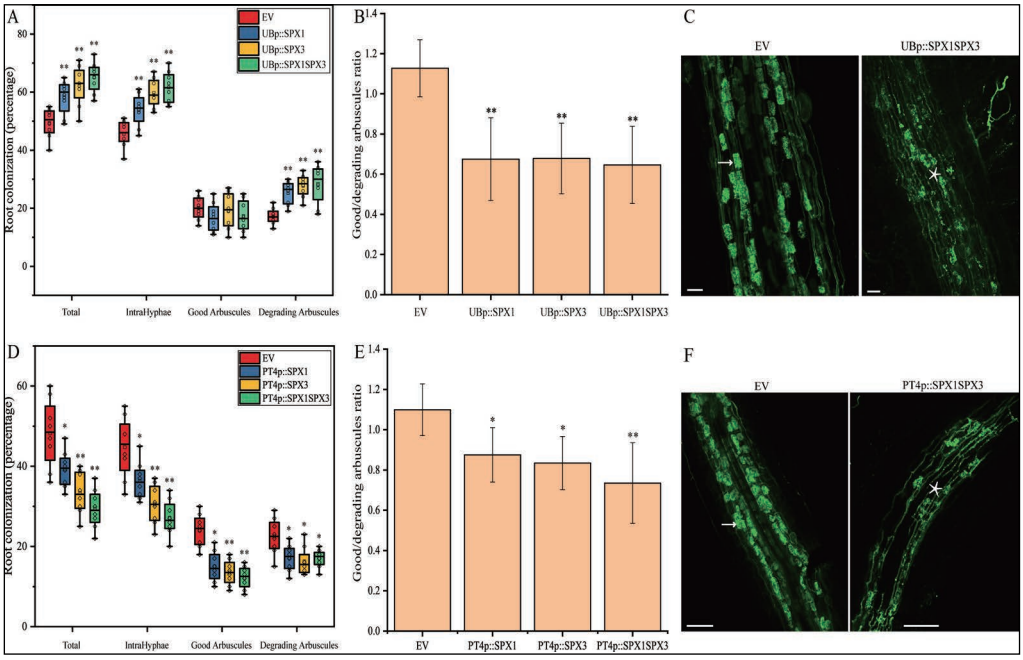

Fig. 7 Overexpression of *SPX1/3* under the control of the *LjUbiquitin* or *MtPT4* promoter increased AM colonization and/or arbuscule degradation. (A) Quantification of mycorrhization level in *M. truncatula* A17 roots expressing EV, *UBp::SPX1*, *UBp::SPX3*, and *UBp::SPX1-UBp::SPX3* 3 weeks post inoculation with *R. irregularis*. 8 independently transformed plants were used as replicas for each sample. Quantification was performed using the magnified intersections method (McGONIGLE et al., 1990). (B) Good-to-Degrading arbuscule ratio of EV, *UBp::SPX1*, *UBp::SPX3* and *UBp::SPX1-UBp::SPX3* mycorrhizal samples from (A). Values represent mean ± standard deviation of 8 independently transformed roots. (C) Representative confocal images of WGA-Alexa488 stained *R. irregularis* in EV and *UBp::SPX1-UBp::SPX3* roots. White arrow marks a good arbuscule. Asterisk marks a degrading arbuscule. Scale bar = 80 µm. (D) Quantification of mycorrhization level in *M. truncatula* A17 roots expressing EV, *PT4p::SPX1*, *PT4p::SPX3* and *PT4p::SPX1-PT4p::SPX3* 3 weeks post inoculation with R. irregularis. 8 independently transformed plants were used as replicas for each sample. Quantification was performed using the magnified intersections method (McGONIGLE et al., 1990). (E) Good-to-Degrading arbuscule ratio of EV, *PT4p::SPX1*, *PT4p::SPX3* and *PT4p::SPX1-PT4p::SPX3* mycorrhizal samples from (D). Values represent mean ± standard deviation of 8 independently transformed roots. (F) Representative confocal images of WGA-Alexa488 stained *R. irregularis* in EV and *PT4p::SPX1-PT4p::SPX3* roots. White arrow marks a good arbuscule. Asterisk marks a degrading arbuscule. Scale bar = 100 µm. All data in (A, B, D, E) significantly different from the corresponding EV controls are indicated * $P < 0.05$; ** $P < 0.01$ (Student's t-test).

levels in individual *LjUBp:SPX1* and *LjUBp:SPX3* transgenic roots as well as double transgenic lines compared to empty vector control roots 3 weeks post inoculation (Fig. 7A). Furthermore, the ratio of good/degrading arbuscule was significantly lower in the *SPX1/3* overexpression roots indicating a premature degradation of arbuscules (Fig. 7A-C). qRT-PCR analyses confirmed the observed phenotypes (Fig. S11A). *RiEF* was higher expressed in *SPX1* and *SPX3* overexpression roots compared to empty vector (EV) controls expressed roots. The expression level of *PT4* as a marker for healthy arbuscules was similar between EV control roots and the *SPX* overexpressing roots. However, arbuscule degradation related genes *CP3* and *Chitinase* were enhanced in the *SPX* overexpressing roots. We observed a differential effect of SPX1 and SPX3 overexpression on *MYB1* expression, with only *SPX3* overexpression causing increased *MYB1* expression (Fig. S11A).

To separate the arbuscule-specific effects of SPX1/3 from non-symbiotic roles, we expressed *SPX1*, *SPX3*, or both, using the arbuscule-specific *PT4* promoter. Interestingly, compared to EV transformed roots decreased colonization levels were observed in all *SPX* overexpressing roots when expressed from the *PT4* promoter (Fig. 7D). This coincided with decreased arbuscule abundance and an increased ratio of degrading arbuscule compared to good arbuscule classes (Fig. 7D-F). Transcript levels of the markers for fungal biomass (*RiEF*), healthy arbuscule abundance (*PT4*) and arbuscule degradation (*MYB1*, *CP3* and *Chitinase*) all confirmed the visual phenotyping results (Fig. S11B). Because the colonization levels in *SPX* expressing roots were much lower than EV control roots and because *SPX1* and *SPX3* are normally highly induced in arbuscule-containing cells the overall *SPX1/3* expression levels did not exceed those in the EV controls (Fig. 1B, 7D, S11B). Overall, these results further strengthen the role for SPX1/3 in regulating AM colonization and arbuscule degradation.

PHR2 can induce arbuscule degradation

Next we investigated whether the SPX1/3 interactor PHR2 affects arbuscule development. Surprisingly, overexpression of *PHR2* using the constitutive *LjUB1* promoter caused the induction of *MYB1*, *CP3* and *Chitinase* expression already under non-symbiotic (low Pi) conditions (Fig. S12A). Although the promoters of these genes do not contain the PHR binding *cis*-regulatory P1BS element, we did find this element in the promoters of the potential MYB1 upstream transcriptional regulators *WRI5a* and *RAM1* (Fig. S13A). This suggested that PHR2 may induce *RAM1* and *WRI5a* leading to *MYB1* expression. Indeed, we observed that both *RAM1* and *WRI5a* were induced upon *PHR2* overexpression under non-symbiotic conditions (Fig. S12A). In line with this, *WRI5a* overexpression induced *MYB1* expression (Fig. S12B).

To determine whether overexpression of PHR2 would also lead to premature arbuscule degradation we overexpressed *PHR2* under the control the arbuscule-specific *PT4* promoter. Strikingly, this resulted in an even more severe phenotype than observed upon *PT4p::SPX1/3* overexpression three weeks after inoculation with *R. irregularis*. Colonization levels were strongly reduced and very few “good” arbuscules were observed (Fig. S12C). Furthermore, most arbuscules appeared to be completely degraded (Fig. S12C, D, F). These observations were corroborated by the expression levels of *RiEF* and *PT4* in these roots, compared to EV control roots (Fig. S12E). However, despite the high level of degraded arbuscules, the arbuscule degeneration markers *CP3* and *Chitinase* were also much lower ex-

pressed in the *PT4::PHR2* roots when compared to EV control roots. RNAseq data suggest that *PHR2* is weakly expressed in arbuscule-containing cells (Fig. S13B; Zeng et al., 2018). This suggests that the very strong induction of *PHR2* leads to the abortion of arbuscule development already at a very early stage.

The ability of both SPX1/3 and PHR2 to induce arbuscule degradation is difficult to reconcile with the observed negative effect of SPX1/3 on PHR2 activity. Although the temporal Pi status of arbuscule-containing cells is not known it can be expected that there is no Pi shortage in these cells as long as the arbuscules are active. Therefore, SPX1/3 would be expected to suppress PHR2 activity in cells with active arbuscules. Nevertheless, our data showed that timely arbuscule degradation requires both SPX1 and SPX3, and their overexpression induced premature arbuscule degradation. This raises the question how SPX1/3 can then induce arbuscule degradation?

SPX1 and SPX3 in relation to known transcriptional regulators of arbuscule degradation

The MYB1 transcription factor was reported to be required for arbuscule degradation when the fungus does not provide sufficient nutrients. Knock-down of *MYB1* could rescue the premature arbuscule degradation phenotype observed in *pt4* mutants that lack a functional symbiotic PT4 phosphate transporter (Floss et al., 2017). To study whether SPX1/3 can also rescue the *pt4* phenotype, we knocked down both *SPX1* and *SPX3* using RNAi in the *pt4-1* mutant background (Javot et al., 2007). This resulted in strongly reduced mycorrhization levels in *EFp:SPX1-SPX3-rnai* transformed *pt4-1* mutant roots compared to EV controls 3 week after inoculation (Fig. S14A). However, the ratio of "Good" to "degrading" arbuscules was not significantly different between *SPX1/3 RNAi-pt4* and *EV-pt4* samples (Fig. S14A, B). qPCR analyses further confirmed the observed phenotypes (Fig. S14C). This suggests that SPX1/3 function is not essential for arbuscule degradation in this setting.

It was further shown that overexpression of *MYB1* can trigger the premature degradation of arbuscules (Floss et al., 2017). To position the action of SPX1/3 on arbuscule development in relation to MYB1, we overexpressed *MYB1* under the control of the constitutive *CaMV35S* promoter in the *spx1spx3* double mutant and checked whether *CP3* and *Chitinase* could still be activated. Compared to EV transformed roots, *CP3* and *Chitinase* expression were significantly induced by MYB1 in the *spx1spx3* double mutant 3 weeks post inoculation and lower colonization levels, with less *RiEF* and *PT4* expression, and signs of premature arbuscule degradation were detected (Fig. S14D, S15). This indicates that SPX1/3 functions either upstream or parallel of MYB1 to control arbuscule turnover. To distinguish between these possibilities, we overexpressed both *SPX1* and *SPX3* together and studied the effect on *MYB1* expression and its target genes under non-symbiotic conditions. At both high and low Pi conditions, overexpression of *SPX1* and *SPX3* (*LjUB1p:SPX1- LjUB-1p:SPX3*) did not (significantly) affect *MYB1* expression (Fig. S14E, F), which suggests that SPX1 and SPX3 likely do not function upstream of *MYB1* to directly control its expression. The expression of the hydrolase-encoding gene *CP3* was also not induced upon overexpression of *SPX1&3* and the expression of *Chitinase* was only weakly affected at low Pi conditions (Fig. S14E, F). The lack of/weak effect on *CP3* and *Chitinase* expression may be caused by the low expression levels of *MYB1* under non-symbiotic conditions.

Based on the results obtained in this study we propose the following model (Fig. 8), where

SPX1 and SPX3 act as negative regulators of a yet-to-identify negative regulator of MYB1 activity. This negative regulation of MYB1 activity likely requires sufficient Pi conditions in the arbuscule containing cells. When cells have acquired sufficient Pi SPX1/3 will ensure the timely degradation of the arbuscules.

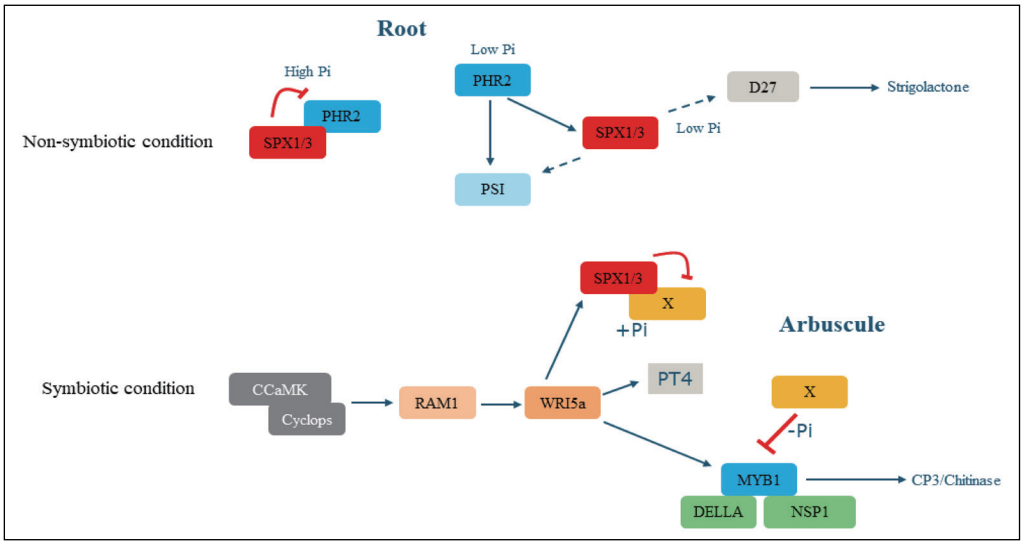

Fig. 8 Proposed model for SPX1/3 function. In high Pi conditions, SPX1 and SPX3 interact with PHR2, inhibiting PHR2-induced PSI gene expression. In low Pi conditions, PHR2 induces phosphate starvation induced (PSI) genes as well as *SPX1/3* expression. SPX1 and SPX3 play a positive role in the expression of PSI genes (*Mt4* and *PT6*) and *D27*. *D27* is a key gene involved in strigolactone biosynthesis. Strigolactones act as signaling molecules to enhance the growth and metabolism of AM fungi. In symbiotic conditions, SPX1 and SPX3 redundantly regulate arbuscule degeneration likely through an yet-to-be-identified factor X, which negatively regulate MYB1 activity. *SPX1* and *SPX3* are induced by the RAM1-WRI5 transcriptional cascade that also induces *PT4* and *MYB1* expression. The activity of X is suppressed by binding of SPX1/3 in Pi-dependent manner. This relieves the inhibition of MYB1 activity that, together with DELLA and NSP1 transcription factors, induces arbuscule degradation genes such as *CP3* and *Chitinase* leading to arbuscule degradation. Red lines indicate Pi dependent negative regulation at the protein level. Solid arrows indicate known transcriptional induction. Dashed arrows indicate direct/indirect transcriptional regulation based on the data presented.

Discussion

SPX proteins have emerged as key sensors and signaling regulators of cellular phosphate status in plants (Wild et al., 2016; Wang et al., 2014b; Puga et al., 2014; Shi et al., 2014; Hu et al., 2019). Here we show that the Medicago single SPX-domain proteins SPX1 and SPX3 not only regulate Pi homeostasis under non-symbiotic conditions, but also regulate root colonization and arbuscule degradation during AM symbiosis. This offers important novel insight into the Pi-dependent regulation of this agriculturally and ecologically important symbiosis.

Under non-symbiotic conditions, SPX1 and SPX3 control Pi homeostasis in part through the regulation of PHR2 activity. In analogy to the situation in Arabidopsis and rice, phosphate starvation leads to the activation of PHR activity to control transcriptional responses.

Among the targets of PHR2 are the *SPX1/3* genes. Both SPX1 and SPX3 can bind PHR2 at high Pi conditions and negatively affect the PSR response to prevent overaccumulation of Pi. We show that SPX1 and SPX3 also control the induction of strigolactone biosynthesis gene *D27* (Liu et al., 2011) under Pi-limiting conditions. This suggests that SPX1 and SPX3 play an additional positive role in the transcription of Pi-starvation induced genes under low Pi conditions. This is further supported by the observation that SPX1 and SPX3 play a positive role in the PSR response at low Pi conditions, in addition to their negative regulation of PSR at high Pi conditions. Such additional, possibly PHR-independent roles, have also been suggested for OsSPX3 and OsSPX5 (Shi et al., 2014). Since D27 plays an essential role in the biosynthesis of strigolactones (Hao et al., 2009), which activate AM fungi, the role of SPX1 and SPX3 in its induction could explain the lower colonization levels observed in the *spx1* and *spx3* mutants. This hypothesis is strongly supported by the reduced stimulatory effect of root exudates from the *spx1* and *spx3* mutant on AM hyphal branching compared to the R108 wild type and *P. ramosa* germination. However, the current inability to measure strigolactone levels in the R108 genetic background prevented us from confirming this directly. Therefore, it cannot be excluded that other stimulatory components in the exudates are also affected in the *spx* mutants. The effect on strigolactone/root exudates would also explain the stimulatory effect of overexpression of *SPX1/3* using the constitutive *LjUB1* promoter on fungal colonization levels (Fig. 6a). In contrast, overexpression of *SPX1/3* under the control of the arbuscule-specific *PT4* promoter leads to a decrease in fungal colonization (Fig. 6d). The arbuscule-specific expression likely prevents the stimulatory effect of SPX1/3 on root exudation while still reducing the level of functional arbuscules leading to overall lower colonization levels.

The induction of *SPX1* and *SPX3* upon Pi starvation or PHR2 overexpression fits with the presence of the P1BS *cis*-regulatory element in the promoters of these genes. However, after establishment of the AM symbiosis, the expression of both *SPX1* and *SPX3* becomes restricted from an ubiquitous expression pattern to specific expression in the arbuscule-containing cells. This suggests that activity of PHR in the non-colonized root cortical and epidermal cells is inhibited upon a functional AM symbiosis in a non-cell autonomous manner. It has been proposed that AM fungi may interfere with the direct phosphate uptake of plants (Smith et al., 2004; Christophersen et al., 2009; Yang et al., 2012; Wang et al., 2020), although the mechanisms for this are still unknown. Another possibility is a more systemic regulation of the phosphate starvation response through hormonal or peptide signaling as the plant is obtaining Pi from the fungus (Müller and Harrison, 2019). Although we cannot pinpoint at what time after initiation of the symbiosis, or level of colonization, the shift in expression exactly occurs based on our analyses, the fact that we hardly see expression in non-colonized root cells, nor in non-transgenic roots on the same composite plants, already after 3 weeks of inoculation suggests a rather fast systemic regulation.

It is currently not known whether PHR2 is active in arbuscule-containing cells, as contrasting roles for the P1BS element in the expression of symbiotic phosphate transporters have been reported (Chen et al., 2011; Lota et al., 2013). Overexpression of *PHR2* specifically in arbuscule-forming cells caused the very rapid, premature, degradation of arbuscules. This correlated with the ability of PHR2 to induce arbuscule-development related genes, including arbuscule degradation genes under low Pi conditions. However, PHR2 is very weakly expressed in arbuscule-containing cells as discussed above (Fig. S13B). Furthermore, the presence of SPX1/3 would be expected to suppress PHR2 activity upon Pi supply by the

arbuscules as it does under non-symbiotic conditions. Instead, the induction of *SPX1* and *SPX3* in arbuscule-containing cells correlates with the presence of multiple AW-boxes and CTTC elements in the promoters of both genes. These *cis*-regulatory elements are found in many genes that are induced in arbuscule-containing cells, and are bound by WRINKLED1-like TFs that are in turn activated by the key GRAS transcription factor RAM1 that controls arbuscule formation (Jiang et al., 2018; Xue et al., 2018; Limpens and Geurts, 2018; Pimprikar et al., 2018). In line with involvement of WRI1-like TFs in the regulation of SPX1/3 expression, overexpression of *WRI5a* indeed induced *SPX1* and *SPX3* expression (Fig. S4B). A further link between *RAM1*, *WRI5a* and *SPX3* expression is supported by the lack of *SPX3* induction in the *ram1* mutant (table S3) (Luginbuehl et al., 2017).

Since Pi levels are most likely not limiting in cells containing active arbuscules, the impaired induction of *CP3* and *Chitinase* and associated arbuscule degradation in the *spx1spx3* double mutant argues for the involvement of SPX1/3 interacting proteins other than PHR2. The observation that *MYB1* overexpression was able to trigger premature arbuscule degradation in the *spx1spx3* double mutant indicates that MYB1 can bypass SPX1/3 to induce arbuscule degradation. We were unable to detect a significant interaction between SPX1 or SPX3 with the currently known regulators of arbuscule degradation, MYB1 and its interacting partners NSP1 and DELLA (Floss et al., 2017); see Chapter 5. This leaves us with the question how SPX1 and SPX3 might control arbuscule degradation? Based on our findings we propose that SPX1 and SPX3 negatively regulate a yet unknown negative regulator of MYB1 activity in a Pi-dependent manner (Fig. 8). *MYB1* expression is already strongly induced at an early stage of arbuscule formation, most likely due to the RAM1-WRI5 transcriptional cascade. However this induction does not lead to the degradation of the arbuscules (Floss et al., 2017). Therefore, it seems that the activity of MYB1 is suppressed as long as the fungus provides (sufficient) Pi to the host cell. Ectopic overexpression of *MYB1* can trigger the premature degradation of the arbuscules suggesting that the proposed negative regulator is not expressed yet or that high MYB1 levels can override the negative regulation. SPX1 and SPX3 are predicted to sense the amount of Pi provided by the fungus in the arbuscule-containing cells. If Pi levels exceed the demand SPX1 and SPX3 may redundantly inhibit the negative regulation of MYB1 activity thereby terminating the arbuscule.

It is tempting to speculate that SPX proteins may also be involved in the cross-talk with other nutrients supplied by the fungus, such as nitrogen. This suggestion is based on the involvement of OsSPX4 in nitrate signaling to activate the phosphate starvation response (Hu et al., 2019) and the reported nitrogen-control of arbuscule development (Breuillin-Sessoms et al., 2015). For example, the premature arbuscule degradation in the *pt4* mutant was also suppressed when the plants were grown under N-limiting conditions (Breuillin-Sessoms et al., 2015). This was shown to depend on the ammonium transceptor AMT2;3. It will therefore be interesting to test whether SPX1 and SPX3 contribute to this nutrient crosstalk in Medicago.

In conclusion, we reveal novel roles for phosphate sensing SPX proteins in the regulation of AM symbiosis to enhance the phosphate acquisition efficiency of plants. SPX proteins show both a role in the initiation of the symbiosis, likely in part through their effect on the expression of the strigolactone biosynthesis gene *D27*, as well as a role in the termination of the symbiosis by controlling the degradation of arbuscules. The latter role can be essential to maintain the beneficial nature of the interaction. In nature plants are most often colonized

by multiple different AM strains that can differ in the amount of nutrients they supply (Kiers et al., 2011). Therefore SPX proteins can provide a means to locally monitor whether a fungal partner provides sufficient nutritional benefits. Further unraveling how nutrient sensing and homeostasis are regulated during AM symbiosis will be pivotal to understand the ecological workings of this key symbiosis and how to best exploit it for more sustainable agriculture practices.

Supplementary Figures

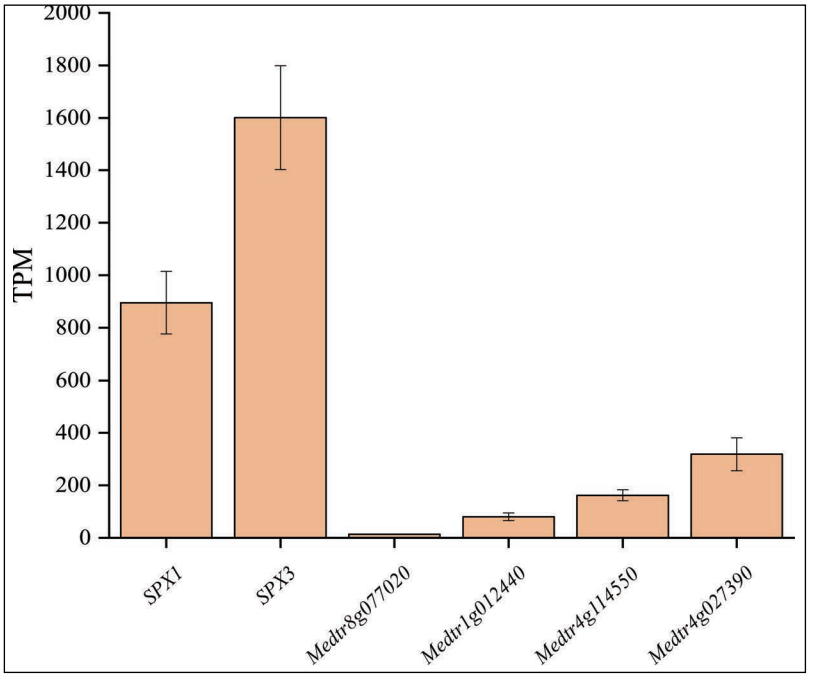

Fig. S1 *SPX1* and *SPX3* are highly expressed in arbuscule-containing cells. RNAseq data of laser microdissected Medicago roots colonized by *R. irregularis* showing that *SPX1* and *SPX3* are the dominant SPX members expressed in arbuscule-containing cells. Data collected from (Zeng et al,. 2018). TPM= transcripts per million.

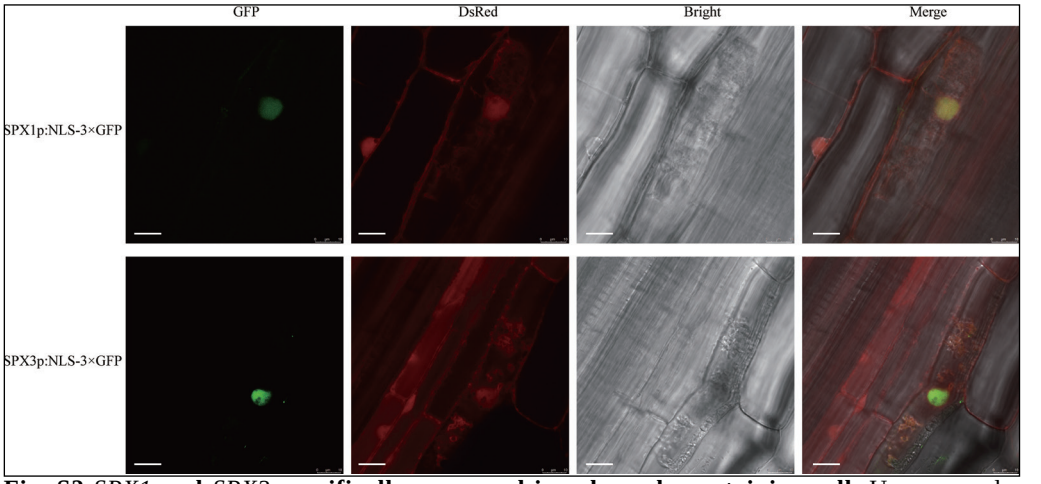

Fig. S2 *SPX1* and *SPX3* specifically expressed in arbuscule-containing cell. Upper panels: Confocal images of nuclear localization signal (NLS)-3×GFP expressed from the *SPX1* promoter in mycorrhized *Medicago truncatula* roots. Bottom panels: Confocal images of NLS-3×GFP expressed from the *SPX3* promoter. A co-expressed *UBp::DsRed* marker localizes to the nucleus and cytoplasm. Different panels represent the following channels (from left to right): GFP, DsRED, Bright field and all channels merged. GFP signal can only be detected in arbuscule-containing cell, while DsRed signal can be detected in neighboring non-colonized cortex cells. Scale bar = 10 μm.

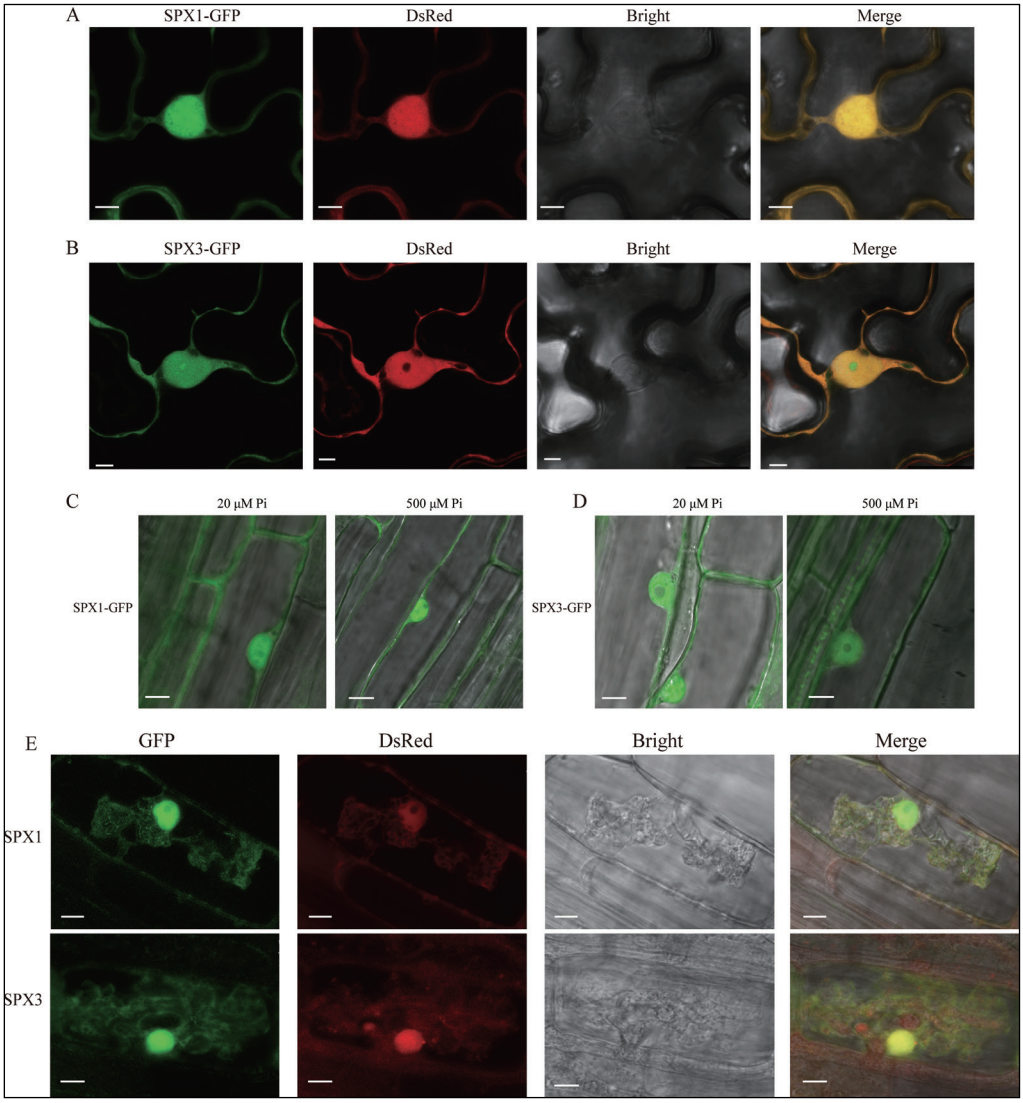

Fig. S3 SPX1 and SPX3 localise to the nucleus and cytoplasm. (A) Confocal images of SPX1-GFP expressed from a constitutive *LjUbiquitin* promoter in *Nicotiana benthamiana* leaves. A co-expressed *UBp::DsRed* marker localizes to the nucleus and cytoplasm. Different panels represent the following channels (from left to right): GFP, DsRED, Bright field and all channels merged Scale bar = 8 µm. (B) Confocal images of *LjUBp::SPX3-GFP* in *N. benthamiana* leaves Scale bar = 5 µm. (C) Confocal images of *LjUBp::SPX1-GFP* in *Medicago truncatula* roots localizing to the nucleus and cytoplasm in low Pi and high Pi conditions. Scale bar = 10 µm. (D) Confocal images of *LjUBp::SPX3-GFP* expressed in *M. truncatula* roots in low Pi and high Pi conditions. Scale bar = 8 µm. (E) Confocal images of SPX1-GFP and SPX3-GFP expressed from their own promoter in *M. truncatula* roots in arbuscule-containing cells. Scale bar = 10 µm.

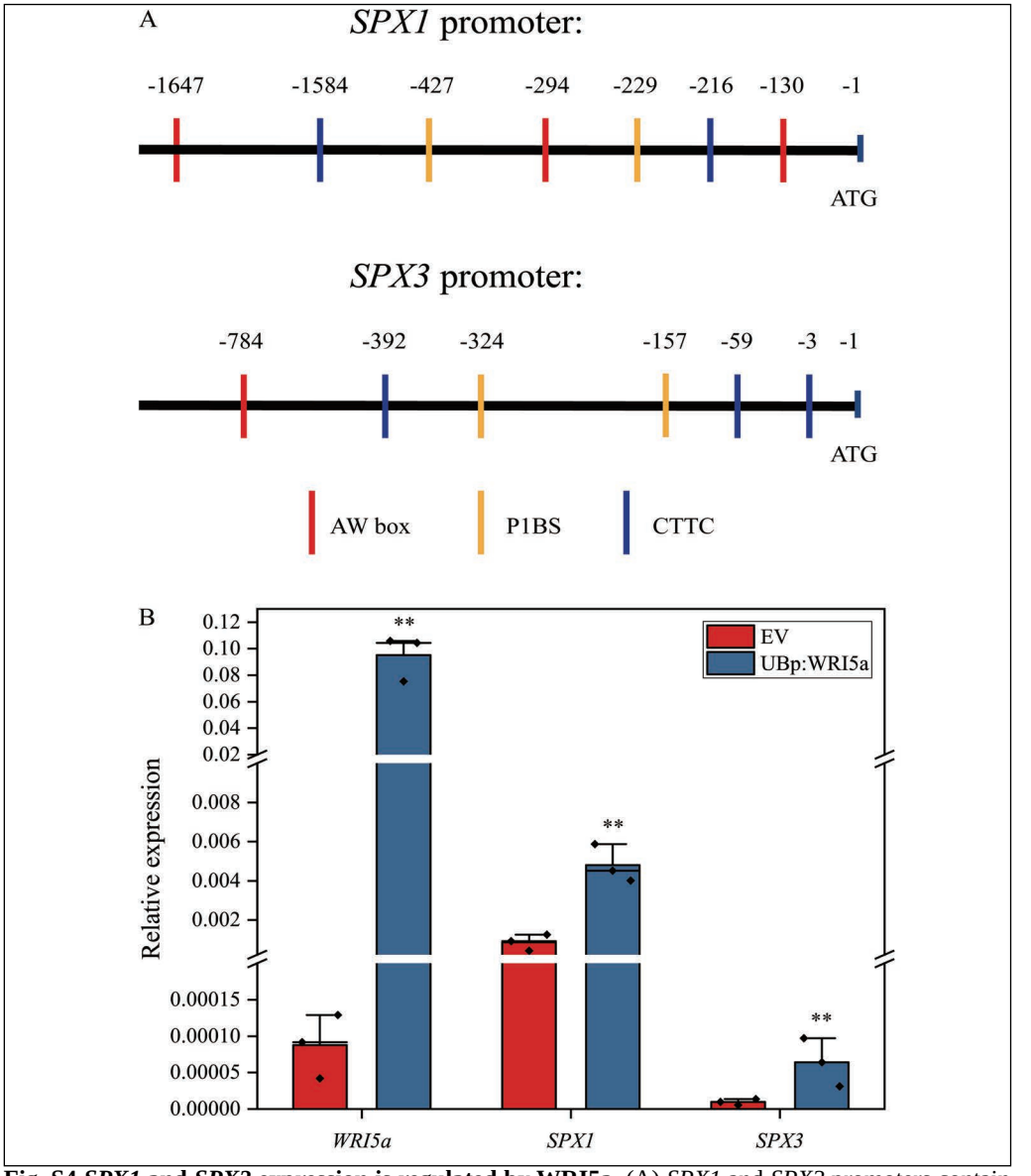

Fig. S4 *SPX1* and *SPX3* expression is regulated by WRI5a. (A) *SPX1* and *SPX3* promoters contain P1BS (GXATATXC), AW box (CG(X)7CXAXG) and CTTC (CTTCTTGTTC) *cis*-regulatory elements. (B) qPCR analyses showing overexpression of *WRI5a* at high Pi conditions induces *SPX1* and *SPX3* expression. Data shown are the individual values of 3 individually transformed roots. Data significantly different from the corresponding EV controls are indicated ** $P < 0.01$ (Student's t-test).

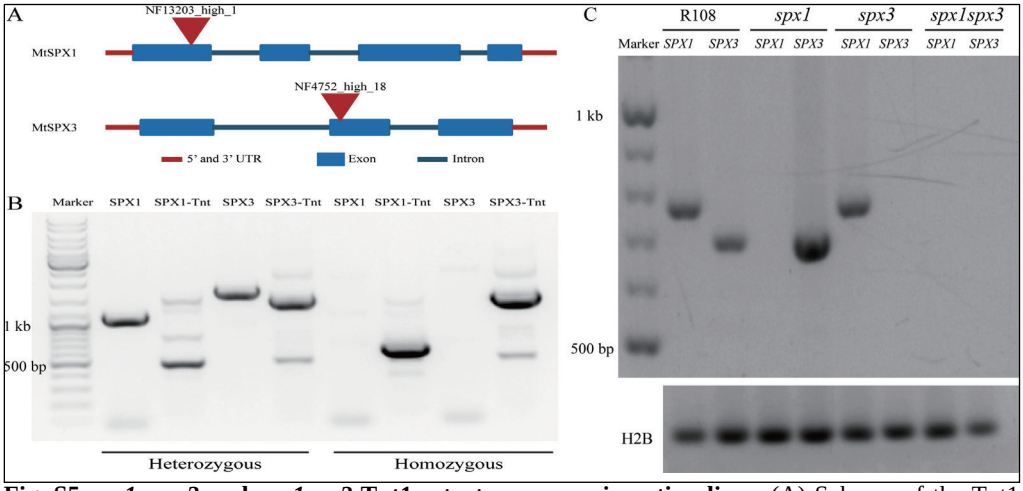

Fig. S5 *spx1*, *spx3* and *spx1spx3* Tnt1-retrotransposon insertion lines. (A) Scheme of the Tnt1 insertions in *spx1* (NF13203) and *spx3* (NF4752), indicated by triangles. (B) PCR using genomic DNA as template confirming the Tnt1 insertions in both *SPX1* and *SPX3* in the *spx1spx3* double mutant. (C) RT-PCR showing the impairment of *SPX1* and *SPX3* expression in the respective mutants. *Histone 2B* (*H2B*) is used as control.

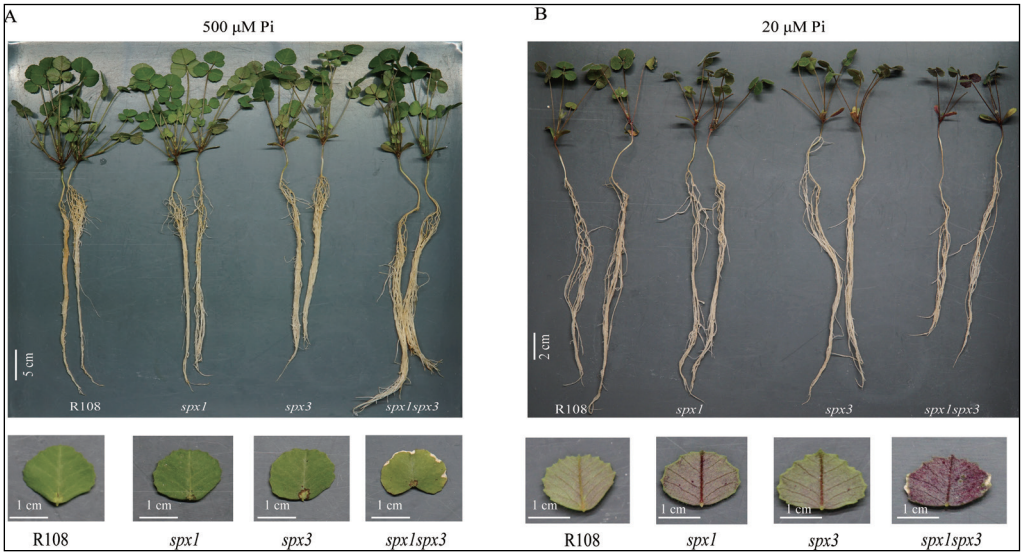

Fig. S6 Phenotypes of *spx1*, *spx3*, and the double-mutant *spx1spx3*. (A) Phenotype of WT, *spx1*, *spx3*, and *spx1spx3* plants grown for 3 weeks in high Pi conditions (upper image). Bottom images show enlarged views of leaves. Note chlorosis of the leaf margins in the *spx1spx3* double mutant. (B) Phenotype of WT, *spx1*, *spx3*, and *spx1spx3* plants grown for 3 weeks in low Pi conditions (upper image). The enlarged views in the bottom images show the accumulation of anthocyanins as purple coloration.

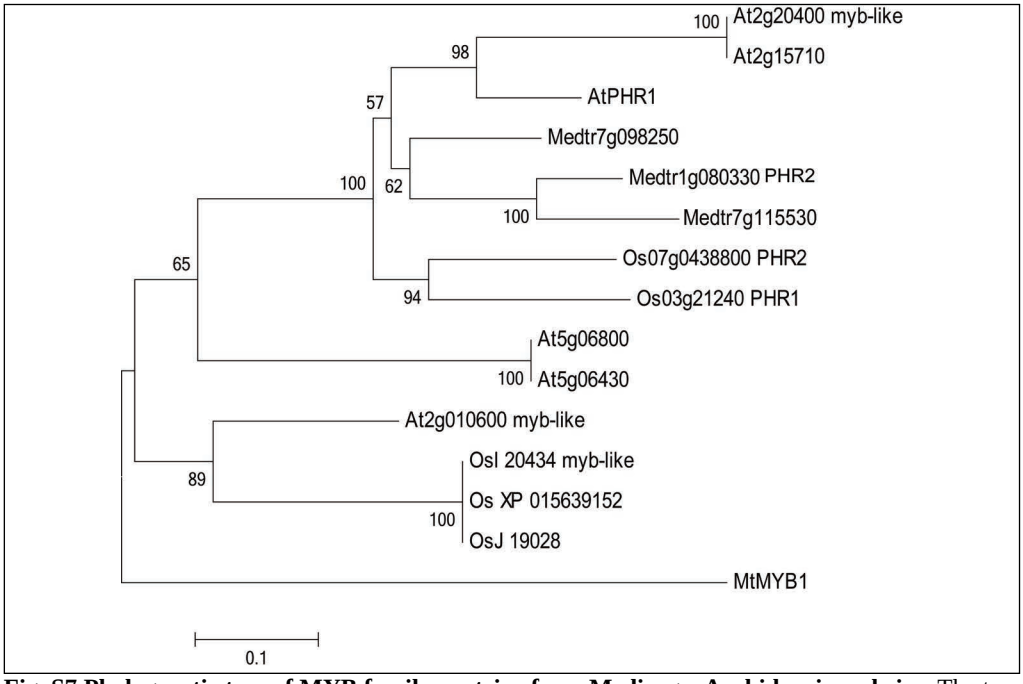

Fig. S7 Phylogenetic tree of MYB family proteins from Medicago, Arabidopsis and rice. The tree were generated using the neighbour-joining tree builder in Geneious R11.0 (https://www.geneious.com). 1000 bootstraps were used. Identifiers for the PHR genes are listed in Table S4.

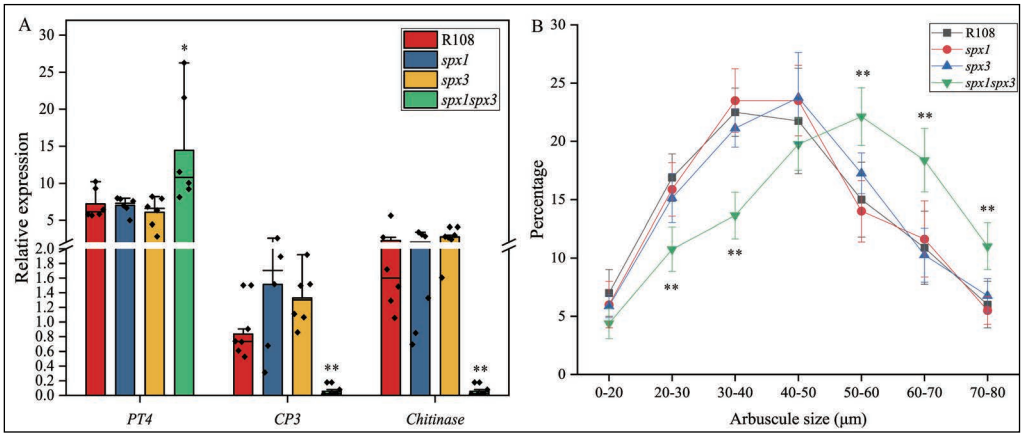

S8 SPX1 and SPX3 regulate arbuscule degradation. (A) qPCR analyses of *PT4*, *CP3* and *Chitinase* expression in mycorrhized mutant root sample from Fig. 5B. The expression are normalised to the fungal *RiEF*. Data shown are individual values of each replicate. Data significantly different from R108 controls are indicated * $P < 0.05$; ** $P < 0.001$ (Student's t-test). (B) Analysis of arbuscule size in R108, *spx1*, *spx3* and *spx1spx3* after 3 weeks inoculated with *R. irregularis*. Frequency graphs showing arbuscule size distribution. 100 arbuscules were counted for each of the 8 replicates. Data in *spx1spx3* double mutants significantly different from R108 controls are indicated ** $P < 0.01$ (Student's t-test).

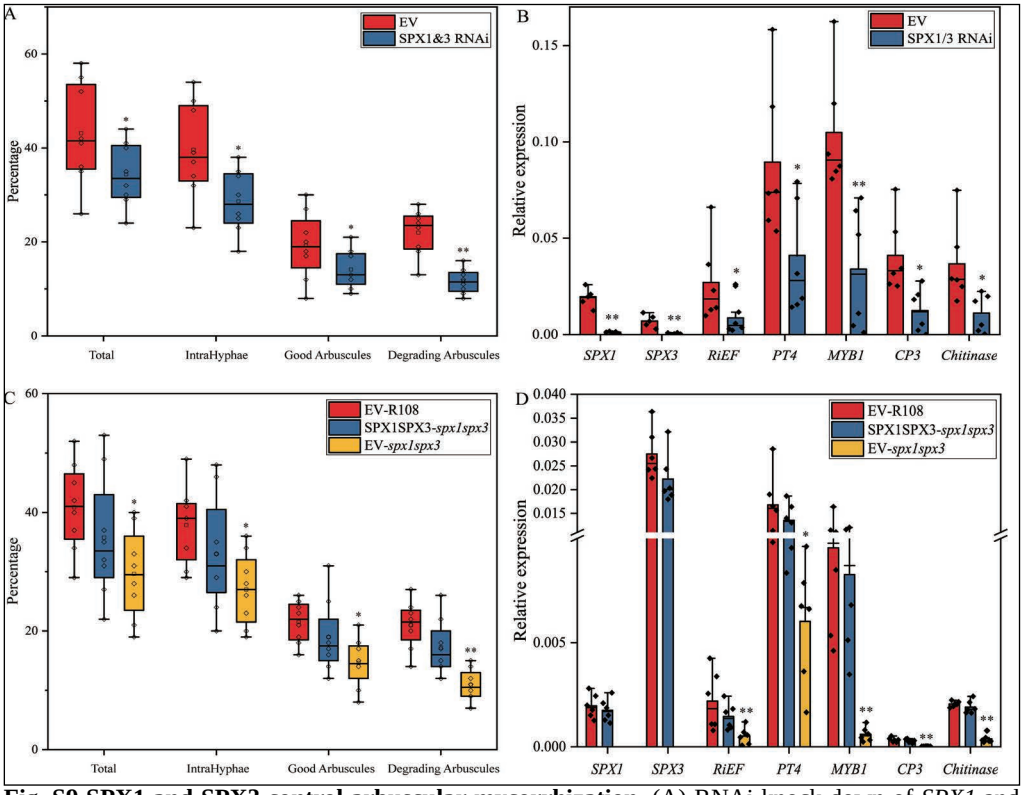

Fig. S9 SPX1 and SPX3 control arbuscular mycorrhization. (A) RNAi knock down of *SPX1* and *SPX3* expression showing decreased arbuscular mycorrhization levels 3 weeks after inoculation in *Medicago truncatula* A17 roots compared to empty vector (EV) transformed roots. Significantly less degrading arbuscules were observed. 8 independent transformed roots were used as replicates for each sample. Total = presence of mycorrhiza in root segments, IntraHyphae = root segments containing intraradical hyphae; examples of good and degrading arbuscule classes are shown in Fig. 5. (B) Relative expression levels of *SPX1*, *SPX3*, *RiEF*, *PT4*, *CP3*, *Chitinase* and *MYB1* in root samples from (A) compared to empty vector (EV) controls. (C) Expression of *SPX1* and *SPX3* under the control of their own promoters in the *spx1spx3* double mutant complemented the AM phenotype. 8 independent transformed plants were used as replicates for each sample. (D) Expression levels of *SPX1*, *SPX3*, *RiEF*, *PT4*, *CP3*, *Chitinase* and *MYB1* in root samples from (C). *MtEF1* was used as internal reference in the qPCR experiments shown in (B) and (C). Data shown are individual values of each root. In (A-D) data significantly different from EV controls are indicated * $P < 0.05$; ** $P < 0.01$ (Student's t-test).

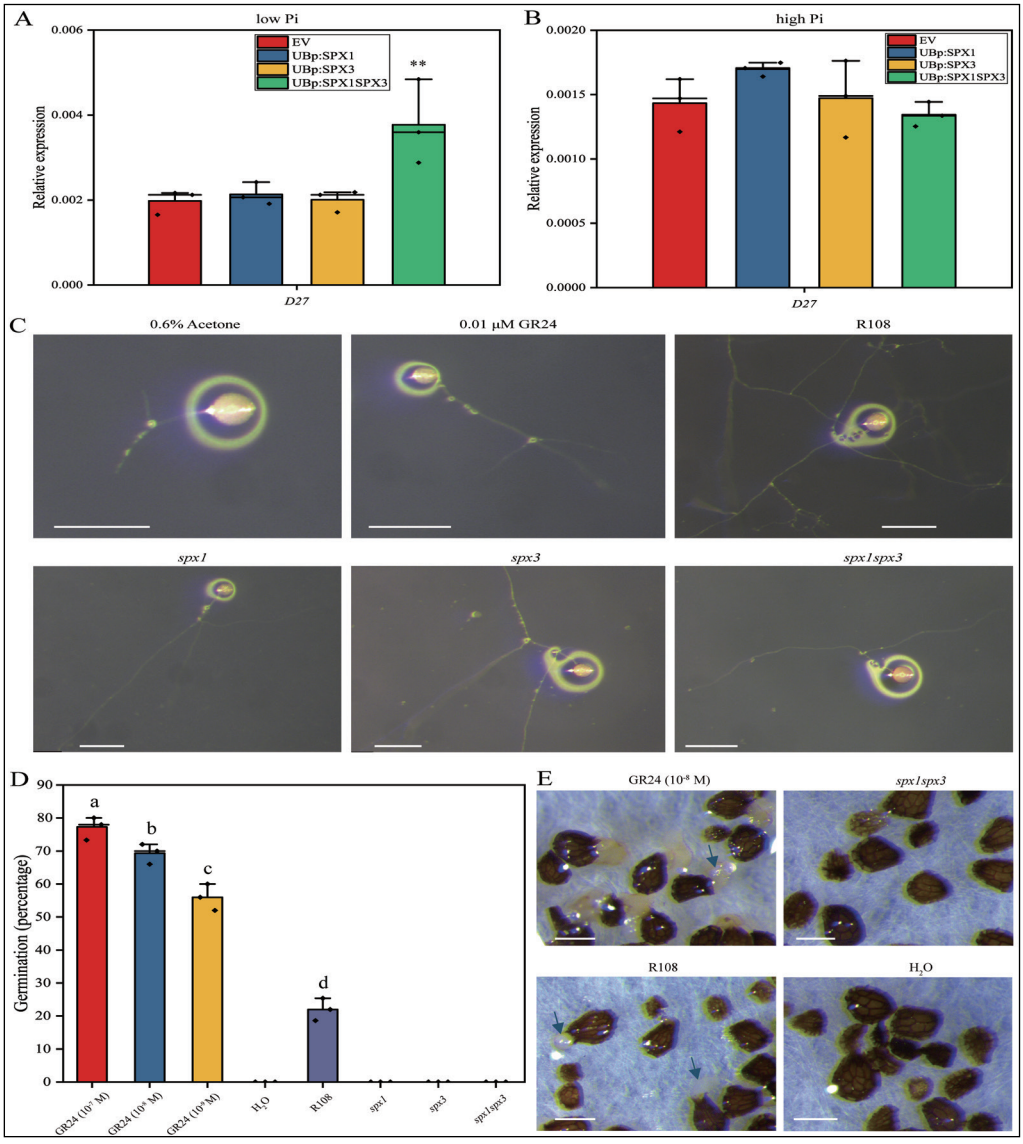

Fig. S10 SPX1 and SPX3 likely regulate strigolactone biosynthesis. (A) Overexpression of *SPX1* and *SPX3* together in low Pi conditions induced *D27* expression. The samples correspond to Fig. 4D. (B) Overexpression of *SPX1* and *SPX3* in high Pi conditions did not affect *D27* expression. Data shown are individual values of 3 independently transformed roots. *MtEF1* was used as reference gene in the qPCR experiment shown in A-B. Data significantly different from the corresponding empty vectors transformed controls are indicated ** $P < 0.01$ (Student's t-test). (C) Representative images of *Rhizophagus irregularis* spores treated with 0.6% acetone, 0.01 µM GR24, roots exudates of R108, *spx1*, *spx3* and *spx1spx3*. Scale bar = 250 µm. (D) Germination of *Phelipanche ramosa* seeds induced by root exudates and GR24. Data shown are individual values of 3 replicates. Different letters indicate significant differences ($P < 0.05$) between treatments (ANOVA followed by Tukey's honestly significant difference). (E) Representative images of *P. ramosa* seeds treated with 10^{-8} M of GR24, H2O, roots exudates of R108 and *spx1spx3*. Arrows point to germinated seeds. Scale bar = 1 mm.

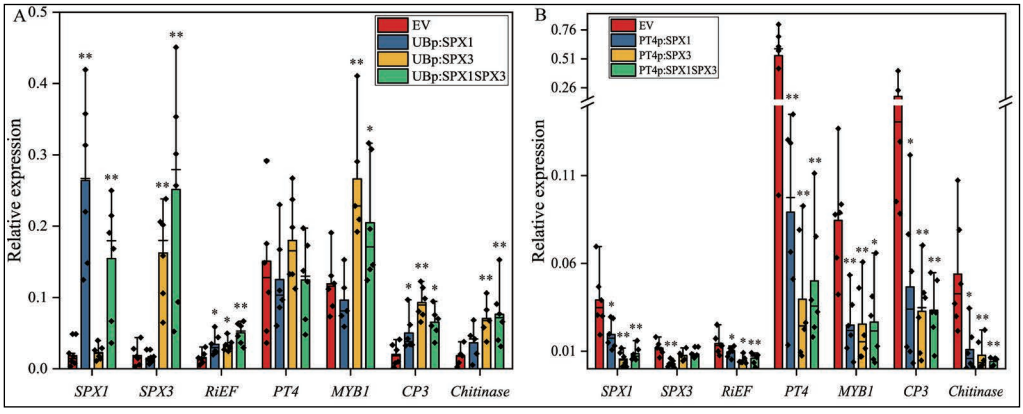

Fig. S11 qPCR analysis of overexpression of *SPX1/3* under the control of the *LjUbiquitin1* or *PT4* promoter increased AM colonization and/or arbuscule degradation. (A) Expression levels of *SPX1*, *SPX3*, *RiEF*, *PT4*, *CP3*, *Chitinase*, *MYB1* in root samples from Fig. 7A as determined by qPCR. *MtEF1* was used as internal reference. (B) Expression levels of *SPX1*, *SPX3*, *RiEF*, *PT4*, *CP3*, *Chitinase*, *MYB1* in root samples from Fig. 7D as determined by qPCR. *MtEF1* was used as internal reference. Data shown are individual values of each root. Expression data significantly different from EV controls are indicated * $P < 0.05$, ** $P < 0.01$ (Student's t-test).

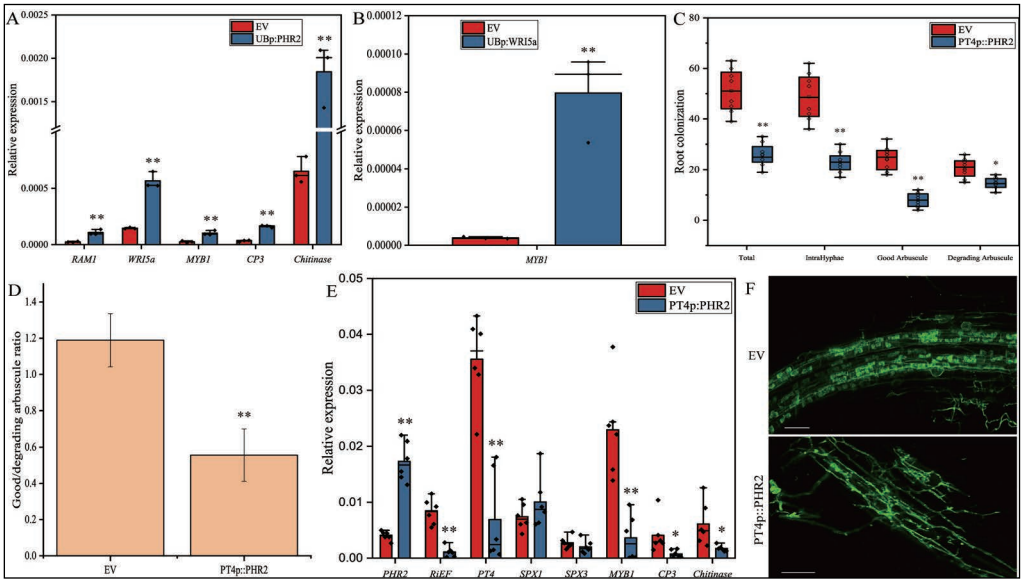

Fig. S12 PHR2 can induce arbuscule degradation. (A) Overexpression of *PHR2* under the control of the *LjUbiquitin* promoter induced symbiosis related genes expression under non-mycorrhizal conditions. The same cDNA samples as shown in Fig. 4B are used. Data shown are individual values of 3 independently transformed roots. Data significantly different from the corresponding empty vector (EV) transformed controls are indicated ** $P < 0.01$ (Student's t-test). (B) Overexpression of *WRI5a* induced *MYB1* expression under non-mycorrhizal conditions. The same cDNA samples as shown in Fig. S4B are used. Data shown are individual values of 3 independently transformed roots. Data significantly different from the corresponding EV transformed controls is indicated ** $P < 0.01$ (Student's t-test). (C) Quantification of mycorrhization level in *M. truncatula* roots expressing EV and *PT4p:PHR2* 3 weeks post inoculation with *R. irregularis*. 8 independently transformed plants were used as replicates. Quantification was performed using the magnified intersections method (McGONIGLE et al., 1990). Data significantly different from EV controls are indicated * $P < 0.05$; ** $P < 0.01$ (Student's t-test). (D) Good-to-Degrading arbuscule ratio of EV and *PT4p::PHR2* mycorrhizal samples from (C). Values represent mean ± standard deviation of the 8 independently transformed plants. Data significantly different from EV controls are indicated ** $P < 0.01$ (Student's t-test). (E) Relative expression levels of *PHR2*, *RiEF*, *PT4*, *SPX1*, *SPX3*, *MYB1*, *CP3* and *Chitinase* in root samples from (C) as determined by qPCR. *MtEF1* was used as internal reference. Data shown are individual values of each replicates. Expression data significantly different from EV controls are indicated * $P < 0.05$; ** $P < 0.01$ (Student's t-test). (F) Representative confocal images of WGA-Alexa488 stained *R. irregularis* in EV and *PT4p::PHR2* roots. Scale bar = 100 µm.

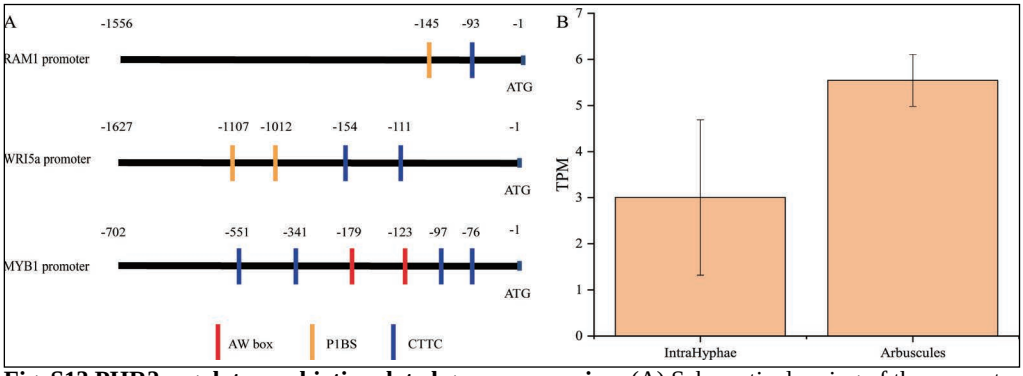

Fig. S13 PHR2 regulate symbiotic related genes expression. (A) Schematic drawing of the promoter regions of *RAM1*, *WRI5a* and *MYB1* showing the location of AW box (CG(N)7CNANG), P1BS (GNATATNC) or CTTC (CTTCTTGTTC) *cis*-regulatory elements. (B) PHR2 is (weakly) expressed in arbuscule-containing cells based on RNAseq data (Zeng et al,. 2018) of laser microdissected roots colonized by *R. irregularis*. IntraHyphae = cortical cells with intercellular hyhpae. TPM= transcripts per million.

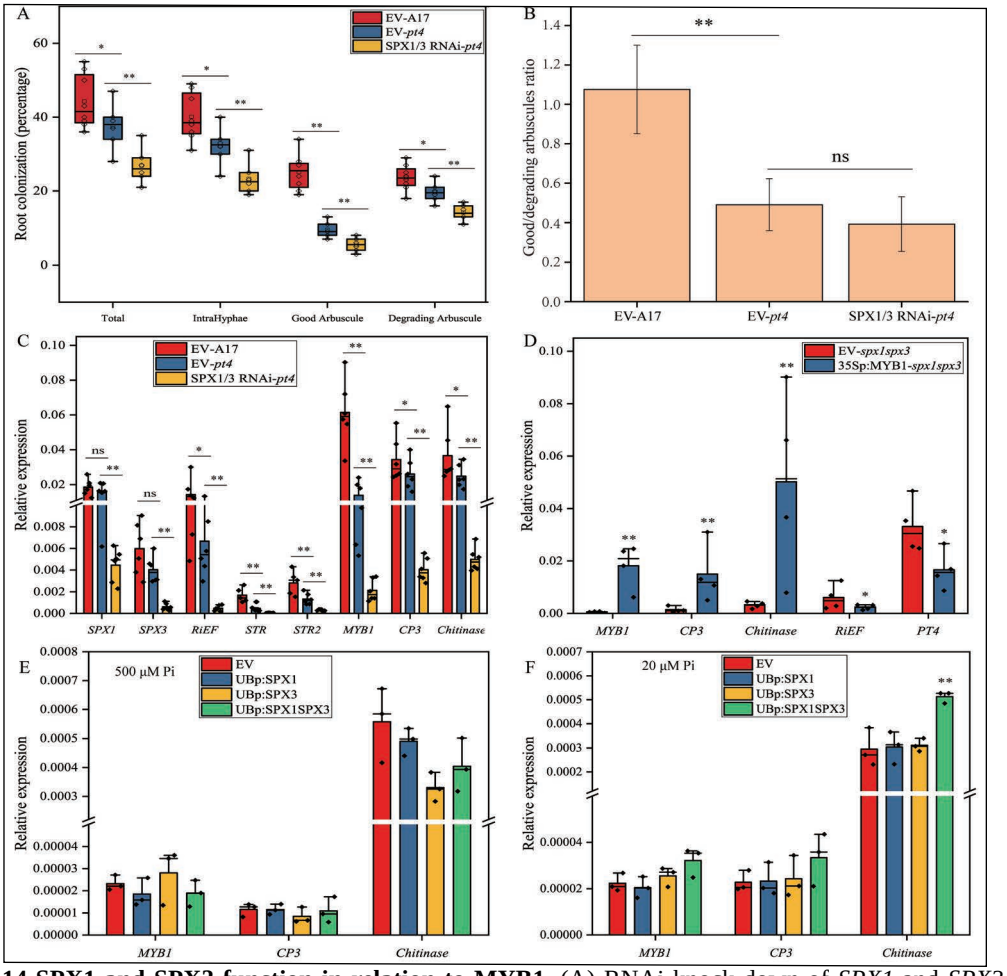

S14 SPX1 and SPX3 function in relation to MYB1. (A) RNAi knock down of *SPX1* and *SPX3* expression in the *pt4* mutant background decreased AM colonization but did not affect the good/degrading arbuscules ratio. 6 independently transformed plants were used as replicas for each sample. Data significantly different from indicated groups are indicated * $P < 0.05$; ** $P < 0.01$ (Student's t-test). (B) Good-to-Degrading arbuscule ratio of mycorrhizal samples from (A). Values represent mean ± standard deviation of 6 independent replicates. Data significantly different from indicated groups are indicated ** $P < 0.01$; ns: not significant (Student's t-test). (C) Relative expression levels of *SPX1*, *SPX3*, *RiEF*, *STR*, *STR2*, *MYB1*, *CP3* and *Chitinase* in samples from (A) compared to EV controls. Data shown are individual values of each root. Data significantly different from indicated groups are indicated * $P < 0.05$; ** $P < 0.01$; ns: not significant (Student's t-test). (D) Overexpression of *MYB1* under the control of *35S* promoter in the *spx1spx3* mutant background induced *CP3* and *Chitinase* expression and resulted in reduced *RiEF* and *PT4* expression compared to EV transformed roots 3 weeks post-inoculation. Data shown are individual values of 4 independent replicates. Data significantly different from EV controls are indicated * $P < 0.05$; ** $P < 0.01$ (Student's t-test). (E) Overexpression of *SPX1* and *SPX3* in high Pi conditions had no effect on *MYB1*, *CP3* and *Chitinase* expression. Data shown are individual values of 3 independently transformed plants. (F) Overexpression of *SPX1* and *SPX3* together in low Pi conditions slightly increased *Chitinase* expression. cDNA samples used correspond to Fig. 4D. Data shown are individual values of 3 independently transformed plants. *MtEF1* was used as internal reference in the qPCR experiments shown in C-F.

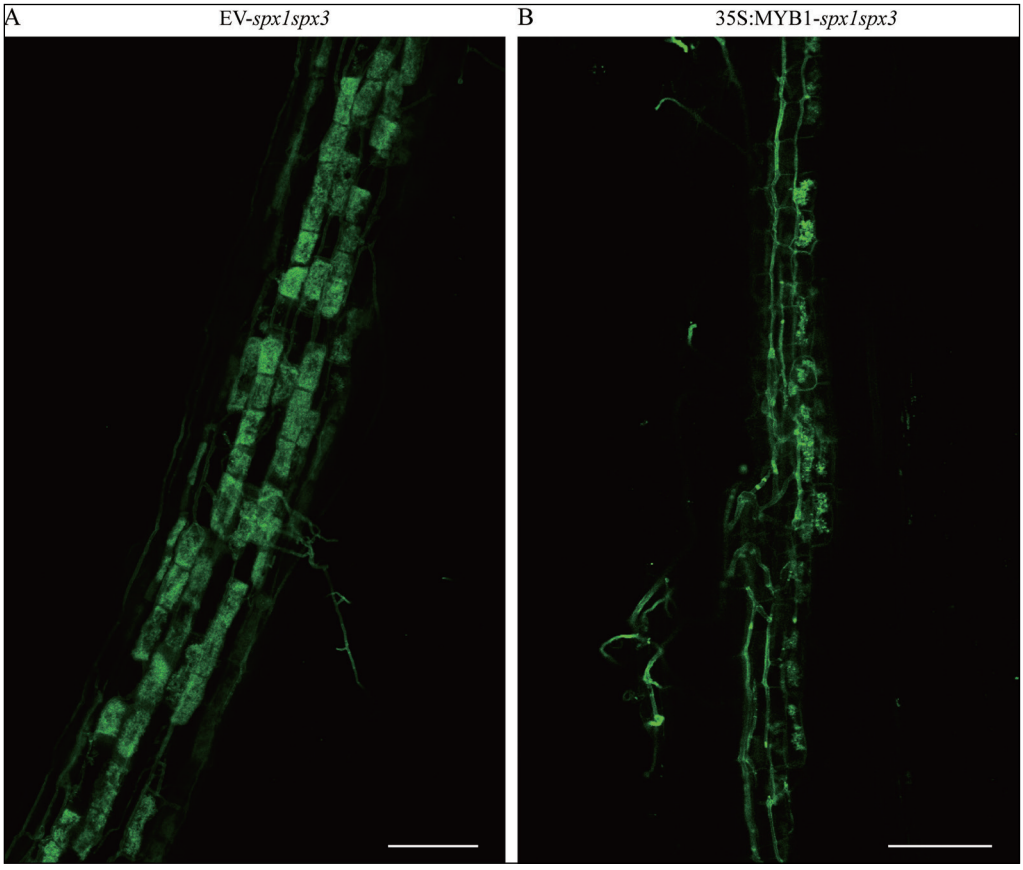

Fig. S15 Representing images of *MYB1* overexpression mycorrhizal roots in the *spx1spx3* double mutant background. (A) Confocal picture of WGA-alexa488 stained empty vector transformed spx1spx3 roots. Scale bar = 100 µm. (B) Confocal picture of WGA-alexa488 stained *35Sp:MYB1* transgenic *spx1spx3* roots. Scale bar = 100 µm.

Supplementary tables

Table S1. Primers list used in this study

Experiment	Primer name	Primer sequence
Goldengate	F-SPX1-CDS1-NS	AGAAGACTCAATGAAGTTCTGGAAGATCTTGAAGA
Goldengate	R-SPX1-CDS1-NS	GGAAGACAGCGAATGAATGTGCTACCTTTTCCTTGT
Goldengate	F-SPX3-CDS1-NS	AGAAGACTCAATGAAGTTTGCAAAGATATATATTGATG
Goldengate	R-SPX3-CDS1-NS	GGAAGACAGCGAACGCTCGTTTTGCATAGAAGTCG-TACC
Goldengate	F-PT4-Pro-CCAT	AGAAGACTCGGAGGACTCGATCCACAACAAAGATTA-ATTTTTG
Goldengate	R-PT4-Pro-CCAT	GGAAGACGCATGGGACTCTCTCAAGTTGGTTTTTG-GAGTTAA
Goldengate	F-PT4-Pro-AATG	AGAAGACTCGGAGGACTCGATCCACAACAAAGATTA-ATTTTTG
Goldengate	R-PT4-pro-AATG	GGAAGACGCATGGAAAAAGGAAGACTCTCT-CAAGTTGG
Goldengate	F-SPX1-Pro-AATG	AGAAGACTCGGAGGTAGACCTAGACCGAGTTTTACA
Goldengate	R-SPX1-Pro-AATG	GGAAGACGCCATTGACAATGTTAAGATCCTTTGCTCACT
Goldengate	F-SPX3-Pro-AATG	AGAAGACTCGGAGGACCACATATGTTGTGTATCGTGA
Goldengate	R-SPX3-Pro-AATG	GGAAGACGCCATTATTCTTCTTCTCTAAGATTAAT-TCAACTTTG
Goldengate	F-LjUB1-Pro-CCAT	AGAAGACTCGGAGGGAGAGAGGATTTTGAGGAAATA
Goldengate	R-LjUB1-Pro-CCAT	GGAAGACGCATGGCTGTAATCACATCAACAACAGATAA
Goldengate	F-LjUB1-Pro-AATG	AGAAGACTCGGAGGGAGAGAGGATTTTGAGGAAATA
Goldengate	R-LjUB1-Pro-AATG	GGAAGACGCCATTCTGTAATCACATCAACAACAGATAA
Goldengate	F-PHR2-CDS1	AGAAGACTCAATGATGTCTTCGTCTATTCCATCTTCCT
Goldengate	R-PHR2-CDS1	GGAAGACAGAAGCCTACTTGTCAGTCTTCACTCGT
qPCR	SPX1-qF	TCAGCATTGCGTACCTTGGA
qPCR	SPX1-qR	TCCACAAGCTTCACCTGACG
qPCR	SPX3-qF	AAGGAGAAGCAGCCAGGATG
qPCR	SPX3-qR	ACTCTGCCTCCTCACTTCCA
qPCR	Medtr1g012440-qF	CAAGACAAAGTTGCCTGGGC
qPCR	Medtr1g012440-qR	CACGCGCAACTTCCTCAAAA
qPCR	Medtr4g027390-qF	ATCGATGCAGTGTTTCCGGT
qPCR	Medtr4g027390-qR	GTAAAGCCGCAACCGTGTTT
qPCR	Medtr4g114550-qF	AGAACTGGTGCCCTCATTCG
qPCR	Medtr4g114550-qR	CCACTTGATTGCAACGGTGG
qPCR	Medtr8g077020-qF	TCTTGCTGCAATGAGAGCCA
qPCR	Medtr8g077020-qR	TGGAGAATTTGCCGCAGAGT
qPCR	PHR2-qF	GCAGCGCTTCAGAGAACATG

qPCR	PHR2-qR	AGCTCAAGTTCACCGGTAGC
qPCR	WRI5a-qF	AAAGGCGGCGAAGAGAATCA
qPCR	WRI5a-qR	TGGATTGACCACTCACTGGC
qPCR	MtD27-qF	TTGCTTGGTTACTCGGTCCC
qPCR	MtD27-qR	CATCAGTTGATGCTGGGGGT
qPCR	Mt4-qF	GGAGAAGTGGATGGTGTGTGT
qPCR	Mt4-qR	GCCAAAGGATCGAAGTTGCC
qPCR	STR-qF	GCTCAGGGTGGTAGCATTGT
qPCR	STR-qR	AAGTCCAACCGTCGCTTGAT
qPCR	STR2-qF	ATGGTCCTCACCTTCATGGG
qPCR	STR2-qR	AAAGCTTGGAGCGCAAGAAA
qPCR	MtEF-qF	GATTGCCACACCTCTCACAT
qPCR	MtEF-qR	TCAGCGAAGGTCTCAACCAC
qPCR	PT4-qF	GGATTCTTTTGCACGTTCTTGG
qPCR	PT4-qR	GCTGTCATTTGGTGTTGCAGTG
qPCR	RiEF-qF	ATTGTTCGTGGTGCATTTCA
qPCR	RiEF-qR	AACCCCTTCGTCTTCCACTT
qPCR	MtPT6-qF	CGTGGTGCGTTTATAGCTGC
qPCR	MtPT6-qR	TAATCGGCTTGCGGAACAGT
qPCR	MYB1-qF	TAAGAGAGTTGATGATGATTGTC
qPCR	MYB1-qR	GATGAGTGATTCTGTTGAACC
qPCR	CP3-qF	AACAATGATGCCAATAACAAGC
qPCR	CP3-qR	GGAGCACATATGACCCTTGA
qPCR	Chitinase-qF	GGCATGTCAGAGGTTGAAGAG
qPCR	Chitinase-qR	GCCAAAAGTGCTTGTGATTG
RNAi	F-SPX3-RNAi	CACCATGGAGGGACAAGTTCTTGTC
RNAi	R-SPX3-RNAi	TTTGGTCT**C**ACTCTTTCGGCTGCTTCACCA
RNAi	F-SPX1-RNAi	TTTGGTCTCAAGAGCCAAATCGAGCAGACC
RNAi	R-SPX1-RNAi	GCAAGGGCAAGAAGGGCTAT
Genotyping	Tnt1-F1	TCCTTGTTGGATTGGTAGCCAACTTTGTTG
Genotyping	Tnt1-R1	TGTAGCACCGAGATACGGTAATTAACAAGA
Genotyping	SPX1-F	ATGAAGTTCTGGAAGATCTTGAAGA
Genotyping	SPX1-R	CGAATGAATGTGCTACCTTTTCCTTGT
Genotyping	SPX3-F	AATGAAGTTTGCAAAGATATATATTGATG
Genotyping	SPX3-R	CGAACGCTCGTTTTGCATAGAAGTCGTACC

Table S2. Constructs made using the golden gate cloning system

Level 0	Level 1	Level 2
pAGM1251-MtPT4p-CCAT	pICH47732-MtPT4p::SPX1-FLAG	pAGM4723-LjUBQ1p::SPX1-GFP-AtUBQ10p::DsRed
pICH41295-MtPT4p-AATG	pICH47751-MtPT4p::SPX3-FLAG	pAGM4723-LjUBQ1p::SPX3-GFP-AtUBQ10p::DsRed
pICH41295-LjUBQ1p-AATG	pICH47732-MtPT4p::-FLAG-PHR2	pAGM4723-LjUBQ1p::SPX1-FLAG-AtUBQ10p::DsRed
pAGM1251-LjUBQ1p-CCAT	pICH47732-LjUBQ1p::SPX1-FLAG	pAGM4723-LjUBQ1p::SPX3-FLAG-AtUBQ10p::DsRed
pICH41295-SPX1p-AATG	pICH47732-LjUBQ1p::SPX3-FLAG	pAGM4723-SPX1p::SPX1-GFP-AtUBQ10p::DsRed
pICH41295-SPX3p-AATG	pICH47732-LjUBQ1p::SPX1-GFP	pAGM4723-SPX3p::SPX3-GFP-AtUBQ10p::DsRed
pAGM1287-SPX1 CDS1 no stop	pICH47732-LjUBQ1p::SPX3-GFP	pAGM4723-LjUBQ1p::SPX1-FLAG-AtUBQ10p::DsRed-LjUBQ1p::SPX3-FLAG
pAGM1287-SPX3 CDS1 no stop	pICH47751-LjUBQ1p::SPX3-GFP	pAGM4723-PT4p::SPX1-FLAG-AtUBQ10p::DsRed-PT4p::SPX3-FLAG
pICH41308-PHR2 CDS1	pICH47761-LjUBQ1p::GFP-MYB1	pAGM4723-PT4p::SPX1-FLAG-AtUBQ10p::DsRed
pICH41308-MYB1-CDS1	pICH47751-LjUBQ1p::GFP-PHR2	pAGM4723-PT4p::SPX3-FLAG-AtUBQ10p::DsRed
pICH41308-NSP1-CDS1	pICH47732-SPX1p::SPX1-GFP	pAGM4723-PT4p::FLAG-PHR2-AtUBQ10p::DsRed
pICH41308-DEL-LAΔ18-CDS1	pICH47751-SPX3p::SPX3-GFP	pAGM4723-LjUBQ1p::FLAG-PHR2-AtUBQ10p::DsRed
pICH41308-WRI5a-CDS1	pICH47811-AtUBQ10p::DsRed	pAGM4723-LjUBQ1p::GFP-PHR2-AtUBQ10p::DsRed
	pICH47751-LjUBQ1p::GFP-NSP1	pAGM4723-LjUBQ1p::SPX1-FLAG-AtUBQ10p::DsRed-LjUBQ1p::GFP-PHR2
	pICH47732-LjUBQ1p::GFP-DEL-LAΔ18	pAGM4723-LjUBQ1p::SPX3-FLAG-AtUBQ10p::DsRed-LjUBQ1p::GFP-PHR2
	pICH47751-LjUBQ1p::FLAG-NSP1	pAGM4723-LjUBQ1p::GFP-MYB1-AtUBQ10p::DsRed
	pICH47732-LjUBQ1p::Flag-WRI5a	pAGM4723-LjUBQ1p::GFP-PHR2-AtUBQ10p::DsRed
		pAGM4723-LjUBQ1p::GFP-NSP1-AtUBQ10p::DsRed
		pAGM4723-LjUBQ1p::SPX1-FLAG-AtUBQ10p::DsRed-LjUBQ1p::GFP-NSP1
		pAGM4723-LjUBQ1p::SPX3-FLAG-AtUBQ10p::DsRed-LjUBQ1p::GFP-NSP1

pAGM4723-LjUBQ1p::GFP-DEL-LAΔ18-AtUBQ10p::DsRed
pAGM4723-LjUBQ1p::Flag-WRI5a-AtUBQ10p::DsRed

Table S3 SPX1 and SPX3 expression fold changes in wild-type and *ram1-1* roots during mycorrhization. Fold changes with an FDR-corrected p-value < 0.05 are shown. Data collected from (Luginbuehl et al., 2017).

Gene	wild type			*ram1-1*		
	8 dpi	13 dpi	27 dpi	8 dpi	13 dpi	27 dpi
SPX1	4	5	7	3	3	n.s.
SPX3	n.s.	57	19	n.s.	9	5
WRI5a	86	1053	1152	n.s.	n.s.	n.s.

Table S4 Identifier of genes used for Phylogenetic analyses

Name	Gene ID
AtSPX1	AT5G20150
AtSPX2	AT2G26660
AtSPX3	AT2G45130
AtSPX4	AT5G15330
OsSPX1	LOC_Os06g40120
OsSPX2	LOC_Os02g10780
OsSPX3	LOC_Os10g25310
OsSPX4	LOC_Os03g61200
OsSPX5	LOC_Os03g29250
OsSPX6	LOC9271158
AtPHR1	AT4G28610
MtMYB1	Medtr7g068600
MtSPX1	Medtr3g107393
MtSPX3	Medtr0262s0060

Chapter 5

Medicago SPX1 and SPX3 interact with PIP2 plasma membrane aquaporins

Peng Wang[a], Sjef Boeren[b], Ton Bisseling[a], Erik Limpens[a*]

[a] Laboratory of Molecular Biology, Wageningen University & Research, 6708 PB Wageningen, the Netherlands

[b] Laboratory of Biochemistry, Wageningen University & Research, Wageningen 6708 WE, the Netherlands

[*]To whom correspondence should be addressed. Email: erik.limpens@wur.nl

Abstract

SPX proteins have emerged as key phosphate sensors that control phosphate homeostasis in plants. In *Medicago truncatula SPX1* and *SPX3* are strongly induced in arbuscule-containing cells, where arbuscular mycorrhiza fungi exchange Pi for carbon sources from the host plant. To ensure a mutualistic interaction, the host plant must be able to control arbuscule development in a nutrient-dependent manner. In chapter 4 we showed that SPX1 and SPX3 redundantly regulate arbuscule degeneration/arbuscule lifetime. However the molecular mechanism underlying this regulation remained to be unraveled. Here we show that SPX1 and SPX3 do not directly interact with known transcriptional regulators of arbuscule degradation. Instead, through co-immunoprecipitation coupled with liquid chromatography–mass spectrometry, we identified PIP2 plasma membrane intrinsic proteins, better known as aquaporins, as interactors of both SPX1 and SPX3. Overexpression of *PIP2;7*, which localizes on the peri-arbuscular membrane in arbuscule-containing cells, reduced overall arbuscule abundance while causing a shift towards larger arbuscules, suggesting reduced degradation. These results now offer a basis to investigate the intriguing possibility that SPX1 and SPX3 help to regulate Pi transport and/or arbuscule degeneration through the regulation of PIP2 activity.

Introduction

Plants increase their phosphate acquisition efficiency by establishing a symbiosis with arbuscular mycorrhizal fungi. The thin fungal hyphae can more easily scavenge scarcely available mineral nutrients and water in the soil, which they deliver to the plant at highly branched hyphal structure, called arbuscules, inside root cortical cells in exchange for sugars and lipids (Gutjahr and Parniske, 2013; Luginbuehl and Oldroyd, 2017). Since arbuscules form the market place for nutrient exchange, their development is tightly controlled by both partners.

Individual arbuscules have a short lifetime of about 2–5 days at maturity, after which they are actively removed from the cortical cell (Kobae and Hata, 2010). After removal, a new arbuscule can be formed again in the same cell (Kobae and Fujiwara, 2014). This phenomenon has been postulated to be important to keep the symbiosis beneficial (Gutjahr and Parniske, 2017). However, the molecular mechanisms that control arbuscule lifetime and function are far from understood.

Failure to provide phosphate by the fungus has been shown to cause the premature degradation of arbuscules. Recently, it was suggested that Pi supply from the extraradical hyphae to the arbuscules is facilitated by aquaporin-mediated long-distance translocation (Kikuchi et al., 2016). Knock-down of a fungal plasma membrane aquaporin (RcAQP3 from *Rhizophagus clarus*) as well as the suppression of host transpiration impaired the translocation of polyphosphate by the fungus. How AM fungi release phosphate at the arbuscules is currently unknown (Ezawa and Saito, 2018). Subsequent uptake of Pi by the plant involves the activity of the arbuscule-specific Pi-transporter PT4, which is located at the plant-derived peri-arbuscular membrane. Pi transport is powered by a proton-gradient generated by the HA1 proton pump (Krajinski et al., 2014). Knock-out mutations in the corresponding genes cause the premature degradation of the arbuscules. Interestingly, simultaneous nitrogen star-

vation was shown to rescue the premature arbuscule degradation in a pt4 mutant suggesting that both phosphate and nitrogen provision, and possibly other nutrients, are monitored by the plant to determine the lifetime of the arbuscules (Breuillin-Sessoms et al., 2015).

In Chapter 4 we reported that two Pi-sensing SPX proteins, SPX1 and SPX3 in *Medicago truncatula* (Medicago), are highly induced in arbuscule containing cells and are involved in the timely degradation of arbuscules. SPX proteins are well known to regulate plant Pi starvation responses to control Pi homeostasis in plants (Puga et al., 2014; Wang et al., 2014b). They sense Pi status in a cell by directly binding inositol polyphosphates, which act as signalling molecules for Pi availability (Wild et al., 2016). Furthermore, SPX proteins also play a role in the crosstalk between nitrogen and phosphate homeostasis (Hu et al., 2019). Based on mutant analyses we hypothesized that SPX1 and SPX3 redundantly control the timely degradation of arbuscules when the cortical cells have obtained sufficient Pi. This raises the question how these Pi-sensing proteins control arbuscule degradation.

Recently it was shown that premature arbuscule degradation due to a lack of fungal Pi-supply involves the action of the MYB1 transcription factor (Floss et al., 2017). MYB1 was shown to form a complex with the NSP1 and DELLA transcriptional regulators to induce the expression of a number of hydrolytic enzymes such as chitinases, proteases and lipases, that degrade the underperforming arbuscules (Floss et al., 2017).

Here, we show that SPX1 and SPX3 do not regulate arbuscule degradation via direct interaction with the MYB1 complex members. To identify potential targets of SPX1 and SPX3 that control arbuscule degeneration, we performed co-immunoprecipitation (Co-IP) followed by liquid chromatography tandem-mass spectroscopy analyses. This identified PIP2 plasma membrane intrinsic protein as potential interactors of both SPX1 and SPX3. Further independent Co-IP and membrane yeast-two hybrid analyses confirmed the interaction between SPX1&3 and the aquaporin PIP2;7. PIP2;7 localizes to the peri-arbuscular membrane and ectopic overexpression of *PIP2;7* reduced arbuscule numbers, while increasing the “good” to “degrading” arbuscule ratio. These results make PIP2;7 a very interesting candidate for future study to provide a link between phosphate sensing by SPX1/3 and the nutrient-dependent regulation of arbuscule development.

Materials and methods

Plant and fungal material

Medicago truncatula Jemalong A17 (Medicago) were germinated and transformed as described (Limpens et al., 2004). *Rhizophagus irregularis* DAOM197198 spores were obtained from Agronutrion, France. Spores were washed three times through three layers of filter mesh (220 µm, 120 µm, 38 µm) with sterile demi water. For arbuscular mycorrhization assays, plant were grown in a SC10 RayLeach cone-tainer (Stuewe and Sons, Canada) with premixed sand:clay (1:1 V/V) mixture. Fungal spores were inoculated by placing ~200 pores ~2 cm below plant seedling roots. Plants were grown in a 16 h daylight chamber at 21°C and watered with 10 ml ½ Hoagland medium containing 20 µM phosphate twice a week, for three weeks.

Constructs

Except Y2H assays related constructs, all the others SPX1 (Medtr3g107393), SPX3 (Medtr0262s0060) and PIP2;7 (Medtr2g094270) constructs were made using the Golden gate cloning system (Engler et al., 2014). Primers used are listed in table S1. Different Golden gate modules created are listed in table S2. All newly made constructs were confirmed by Sanger sequencing.

Co-immunoprecipitation and liquid chromatography tandem-mass spectrometry (LC-MS/MS)

Co-IP/MS experiments were done as described (Wang et al., 2021). In brief, *LjUB1p::SPX1-FLAG* and *LjUB1p::SPX3-FLAG* constructs were transformed into Medicago roots via Agrobacterium rhizogenes mediated transformation. *LjUB1p::FLAG-GFP* transformed Medicago roots were used as negative control. After 4 weeks of inoculation with *R. irregularis* spores, total proteins were extracted from well-mycorrhized transgenic roots using Co-IP buffer (10% glycerol, 50 mM Tris-Hcl pH=8.0, 150 mM NaCl, 1% Igepal CA 630, 1 mM PMSF, 20 µM MG132, 1 tablet protease inhibitor cocktail). The protein extract was centrifuged at 15000 g for 10 min at 4 °C, and the supernatant transferred to a fresh 15 ml tube. After repeating the centrifugation the FLAG-tagged protein was pulled down from the supernatant by using µMACS and MultiMACS FLAG Isolation beads, according to manufacturer's instructions (Miltenyi Biotec). Immunoprecipitated protein samples were digested into peptides using trypsin (Sigma-Aldrich).

The digested peptides were measured using a Proxeon EASY nLC1000 and a LTQ-Orbitrap XL mass spectrometer as described (Lu et al., 2011; Wendrich et al., 2017). Briefly, 18 ul of peptide sample was injected into a 0.10 * 32 mm Magic C18AQ 200A 5 µm beads (Bruker Nederland B.V.) Pre-concentration column (prepared in-house) and the peptides were eluted onto a 0.10 * 250 mm ReproSil-Pur 120 C18-AQ 1.9 µm beads analytical column (prepared in-house) with an acetonitril gradient at a flow of 0.5 ul/min with a Thermo EASY nanoLC1000. A gradient from 9 to 34% acetonitril in water with 1 ml/l formic acid was applied in 50 minutes. An electrospray potential of 3.5 kV was applied directly to the eluent and full scan positive mode FTMS spectra were measured between m/z 380 and 1400 in the Orbitrap at high resolution (60000) and MSMS spectra were measured in the ion trap.

LC-MS/MS data analysis (false discovery rates were set to 0.01 on peptide and protein levels) and additional result filtering (minimally 2 peptides are necessary for protein identification of which at least one is unique and at least one is unmodified) were performed as described before using MaxQuant (Smaczniak et al., 2012; Wendrich et al., 2017). Peptide data were mapped to *M. truncatula* uniprot 2018 and *R. irregularis* DAOM197198 Uniprot 2018 to identify proteins. To analyse the relative abundance of proteins, their normalized label-free quantification (LFQ) intensities were compared (Cox et al., 2014). nLC-MS/MS system quality was checked with PTXQC (Bielow et al., 2016) using the MaxQuant result files.

Agroinfiltration of *Nicotiana benthamiana* and western blotting

To study the interaction between SPX1/3 and MYB1 complex members in *Nicotiana benthamiana* (Nicotiana) leaves, agro-infiltration of 5 week-old Nicotiana leaves was performed

as described before (Zeng et al., 2018). Briefly, *Agrobacterium tumefaciens* C58 containing the corresponding vectors were grown in LB medium (1% tryptone, 0.5% yeast extract, 1% NaCl) overnight at 28 °C. After centrifugation for 10 minutes at 4000 g the bacteria were resuspended in MMAi medium (2% sucrose, 0.5% MS basal salts, 0.2% MES, 200 uM acetosyringone, pH 5.6) and the OD_{600} adjusted to 1.0. After incubation for 1 hour at room temperature, the culture was mixed 1:1 with a similarly grown *A. tumefaciens* strain containing P19 as silencing inhibitor. Infiltrated Nicotiana plants were grown for 2 days and total proteins were isolated using Co-IP buffer as described above. GFP-Trap agarose beads (Chromotek) were used to immunoprecipitate GFP protein complexes. Western blot was performed as described (Bungard et al., 2010). 1:5000 diluted anti-GFP-HRP and anti-FLAG-HRP antibodies (Miltenyi biotec, USA) were used for detection.

RNA isolation and qPCR

RNA was isolated using the Qiagen plant RNA mini kit according to manufacturer's instruction. cDNA was made from 400 ng total RNA using the iScript cDNA Synthesis kit (Bio-Rad). iQ SYBR Green Supermix (Bio-Rad) was used for qPCR analysis in a Bio-Rad CFX connect real-time system. Primers used are listed in supplementary table S1. Medicago *Elongation factor 1* (*EF1*) was used for gene expression normalization. Relative expression levels were calculated as $2^{-\triangle ct}$. Three technical replicates were used for biological replicate. Six biological replicates were used to investigate gene expression. Significance was tested using Student's t-test.

***MtPIP2;7* constitutive overexpression**

For constitutive *PIP2;7* overexpression, *PIP2;7* was expressed in Medicago hairy roots under the control of the Lotus *Ubiquitin 1* promoter. An empty vector construct was transformed as control. Transgenic roots were collected based on DsRed marker three weeks post inoculation for mycorrhizal quantification and RNA isolation. Roots for mycorrhizal quantification were stained with WGA-Alexafluor 488 (Thermo Fisher Scientific, USA) according to Wang et al. (2021) and scored using the gridline intersect method (McGONIGLE et al., 1990).

Yeast two hybrid

To investigate the interaction between SPX1/3 and PIP2, the DUALmembrane 3 Kit (Dualsystems Biotech AG) was used. The *PIP2;7* CDS fragment was amplified using primer with SfiI restriction sites and inserted into the pBT3-N bait vector. *SPX1* and *SPX3* CDS fragments with SfiI restriction site were inserted in the pPR3-N prey vector. Primers used are listed in supplemental table S1. The bait and prey constructs were co-transformed into yeast strain NMY51 according to manufacturer's instructions. Positive colonies from SD-LT plates (DDO) were plated to SD-AHLT plates (QDO) for interaction investigation. pCCW-Alg5 and pAI-Alg5 provided by the kit were used as positive control.

To investigate the interaction between SPX1/3 and MYB1/NSP1/DELLA, the Matchmaker Gold Y2H System was applied (Clontech, USA) according to manufacturer's instructions. *SPX1/3* was inserted into the pGBKT7 bait vector, and *MYB1/NSP1/DELLA1Δ18* was inserted in the pGADT7 prey vector via Gibson assembly. Bait and prey constructs were transformed into respectively Y2H Gold and Y187 strains. Bait and prey strains were subse-

quently mated according to manufacturer's instructions. After mating, the strains were plated on DDO and QDO/Aureobasidin plates to analyse mating and protein-protein interaction results, respectively.

Results

SPX1 and SPX3 do not interact with the MYB1 complex

To investigate how SPX1 and SPX3 may control arbuscule degradation, we first studied whether SPX1 and SPX3 directly interact with the known transcriptional regulator MYB1 and its interactors NSP1 and DELLA involved in arbuscule degradation (Floss et al., 2017). Co-immunoprecipitation analyses of FLAG-tagged SPX1 and SPX3 transiently ex-

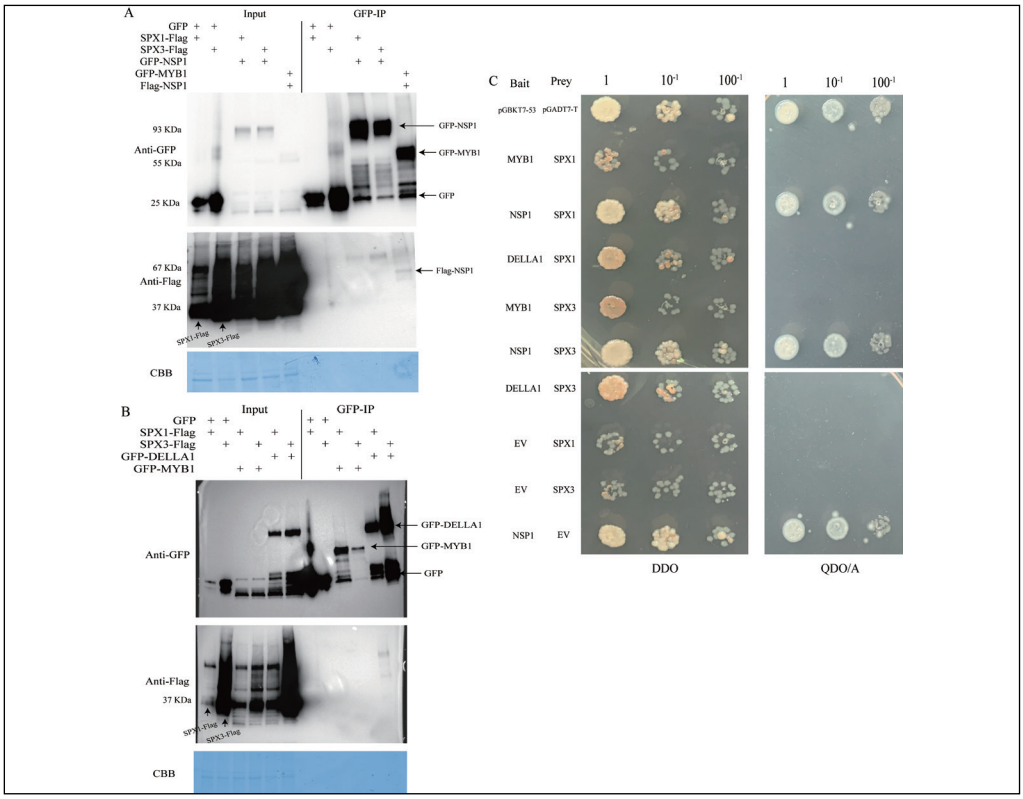

Fig. 1 SPX1 and SPX3 do not interact with the MYB1 complex. (A, B) Co-immunoprecipitation (Co-IP) assay showing that SPX1 and SPX3 do not interact with MYB1, NSP1 and DELLA1Δ18 in transiently transformed *Nicotiana benthamiana* leaves. The Flag tagged SPX1 and SPX3 proteins cannot be detected in GFP-IP enriched MYB1, NSP1 and DELLA1 samples indicating there is no interaction, while the interaction between NSP1 and MYB1 is confirmed (A). (C) Y2H assay showing no interaction between SPX1/3 and MYB1/DELLA1, using MYB1 or DELLA1 as bait (pGBKT7) and SPX1 or SPX3 as prey (pGADT7). Serial dilutions of mated yeast cultures were plated on selective medium. DDO (-LT) was used as control plate to show mating was successful. Selection was carried out on QDO (-LTHA) plates plus aureobasidin as additional selection markers. pGBKT7_53 + pGADT7_T was used as positive control. Expression of NSP1-BD caused the autoactivation of reporters in our yeast-two-hybrid system preventing the observation of a potential interaction.

pressed in *Nicotiana benthamiana* leaves together with either GFP-MYB1, NSP1-GFP or GFP-DELLA1-Δ18 (a dominant version of DELLA1 (Floss et al., 2013)) failed to detect a significant interaction between any of these proteins (Fig. 1A, B). In contrast, we did detect an interaction between MYB1 and NSP1 as reported by Floss et al. (2017) (Fig. 1A). As a second method to check for interaction we performed yeast-two hybrid analyses. Co-expression of SPX1/3-AD (prey) and MYB-BD or DELLA1-Δ18-BD (bait) again did not detect a significant interaction between these proteins (Fig. 1C). Expression of NSP1-BD caused the autoactivation of reporters in our yeast-two-hybrid system preventing the observation of a potential interaction. Together these analyses suggested that regulation of arbuscule degeneration by SPX1 and SPX3 does not involve direct interaction with the MYB1 complex.

SPX1 and SPX3 interact with Medicago aquaporin PIP2

To identify potential novel targets of SPX1 and SPX3, we next performed an unbiased co-immunoprecipitation (Co-IP) experiment coupled with liquid chromatography tandem-mass spectrometry (LC-MS/MS). FLAG-tagged SPX1 and SPX3 were expressed from the *LjUB1* promotor in Medicago hairy roots. Five weeks after inoculation with *R. irregularis* we immuno-precipitated FLAG-tagged SPX1 and SPX3 and their potential plant interactors using anti-FLAG magnetic beads. Root expressing FLAG-tagged GFP were used as a negative control. LC-MS/MS identified multiple peptides that were significantly enriched compared to the FLAG-GFP control in the different samples (Fig. 2A,B; Table S3). In line with the previous analyses MYB1, NSP1 or DELLAs were not detected in the mass-spectroscopy data. Since SPX1 and SPX3 redundantly control arbuscule degradation (Chapter 4) we looked for proteins co-enriched in both SPX1 and SPX3 co-IP samples. This identified peptides corresponding to major intrinsic proteins (MIP) as co-enriched in both samples (Fig. 2A, B). Upon closer examination, the MIP peptides all corresponded to the plasma membrane intrinsic protein PIP2 family, also known as plasma membrane aquaporins (Young et al., 2011). There are 10 *PIP2* genes in the Medicago genome, and peptides corresponding to 3 of them were detected in our data. From these we selected *PIP2;7* (Medtr2g094270) (Hachez et al., 2014; Li et al., 2020) for further research, because it is highly expressed in AM roots and arbuscule-containing cells (Table S4) (Zeng et al., 2018).

To confirm the mass-spectroscopy data, we performed an independent Co-IP experiment on 3-week old mycorrhized Medicago roots expressing FLAG-tagged SPX1 or SPX3 together with GFP-PIP2. A FLAG-tagged fungal effector RirT167760, that localizes to both the cytoplasm and the nucleus was used as negative control. Western blot analyses confirmed the interaction of PIP2;7 with SPX1 and SPX3 (Fig. 3A). To further confirm the potential interaction, we used the split-ubiquitin membrane yeast-two hybrid system (Snider et al., 2010). Co-expression of PIP2;7 as bait with SPX1 or SPX3 as prey also showed a positive interaction in this assay (Fig. 3B). Together these results indicate that both SPX1 and SPX3 can interact with PIP2.

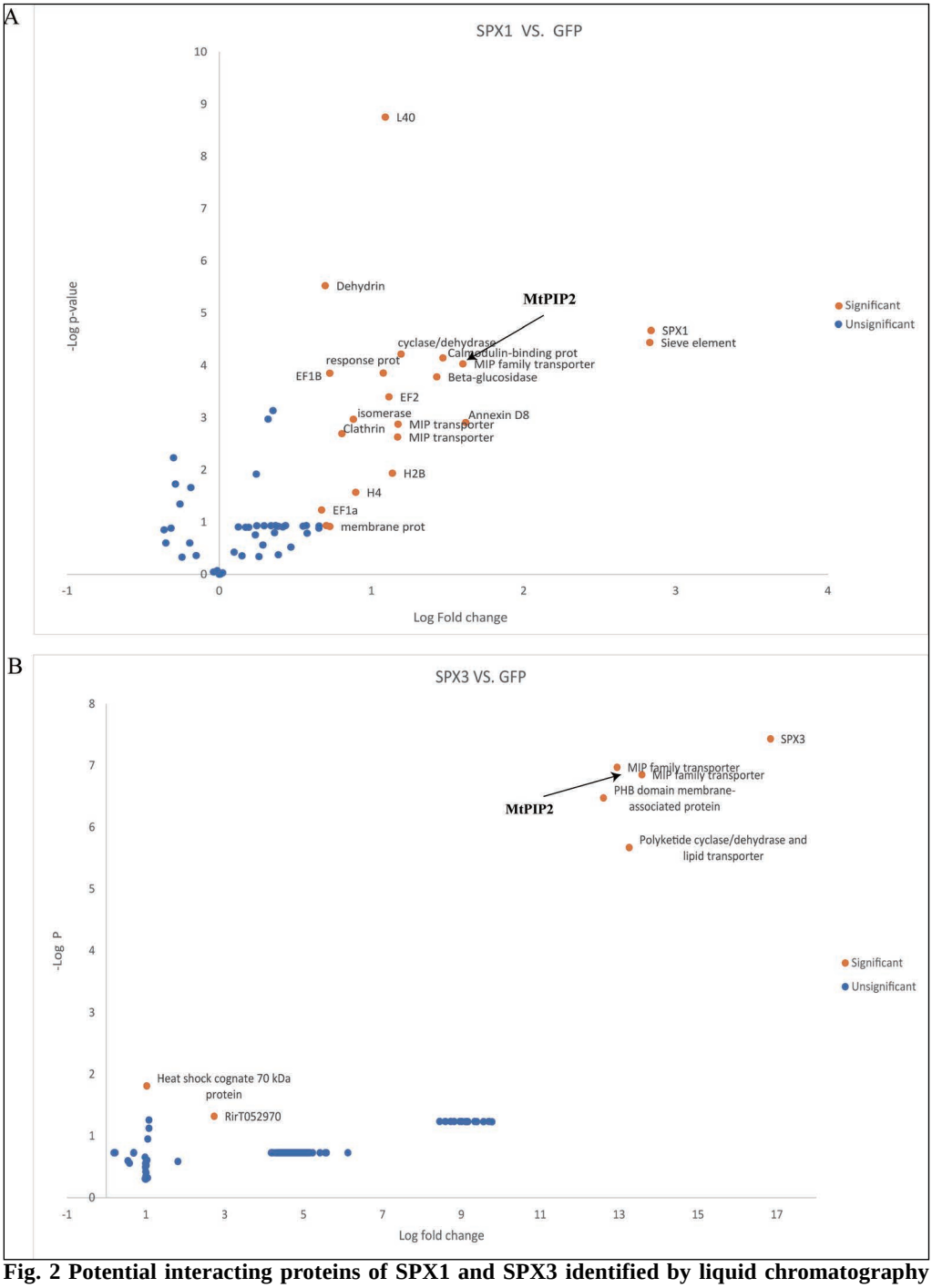

Fig. 2 Potential interacting proteins of SPX1 and SPX3 identified by liquid chromatography tandem-mass spectrometry. SPX1-Flag and SPX3-Flag fusion protein expressed in mycorrhizal *Medicago truncatula* roots under the control of *LjUB1* promoter were used for anti-Flag immunoprecipitation. The Flag-GFP fusion protein was used as control. Among the enriched proteins, MIP family transporters are significantly enriched both in SPX1 and SPX3 samples. Genome annotation shows that they are all PIP2 proteins.

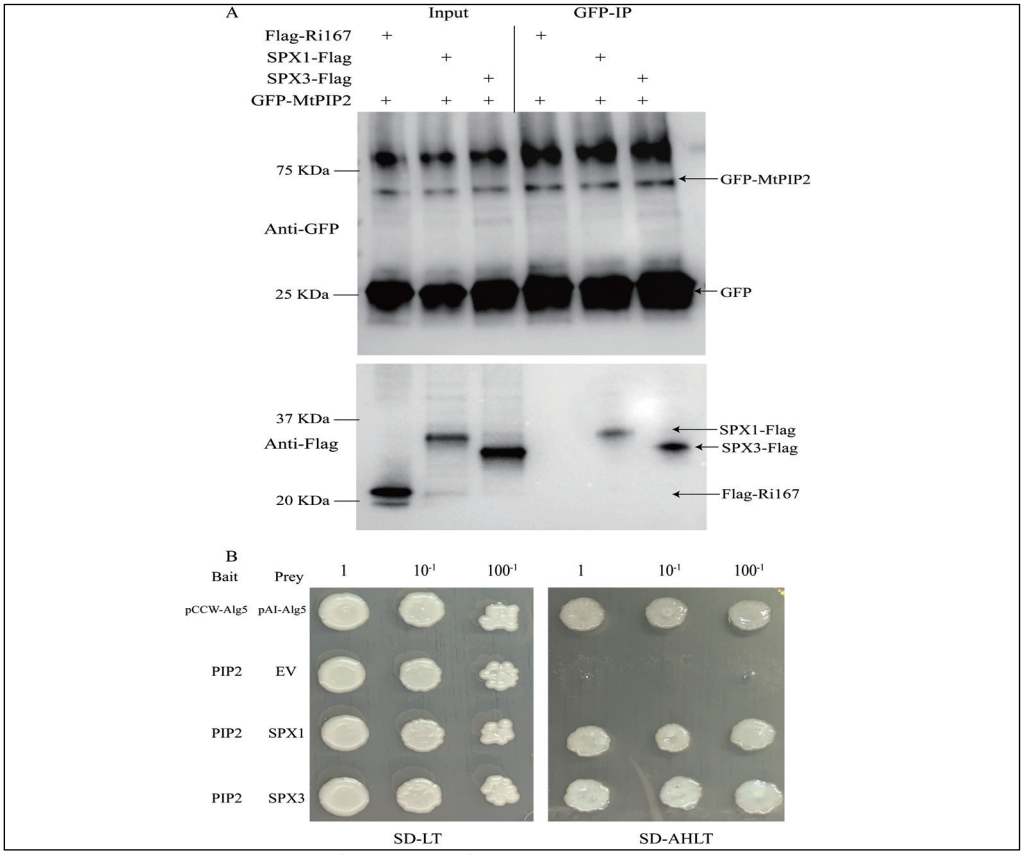

Fig. 3 MtPIP2;7 interacts with SPX1 and SPX3. (A) Co-immunoprecipitation (Co-IP) assay showing interaction between MtPIP2;7 and SPX1 and SPX3 in transiently transformed *Nicotiana benthamiana* leaves. SPX1-Flag and SPX3-Flag fusion protein can be detected in GFP-IP enriched GFP-MtPIP2 samples, while the negative control protein Flag-Ri167 cannot be detected. Ri167 is a fungal effector that has a similar localization as SPX1 and SPX3 in Nicotiana leaves. (B) Membrane Y2H assay showing that MtPIP2;7 interacts with SPX1 and SPX3. MtPIP2;7 was expressed in the bait vector pBT3-N. SPX1 and SPX3 were expressed in the prey vector pPR3-N. pCCW-Alg5 and pAI-Alg5 vectors in the DUALmembrane 3 Kit (Dualsystems Biotech AG) were used as positive control. Serial dilutions of dual transformed yeast cultures were plated on selective medium. SD-LT was used as control plate to show that the co-transformation was successful. Selection was carried out on SD-AHLT plates.

MtPIP2 localizes to the plasma membrane and peri-arbuscule membrane

As a first step to study the role of PIP2;7 in the symbiosis, we studied its subcellular localization in mycorrhized roots. Therefore, GFP-MtPIP2 was expressed in Medicago roots under the control of the constitutive *Lotus japonicus Ubiquitin 1* (*LjUB1*) promotor. This showed that GFP-PIP2;7 accumulated in the plasma membrane in non-mycorrhizal cells in line with its annotation as an plasma membrane aquaporin (Fig. 4A). In arbuscule-containing cells GFP-PIP2;7 was expressed under the control of the *PT4* promotor. This showed that GFP-PIP2;7 localized mostly to the peri-arbuscular membrane (Fig. 4B). Given the relatively strong expression of *PIP2;7* in arbuscule containing cells (Table S4) this suggests that it may play a role at the symbiotic interface.

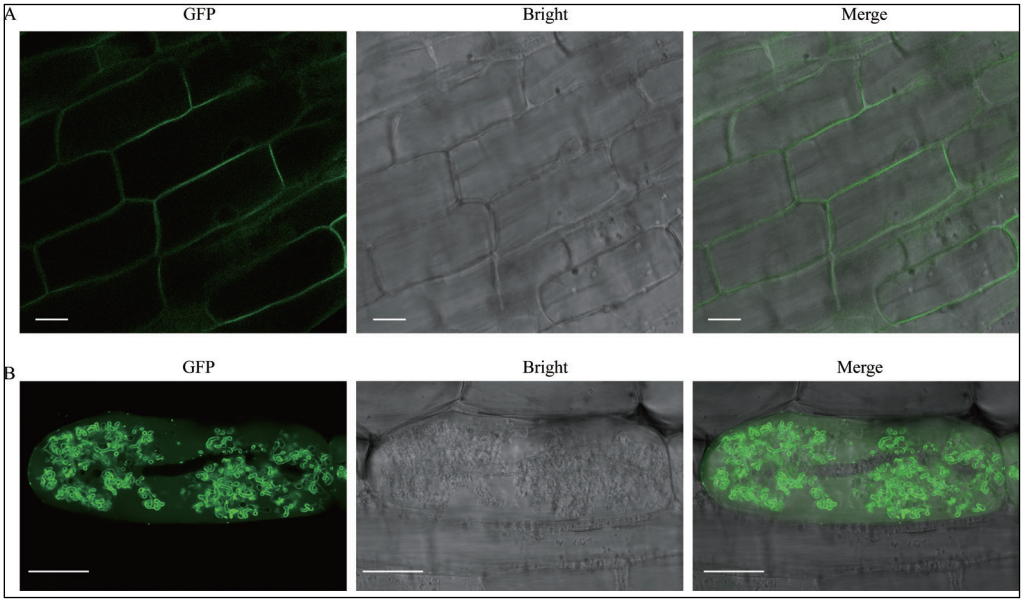

Fig. 4 MtPIP2;7 localizes to the plasma membrane and peri-arbuscular membrane. (A) GFP-MtPIP2 fusion protein expressed under the control of the *LjUB1* promoter in *Medicago truncatula* roots shows localization to plasma membrane. Different panels represent the following channels (from left to right): GFP, Bright field and all channels merged. (B) GFP-MtPIP2 fusion protein expressed under the control of the *PT4* promoter in *M. truncatula* mycorrhizal roots shows localization to peri-arbuscule membrane. Different panels represent the following channels (from left to right): GFP, Bright field and all channels merged. Scale bar in (A-B) is 10 μm. Images from (B) are kindly provided by Rik Huisman.

Overexpression of *MtPIP2* reduces arbuscule abundance

Next, we overexpressed untagged *PIP2;7* under the control of strong constitutive *LjUbiquitin1* promoter and examined its effect on the symbiosis. Empty vector (EV) transformed roots were used as controls. Three weeks after inoculation arbuscular mycorrhization levels were quantified using the intersect method (McGONIGLE et al., 1990). Overall fungal colonization levels and hyphal intensity showed no significant difference between *MtPIP2;7* overexpression and control samples (Fig. 5A). However the number of arbuscules (arbuscule abundance) was significantly lower in *MtPIP2* overexpression samples compared to the EV control (Fig. 5A, C, D). qPCR analyses confirmed the overexpression of *MtPIP2;7* as well as the observed phenotype; the fungal *RiEF1* reference gene was not significantly different in *UBQp::MtPIP2;7* roots compared to control roots, while MtPT4 expression, a marker for arbuscule abundance, was significantly lower in *UBQp::MtPIP2;7* roots (Fig. 5B). To rule out a specific effect on *PT4* expression, we analysed the expression of the fungal arbuscule specific *RiNLE1* effector (Wang et al., 2021; Chapter 1) as an additional marker gene for arbuscule abundance. Similar to *PT4*, the expression of *RiNLE1* was significantly lower in *MtPIP2;7* overexpressing roots as well (Fig. 5B), indicating a general effect on arbuscule abundance. Therefore, we examined arbuscule morphology in more detail, similar to the method used in Chapter 4. First, we quantified arbuscules in two classes where arbuscules larger or equal than 40 μM were quantified as “good” arbuscules, and arbuscules smaller

than 40 µm with typical features of degradation as "degrading" arbuscules. Interestingly, the ratio of "good" arbuscules was significantly higher in *MtPIP2;7* overexpression samples compared to EV control samples (Fig. 5A, 6A). This suggested that *MtPIP2;7* overexpressing roots contained less degraded arbuscules. Additionally, we quantified the arbuscule size distribution in EV and *MtPIP2;7* overexpressing roots by measuring 100 arbuscules per transgenic root (n = 8). This method also showed more larger developed (50-70 µm) arbuscules in *MtPIP2;7* overexpressing roots compared to EV controls (Fig. 6B), and less small (20-40 µm) arbuscules with septa. This arbuscule phenotype is somewhat similar to, but less severe than, that observed in the *spx1spx3* double mutant (Chapter 4). In contrast, the

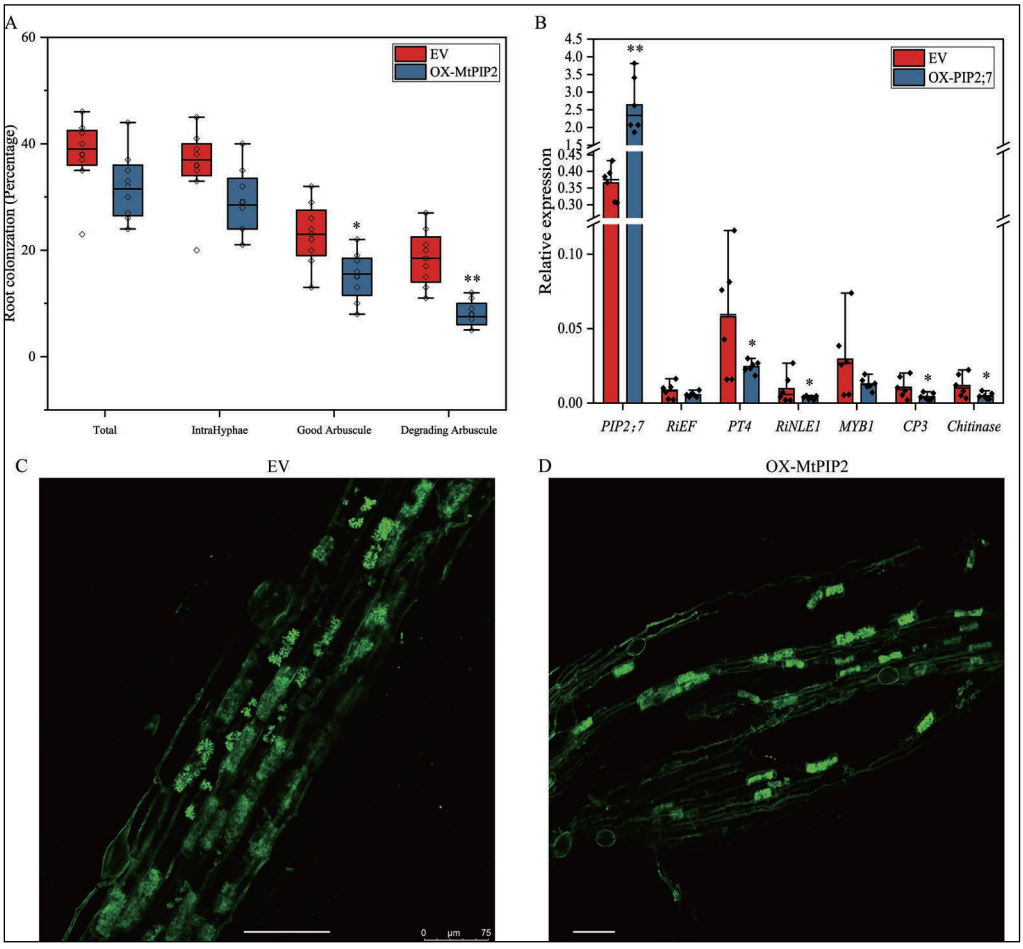

Fig. 5 Overexpression of *MtPIP2;7* reduced arbuscule abundance. (A) Quantification of the level of mycorrhization in *UBp:Flag-MtPIP2;7* transgenic roots and empty vector (EV) control roots, 3 weeks post inoculation. Indicated are the percentage of total colonization levels, intraradical hyphae (IntrHyphae), "good" arbuscules and "degrading" arbuscules. Eight independently transformed plants were used as replicates for each construct. (B) Expression levels of *RiEF*, *PT4*, *RiNLE1*, *MYB1*, *CP3* and *Chitinase* in root samples from (A) determined by qPCR analyses. *MtEF1* was used as internal reference. Data shown are the individual values of each biological replicates. Data significantly different from EV controls are indicated * $P < 0.05$; ** $P < 0.01$ (Student's t-test). (C) and (D) Representative images of WGA-Alexa488 stained *R. irregularis* in EV and *MtPIP2;7* overexpression samples. Scale bar = 100 µm.

expression levels of the arbuscule degradation-related genes *CP3* and *Chitinase* were not significantly reduced in the *MtPIP2;7* overexpressing roots relative to *PT4* or *MYB1* (Fig. 5B).

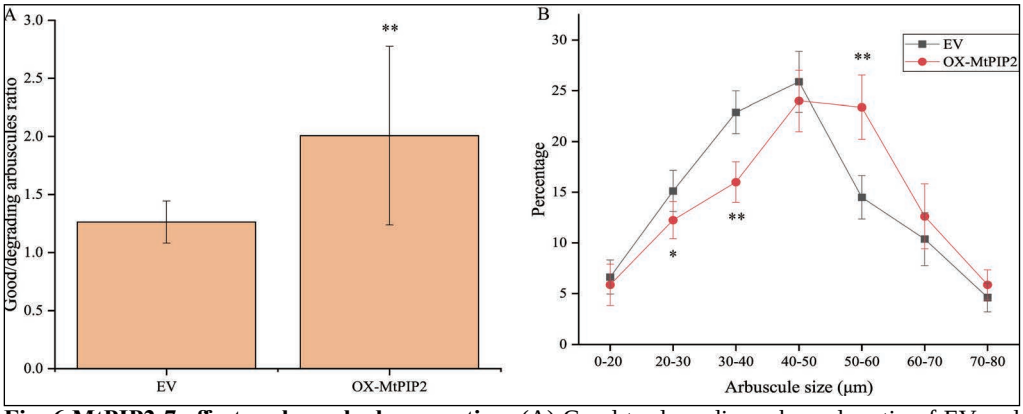

Fig. 6 MtPIP2;7 affects arbuscule degeneration. (A) Good-to-degrading arbuscule ratio of EV and *MtPIP2;7* overexpression mycorrhizal samples from (Fig. 5A). Values represent mean ± standard error of 8 independently transformed roots. Data significantly different from EV controls are indicated ** $P < 0.01$ (Student's t-test). (B) Analysis of arbuscule size in EV and *MtPIP2;7* overexpression mycorrhizal samples from (Fig. 5A). Frequency graphs showing arbuscule size distribution. 100 arbuscules were counted for each of the 8 replicates. Data significantly different from EV controls are indicated ** $P < 0.01$ (Student's t-test).

Discussion

The ability to control arbuscule development and lifetime according to the fungal supply of nutrients such as phosphate is of key importance to keep the AM symbiosis beneficial. In Chapter 4 we showed that the phosphate-sensing SPX1 and SPX3 proteins redundantly control arbuscule degradation. Here we show that SPX1 and SPX3 do not regulate arbuscule lifetime through direct interaction with the MYB1 transcriptional complex, known to be required for arbuscule degradation when the fungus does not deliver Pi (Floss et al., 2017). Instead SPX1 and SPX3 were both found to interact with PIP2 aquaporins in Medicago roots. PIP2 aquaporins form a small protein family of 10 members in Medicago. Many of these are strongly, yet variably, expressed throughout plant development, and several are also highly expressed in arbuscule-containing cells. Peptides from 3 PIP2 aquaporins were enriched in both samples. Therefore, we cannot conclude whether there is any isoform specificity in the interactions. However, we did verify the interaction of SPX1 and SPX3 with MtPIP2;7 (Medtr2g094270), which is abundantly present in arbuscule containing cells and which localizes to the peri-arbuscular membrane.

PIP2s are known to form hetero-tetramers with the PIP1 class of plasma membrane intrinsic proteins (Fetter et al., 2004; Bienert and Chaumont, 2014). In general PIP1 requires PIP2 for efficient transport the plasma membrane and lacks significant water transport ability by itself (Chaumont et al., 2000). However, interaction between PIP1 and PIP2 can increase water permeability of the aquaporin complex as well as solute specificity. We did not detect PIP1 peptides in our Co-IP mass spectroscopy data indicating specificity for PIP2. However it would be interesting to test whether the SPX-PIP2 interaction affects the ability of PIP2

to homo- or heteromerization.

A major focus for further research will be to determine whether SPX1 and SPX3 affect PIP2 transport activities. The water transport activity of plasma membrane aquaporins has been previously postulated to play an important role during AM symbiosis. Interestingly, *PIP2;7* expression in Medicago has been shown to be induced in arbuscular mycorrhizal roots to optimize water and ammonium transport (Uehlein et al., 2007). In maize, the phosphorylation status of maize PIP2 levels increased in AM roots subjected to water shortage, which caused a higher water permeability of root cells (Quiroga et al., 2019). This correlated with increased photosynthetic capacity and stomatal conductance, suggesting a connection between shoot and root parameters. Increased transpiration and increased water transport from the roots was further suggested to facilitate the transport of poly-P from the extraradical hyphae to the arbuscules (Kikuchi et al., 2016). In this model, increased water flow due to PIP activity could lead to increased Pi transfer at the arbuscules.

Besides acting as key water channels, plasma membrane aquaporins have been shown to play additional roles, such as transport of small solutes like ions, peptides, H_2O_2, urea or glycerol. Furthermore, it is increasingly becoming clear that aquaporins act as hubs in signal transduction and response to abiotic stress (Hachez and Chaumont, 2010; Bienert and Chaumont, 2014). Indeed, PIPs have been shown to be involved in a wide range of cellular and developmental processes (Tyerman et al., 2002; Martre et al., 2002). Interactomics studies have revealed PIPs to behave as important platforms for the recruitment of a wide range of transport activities (Bellati et al., 2016). In Arabidopsis PIP1 and PIP2 were found to share ~400 interacting proteins, which include many transporters, including phosphate transporters, as well as various protein kinases (Bellati et al., 2016). Furthermore, a PIP2 aquaporin in rose was recently shown to interact with a membrane-tethered MYB transcription factor to regulate growth and stress responses according water availability (Zhang et al., 2019). In turn, post-translational modifications such as phosphorylation and ubiquitination of PIPs play an important role in the control of their transport activities (Bellati et al., 2016; Zhang et al., 2019).

A role for PIP2 in the control of arbuscule development was strengthened by the observation that constitutive overexpression of *MtPIP2;7* caused an overall reduction in arbuscule numbers, while at the same time increasing the ratio of “good” versus “degrading” arbuscules. It should be noted that we only measured arbuscule phenotypes at a single time point, three weeks after inoculation. Therefore, we cannot rule out a possible delay in mycorrhization due to the overexpression of *PIP2*. To circumvent potential pleiotropic effects future experiments should examine the effect of arbuscule-specific overexpression of *PIP2* along a time course. Nevertheless, the increased “good to degraded” arbuscule ratio in *MtPIP2;7* overexpression roots somewhat resembles the reduced arbuscule degradation phenotype seen in the *spx1spx3* double mutant (Chapter 4). In contrast to the *spx1spx3* mutant the expression of arbuscule degradation-related genes did not appear to be significantly affected in the *PIP2* overexpressing roots. This might be because *MtPIP2* overexpression showed a much milder effect on arbuscule degeneration.

Based on these results it is tempting to speculate that SPX1 and SPX3 might function to inhibit PIP2 activity in a Pi-dependent manner; if an arbuscule-containing cell has acquired sufficient Pi, binding of SPX1/3 to PIP2 may inhibit its activity to stop the translocation

of Pi from the arbuscule. A similar role might be played under non-symbiotic conditions. Transport of Pi out of the arbuscule cell towards the vasculature, could subsequently reduce Pi levels and lead to the activation of MYB1 to activate the arbuscule degradation program. It will now be exciting to test this hypothetical model in future experiments.

Supplementary tables

Table S1. Primers list used in this study

qPCR	MtEF-qF	GATTGCCACACCTCTCACAT
qPCR	MtEF-qR	TCAGCGAAGGTCTCAACCAC
qPCR	PT4-qF	GGATTCTTTTGCACGTTCTTGG
qPCR	PT4-qR	GCTGTCATTTGGTGTTGCAGTG
qPCR	RiEF-qF	ATTGTTCGTGGTGCATTTCA
qPCR	RiEF-qR	AACCCCTTCGTCTTCCACTT
qPCR	MYB1-qF	TAAGAGAGTTGATGATGATTGTC
qPCR	MYB1-qR	GATGAGTGATTCTGTTGAACC
qPCR	CP3-qF	AACAATGATGCCAATAACAAGC
qPCR	CP3-qR	GGAGCACATATGACCCTTGA
qPCR	Chitinase-qF	GGCATGTCAGAGGTTGAAGAG
qPCR	Chitinase-qR	GCCAAAAGTGCTTGTGATTG
qPCR	MtPIP2-qF	GGCTGTGACCTTTGGGCTAT
qPCR	MtPIP2-qR	CTTTGCAAGTCCAGCACCAC
Goldengate	F-LjUB1-Pro-CCAT	AGAAGACTCGGAGGGAGAGAGGATTTTGAGGAAATA
Goldengate	R-LjUB1-Pro-CCAT	GGAAGACGCATGGCTGTAATCACATCAACAACAGATAA
Goldengate	MtPIP2-CDS1-F	AGAAGACTCAATGGGCAAAGATGTTGAGGT
Goldengate	MtPIP2-CDS1-R	GGAAGACAGAAGCTTAAGCATTGCTCCTGAAGGA

Table S2. Constructs made using the golden gate cloning system

Level 0	Level 1	Level 2
pICH41295-LjUBQ1p-AATG	pICH47732-LjUBQ1p::SPX1-FLAG	pAGM4723-LjUBQ1p::SPX1-FLAG-AtUBQ10p::DsRed
pAGM1251-LjUBQ1p-CCAT	pICH47732-LjUBQ1p::SPX3-FLAG	pAGM4723-LjUBQ1p::SPX3-FLAG-AtUBQ10p::DsRed
pAGM1287-SPX1 CDS1 no stop	pICH47732-LjUBQ1p::SPX1-GFP	pAGM4723-SPX1p::SPX1-GFP-AtUBQ10p::DsRed
pAGM1287-SPX3 CDS1 no stop	pICH47732-LjUBQ1p::SPX3-GFP	pAGM4723-SPX3p::SPX3-GFP-AtUBQ10p::DsRed
pICH41308-MYB1-CDS1	pICH47751-LjUBQ1p::SPX3-GFP	pAGM4723-LjUBQ1p::SPX1-FLAG-AtUBQ10p::DsRed-LjUBQ1p::SPX3-FLAG
pICH41308-NSP1-CDS1	pICH47811-AtUBQ10p::DsRed	pAGM4723-LjUBQ1p::SPX1-FLAG-AtUBQ10p::DsRed-LjUBQ1p::GFP-PHR2
pICH41308-DELLAΔ18-CDS1	pICH47751-LjUBQ1p::GFP-NSP1	pAGM4723-LjUBQ1p::SPX3-FLAG-AtUBQ10p::DsRed-LjUBQ1p::GFP-PHR2
pICH41308-WRI5a-CDS1	pICH47732-LjUBQ1p::GFP-DELLAΔ18	pAGM4723-LjUBQ1p::GFP-MYB1-AtUBQ10p::DsRed

pICH47751-LjUBQ1p::-FLAG-NSP1	pAGM4723-LjUBQ1p::GFP-PHR2-AtUBQ10p::DsRed pAGM4723-LjUBQ1p::GFP-NSP1-AtUBQ10p::DsRed pAGM4723-LjUBQ1p::SPX1-FLAG-AtUBQ10p::DsRed-LjUBQ1p::GFP-NSP1 pAGM4723-LjUBQ1p::SPX3-FLAG-AtUBQ10p::DsRed-LjUBQ1p::GFP-NSP1 pAGM4723-LjUBQ1p::GFP-DELLAΔ18-AtUBQ10p::DsRed pAGM4723-LjUBQ1p::Flag-WRI5a-AtUBQ10p::DsRed

Table S3 LC-MS/MS identified significantly enriched peptides intensity information for SPX1-Flag and SPX3-Flag Co-immunoprecipitation in mycorrhizal roots. Flag-GFP Co-immunoprecipitation samples were used as control. LFQ (label-free quantification). Data significantly enriched from Flag-GFP controls are indicated with a + ; P < 0.05 (Student's t-test).

Table S3 can be found at https://doi.org/10.1101/2021.02.09.430431

Table S4 PIP2-like genes expression levels in arbuscule-containing cells (Data collected from Zeng et al., 2018). Indicated are mean TPM values of arbuscules, intracellular hyphae and their ratio.

Gene ID	Arbuscule- Means	Hyphae - Means	ARB/HYP
Medtr2g094270 (MtPIP2;7)	269.1270478	595.2571645	0.45211896
Medtr4g059390	70.08439423	354.0473346	0.19795205
Medtr7g101190	5.406852815	6.212832892	0.87027173
Medtr3g118010	0	1.132900987	0
Medtr8g098375	0.070199656	0.29858184	0.23511027
Medtr5g010150	0.312280721	0.853651893	0.36581741
Medtr4g415300	0.30993739	1.504937422	0.20594703
Medtr5g082070	182.5898567	424.7497697	0.42987629
Medtr3g070210	287.0355621	553.906888	0.51820183
Medtr1g095070	2.591271765	2.853930922	0.90796583

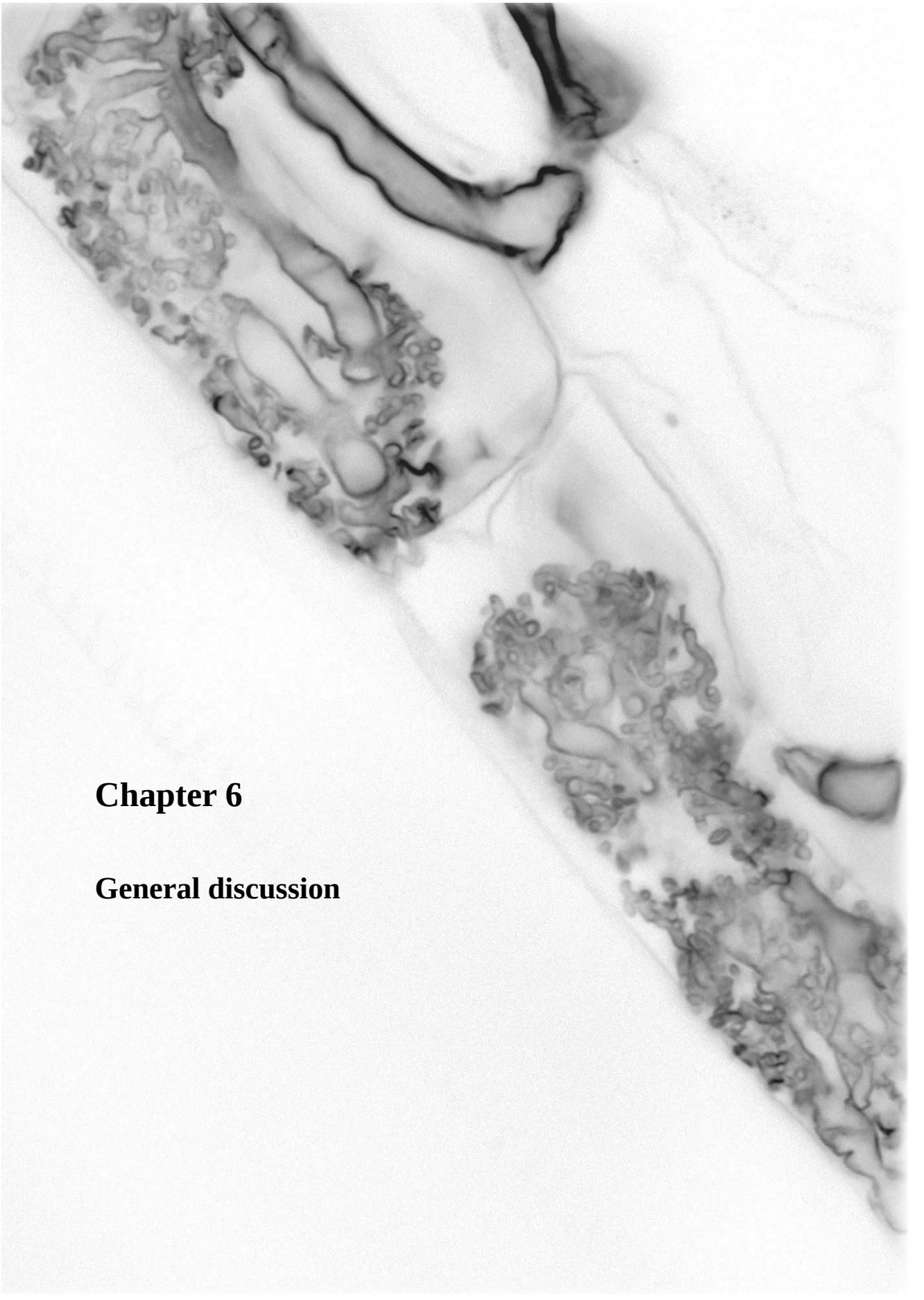

Chapter 6

General discussion

Arbuscular mycorrhizal fungi are widely recognized for their potential as sustainable biofertilizers. The fact that the AM symbiosis originated ~450 million years ago and has since been maintained in the vast majority of land plants highlights their integral part of plant life in natural ecosystems (Redecker et al., 2000; Smith and Read, 2008). In the field, plants are most often colonized by multiple AM fungal species (Vandenkoornhuyse et al., 2007) and a single fungus can simultaneously colonize a large variety of host plants (Mikkelsen et al., 2008). However, significant variation in plant growth responses to different fungi has been reported (Klironomos, 2003; Helgason et al., 1998; Vandenkoornhuyse et al., 2003; Martínez-García and Pugnaire, 2011; Torrecillas et al., 2012; van der Heijden et al., 2015). Furthermore, under natural conditions different plants preferentially associate with distinct AM fungi. However, the molecular mechanisms underlying such partner selection in AM symbiosis are still largely unknown. In this chapter I will discuss my results in the broader context of partner preferences and how both partners may ensure a mutually beneficial interaction. I will especially focus on two questions: 1) Does the plant immune system contribute to partner selection; and 2) How can nutrient sensing and exchange influence partner preference?

Partner preferences

The fact that globally distributed AM fungi like *Rhizophagus irregularis* have been observed to infect the majority of land plants they encounter in nature has led to the perspective that there is very little host specificity in the AM symbiosis (Smith and Read, 2008; Parniske, 2008). However, AM fungal species isolated from roots of different plants collected at the same place showed that different plant species harbour quite distinct AM fungal communities in natural settings (Helgason et al., 2002; Vandenkoornhuyse et al., 2003; Helgason et al., 2007). This indicates that certain AM fungi prefer certain host plants or that different host plants are able to select fungal species that they prefer to cooperate with. Furthermore, laser dissection of individual roots showed that the AM fungal communities that colonize the root do not contribute equally to arbuscule formation (Berruti et al., 2013), indicating different contributions to plant nutrition. In line with this, the effect of plant growth responses to different AM fungi, the so-called mycorrhizal growth response, can range from parasitic to mutualistic (Klironomos, 2003; McHaffie and Maherali, 2020). This has led to the suggestion that different AM fungi may provide different benefits to the plant / ecosystems functions (van der Heijden et al., 2015). Thus an optimal mycorrhiza depends on both plant and fungal genotypes. In addition, environmental context, such as nutrient availability, influences the partner preference. For example, plants grown in conditions with increasing CO2 levels were found to allocate more carbon to higher quality mutualists, which over time resulted in a reduction in the abundance of lower quality AM fungi (Werner et al., 2018). It has also been shown that plants, when given the choice allocate more carbon to a fungus that provide more phosphate, and vice versa (Kiers et al., 2011). This reciprocal exchange of nutrients has been suggested to represent a biological market place, where both partners trade their specialized resources (Kiers and Van Der Heijden, 2006; Werner et al., 2014; van der Heijden et al., 2015). Reciprocal rewarding was suggested to stabilize the symbiosis (Kiers et al., 2011), where partners that offer the best rate of nutrient exchange are favoured (Noë and Kiers, 2018; van't Padje et al., 2021).

Despite such theoretical frameworks, the molecular basis for partner preference, reciprocal nutrient exchange or variation in mycorrhizal growth responses is still far from understood.

Below I will discuss several mechanisms that might be at play.

Pre-contact signalling

Partner selection may already start at the pre-contact phase, when the plant secretes chemical cues to attract AM fungi. Plant roots secrete a plethora of molecules into the environment with substantial influence on the soil microbiome surrounding them (Jacobowitz and Weng, 2020). Various molecules have been identified to stimulate AM fungal germination, hyphal branching and growth to promote fungal–host encounters. These include for example, flavonoids, 2-hydroxy fatty acids and strigolactones (Becard et al., 1992; Nagahashi and Douds, 2011; Akiyama et al., 2005; Besserer et al., 2006, 2008; see also Chapter 1). Little is known about whether different root exudates confer specificity or whether plants adjust their root exudates to attract distinct AM fungi.

It has been shown that when under pathogen attack, Arabidopsis increased malic acid secretion, which lead to attract root colonization of the beneficial bacteria *Bacillus subtilis* (Rudrappa et al., 2008). Plant exudates varied among different genotype, as observed in 19 Arabidopsis accessions with distinct exudation patterns (Monchgesang et al., 2016). Different exudation patterns have been suggested to explain the association of distinct microbiomes with different plant accessions (Etemadi et al., 2018). Furthermore, plant exudation changes with different developmental stages of the plant, which in turn affects the root microbiome (Chaparro et al., 2014; Sasse et al., 2018). It can therefore be expected that also in AM symbiosis changes in root exudates play a role in partner selection. In line with this, it was for example shown that specific flavonoids were induced before and during AM symbiosis in Medicago suggesting mycorrhizal-fungal specificity (Larose et al., 2002; Schliemann et al., 2008). Specific flavonoids where found to be able to enhance AM colonization, while others had negative effects (Abdel-Lateif et al., 2012). Furthermore, several flavonoid compounds of white clover were found to differently affect growth of Glomus and Gigaspora species (Scervino et al., 2005).

As mentioned, nutrient status has a major effect on root exudation. For example in relation to AM symbiosis, phosphate and nitrogen starvation were shown to induce the production and exudation of strigolactones, derived from the carotenoid pathway (Yoneyama et al., 2007a, 2007b, 2008; López-Ráez et al., 2008; Umehara et al., 2008) How nutrient availability modulates SLs production and exudation remains elusive (Yoneyama et al., 2020). Several SL biosynthesis genes have been found to be regulated at the transcriptional level by Pi conditions (Umehara et al., 2010; Sun et al., 2014). One of the key strigolactone biosynthesis genes, *DWARF27* (*D27*), was shown to be induced under phosphate-limited conditions in an NSP1/NSP2-dependent manner in Medicago (Liu et al., 2011). NSP1 and NSP2 are GRAS transcription factors that are also implicated in the common symbiotic signaling pathway (Smit et al., 2005; Kaló et al., 2005). In Chapter 4 we show that induction of *MtD27* expression upon Pi starvation does not involve direct regulation by the MYB transcription factor PHR, a key regulator of phosphate starvation induced gene expression (Rubio et al., 2001; Zhou et al., 2008). Instead we found that induction of *D27* at low Pi conditions involved the AM-regulated SPX proteins SPX1 and SPX3, that also act as Pi-dependent negative regulators of PHR activity.

Gibberellins (GAs), in addition to several other plant hormones, have also been suggested to affect SL production and exudation (Ito et al., 2017). High Pi conditions correlate with

increased GA levels in the roots and application of GA was shown to reduce SL levels in roots and root exudates. GA levels also play a key role in the regulation of AM symbiosis, through the regulation of DELLA transcription factors (Foo et al., 2013). GA perception leads to the degradation of DELLAs. Therefore DELLAs may be regulators of SL biosynthesis. DELLAs were further reported to interact with NSP2-NSP1 and to bridge a connection between CYCLOPS and NSP2 to control the output of the common symbiotic signaling pathway to allow the formation of arbuscules (Floss et al., 2013; Jin et al., 2016; Pimprikar et al., 2016). This raises the question whether there may be a link between SPX1/3, NSP1/2 and/or DELLA activity under low Pi conditions, which remains to be investigated; see also the discussion on "Nutrient sensing and exchange" below.

Different plants have been shown to produce and exude strigolactones with different structures (Liu et al., 2011; Kohlen et al., 2011; Monchgesang et al., 2016; Umehara et al., 2010). This could also be the case for the Medicago ecotypes A17 and R108. In Medicago A17, the strigolactone didehydro-orobanchol can easily be detected in the exudates of roots grown under Pi limiting conditions (Liu et al., 2011). However, using a similar setup we were not able to measure (known) strigolactones in the exudates of R108 (Chapter 4). Nevertheless, the exudate of R108 was able to induce hyphal branching in *Rhizophagus irregularis* as well as seed germination of the parasitic Orobanchae plant *Phelipe ramosa* in an SPX1/3 dependent manner. Together with the SPX1/3-dependent regulation of *D27* expression this strongly suggests that SL levels are affected in the *spx* mutants. Reduced SL exudation in the *d27* mutant (as well as other strigolactone biosynthesis mutants) has been correlated with lower fungal colonization levels (Liu et al., 2011), and a similar reduction in colonization was seen in the *spx* mutants (Chapter 4). However, we cannot rule out that SPX1/3 may affect other root exudates to facilitate root colonization.

It is currently not known whether different SLs vary in their ability to recruit or activate distinct AM fungi. In analogy to the role of flavonoids, it would be interesting to test whether plants varying in SL profile preferentially associate with different AM fungi. Currently it is not known how AM fungi perceive SLs. Homologs of the plant SL receptor D14 (Yao et al., 2016) have not been identified in any of the currently sequenced AM fungal genomes. Therefore, future insight into how SL are perceived by AM fungi might give insight into SL structure-function relationship during AM symbiosis.

Given the wealth of metabolites produced by both plants and fungi, it is likely that additional compounds remain to be identified that influence partner choice and how plants select for beneficial microbes while restricting pathogens. The essential role of the putative GlcNac transporter NOPE1 and the karrikin receptor D14L in rice clearly point in this direction (Nadal et al., 2017; Gutjahr et al., 2015; see also Chapter 1).

The involvement of the plants immune system in partner control

Like pathogenic fungi, AM fungi contain conserved microbe/pathogen-associated molecular patterns (MAMPs/PAMPs) such as β-glucan and chitin in their cell walls, which trigger a first line of plant defense responses called PAMP-triggered immunity (PTI (Jones and Dangl, 2006; Fesel and Zuccaro, 2016). Indeed, AM fungi were shown to trigger plant defense response at the early stages of AM symbiosis, however such defense response were subsequently rapidly inhibited (Kapulnik et al., 1996; García-Garrido and Ocampo, 2002). It could be that the host plant actively reduces its immune responses to welcome the AM

fungus, or that the AM fungus is able to subvert the plant immune response, or a combination of both.

It has recently become clear that immune responses are intertwined with nutrient signaling. For example, phosphate deprivation was found to the suppress the plant immune system, opening the door for plant–microbe interactions (Hacquard et al., 2016). Follow-up work identified PHR1 as a central regulator in this balance between nutrient stress response and immune regulation in Arabidopsis to regulate plant-microbe interactions (Castrillo et al., 2017; Finkel et al., 2019). How PHR1 regulates immune signaling remains to unravel. However, a lowered immune response makes the plant at the same time vulnerable to pathogens. Therefore, there must be specific check points by which a plant can distinguish between friend from foe. Several recent findings support a role for plant immune responses in partner selection during AM symbiosis.

MAMP perception

The initiation of symbiosis and defense responses both involve the recognition of chitooligosaccharides (COs) signal molecules (Maillet et al., 2011; Genre et al., 2013; Newman et al., 2013; Akamatsu et al., 2016; Chapter 1). For example, both CO4 and CO8 have been shown to activate symbiotic signaling and defense signaling in *M. truncatula* (Feng et al., 2019). When in combination with lipo-chitooligosaccharides (LCOs), symbiotic signaling was enhanced while immune signaling was suppressed (Feng et al., 2019). This suggested that the perception of mixes of COs and LCOs is important for host plant to recognize AM fungi. It is currently not known whether different AM fungi species secret different composition/levels of (lipo-)chitooligosaccharides to affect the interaction with the host plant. Both CO's and LCO's are recognized by Lysin-motif (LysM) containing receptors (Limpens et al., 2003; Amor et al., 2003; Radutoiu et al., 2003; Madsen et al., 2003; Miyata et al., 2014; Bozsoki et al., 2017). In rice, the LysM receptor OsCERK1 was demonstrated to regulate both chitin-triggered immune responses and AM symbiosis (Shimizu et al., 2010; Miyata et al., 2014). Upon chitin-triggered immune signaling, OsCERK1 forms a complex with the co-receptor OsCEBiP to activate defense response (Akamatsu et al., 2013). Upon symbiotic signaling, OsCERK1 forms a complex with the co-receptor OsMYR1 (He et al., 2019). This discrimination is achieved through receptor competition for CO4, which binds preferentially to OsMYR1 and inhibits the interaction between OsCERK1 and OsCEBiP (Zhang et al., 2021). In turn, OsCEBiP has been shown to interfere with OsCERK1 and OsMYR1 interaction in a CO8 dependent manner (Zhang et al., 2021). Furthermore, the *Oscebip* mutant showed a higher level of mycorrhizal infection at the early stages of AM symbiosis. This correlated with lower expression of immunity markers genes in *Oscebip* mutant (Zhang et al., 2021). A competition between LysM receptor complexes was also proposed in legumes such as Lotus and Medicago (Van Zeijl et al., 2015; Bozsoki et al., 2020).

Recently, it was shown that variation in the efficiency of AM colonization is influenced by OsCERK1 allelic variants in different rice varieties (Huang et al., 2020). Dongxiang wild rice showed higher colonization levels by *R. irregularis* than the rice cultivar Zhongzao 35. This was found to be caused by two amino acids differences in the second lysine-motif domain of OsCERK1 between Dongxiang and Zhongzao 35 (Huang et al., 2020). Introduction of the Dongxiang OsCERK1 allele in Zhongzao 35 rice increased fungal colonization levels and led to higher phosphorus content and grain yield (Huang et al., 2020). This suggests

that host plants can discriminate between different microbes and possibly different AM fungi through their LysM receptor repertoire, by balancing between symbiotic and immune signaling. It would be interesting to test whether Dongxiang and Zhongzao 35 rice show differences in colonization efficiency with different AM fungi in an OsCERK1 dependent manner. In this respect, it is also relevant to study whether different AM fungi make different CO/LCO molecules. LCO structure is well known to plays a key role in the regulation of host specificity in the rhizobium-legume symbiosis (Schultze and Kondorosi, 1996; Radutoiu et al., 2007; Bozsoki et al., 2020).

Intriguingly, it was recently found that LCOs are also produced by non-symbiotic and pathogenic fungi (Rush et al., 2020). However, solid evidence that pathogens make use of the symbiotic signaling pathway to colonize plants is strikingly lacking. Therefore, activation of symbiotic signaling alone is likely not enough for a microbe to be perceived as friend. Besides PAMPs as inducers of immune responses, cellular damage inflicted by microbes may play an important additional role to distinguish between microbes (Poncini et al., 2017; Hander et al., 2019; Zhou et al., 2020). A wide variety of damage associated molecular pattern (DAMP) molecules has been identified that are perceived by distinct pattern recognition receptors (Brutus et al., 2010; Hou et al., 2014; Jewell et al., 2019; Pham et al., 2020). This has led to the proposition that plants have the potential to identify the diverse types of damage that microbes can elicit and that a combination of MAMP and DAMP perception ultimately sets an immune threshold (Thoms et al., 2021). The loss of many plant cell wall degrading enzymes from AM fungal genomes (Tisserant et al., 2013), may therefore be of key relevance to be perceived as potential friend.

Effectors

Besides modulating the production or recognition of PAMP/DAMP signals, fungi also use secreted effector proteins to actively suppress the plant immune system and to facilitate infection (Lo Presti et al., 2015). Such effector proteins, which act either in the apoplast or are translocated in plant host cells, play a key role in the host range of pathogenic fungi. It has become clear that also mutualistic fungi use effector proteins to facilitate their interaction with the plant (Kloppholz et al., 2011; Plett et al., 2014; Wawra et al., 2016; Zeng et al., 2020).

Transcriptome analyses of *R. irregularis* revealed the expression of several hundreds of putative effectors in different host plant interactions (Tisserant et al., 2013; Zeng et al., 2018; Kamel et al., 2017). These putative effectors can be roughly divided in into members that are more or less equally induced by a wide range of plant species and members that show a much more host-dependent regulation. Furthermore, genome sequencing of a range of AM fungal plant species and isolates has revealed a large variety in the potential effector repertoire of different AM fungi (Tisserant et al., 2013; Sędzielewska Toro and Brachmann, 2016; Kobayashi et al., 2018; Morin et al., 2019). Based on such comparisons effectors may be further divided into conserved and strain-specific members (Sędzielewska Toro and Brachmann, 2016). For example, the expressed effector repertoire of two AM fungi, *R. irregularis* DAOM 197198 and *Gigaspora rosea* was compared (Kamel et al., 2017). *R. irregularis* DAOM 197198 has a very broad host spectrum and occurs globally across the world, while *G. rosea* shows a narrower host range and a more restrictive geographic distribution (Öpik et al., 2010). Comparative expression analyses indicated that *G. rosea*

expressed more putative effectors in a host-dependent manner than *R. irregularis* DAOM 197198 (Kamel et al., 2017). This suggests that the number of core symbiotic effectors, that are more or less similarly expressed in all host plants, correlates with the host range of different AM fungi (Kamel et al., 2017), further strengthening the idea that effectors contribute to the host range of AM fungi.

Among the core effector classes that seems to be widely applied by both AM fungi and pathogenic fungi are LysM domain containing effectors (Jonge et al., 2010; Sánchez-Vallet et al., 2013; Schmitz et al., 2019; Zeng et al., 2020). A single LysM domain containing effector, called Secreted LysM (RiSLM) protein, was identified in *R. irregularis* (Schmitz et al., 2019; Zeng et al., 2020). Similar to several LysM effector proteins from pathogenic fungi, RiSLM was found to bind chitooligosaccharides and to inhibit chitin-triggered immunity as well as protect fungal hyphae against the activity of chitinases (Jonge et al., 2010; Sánchez-Vallet et al., 2013; Schmitz et al., 2019; Zeng et al., 2020; Sánchez-Vallet et al., 2020). The relative low (micromolar range) affinity of RiSLM for various CO and LCO molecules suggests that RiSLM, in analogy to the receptor competition described above, may help to shift the balance of CO perception towards a symbiotic outcome. Indeed, RiSLM did not interfere with LCO-mediated symbiotic gene expression in Medicago which involves LysM receptors with a much higher affinity for LCO's (Broghammer et al., 2012). Intriguingly, although RiSLM homologs were identified in all sequenced AM fungal genomes, their amino acid sequence showed a strikingly high level of variation and signs of diversifying selection even between different fungal isolates of *R. irregularis* (Schmitz et al., 2019; Zeng et al., 2020). This may suggest that the different SLM homologs vary in their affinity for different chitoologisaccharides and thereby show different abilities to interfere with receptor complex formation. Another explanation for the observed variation could be that the LysM effectors may diversify to escape recognition by host-specific resistance (R) proteins that trigger so-called effector-triggered immune responses (Jones and Dangl, 2006). In case of pathogenic fungi, there is a continuously evolving arms race between effectors and R proteins that determining the host range of pathogenic fungi. The recognition of effectors by host R proteins gives a high evolutionary pressure to pathogens to circumvent this recognition (Thordal-Christensen et al., 2018; Bertazzoni et al., 2018). A high mutation rate combined with a faster reproduction rate than the host plant enables the pathogen to outrun the host immune system to remain virulent or to jump to a new host (Thines, 2019). For example, the *F. oxysporum* f. sp. Lycopersici effector Avr2 is required for infection in a susceptible host but also induces resistance in tomato host carrying the R protein I-2 (Houterman et al., 2009). Since LysM domain effectors are used by both mutualists and pathogens, such an arms race could drive variation in SLM sequence.

One of the first identified effector proteins from *R. irregularis* is Secreted Protein 7 (RiSP7) (Kloppholz et al., 2011). Like RiSLM, the presence of this effector is conserved in a wide variety of AM fungi. RiSP7 was shown to be able to translocate into plant host cells where it localized to the nucleus and interacted with a pathogenesis-related ERF transcription factor (Kloppholz et al., 2011). Stage-specific transcriptome analyses showed that *RiSP7* is strongly induced when the fungus comes into close contact with the root. However as soon as the fungus enters the root the expression of *SP7* is largely shut down (Zeng et al., 2018). This indicates that distinct effectors play a role at different stages of the interaction. Even plant age was shown to influence the expression of some effectors, suggesting a link with changes in the age-dependent metabolic profile of the host (Zeng et al., 2018).

In chapter 2, I studied another core effecter, called Nuclear Localized Effector1 (RiNLE1), that is conserved in different AM fungi and highly induced specifically in the arbuscules in a wide range of host plants. Like RiSP7 this effector was also able to translocate into host cells, where it localized to the nucleus and especially accumulated in the nucleolus as well as (undefined) nuclear bodies (Wang et al., 2021). Our ability to functionally study AM effectors is strongly limited by the fact that AM fungi cannot be stably transformed yet (Helber and Requena, 2008). This is caused by the extreme coenocytic nature of AM fungi, where millions of nuclei share a common cytoplasm and the fact that there is never a stage where a single nucleus generates the next generation (Kokkoris et al., 2021). Therefore, alternative approaches are required to investigate the function of AM effectors. One of these approaches is host-induced gene silencing (HIGS) where a hairpin-construct targeting a fungal gene is expressed in the plant to generate double stranded RNA that then leads to RNA interference also in the fungus (Nowara et al., 2010). However, although occasionally successfully applied on AM fungi (Tsuzuki et al., 2016; Voß et al., 2018; Zeng et al., 2020), the efficiency of this approach is highly variable and it often does not work. In case of RiNLE1 we found that (inducible) overexpression could significantly increase root colonization and suppressed the expression of a set of defense-related genes (Chapter 2). Using co-immunoprecipitation in combination with mass-spectroscopy we identified Medicago Histone 2B (H2B) as an interactor RiNLE1. Furthermore, we showed that RiNLE1 could impair the mono-ubiquitination of H2B, which suppressed defense-related gene expression and enhanced fungal colonization. This again suggests that AM colonization levels are controlled by immune responses. However it should be noted that we especially focused on the set of down-regulated defense-related genes in a whole root setting. Therefore it might be that additional targets of RiNLE1, specifically in arbuscule-containing cells, play important roles in the symbiosis. Interestingly, we identified RiNLE1 homologs in several other biotrophic fungi that intimately interact with plants or that intracellularly colonize other hosts. Therefore it would be interesting to study whether such homologs similarly target H2B to facilitate intracellular colonization. Targeting histones directly or indirectly via histone modifying enzymes appears to be a widely used strategy of a wide variety of microbes to epigenetically control the plant immune. For example, the *Phytophthora sojae* effectors Avh52 and PsAvh23 were reported to target host histone acetyltransferases to modify histone acetylation levels, which resulted in the inhibition of defense gene expression or the activation of susceptibility genes (Kong et al., 2017; Li et al., 2018).

Besides conserved or commonly-expressed effectors, other effectors are only found in certain fungal strains or are induced specifically in the interaction with distinct plants. These effectors are called host specific or host dependent and they are suggested to contribute to host preference or specificity. For example, a single effector Tom1 in *Verticillium dahlia* was shown to specifically mediate pathogenicity on tomato (Li, 2019). Introduction of Tom1 into a non-pathogenic *V. dahlia* strain transferred the ability to cause disease in tomato to this strain (Li, 2019). Also in mutualistic root endophytes such as *Piriformospora indica* it was found that effector genes showed diverse expression patterns when interacting with either barley or Arabidopsis. This was found to be correlated with different colonization strategies of *P. indica* in barley and Arabidopsis (Lahrmann et al., 2013). Several host-dependent effector candidates have been identified in *R. irregularis* (Kamel et al., 2017; Zeng et al., 2018).

In chapter 3, I studied the function of such a host-dependent effector, called RiFGB1.

RiFGB1 expression is highly induced when the *R. irregularis* DAOM197198 strain colonizes chives, but not upon colonization of dicot hosts like Medicago and Nicotiana. This effector was called RiFGB1 because it shows homology to the Fungal Glucan Binding 1 (FGB1) effector from *P. indica*. *P. indica* FGB1 was reported to bind fungal β-glucans and to suppress β-glucan-triggered immune responses in plants (Wawra et al., 2016). It was hypothesized to act as a camouflage coat to conceal fungal sugar molecules from the plants immune system or to actively disrupt immune receptor complexes, in analogy to the proposed role of LysM effectors (Wawra et al., 2016). How fungal β-glucans are perceived by plants is still largely unknown (Fesel and Zuccaro, 2016). Interestingly, it was recently found that the LysM receptor AtCERK1 acts as an immune co-receptor in the perception of linear 1,3-β-d-glucans (Mélida et al., 2018). This might suggest a potential intimate cross-talk between chitin and glucan triggered immune responses. We found that RiFGB1 could also bind to β-glucans, however unlike PiFBG1, it was not specific for β-1,6-linked glucans that are uniquely found in the cell walls of fungi. Furthermore, RiFGB1 also seemed to bind chitin and even xylan, but not deacetylated chitin. RiFGB1 could interfere with both laminarin (a β-1,3-linked glucose polymer containing β-1,6-glycosidic side branches) and chitooligosaccharide triggered immune responses (Chapter 3). Strikingly, RiFGB1 could also interfere with flg22-triggered immune responses. Various pattern recognition receptors such as FLS2 and CERK1 have been shown to require proper glycosylation of their activity (Van Der Hoorn et al., 2005; Zipfel et al., 2006; Häweker et al., 2010; Petutschnig et al., 2010). Though preliminary, our results therefore raise the intriguing possibility that RiFGB1 might actually bind to glycan-modifications of a wide variety of immune receptors to interfere with their activity. Differences in glucan patterns in chives, as reported for other monocots (Fesel and Zuccaro, 2016), might be correlated with the host-dependent expression or RiFGB1.

As a first clue that RiFGB1 may actually play a role in the host range of *R. irregularis* we found that the *R. irregularis* C3 isolate, in contrast to DAOM197198, did not contain a FGB1 homolog that showed similar chives-dependent expression. Furthermore, our preliminary data indicate that C3 has a reduced colonization efficiency on chives compared to DAOM197198, while in Medicago overexpression of *RiFGB1* had a positive effect on fungal colonization levels (Chapter 3). It would therefore be interesting to test whether the differential colonization levels in chives are caused by the difference in *RiFGB1* expression.

A role for nutrient sensing and exchange in partner control

Above we discussed that nutrient levels influence the plants immune system, which may differentially affect the interaction with different AM fungi. However, nutrient levels and exchange also play a more direct role in partner control during the symbiosis.

In Medicago it was shown that an AM fungus that is less cooperative, i.e. which stores more Pi as poly-P , receives less carbon from the host than a more cooperative fungus that gives Pi more easily to the plant (Kiers et al., 2011; Fellbaum et al., 2014). This rewards a fungus that is more beneficial in terms of carbon costs. On the other hand, when the plant gives less carbon to the fungal partner, the fungus shows a reciprocal response and provide less phosphate to the plant (Kiers et al., 2011; Fellbaum et al., 2014). This may be important to balance the carbon costs with the nutrient demand of the plant and to keep the symbiosis beneficial. It indicates that the plant can tightly monitor the amount of nutrients it obtains

from its partners and to integrate it with its own demands. If the fungus does not provide sufficient nutrients it will ultimately lead to the (premature) degradation of the arbuscules, where nutrient exchange takes place. Therefore, the plant seems to control its partner by regulating 1) the carbon supply and 2) arbuscule development and lifetime, in a nutrient dependent manner.

Below, I will discuss our current insight into the molecular regulation of nutrient exchange, focusing on phosphorus (P) and nitrogen (N), and arbuscule development in relation partner control.

From plant to fungus

It was long believed that sugars (hexoses) were the main carbon source that was provided by the host plants across the peri-arbuscular membrane to the AM fungi (Roth and Paszkowski, 2017). This was mainly based on studies using isotope-labeled sugars added to mycorrhized roots coupled with detailed Nuclear Magnetic Resonance spectroscopy analyses. These suggested that glucose is provided to the fungus by host roots (Shachar-Hill et al., 1995; Pfeffer et al., 1999; Bago et al., 2000, 2003). In agreement with a role for plant-derived sugars as carbon source, a proton-coupled high-affinity monosaccharide transporter, RiMST2 from *R. irregularis*, was shown to be required for the appropriate development of arbuscules and fungal colonization (Helber et al., 2011). RiMST2 is most highly induced in arbuscules but also showed expression in the intraradical mycelium and extraradical mycelium (Helber et al., 2011; Zeng et al., 2018). This led to the hypothesis that AM fungi may not only take up sugars from the arbuscular interface but also from the apoplast through their intraradical hyphae. In addition, RiMST2 showed affinity for plant cell wall-derived xylose and its expression was shown induce upon addition of xylose. This suggested that cell wall derived monosaccharides may be taken up by AM fungi as well (Helber et al., 2011). Furthermore, several monosaccharide transporter members were shown to be specific expressed in the extraradical mycelium, where they were suggested to play a role in the uptake of organic carbon (Lahmidi et al., 2016; Roth and Paszkowski, 2017).

In recent years, the view of sugars as the major carbon source provided to AM fungi has been challenged when it was revealed that AM fungi lack a key enzyme, type-I multidomain fatty acid synthase (FAS), required to de novo synthesize long chain (C16:0) fatty acids (Tisserant et al., 2013; Wewer et al., 2014). This makes AM fungi in fact fatty acid auxotroph. This finding was striking as lipids are actually found to be the major carbon storage form in AM fungi (Wang et al., 2017). It suggested that AM fungi need to obtain fatty acid precursors from the host plant. In agreement with this, a set of genes involved in fatty acid biosynthesis are specifically induced in the arbuscule-containing cells during AM symbiosis (Bravo et al., 2017; Luginbuehl et al., 2017; Jiang et al., 2017). Mutations in these genes typically lead to the premature collapse or underdevelopment of arbuscules and reduced AM fungal colonization. By expressing a fatty acyl–ACP thioesterase (UcFatB) from *Umbellularia californica* that produces lauric acid (C12:0), which is normally not or very lowly exist in plant and AM fungi, it was ultimately proven that plants provide fatty acids to AM fungi (Luginbuehl et al., 2017; Jiang et al., 2017). It has been suggested that fatty acid precursors are transported to as β-monacylglycerol (β-MAG), which is then is converted into the storage form triacylglycerol (TAG) to be transmitted to the extraradical mycelium and stored in spores and vesicles. TAG can be broken to sugars via the glyoxylate cycle and glu-

coneogenesis (Bago et al., 2003). Therefore fatty acids are likely the major nutritive carbon source for the fungus. However, the physiological relevance of the different contributions of sugars and fatty acids to feed the fungus remains to be addressed. Interestingly, it has been shown that fatty acids can stimulate asymbiotic sporulation of AM fungi, and that different AM fungi seem to prefer different kinds of fatty acids (Kameoka et al., 2019; Sugiura et al., 2020). For example, anteiso-C15:0 induced hyphal branching and sporulation in *R. irregularis* and *R. clarus*, but failed to do so in *Gigaspora margarita* (Kameoka et al., 2019). This raises the intriguing possibility that the lipid profile of plants may in fact determine the reproductive success of their fungal partner, which will affect host-preferential associations. In line with this suggestion, the isotope profile of 16:0 fatty acids in *R. irregularis* extraradical mycelium growing on Lotus and carrot roots were significantly different (Keymer et al., 2017).

How do plants regulate carbon flow to the fungus at the arbuscules?

AM symbiosis creates a sink for sucrose transport to the roots where it is converted to glucose through the action of symbiotically induced sucrose synthases and invertases. Knockdown of the symbiotically induced sucrose synthase *MtSucS1* impaired arbuscule development and colonization levels (Baier et al., 2010). On the other hand, knockdown of the sucrose transporter *SlSUT2* led to increased colonization levels and abolished the positive growth response to AM symbiosis in tomato (Bitterlich et al., 2014). Because sucrose transport activity could not be shown it was suggested that SlSUT2 may have a signaling activity. It was found to physically interact with components of brassinosteroid (BR) signaling and biosynthesis (Bitterlich et al., 2014). Tomato mutants defective in BR biosynthesis also showed decreased mycorrhization, indicating that sucrose and BRs cross talk to control colonization levels. Interestingly, BRs are known to antagonize plant innate immune responses through the co-receptor BAK1 (Lozano-Durán and Zipfel, 2015). Furthermore, extracellular sugar levels are important regulators of immune responses. For example, the Arabidopsis homologue of the AM-induced Medicago Hexose 1 transporter (MtHEX1), AtSTP13, interacts with the immune receptor FLS2 and its interactor BAK1 resulting in an increased hexose uptake from the apoplast and thereby enhanced basal resistance (Yamada et al., 2016). Upregulation of MtHex1 during AM colonization may suggest a similar crosstalk between sugar signalling and immune receptor complexes to control the symbiosis (Roth and Paszkowski, 2017).

Transport of glucose across the peri-arbuscular membrane was recently suggested to be regulated by SWEET (Sugars Will Eventually be Exported) transporters (Manck-Götzenberger and Requena, 2016; Kafle et al., 2019). Recently, a single *SWEET* gene (*MtSWEET1b*) in Medicago was shown to be specifically expressed in arbuscule-containing cells where it localized to the peri-arbuscular membrane (An et al., 2019). MtSWEET1b was shown to transport glucose and arbuscule-specific overexpression of dominant-negative forms of MtSWEET1b caused an early collapse of arbuscules (An et al., 2019). This suggests that the transport of glucose to arbuscules is important for the maintenance of proper arbuscule development. *SWEET* genes can be differently regulated in different plant species. However, whether this may affect the preferential association with distinct AM fungi remains to be investigated.

In case of fatty acids, two ATP-binding cassette (half-ABC) transporters, called STUNTED

ARBUSCULES (STR) and STR2, were found to be required for the delivery of the fatty acid precursors to the AM fungi (Zhang et al., 2010; Gutjahr et al., 2012). Their expression is also induced in arbuscule containing cells and they are localized to the peri-arbuscular membrane (Zhang et al., 2010; Gutjahr et al., 2012). Knock-out of these lipid transporters caused a strong underdevelopment of arbuscules and correspondingly reduced colonization levels. It is currently not known whether or how these transporters are regulated post-transcriptionally, however transcriptional regulation of STR/STR2 expression in arbuscule-containing cells was shown to involve WRINKLED1-like transcription factors (TFs). These TFs, LjCBX1 in Lotus and WRI5a-c in Medicago, induce many of the genes that are specifically induced in arbuscule containing cells, such as the fatty acid regulon as wells *MtHA1* and *MtPT4* required for phosphate uptake from the arbuscules (Jiang et al., 2018; Xue et al., 2018). Furthermore, the same transcriptional network regulates genes required for arbuscule degradation such as *MtMYB1* and the phosphate sensing *MtSPX1* and *MtSPX3* studied in Chapter 4 and 5 (discussed further below). The WRI1-like genes are transcriptionally regulated by the GRAS TF RAM1, which is essential for arbuscule development after the entry of fungal hyphae into inner cortex cells (Gobbato et al., 2012). AM-specific induction of RAM1 is in turn controlled by the common symbiotic signaling TFs CYCLOPS and DELLAs (Pimprikar et al., 2016). Although the picture is still incomplete, these data are starting to unveil the transcriptional network that controls nutrient exchange during AM symbiosis (Limpens and Geurts, 2018). How different fungal partners and environmental conditions affect this transcriptional network will be a great challenge for the future.

From fungus to plant

The relatively thin AM fungal hyphae form an extensive mycelial network in the soil that is much better able to scavenge for scarce mineral sources and water than the relatively large plant roots. Furthermore, plant roots can only take up soluble inorganic orthophosphate, while most phosphate in the soil is present in bound forms, with large parts as organic phytate. AM fungi have been shown to be able to mineralize organic phosphate with the help of hyphosphere bacteria (Wang et al., 2017; Jiang et al., 2021; Emmett et al., 2021). Mineralized phosphate is then taken-up by the fungal phosphate transporters that are expressed in the extraradical mycelium. These transporters are energized by proton (H^+/Pi) or sodium (Na^+/Pi) gradients (Harrison and Van Buuren, 1995; Maldonado-mendoza et al., 2001; Fiorilli et al., 2013; Tisserant et al., 2013 Ferrol et al., 2000; Requena et al., 2003). Many of the fungal phosphate transporters are not exclusively expressed in the extraradical hyphae but also show significant expression in the arbuscules. This was suggested to either reflect a competition for Pi between fungus and host plant at the peri-arbuscule membrane, or a role for these transporters in phosphate secretion from the arbuscules (Xie et al., 2016; Ferrol et al., 2019). A high-affinity fungal phosphate transporter GigmPT in *Gigaspora margarita* was found to function both as transporter and Pi sensor, acting as transceptor to regulate Pi-dependent signaling (Xie et al., 2016). *GigmPT* expression in extraradical hyphae was induced by increased carbon supply, which corresponded with more phosphate transport to the host (Xie et al., 2016). HIGS of *GigmPT* led to reduced AM colonization and the premature collapse of arbuscules (Xie et al., 2016). Such a signaling role may also play a role in the distribution of Pi along the fungal network, which was recently visualized using a novel the fluorescing tagged phosphate (using quantum dots) technique (van't Padje et al., 2020).

Once taken up, phosphate is polymerized to polyphosphate (poly-P) in the fungal vacuoles

(Ezawa et al., 2002). This is likely carried out by the vacuolar transporter chaperon complex (VTC), which has been shown to control poly-P synthesis in yeast. In line with this, the expression of several VTC components is upregulated when phosphate is added to extraradical hyphae (Kikuchi et al., 2014). The poly-P is subsequently transported to the intraradical hyphae through the mobile vacuolar system as well as via cytoplasmic streaming (Uetake et al., 2002). Recently it was shown that poly-P transport is influenced by water transport across the plasma membrane in the intraradical hyphae (Kikuchi et al., 2016). Virus-induced silencing of an aquaporin *RcAQP3* from *Rhizophagus clarus* as well as the reduction of host plant transpiration decreased the rate of poly-P translocation from fungal extraradical to intraradical hyphae (Kikuchi et al., 2016). This suggests that host transpiration drives water transportation through the hyphae, in turn, mediates poly-P transportation (further discussed below).

A major question that remains to be solved is how phosphate is released by the AM fungi to be taken up by the host plant at the arbuscules. It is suggested that poly-P is first hydrolyzed in the intraradical hyphae (Kikuchi et al., 2014), after which it is transported across the vacuolar membrane, probably by the vacuolar phosphate transporter PHO91 (Tisserant et al., 2012). Subsequently, the phosphate is pumped into the peri-arbuscular space from where it is taken up by specific phosphate transporters such as PT4 into the plant cells (Ferrol et al., 2019). Several candidate phosphate efflux transporters have been proposed but their involvements remains to be demonstrated (Ezawa and Saito, 2018). Alternatively, poly-P might be exported by a fungal plasma membrane localized VTC complex and hydrolyzed by plant acid phosphatases in the peri-arbuscular space (Ezawa and Saito, 2018). Yet another possibility could be the involvement of extracellular vesicles in the transport of nutrients (Ivanov et al., 2019; Roth et al., 2019).

Besides phosphate, AM fungi also play a key role in providing nitrogen to host plants (Garcia et al., 2016; Wipf et al., 2019). The fungal extraradical mycelium can take up inorganic (NH_4^+ or NO^{3-}) and organic nitrogen (amino acids or short peptides) from the soil. High affinity nitrate transporters and ammonium transporters have been identified in AM fungi (Tian et al., 2010; Koegel et al., 2015; Pérez-Tienda et al., 2011; Calabrese et al., 2016). Similar to phosphate transporters, several of these nitrogen transporter, such as RiNRT2, are expressed in both the extraradical mycelium and intraradical mycelium (Wipf et al., 2019). This suggests that competition for nutrient sources symbiotic interface may be integral market strategy. Once taken up, nitrogen ions in the fungal hyphae are converted via glutamine into arginine through the GS/GOGAT cycle (Wipf et al., 2019). Arginine is then transferred to the intraradical mycelium possibly through formation of complexes with the negatively charged poly-P granules, after which the arginine is broken down to urea and ornithine (Govindarajulu et al., 2005; Jin et al., 2005). The urea is then hydrolyzed to ammonia/ammonium in the arbuscules, and exported into the peri-arbuscular space (Kobae et al., 2010; Breuillin-Sessoms et al., 2015). Interestingly, it was shown that the premature arbuscule degeneration phenotype of the Medicago *pt4* mutant, lacking the key symbiotic phosphate transporter PT4 (Javot et al., 2007), was restored when plants were grown in nitrogen starvation conditions (Breuillin-Sessoms et al., 2015). This complementation required the ammonium transporter MtAMT2;3. Because MtAMT2;3 did not show ammonium transport activity when expressed in yeast, it was suggested to function in N-sensing and signaling (Breuillin-Sessoms et al., 2015). Recently, a low-affinity nitrate transporter OsNPF4.5 in rice was reported to be specifically expressed in arbuscule-containing cells (Wang et al.,

2020). Knockout of OsNPF4.5 resulted in a 45% decrease in plant AM-related nitrogen uptake, indicating that AM fungi trade nitrate with the host as well.

Nitrogen and phosphorus are the two most important mineral nutrients and they need to be balanced for optimal plant growth. At low N : P ratios nitrogen addition negatively affects AMF colonization (Johnson et al., 2003). But at high N : P ratios nitrogen positively affects AMF colonization (Johnson et al., 2015). However, the molecular mechanisms by which P and N collectively regulate AM symbiosis are unknown. Since both P and N supply ultimately determines whether mycorrhizal benefits outweigh their costs it is important that the plant can sense how much nutrients it receives.

In Chapter 4 , we studied two SPX proteins that are strongly induced in arbuscule containing cells. SPX proteins have been well studied for their role as phosphate sensors and regulators of phosphate homeostasis in plants (Puga et al., 2014; Wang et al., 2014b; Zhong et al., 2018; Wild et al., 2016). Under non-symbiotic conditions SPX1 and SPX3 negatively regulated the key phosphate starvation response regulator PHR2 in Medicago in a Pi-dependent manner, similar to the role of SPX proteins reported in rice and arabidopsis where it prevents potential toxic effects of too much Pi acquisition. In arbuscule-containing cells, the induction of *SPX1* and *SPX3* appeared to be controlled by the WRI1-like transcription factors, discussed above. There, SPX1 and SPX3 redundantly controlled in the timely degradation of arbuscules. Overexpression of SPX1/3 caused the premature degradation of arbuscules, while the *spx1spx3* double mutant showed a higher “good” to “degrading” arbuscule ratio. Knockdown of *SPX1* and *SPX3* expression in the *pt4* mutant could not suppress the premature arbuscule degradation in this mutant. Furthermore, overexpression of the MYB1 transcriptional regulator of arbuscule degradation genes in the *spx1spx3* double mutant still induced the premature degradation of arbuscules. This suggested that SPX1 and SPX3 may act to sense when an arbuscule-containing cell has obtained sufficient Pi and to prevent too much Pi from entering the cells, in analogy to its role under non-symbiotic conditions. Interestingly, a role for SPX proteins in the integration of N and P signaling was recently reported. In rice, OsSPX4 was shown to interact with the nitrate sensor NRT1.1B (Hu et al., 2019). Nitrate perception leads to the degradation of SPX4, which releases both PHR2 and OsNLP3 TFs to move to the nucleus and to induce respectively phosphate starvation genes and nitrate-responsive genes. Since both P and N collectively control arbuscule degradation it would be interesting to study whether SPX1/3 also play a role in the N-control of arbuscule development.

To understand how SPX1 and SPX3 might facilitate arbuscule degradation we first investigated their ability to interact with the currently known regulators of arbuscule degradation (Chapter 5). However, no interaction with either MYB1, NSP2 or DELLA proteins, which form a TF complex to induce the expression of arbuscule degrading enzymes, was observed (Floss et al., 2017). Since SPX1 and SPX3 redundantly controlled arbuscule degradation we reasoned that they must share interacting partners. To identify these we used a co-IP approach coupled with tandem mass-spectroscopy. This identified a PIP2 plasma membrane aquaporin as interactor of both SPX1 and SPX3 (Chapter 5). Aquaporins act as water channels that selectively allow water or other small uncharged molecules to pass along an osmotic gradient. In addition some aquaporins may also mediate the transport of volatiles such as NH_3 or CO_2 and small solutes such as ions, peptides, H_2O_2, urea, or glycerol across membranes (Tyerman et al., 2002; Hachez and Chaumont, 2010; Bienert and Chaumont,

2014). Water flow has been postulated to play an important role to facilitate the flow of nutrients from the fungus to the arbuscules (Kikuchi et al., 2016). In AM fungi, an aquaporin RcAQP3 was found to mediate long-distance poly-P translocation to the host plant (Kikuchi et al., 2016). Furthermore, several studies have shown a correlation between the transpiration of the plant and nutrient transport by AM fungi (Birhane et al., 2012; Kikuchi et al., 2016; Quiroga, 2019; Quiroga et al., 2019), and various aquaporins have been found to be transcriptionally regulated during the AM symbiosis (Uehlein et al., 2007; Quiroga et al., 2019). It can therefore be hypothesized that the interaction with SPX1 and SPX3 controls PIP2 activity in a Pi-dependent manner. One possibility is that when the plant cell has acquired sufficient Pi, SPX binding will block the water transport activity of PIP2, to inhibit the flow of nutrients and thereby further Pi transfer. The transport of Pi out of the arbuscule-containing cells to the vasculature will lead to a drop in the Pi levels, which subsequently can trigger MYB1 leading to the degradation of the arbuscule. This hypothesis remains to be tested. A role for plant-mediated water transport in the transport of nutrients by the fungi might also explain the unequal contribution of *R. irregularis* in a common mycorrhizal network between flax and sorghum, reported by Walder et al. (2012). Flax was found to invest little carbon but gained most of the nitrogen and phosphorus while the connected sorghum plant received little in return despite providing more carbon (Walder et al., 2012). It would be interesting to investigate whether this unbalance may be caused by differences in the plants hydraulic strength between the two plant species. Of course, other roles of aquaporins can also be envisioned since it is increasingly becoming clear that aquaporins act as hubs in various signal transduction pathways in response to abiotic stress (Hachez and Chaumont, 2010; Bienert and Chaumont, 2014; Zhang et al., 2019).

In addition to PIP2, one other protein (G7LFU4) was identified in the mass-spec data as potential interactor of both SPX1 and SPX3. This protein is annotated as a putative polyketide cyclase/dehydrase and lipid transporter, with homology to Betv_1 type Major Latex Protein-like 43. MLP43 in arabidopsis has been found to function as a positive regulator during abscisic acid responses and to confer drought tolerance (Wang et al., 2016). This might offer another clue towards water relations and the SPX proteins. However, whether this is a true interactor of SPX1/3 first remains to be verified.

Concluding remarks

In summary, our insight into potential mechanisms of partner control in AM symbiosis have significantly increased in recent years. It has become clear that complex and interconnected signalling pathways concerning nutrient status and defense responses are integrated at local and systemic levels to control AM symbiosis development. This may not be surprising given the ancient origin and widespread nature of this fundamental plant endosymbiosis. Especially the availability of various AM fungal genomes and transcriptome data in different host plants and at different AM development stages, now offers a rich resource to gain further insight in this fascinating aspect of the symbiosis. One of the major questions to be studied is how the symbiotic efficiency of different plant-fungus combinations is controlled at the molecular level in natural settings. A better knowledge of partner control, both from the plant as well as the fungal side of the interaction, will be pivotal to realize and apply the widely recognized potential of AM fungi as sustainable biofertilizers.

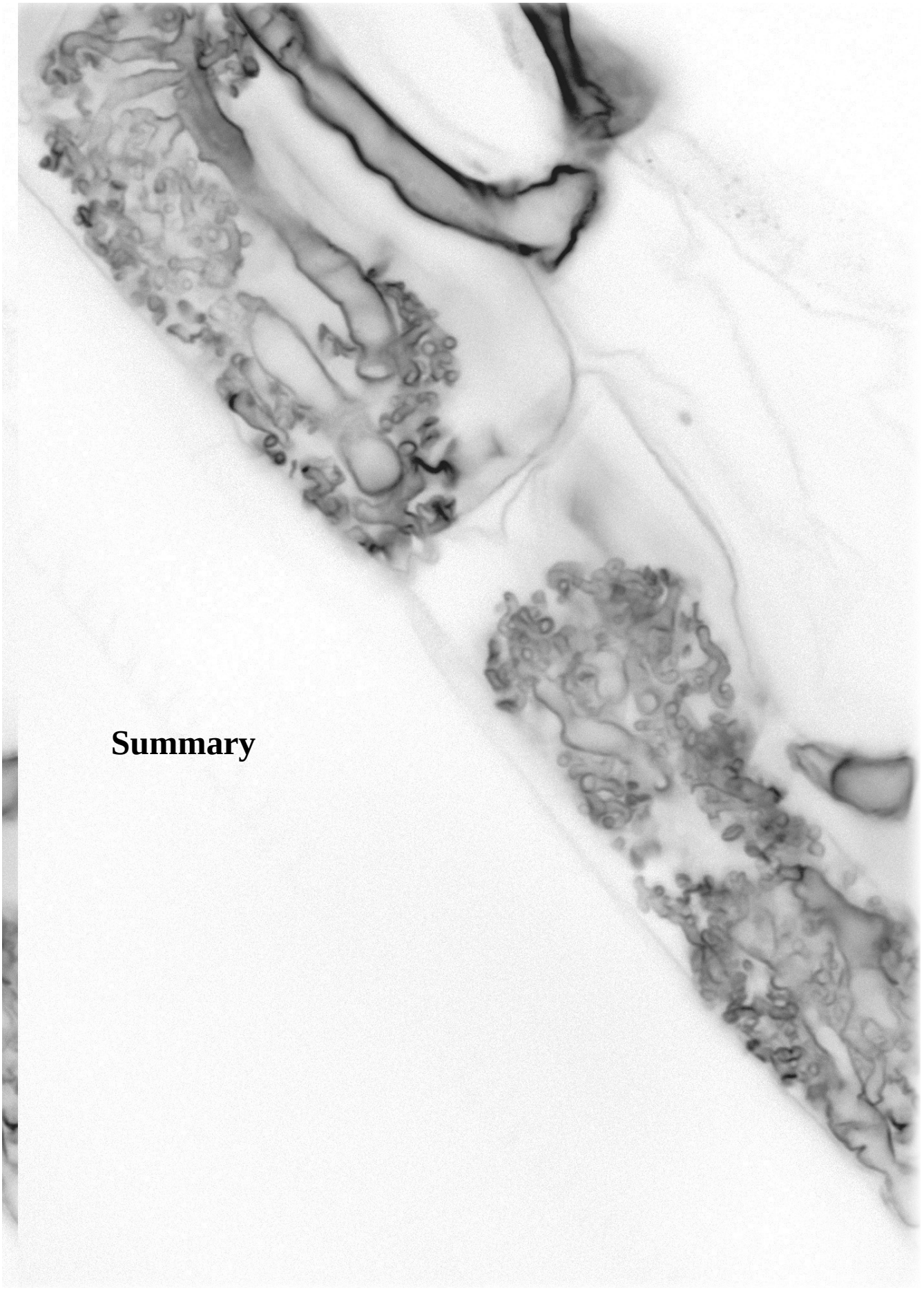

Summary

The arbuscular mycorrhizal (AM) symbiosis is the most widespread symbiotic association between land plants and arbuscular mycorrhizal fungi belonging to Glomeromycotina subphylum. This mutualistic association can have a range of benefits for the plant, such as increased access to mineral nutrients (especially phosphate and nitrogen) and water in the soil as well as protection from various biotic and abiotic stresses. In return for these services, the fungi receive fixed carbon from their hosts to complete their life cycle. To keep this interaction beneficial, multiple layers of control are exerted by both partners at different stages of the interaction. In this thesis, we studied the role of AM fungal effectors to facilitate colonization and how host plants sense how much phosphate they receive from their partner to control the development of the arbuscules.

Similar to pathogenic fungi, the cell walls of AM fungi contain common microbe-associated molecular patterns (MAMPs), such as chitin and β-glucans, that can trigger plant immune responses. The extreme host range of AM fungi raises the question how they can efficiently deal with the immune system of such a wide variety of plants. It has recently become clear that secreted AM fungal effector proteins can play a key role. In **chapter 2**, we studied the role of a secreted nuclear-localization signal containing effector from *Rhizophagus irregularis*, called Nuclear Localized Effector1 (RiNLE1), which is highly and specifically expressed in arbuscules in wide variety of plant species. RiNLE1 was able translocate to the host nucleus where it could interact with the core nucleosome component Histone 2B (H2B) and impair its mono-ubiquitination. This resulted in the suppression of defense-related gene expression and enhanced colonization levels. This chapter highlighted a novel mechanism by which AM fungi can effectively affect the plants epigenome via direct interaction with a core nucleosome component to facilitate colonization. RiNLE1-like effectors were found in a range of fungi that establish intimate interactions with plants, suggesting that this type of effector may be more widely recruited to manipulate host defense responses.

Despite the fact that there seems to be little to no strict host specificity in the AM interaction. so-called host preferences have been widely observed in the field. In **chapter 3**, we studied an effector from *Rhizophagus irregularis* DAOM197198, called RiFGB1, that is expressed in a host-dependent manner. RiFGB1 is highly induced in the interaction with *Allium schoenoprasum* (chives) as host plant but not in the interaction with dicot hosts like *Medicago truncatula* and *Nicotiana benthamiana*. RiFGB1 was shown to be a homolog of the *Piriformospora indica* fungal β-glucan-binding lectin (FGB1). We found that RiFGB1 can bind a variety of glycan molecules such as β-glucan, chitin and xylan. Furthermore RiFGB1 could interfere with a wide range of MAMP-triggered immune responses. Furthermore, different expression levels of *FGB1* homologs in another *R. irregularis* isolate seemed to correlate with a reduced colonization of this isolate on chives. These data suggest that effectors may contribute to host preferences through their ability to regulate the host immune system.

To keep the symbiosis beneficial a plant must be able to sense how much nutrients it obtains from its partner and to integrate it with its needs. For example, if the fungus fails to provide phosphate the plant can terminate the interaction by degrading the arbuscules to prevent a carbon drain by the fungus. How plants sense the phosphate status in arbuscule-containing cells and accordingly control arbuscule lifetime or function is therefore a major question. In **chapter 4**, we identified two *Medicago truncatula* phosphate-sensing SPX-domain containing proteins, SPX1 and SPX3, as key regulators of phosphate starvation responses

as well as fungal colonization and arbuscule degradation. *SPX1* and *SPX3* are induced by phosphate starvation but become restricted to arbuscule-containing cells upon establishment of AM symbiosis. Under non-symbiotic conditions they control phosphate homeostasis in part through their interaction with the phosphate starvation response factor PHR2. Furthermore, upon phosphate deficiency they facilitate expression of the strigolactone biosynthesis gene *DWARF27*, which correlates with increased fungal branching by root exudates and increased root colonization. Later, in the arbuscule-containing cells SPX1 and SPX3 redundantly control the timely degradation of arbuscules.

To understand how SPX1 and SPX3 control arbuscule lifetime, we searched for interacting partners in **chapter 5**. We did not find any interaction with the known transcriptional regulators of arbuscule degradation MYB1, NSP1 and DELLA. Instead, through co-immunoprecipitation coupled with liquid chromatography–mass spectrometry, we identified PIP2 aquaporins as interactors of both SPX1 and SPX3. Overexpression of *MtPIP2;7* reduced overall arbuscule abundance but also caused a higher "good" to "degrading" arbuscule ratio, suggesting reduced arbuscule degradation. These results now offer a basis to study the intriguing possibility that SPX1 and SPX3 help to regulate phosphate transport and/or arbuscule degeneration through the regulation of PIP2 activity.

In **chapter 6**, the results generated during my thesis research are discussed in the broader perspective of partner preferences during AM symbiosis. It has become clear that complex and interconnected signaling pathways concerning nutrient status and defense responses are integrated to control AM symbiosis development. Extending this knowledge will be important realize to the widely recognized potential of AM fungi as sustainable biofertilizers.

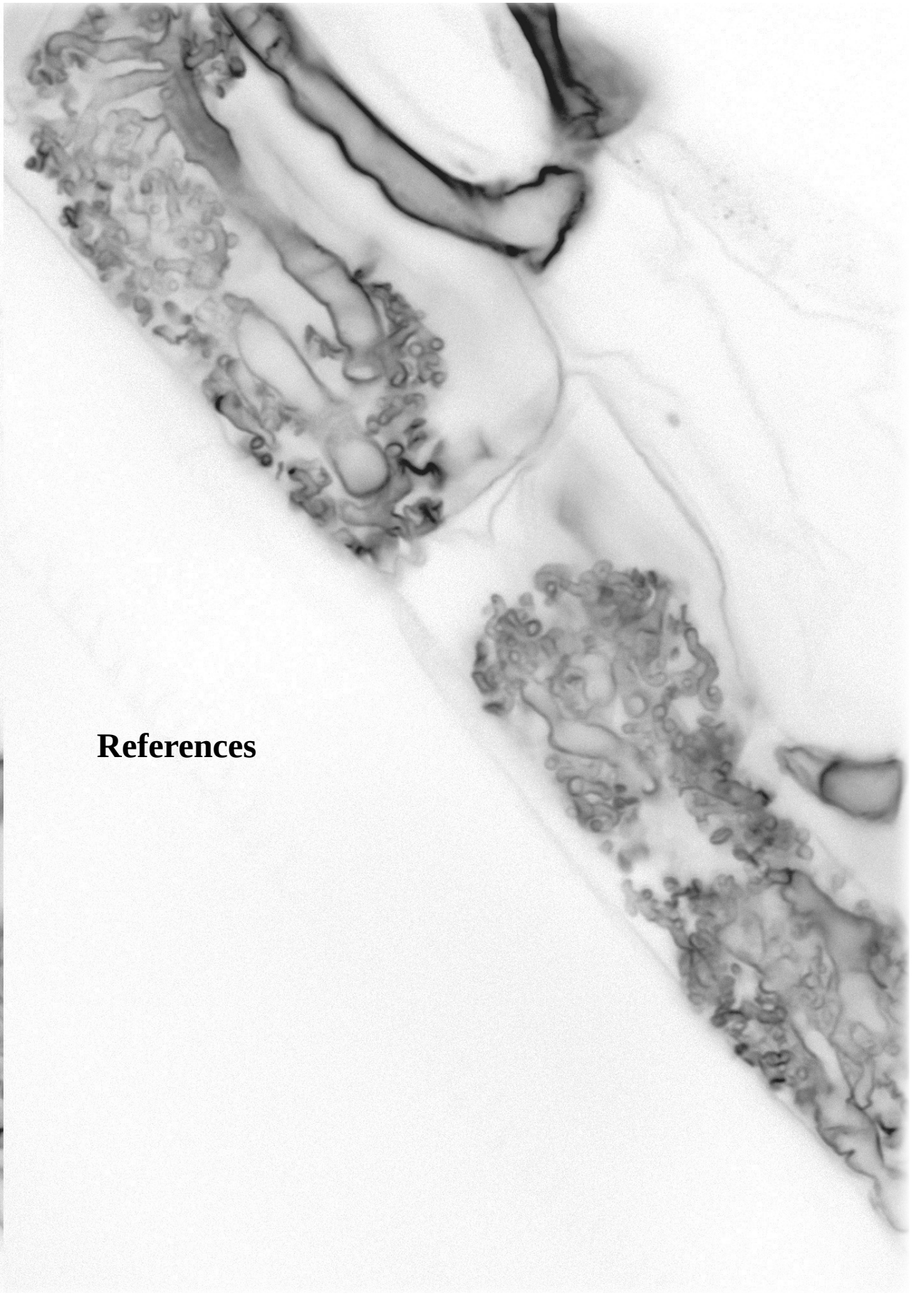

References

Abdel-Lateif, K., Bogusz, D., and Hocher, V. (2012). The role of flavonoids in the establishment of plant roots endosymbioses with arbuscular mycorrhiza fungi, rhizobia and Frankia bacteria. Plant Signal. Behav. **7**: 636–641.

Ahmad, M., Hirz, M., Pichler, H., and Schwab, H. (2014). Protein expression in Pichia pastoris: Recent achievements and perspectives for heterologous protein production. Appl. Microbiol. Biotechnol. **98**: 5301–5317.

Akamatsu, A., Shimamoto, K., and Kawano, Y. (2016). Crosstalk of Signaling Mechanisms Involved in Host Defense and Symbiosis Against Microorganisms in Rice. Curr. Genomics **17**: 297–307.

Akamatsu, A., Wong, H.L., Fujiwara, M., Okuda, J., Nishide, K., Uno, K., Imai, K., Umemura, K., Kawasaki, T., Kawano, Y., and Shimamoto, K. (2013). An OsCEBiP/OsCERK1-OsRacGEF1-OsRac1 module is an essential early component of chitin-induced rice immunity. Cell Host Microbe **13**: 465–476.

Akiyama, K., Matsuzaki, K.I., and Hayashi, H. (2005). Plant sesquiterpenes induce hyphal branching in arbuscular mycorrhizal fungi. Nature **435**: 824–827.

Alvarez, F.J. and Konopka, J.B. (2007). Identification of an N-acetylglucosamine transporter that mediates hyphal induction in Candida albicans. Mol. Biol. Cell.

Amor, B. Ben, Shaw, S.L., Oldroyd, G.E.D., Maillet, F., Penmetsa, R.V., Cook, D., Long, S.R., Dénarié, J., and Gough, C. (2003). The NFP locus of Medicago truncatula controls an early step of Nod factor signal transduction upstream of a rapid calcium flux and root hair deformation. Plant J.

An, J., Zeng, T., Ji, C., de Graaf, S., Zheng, Z., Xiao, T.T., Deng, X., Xiao, S., Bisseling, T., Limpens, E., and Pan, Z. (2019). A Medicago truncatula SWEET transporter implicated in arbuscule maintenance during arbuscular mycorrhizal symbiosis. New Phytol. **224**: 396–408.

Antolín-Llovera, M., Ried, M.K., and Parniske, M. (2014). Cleavage of the symbiosis receptor-like kinase ectodomain promotes complex formation with nod factor receptor 5. Curr. Biol. **24**: 422–427.

Bago, B., Pfeffer, P.E., Abubaker, J., Jun, J., Allen, J.W., Brouillette, J., Douds, D.D., Lammers, P.J., and Shachar-Hill, Y. (2003). Carbon export from arbuscular mycorrhizal roots involves the translocation of carbohydrate as well as lipid. Plant Physiol.

Bago, B., Pfeffer, P.E., and Shachar-Hill, Y. (2000). Carbon metabolism and transport in arbuscular mycorrhizas. Plant Physiol.

Baier, M.C., Keck, M., Gödde, V., Niehaus, K., Küster, H., and Hohnjec, N. (2010). Knockdown of the symbiotic sucrose synthase MtSucS1 affects arbuscule maturation and maintenance in mycorrhizal roots of Medicago truncatula. Plant Physiol. **152**: 1000–1014.

Bapaume, L., Laukamm, S., Darbon, G., Monney, C., Meyenhofer, F., Feddermann, N., Chen, M., and Reinhardt, D. (2019). VAPYRIN marks an endosomal trafficking compartment involved in arbuscular mycorrhizal symbiosis. Front. Plant Sci. **10**: 1–19.

Barabote, R.D., Tamang, D.G., Abeywardena, S.N., Fallah, N.S., Fu, J.Y.C., Lio, J.K., Mirhosseini, P., Pezeshk, R., Podell, S., Salampessy, M.L., Thever, M.D., and Saier, M.H. (2006). Extra domains in secondary transport carriers and channel proteins. Biochim. Biophys. Acta - Biomembr. **1758**: 1557–1579.

Bari, R., Pant, B.D., Stitt, M., and Scheible, W.R. (2006). PHO2, microRNA399, and PHR1 define a phosphate-signaling pathway in plants. Plant Physiol.

Becard, G., Douds, D.D., and Pfeffer, P.E. (1992). Extensive in vitro hyphal growth of vesicular-arbuscular mycorrhizal fungi in the presence of CO2 and flavonols. Appl. Environ. Microbiol.

BÉCARD, G. and FORTIN, J.A. (1988). Early events of vesicular–arbuscular mycorrhiza formation on Ri T-DNA transformed roots. New Phytol.

Bellati, J., Champeyroux, C., Hem, S., Rofidal, V., Krouk, G., Maurel, C., and Santoni, V. (2016). Novel aquaporin regulatory mechanisms revealed by interactomics. Mol. Cell. Proteomics **15**: 3473–3487.

Berruti, A., Borriello, R., Lumini, E., Scariot, V., Bianciotto, V., and Balestrini, R. (2013). Application of laser microdissection to identify the mycorrhizal fungi that establish arbuscules inside root cells. Front. Plant Sci. **4**: 1–10.

Bertazzoni, S., Williams, A.H., Jones, D.A., Syme, R.A., Tan, K.-C., and Hane, J.K. (2018). Accessories Make the Outfit: Accessory Chromosomes and Other Dispensable DNA Regions in Plant-Pathogenic Fungi. Mol. Plant-Microbe Interact. **31**: 779–788.

Besserer, A., Bécard, G., Jauneau, A., Roux, C., and Séjalon-Delmas, N. (2008). GR24, a synthetic analog of strigolactones, stimulates the mitosis and growth of the arbuscular mycorrhizal fungus Gigaspora rosea by boosting its energy metabolism. Plant Physiol. **148**: 402–413.

Besserer, A., Puech-Pagès, V., Kiefer, P., Gomez-Roldan, V., Jauneau, A., Roy, S., Portais, J.C., Roux, C., Bécard, G., and Séjalon-Delmas, N. (2006). Strigolactones stimulate arbuscular mycorrhizal fungi by activating mitochondria. PLoS Biol. **4**: 1239–1247.

Bielow, C., Mastrobuoni, G., and Kempa, S. (2016). Proteomics Quality Control: Quality Control Software for MaxQuant Results. J. Proteome Res. **15**: 777–787.

Bienert, G.P. and Chaumont, F. (2014). Aquaporin-facilitated transmembrane diffusion of hydrogen peroxide. Biochim. Biophys. Acta - Gen. Subj. **1840**: 1596–1604.

Birhane, E., Sterck, F.J., Fetene, M., Bongers, F., and Kuyper, T.W. (2012). Arbuscular mycorrhizal fungi enhance photosynthesis, water use efficiency, and growth of frankincense seedlings under pulsed water availability conditions. Oecologia.

Bitterlich, M., Krügel, U., Boldt-Burisch, K., Franken, P., and Kühn, C. (2014). The sucrose transporter SlSUT2 from tomato interacts with brassinosteroid functioning and affects arbuscular mycorrhiza formation. Plant J. **78**: 877–889.

Bonfante-Fasolo, P. (1984). Anatomy and morphology of VA mycorrhizae. VA mycorrhi-

zae **57**: 5–33.

Bonfante, P. and Genre, A. (2008). Plants and arbuscular mycorrhizal fungi: an evolutionary-developmental perspective. Trends Plant Sci.

Borghi, L. (2010). Inducible gene expression systems for plants. (Humana Press: Hertfordshire, UK).

Bozsoki, Z. et al. (2020). Ligand-recognizing motifs in plant LysM receptors are major determinants of specificity. Science (80-.). **369**: 663–670.

Bozsoki, Z., Cheng, J., Feng, F., Gysel, K., Vinther, M., Andersen, K.R., Oldroyd, G., Blaise, M., Radutoiu, S., and Stougaard, J. (2017). Receptor-mediated chitin perception in legume roots is functionally separable from Nod factor perception. Proc. Natl. Acad. Sci. U. S. A. **114**: E8118–E8127.

Bravo, A., Brands, M., Wewer, V., Dörmann, P., and Harrison, M.J. (2017). Arbuscular mycorrhiza-specific enzymes FatM and RAM2 fine-tune lipid biosynthesis to promote development of arbuscular mycorrhiza. New Phytol. **214**: 1631–1645.

Breuillin-Sessoms, F. et al. (2015). Suppression of arbuscule degeneration in Medicago truncatula phosphate transporter4 mutants is dependent on the ammonium transporter 2 family protein AMT2;3. Plant Cell.

Broghammer, A. et al. (2012). Legume receptors perceive the rhizobial lipochitin oligosaccharide signal molecules by direct binding. Proc. Natl. Acad. Sci. U. S. A. **109**: 13859–13864.

Brutus, A., Sicilia, F., Macone, A., Cervone, F., and De Lorenzo, G. (2010). A domain swap approach reveals a role of the plant wall-associated kinase 1 (WAK1) as a receptor of oligogalacturonides. Proc. Natl. Acad. Sci. U. S. A. **107**: 9452–9457.

Bulone, V., Schwerdt, J.G., and Fincher, G.B. (2019). Co-evolution of Enzymes Involved in Plant Cell Wall Metabolism in the Grasses. Front. Plant Sci. 10.

Bungard, D., Fuerth, B.J., Zeng, P.Y., Faubert, B., Maas, N.L., Viollet, B., Carling, D., Thompson, C.B., Jones, R.G., and Berger, S.L. (2010). Signaling kinase AMPK activates stress-promoted transcription via histone H2B phosphorylation. Science (80-.). **329**: 1201–1205.

Burleigh, S.H. and Harrison, M.J. (1999). The down-regulation of Mt4-like genes by phosphate fertilization occurs systemically and involves phosphate translocation to the shoots. Plant Physiol.

Bustos, R., Castrillo, G., Linhares, F., Puga, M.I., Rubio, V., Pérez-Pérez, J., Solano, R., Leyva, A., and Paz-Ares, J. (2010). A central regulatory system largely controls transcriptional activation and repression responses to phosphate starvation in arabidopsis. PLoS Genet. 6.

Calabrese, S., Pérez-Tienda, J., Ellerbeck, M., Arnould, C., Chatagnier, O., Boller, T., Schüßler, A., Brachmann, A., Wipf, D., Ferrol, N., and Courty, P.E. (2016). Gin-

tAMT3-a low-affinity ammonium transporter of the arbuscular mycorrhizal rhizophagus irregularis. Front. Plant Sci.

Camps, C., Jardinaud, M.F., Rengel, D., Carrère, S., Hervé, C., Debellé, F., Gamas, P., Bensmihen, S., and Gough, C. (2015a). Combined genetic and transcriptomic analysis reveals three major signalling pathways activated by Myc-LCOs in Medicago truncatula. New Phytol.

Camps, C., Jardinaud, M.F., Rengel, D., Carrère, S., Hervé, C., Debellé, F., Gamas, P., Bensmihen, S., and Gough, C. (2015b). Combined genetic and transcriptomic analysis reveals three major signalling pathways activated by Myc-LCOs in Medicago truncatula. New Phytol. **208**: 224–240.

Cao, H., Li, X., Wang, Z., Ding, M., Sun, Y., Dong, F., Chen, F., Liu, L., Doughty, J., Li, Y., and Liu, Y.X. (2015). Histone H2B monoubiquitination mediated by HISTONE MONOUBIQUITINATION1 and HISTONE MONOUBIQUITINATION2 is involved in anther development by regulating tapetum degradation-related genes in rice. Plant Physiol. **168**: 1389–1405.

Cao, Y., Dai, Y., Cui, S., and Ma, L. (2008). Histone H2B monoubiquitination in the chromatin of Flowering Locus C regulates flowering time in Arabidopsis. Plant Cell **20**: 2586–2602.

Carotenuto, G., Chabaud, M., Miyata, K., Capozzi, M., Takeda, N., Kaku, H., Shibuya, N., Nakagawa, T., Barker, D.G., and Genre, A. (2017). The rice LysM receptor-like kinase OsCERK1 is required for the perception of short-chain chitin oligomers in arbuscular mycorrhizal signaling. New Phytol. **214**: 1440–1446.

Castrillo, G., Teixeira, P.J.P.L., Paredes, S.H., Law, T.F., De Lorenzo, L., Feltcher, M.E., Finkel, O.M., Breakfield, N.W., Mieczkowski, P., Jones, C.D., Paz-Ares, J., and Dangl, J.L. (2017). Root microbiota drive direct integration of phosphate stress and immunity. Nature **543**: 513–518.

Catoira, R., Galera, C., De Billy, F., Penmetsa, R. V., Journet, E.P., Maillet, F., Rosenberg, C., Cook, D., Gough, C., and Denarie, J. (2000). Four genes of Medicago truncatula controlling components of a Nod factor transduction pathway. Plant Cell **12**: 1647–1665.

Chaparro, J.M., Badri, D. V., and Vivanco, J.M. (2014). Rhizosphere microbiome assemblage is affected by plant development. ISME J. **8**: 790–803.

Chaumont, F., Barrieu, F., Jung, R., and Chrispeels, M.J. (2000). Plasma membrane intrinsic proteins from maize cluster in two sequence subgroups with differential aquaporin activity. Plant Physiol. **122**: 1025–1034.

Chen, A., Gu, M., Sun, S., Zhu, L., Hong, S., and Xu, G. (2011). Identification of two conserved cis-acting elements, MYCS and P1BS, involved in the regulation of mycorrhiza-activated phosphate transporters in eudicot species. New Phytol. **189**: 1157–1169.

Chen, S., Jing, Y., Kang, X., Yang, L., Wang, D.L., Zhang, W., Zhang, L., Chen, P., Chang, J.F., Yang, X.M., and Sun, F.L. (2017). Histone H2B monoubiquitination is a critical epigenetic switch for the regulation of autophagy. Nucleic Acids Res. **45**: 1144–1158.

Choi, J. et al. (2020). The negative regulator SMAX1 controls mycorrhizal symbiosis and strigolactone biosynthesis in rice. Nat. Commun. 11.

Christophersen, H.M., Smith, F.A., and Smith, S.E. (2009). Arbuscular mycorrhizal colonization reduces arsenate uptake in barley via downregulation of transporters in the direct epidermal phosphate uptake pathway. New Phytol. **184**: 962–974.

Cox, J., Hein, M.Y., Luber, C.A., Paron, I., Nagaraj, N., and Mann, M. (2014). Accurate proteome-wide label-free quantification by delayed normalization and maximal peptide ratio extraction, termed MaxLFQ. Mol. Cell. Proteomics **13**: 2513–2526.

van Creij, J., Wang, P., and Limpens, E. (2020). Arbuscular mycorrhiza, a fungal perspective.

Croll, D., Wille, L., Gamper, H.A., Mathimaran, N., Lammers, P.J., Corradi, N., and Sanders, I.R. (2008). Genetic diversity and host plant preferences revealed by simple sequence repeat and mitochondrial markers in a population of the arbuscular mycorrhizal fungus Glomus intraradices. New Phytol. **178**: 672–687.

Czaja, L.F., Hogekamp, C., Lamm, P., Maillet, F., Martinez, E.A., Samain, E., Dénarié, J., Küster, H., and Hohnjec, N. (2012). Transcriptional responses toward diffusible signals from symbiotic microbes reveal MtNFP- and MtDMI3-dependent reprogramming of host gene expression by arbuscular mycorrhizal fungal lipochitooligosaccharidesspi. Plant Physiol.

Czarnecki, O., Yang, J., Weston, D.J., Tuskan, G.A., and Chen, J.G. (2013). A dual role of strigolactones in phosphate acquisition and utilization in plants. Int. J. Mol. Sci. **14**: 7681–7701.

Davière, J.M. and Achard, P. (2013). Gibberellin signaling in plants. Dev. **140**: 1147–1151.

De-la-Peña, C. and Loyola-Vargas, V.M. (2014). Biotic interactions in the rhizosphere: A diverse cooperative enterprise for plant productivity. Plant Physiol. **166**: 701–719.

Dhawan, R., Luo, H., Foerster, A.M., Abuqamar, S., Du, H.N., Briggs, S.D., Scheid, O.M., and Mengiste, T. (2009). HISTONE MONOUBIQUITINATION1 interacts with a subunit of the mediator complex and regulates defense against necrotrophic fungal pathogens in Arabidopsis. Plant Cell **21**: 1000–1019.

Dodds, P.N. and Rathjen, J.P. (2010). Plant immunity: Towards an integrated view of plant-pathogen interactions. Nat. Rev. Genet. **11**: 539–548.

Dumas-Gaudot, E., Slezack, S., Dassi, B., Pozo, M.J., Gianinazzi-Pearson, V., and Gianinazzi, S. (1996). Plant hydrolytic enzymes (chitinases and β-1,3-glucanases) in root reactions to pathogenic and symbiotic microorganisms. Plant Soil **185**: 211–221.

Ehinger, M.O., Croll, D., Koch, A.M., and Sanders, I.R. (2012). Significant genetic and phenotypic changes arising from clonal growth of a single spore of an arbuscular mycorrhizal fungus over multiple generations. New Phytol. **196**: 853–861.

Emmett, B.D., Lévesque-tremblay, V., Harrison, M.J., Emmett, B.D., and Harrison, M.J. (2021). Conserved and reproducible bacterial communities associate with extraradical hyphae of arbuscular mycorrhizal fungi. ISME J.

Endre, G., Kereszt, A., Kevei, Z., Mihacea, S., Kaló, P., and Kiss, G.B. (2002). A receptor kinase gene regulating symbiotic nodule development. Nature **417**: 962–966.

Engler, C., Youles, M., Gruetzner, R., Ehnert, T.M., Werner, S., Jones, J.D.G., Patron, N.J., and Marillonnet, S. (2014). A Golden Gate modular cloning toolbox for plants. ACS Synth. Biol. **3**: 839–843.

Etemadi, M., Zuther, E., Müller, H., Hincha, D.K., and Berg, G. (2018). Ecotype-dependent response of bacterial communities associated with Arabidopsis to cold acclimation. Phytobiomes J. **2**: 3–13.

Ezawa, T. and Saito, K. (2018). How do arbuscular mycorrhizal fungi handle phosphate? New insight into fine-tuning of phosphate metabolism. New Phytol. **220**: 1116–1121.

Ezawa, T., Smith, S.E., and Smith, F.A. (2002). P metabolism and transport in AM fungi. In Plant and Soil.

Fellbaum, C.R., Mensah, J.A., Cloos, A.J., Strahan, G.E., Pfeffer, P.E., Kiers, E.T., and Bücking, H. (2014). Fungal nutrient allocation in common mycorrhizal networks is regulated by the carbon source strength of individual host plants. New Phytol.

Feng, F. et al. (2019). A combination of chitooligosaccharide and lipochitooligosaccharide recognition promotes arbuscular mycorrhizal associations in Medicago truncatula. Nat. Commun. 10.

Ferrol, N., Azcón-Aguilar, C., and Pérez-Tienda, J. (2019). Review: Arbuscular mycorrhizas as key players in sustainable plant phosphorus acquisition: An overview on the mechanisms involved. Plant Sci. **280**: 441–447.

Fesel, P.H. and Zuccaro, A. (2016). β-glucan: Crucial component of the fungal cell wall and elusive MAMP in plants. Fungal Genet. Biol. **90**: 53–60.

Fetter, K., Van Wilder, V., Moshelion, M., and Chaumont, F. (2004). Interactions between Plasma Membrane Aquaporins Modulate Their Water Channel Activity. Plant Cell **16**: 215–228.

Finkel, O.M., Salas-González, I., Castrillo, G., Spaepen, S., Law, T.F., Teixeira, P.J.P.L., Jones, C.D., and Dangl, J.L. (2019). The effects of soil phosphorus content on plant microbiota are driven by the plant phosphate starvation response.

Fiorilli, V., Lanfranco, L., and Bonfante, P. (2013). The expression of GintPT, the phosphate transporter of Rhizophagus irregularis, depends on the symbiotic status and phosphate availability. Planta.

Fleury, D. et al. (2007). The Arabidopsis thaliana homolog of yeast BRE1 has a function in cell cycle regulation during early leaf and root growth. Plant Cell **19**: 417–432.

Fliegmann, J., Mithöfer, A., Wanner, G., and Ebel, J. (2004). An Ancient Enzyme Do-

main Hidden in the Putative β-Glucan Elicitor Receptor of Soybean May Play an Active Part in the Perception of Pathogen-associated Molecular Patterns during Broad Host Resistance. J. Biol. Chem. **279**: 1132–1140.

Floss, D.S., Gomez, S.K., Park, H.J., MacLean, A.M., Müller, L.M., Bhattarai, K.K., Lévesque-Tremblay, V., Maldonado-Mendoza, I.E., and Harrison, M.J. (2017). A Transcriptional Program for Arbuscule Degeneration during AM Symbiosis Is Regulated by MYB1. Curr. Biol. **27**: 1206–1212.

Floss, D.S., Levy, J.G., Lévesque-Tremblay, V., Pumplin, N., and Harrison, M.J. (2013). DELLA proteins regulate arbuscule formation in arbuscular mycorrhizal symbiosis. Proc. Natl. Acad. Sci. U. S. A.

Floss, D.S., Schliemann, W., Schmidt, J., Strack, D., and Walter, M.H. (2008). RNA interference-mediated repression of MtCCD1 in mycorrhizal roots of Medicago truncatula causes accumulation of C27 apocarotenoids, shedding light on the functional role of CCD1. Plant Physiol. **148**: 1267–1282.

Foo, E., Ross, J.J., Jones, W.T., and Reid, J.B. (2013). Plant hormones in arbuscular mycorrhizal symbioses: An emerging role for gibberellins. Ann. Bot. **111**: 769–779.

Forbes, P.J., Millam, S., Hooker, J.E., and Harrier, L.A. (1998). Transformation of the arbuscular mycorrhiza Gigaspora rosea by particle bombardment. Mycol. Res. **102**: 497–501.

Gan, P., Tsushima, A., Hiroyama, R., Narusaka, M., Takano, Y., Narusaka, Y., Kawaradani, M., Damm, U., and Shirasu, K. (2019). Colletotrichum shisoi sp. nov., an anthracnose pathogen of Perilla frutescens in Japan: molecular phylogenetic, morphological and genomic evidence. Sci. Rep. **9**: 13349.

García-Garrido, J.M. and Ocampo, J.A. (2002). Regulation of the plant defence response in arbuscular mycorrhizal symbiosis. J. Exp. Bot. **53**: 1377–1386.

Garcia, K., Doidy, J., Zimmermann, S.D., Wipf, D., and Courty, P.E. (2016). Take a Trip Through the Plant and Fungal Transportome of Mycorrhiza. Trends Plant Sci. **21**: 937–950.

Gendrel, A.V., Lippman, Z., Martienssen, R., and Colot, V. (2005). Profiling histone modification patterns in plants using genomic tiling microarrays. Nat. Methods **2**: 213–218.

Genre, A., Chabaud, M., Balzergue, C., Puech-Pagès, V., Novero, M., Rey, T., Fournier, J., Rochange, S., Bécard, G., Bonfante, P., and Barker, D.G. (2013). Short-chain chitin oligomers from arbuscular mycorrhizal fungi trigger nuclear Ca2+ spiking in Medicago truncatula roots and their production is enhanced by strigolactone. New Phytol.

Genre, A., Chabaud, M., Timmers, T., Bonfante, P., and Barker, D.G. (2005). Arbuscular mycorrhizal fungi elicit a novel intracellular apparatus in Medicago truncatula root epidermal cells before infection. Plant Cell.

Genre, A., Ivanov, S., Fendrych, M., Faccio, A., Žárský, V., Bisseling, T., and Bonfante, P. (2012). Multiple exocytotic markers accumulate at the sites of perifungal membrane bio-

genesis in arbuscular mycorrhizas. Plant Cell Physiol. **53**: 244–255.

Genre, A., Lanfranco, L., Perotto, S., & Bonfante, P. (2020). Unique and common traits in mycorrhizal symbioses. Nature Reviews Microbiology, **18(11)**, 649-660.

Geurts, R. and Bisseling, T. (2002). Rhizobium nod factor perception and signalling. The Plant Cell, **14**(suppl 1), S239-S249.

Gianinazzi-Pearson, V., Dumas-Gaudot, E., Gollotte, A., Tahiri-Alaoui, A., and Gianinazzi, S. (1996). Cellular and molecular defence-related root responses to invasion by arbuscular mycorrhizal fungi. New Phytol. **133**: 45–57.

Gobbato, E. et al. (2012). A GRAS-type transcription factor with a specific function in mycorrhizal signaling. Curr. Biol. **22**: 2236–2241.

Gong, B.Q., Wang, F.Z., and Li, J.F. (2020). Hide-and-Seek: Chitin-Triggered Plant Immunity and Fungal Counterstrategies. Trends Plant Sci. **25**: 805–816.

Govindarajulu, M., Pfeffer, P.E., Jin, H., Abubaker, J., Douds, D.D., Allen, J.W., Bücking, H., Lammers, P.J., and Shachar-Hill, Y. (2005). Nitrogen transfer in the arbuscular mycorrhizal symbiosis. Nature.

Gutjahr, C. et al. (2015). Rice perception of symbiotic arbuscular mycorrhizal fungi requires the karrikin receptor complex. Science (80-.). **350**: 1521–1524.

Gutjahr, C. et al. (2012). The half-size ABC transporters STR1 and STR2 are indispensable for mycorrhizal arbuscule formation in rice. Plant J. **69**: 906–920.

Gutjahr, C., Casieri, L., and Paszkowski, U. (2009). Glomus intraradices induces changes in root system architecture of rice independently of common symbiosis signaling. New Phytol.

Gutjahr, C. and Parniske, M. (2013). Cell and developmental biology of arbuscular mycorrhiza symbiosis. Annu. Rev. Cell Dev. Biol. **29**: 593–617.

Gutjahr, C. and Parniske, M. (2017). Cell Biology: Control of Partner Lifetime in a Plant–Fungus Relationship. Curr. Biol. **27**: R420–R423.

Guyon, K., Balagué, C., Roby, D., and Raffaele, S. (2014). Secretome analysis reveals effector candidates associated with broad host range necrotrophy in the fungal plant pathogen Sclerotinia sclerotiorum. BMC Genomics **15**.

Hachez, C. and Chaumont, F. (2010). Aquaporins: A family of highly regulated multifunctional channels. Adv. Exp. Med. Biol. **679**: 1–17.

Hachez, C., Laloux, T., Reinhardt, H., Cavez, D., Degand, H., Grefen, C., De Rycke, R., Inzé, D., Blatt, M.R., Russinova, E., and Chaumont, F. (2014). Arabidopsis SNAREs SYP61 and SYP121 coordinate the trafficking of plasma membrane aquaporin PIP2;7 to modulate the cell membrane water permeability. Plant Cell **26**: 3132–3147.

Hacquard, S. et al. (2016). Survival trade-offs in plant roots during colonization by closely related beneficial and pathogenic fungi. Nat. Commun. **7**.

Hander, T. et al. (2019). Damage on plants activates Ca^{2+}-dependent metacaspases for release of immunomodulatory peptides. Science (80-.). **363**.

Hao, L., Renxiao, W., Qian, Q., Meixian, Y., Xiangbing, M., Zhiming, F., Cunyu, Y., Biao, J., Zhen, S., Jiayang, L., and Yonghong, W. (2009). DWARF27,an iron-containing protein required for the biosynthesis of strigolactones,regulates rice tiller bud outgrowth. Plant Cell.

Harrison, M.J. and Van Buuren, M.L. (1995). A phosphate transporter from the mycorrhizal fungus Glomus versiforme. Nature.

Harrison, M.J. and Dixon, R.A. (1993). Isoflavonoid accumulation and expression of defense gene transcripts during the establishment of vesicular-arbuscular mycorrhizal associations in roots of Medicago truncatula. Mol. Plant-Microbe Interact. **6**: 643–654.

Harrison, M.J. and Ivanov, S. (2017). Exocytosis for endosymbiosis: membrane trafficking pathways for development of symbiotic membrane compartments. Curr. Opin. Plant Biol. **38**: 101–108.

Hartmann, M., Voß, S., and Requena, N. (2020). Host-Induced Gene Silencing of Arbuscular Mycorrhizal Fungal Genes via Agrobacterium rhizogenes-Mediated Root Transformation in Medicago truncatula. In Arbuscular Mycorrhizal Fungi: Methods and Protocols, N. Ferrol and L. Lanfranco, eds (Springer US: New York, NY), pp. 239–248.

Häweker, H., Rips, S., Koiwa, H., Salomon, S., Saijo, Y., Chinchilla, D., Robatzek, S., and Von Schaewen, A. (2010). Pattern recognition receptors require N-glycosylation to mediate plant immunity. J. Biol. Chem. **285**: 4629–4636.

He, J. et al. (2019). A LysM Receptor Heteromer Mediates Perception of Arbuscular Mycorrhizal Symbiotic Signal in Rice. Mol. Plant **12**: 1561–1576.

van der Heijden, M.G.A., Martin, F.M., Selosse, M.A., and Sanders, I.R. (2015). Mycorrhizal ecology and evolution: The past, the present, and the future. New Phytol. **205**: 1406–1423.

Helber, N. and Requena, N. (2008). Expression of the fluorescence markers DsRed and GFP fused to a nuclear localization signal in the arbuscular mycorrhizal fungus Glomus intraradices. New Phytol.

Helber, N., Wippel, K., Sauer, N., Schaarschmidt, S., Hause, B., and Requena, N. (2011). A versatile monosaccharide transporter that operates in the arbuscular mycorrhizal fungus Glomus sp is crucial for the symbiotic relationship with plants. Plant Cell **23**: 3812–3823.

Helgason, T., Daniell, T.J., Husband, R., Fitter, A.H., and Young, J.P.W. (1998). Ploughing up the wood-wide web? Nature **394**: 431.

Helgason, T., Merryweather, J.W., Denison, J., Wilson, P., Young, J.P.W., and Fitter, A.H. (2002). Selectivity and functional diversity in arbuscular mycorrhizas of co-occurring fungi and plants from a temperate deciduous woodland. J. Ecol. **90**: 371–384.

Helgason, T., Merryweather, J.W., Young, J.P.W., and Fitter, A.H. (2007). Specificity

and resilience in the arbuscular mycorrhizal fungi of a natural woodland community. J. Ecol. **95**: 623–630.

Hitchman, R.B., Possee, R.D., and King, L.A. (2009). Baculovirus expression systems for recombinant protein production in insect cells. Recent Pat. Biotechnol. **3**: 46–54.

Hogekamp, C. and Küster, H. (2013). A roadmap of cell-type specific gene expression during sequential stages of the arbuscular mycorrhiza symbiosis. BMC Genomics **14**: 306 (2013).

Hogenhout, S.A., Van Der Hoorn, R.A.L., Terauchi, R., and Kamoun, S. (2009). Emerging concepts in effector biology of plant-associated organisms. Mol. Plant-Microbe Interact. **22**: 115–122.

Hogland, D.R. (1950). The Water Culture Method for Growing Plants without Soil THE COLLEGE OF AGRICULTURE. Agriculture.

Van Der Hoorn, R.A.L., Wulff, B.B.H., Rivas, S., Durrant, M.C., Van Der Ploeg, A., De Wit, P.J.G.M., and Jones, J.D.G. (2005). Structure-function analysis of Cf-9, a receptor-like protein with extracytoplasmic leucine-rich repeats. Plant Cell.

Horváth, B. et al. (2011). Medicago truncatula IPD3 is a member of the common symbiotic signaling pathway required for rhizobial and mycorrhizal symbioses. Mol. Plant-Microbe Interact.

Hou, S., Wang, X., Chen, D., Yang, X., Wang, M., Turrà, D., Di Pietro, A., and Zhang, W. (2014). The Secreted Peptide PIP1 Amplifies Immunity through Receptor-Like Kinase 7. PLoS Pathog. **10**.

Houterman, P.M., Ma, L., Van Ooijen, G., De Vroomen, M.J., Cornelissen, B.J.C., Takken, F.L.W., and Rep, M. (2009). The effector protein Avr2 of the xylem-colonizing fungus Fusarium oxysporum activates the tomato resistance protein I-2 intracellularly. Plant J. **58**: 970–978.

Hu, B. et al. (2019). Nitrate–NRT1.1B–SPX4 cascade integrates nitrogen and phosphorus signalling networks in plants. Nat. Plants **5**: 401–413.

Huang, R. et al. (2020). Natural variation at OsCERK1 regulates arbuscular mycorrhizal symbiosis in rice. New Phytol. **225**: 1762–1776.

Huisman, R., Hontelez, J., Mysore, K.S., Wen, J., Bisseling, T., and Limpens, E. (2016). A symbiosis-dedicated SYNTAXIN OF PLANTS 13II isoform controls the formation of a stable host-microbe interface in symbiosis. New Phytol. **211**: 1338–1351.

Ito, S. et al. (2017). Regulation of strigolactone biosynthesis by gibberellin signaling. Plant Physiol. **174**: 1250–1259.

Ivanov, S., Austin, J., Berg, R.H., and Harrison, M.J. (2019). Extensive membrane systems at the host–arbuscular mycorrhizal fungus interface. Nat. Plants **5**: 194–203.

Ivanov, S., Fedorova, E.E., Limpens, E., De Mita, S., Genre, A., Bonfante, P., and Bisseling, T. (2012). Rhizobium-legume symbiosis shares an exocytotic pathway required for

arbuscule formation. Proc. Natl. Acad. Sci. U. S. A. **109**: 8316–8321.

Ivanov, S. and Harrison, M.J. (2019). Accumulation of phosphoinositides in distinct regions of the periarbuscular membrane. New Phytol. **221**: 2213–2227.

Jach, G., Binot, E., Frings, S., Luxa, K., and Schell, J. (2001). Use of red fluorescent protein from Discosoma sp. (dsRED) as a reporter for plant gene expression. Plant J.

Jacobowitz, J.R. and Weng, J.K. (2020). Exploring Uncharted Territories of Plant Specialized Metabolism in the Postgenomic Era. Annu. Rev. Plant Biol. **71**: 631–658.

James, T.Y., Pelin, A., Bonen, L., Ahrendt, S., Sain, D., Corradi, N., and Stajich, J.E. (2013). Shared signatures of parasitism and phylogenomics unite cryptomycota and microsporidia. Curr. Biol. **23**: 1548–1553.

Jashni, M.K., Mehrabi, R., Collemare, J., Mesarich, C.H., and de Wit, P.J.G.M. (2015). The battle in the apoplast: Further insights into the roles of proteases and their inhibitors in plant–pathogen interactions. Front. Plant Sci. **6**: 1–7.

Javot, H., Penmetsa, R.V., Breuillin, F., Bhattarai, K.K., Noar, R.D., Gomez, S.K., Zhang, Q., Cook, D.R., and Harrison, M.J. (2011). Medicago truncatula mtpt4 mutants reveal a role for nitrogen in the regulation of arbuscule degeneration in arbuscular mycorrhizal symbiosis. Plant J. **68**: 954–965.

Javot, H., Penmetsa, R.V., Terzaghi, N., Cook, D.R., and Harrison, M.J. (2007). A Medicago truncatula phosphate transporter indispensable for the arbuscular mycorrhizal symbiosis. Proc. Natl. Acad. Sci. U. S. A. **104**: 1720–1725.

Jenner, R.G. and Young, R.A. (2005). Insights into host responses against pathogens from transcriptional profiling. Nat. Rev. Microbiol.: 281–294.

Jewell, J.B., Sowders, J.M., He, R., Willis, M.A., Gang, D.R., and Tanaka, K. (2019). Extracellular atp shapes a defense-related transcriptome both independently and along with other defense signaling pathways. Plant Physiol. **179**: 1144–1158.

Jiang, F., Zhang, L., Zhou, J., George, T.S., and Feng, G. (2021). Arbuscular mycorrhizal fungi enhance mineralisation of organic phosphorus by carrying bacteria along their extraradical hyphae. New Phytol.

Jiang, Y., Wang, W., Xie, Q., Liu, N., Liu, L., Wang, D., Zhang, X., Yang, C., Chen, X., Tang, D., and Wang, E. (2017). Plants transfer lipids to sustain colonization by mutualistic mycorrhizal and parasitic fungi. Science (80-.). **356**: 1172–1173.

Jiang, Y., Xie, Q., Wang, W., Yang, J., Zhang, X., Yu, N., Zhou, Y., and Wang, E. (2018). Medicago AP2-Domain Transcription Factor WRI5a Is a Master Regulator of Lipid Biosynthesis and Transfer during Mycorrhizal Symbiosis. Mol. Plant **11**: 1344–1359.

Jin, H., Pfeffer, P.E., Douds, D.D., Piotrowski, E., Lammers, P.J., and Shachar-Hill, Y. (2005). The uptake, metabolism, transport and transfer of nitrogen in an arbuscular mycorrhizal symbiosis. New Phytol.

Jin, Y., Liu, H., Luo, D., Yu, N., Dong, W., Wang, C., Zhang, X., Dai, H., Yang, J., and

Wang, E. (2016). DELLA proteins are common components of symbiotic rhizobial and mycorrhizal signalling pathways. Nat. Commun. **7**.

Johnson, N.C., Rowland, D.L., Corkidi, L., Egerton-Warburton, L.M., and Allen, E.B. (2003). Nitrogen enrichment alters mycorrhizal allocation at five mesic to semiarid grasslands. Ecology **84**: 1895–1908.

Johnson, N.C., Wilson, G.W.T., Wilson, J.A., Miller, R.M., and Bowker, M.A. (2015). Mycorrhizal phenotypes and the Law of the Minimum. New Phytol. **205**: 1473–1484.

Jones, J.D.G. and Dangl, J.L. (2006). The plant immune system. Nature **444**: 323–329.

Jonge, R. De, Esse, H.P. Van, Kombrink, A., Shinya, T., Desaki, Y., Bours, R., Krol, S. Van Der, Shibuya, N., Joosten, M.H.A.J., and Thomma, B.P.H.J. (2010). Conserved Fungal LysM Effector Ecp6 Prevents Chitin-Triggered Immunity in Plants. Science (80-.). **329**: 953–956.

Jung, J.Y., Ried, M.K., Hothorn, M., and Poirier, Y. (2018). Control of plant phosphate homeostasis by inositol pyrophosphates and the SPX domain. Curr. Opin. Biotechnol. **49**: 156–162.

Kafle, A., Garcia, K., Wang, X., Pfeffer, P.E., Strahan, G.D., and Bücking, H. (2019). Nutrient demand and fungal access to resources control the carbon allocation to the symbiotic partners in tripartite interactions of Medicago truncatula. Plant Cell Environ.

Kagiyama, M., Hirano, Y., Mori, T., Kim, S.Y., Kyozuka, J., Seto, Y., Yamaguchi, S., and Hakoshima, T. (2013). Structures of D14 and D14L in the strigolactone and karrikin signaling pathways. Genes to Cells **18**: 147–160.

Kaló, P. et al. (2005). Nodulation signaling in legumes requires NSP2, a member of the GRAS family of transcriptional regulators. Science (80-.). **308**: 1786–1789.

Kamel, L., Tang, N., Malbreil, M., San Clemente, H., Le Marquer, M., Roux, C., and dit Frey, N.F. (2017). The comparison of expressed candidate secreted proteins from two arbuscular mycorrhizal fungi unravels common and specific molecular tools to invade different host plants. Front. Plant Sci. **8**: 1–18.

Kameoka, H., Tsutsui, I., Saito, K., Kikuchi, Y., Handa, Y., Ezawa, T., Hayashi, H., Kawaguchi, M., and Akiyama, K. (2019). Stimulation of asymbiotic sporulation in arbuscular mycorrhizal fungi by fatty acids. Nat. Microbiol. **4**: 1654–1660.

Kapulnik, Y., Volpin, H., Itzhaki, H., Ganon, D., Galili, S., David, R., Shaul, O., Elad, Y., Chet, I., and Okon, Y. (1996). Suppression of defence responses in mycorrhizal alfalfa and tobacco roots. New Phytol. **133**: 59–64.

Kasprzewska, A. (2003). Plant chitinases - Regulation and function. Cell. Mol. Biol. Lett.

Kelly, S., Radutoiu, S., and Stougaard, J. (2017). Legume LysM receptors mediate symbiotic and pathogenic signalling. Curr. Opin. Plant Biol. **39**: 152–158.

Keymer, A. et al. (2017). Lipid transfer from plants to arbuscular mycorrhiza fungi. Elife **6**: 1–33.

Kiers, E.T. et al. (2011). Reciprocal rewards stabilize cooperation in the mycorrhizal symbiosis. Science (80-.). **333**: 880–882.

Kiers, E.T. and Van Der Heijden, M.G.A. (2006). Mutualistic stability in the arbuscular mycorrhizal symbiosis: Exploring hypotheses of evolutionary cooperation. Ecology **87**: 1627–1636.

Kikuchi, Y., Hijikata, N., Ohtomo, R., Handa, Y., Kawaguchi, M., Saito, K., Masuta, C., and Ezawa, T. (2016). Aquaporin-mediated long-distance polyphosphate translocation directed towards the host in arbuscular mycorrhizal symbiosis: application of virus-induced gene silencing. New Phytol. **211**: 1202–1208.

Kikuchi, Y., Hijikata, N., Yokoyama, K., Ohtomo, R., Handa, Y., Kawaguchi, M., Saito, K., and Ezawa, T. (2014). Polyphosphate accumulation is driven by transcriptome alterations that lead to near-synchronous and near-equivalent uptake of inorganic cations in an arbuscular mycorrhizal fungus. New Phytol.

Kim, D., Paggi, J.M., Park, C., Bennett, C., and Salzberg, S.L. (2019). Graph-based genome alignment and genotyping with HISAT2 and HISAT-genotype. Nat. Biotechnol. **37**: 907–915.

Kirkpatrick, D.S., Bustos, D.J., Dogan, T., Chan, J., Phu, L., Young, A., Friedman, L.S., Belvin, M., Song, Q., Bakalarski, C.E., and Hoeflich, K.P. (2014). Genome of an arbuscular mycorrhizal fungus provides insight into the oldest plant symbiosis. Proc. Natl. Acad. Sci. U. S. A. **111**: 562.

Kistner, C., Winzer, T., Pitzschke, A., Mulder, L., Sato, S., Kaneko, T., Tabata, S., Sandal, N., Stougaard, J., Webb, K.J., Szczyglowski, K., and Parniske, M. (2005). Seven Lotus japonicus genes required for transcriptional reprogramming of the root during fungal and bacterial symbiosis. Plant Cell.

Klironomos, J.N. (2003). Variation in plant response to native and exotic arbuscular mycorrhizal fungi. Ecology **84**: 2292–2301.

Kloppholz, S., Kuhn, H., and Requena, N. (2011). A secreted fungal effector of glomus intraradices promotes symbiotic biotrophy. Curr. Biol. **21**: 1204–1209.

Kobae, Y. and Fujiwara, T. (2014). Earliest colonization events of rhizophagus irregularis in rice roots occur preferentially in previously uncolonized cells. Plant Cell Physiol.

Kobae, Y. and Hata, S. (2010). Dynamics of periarbuscular membranes visualized with a fluorescent phosphate transporter in arbuscular mycorrhizal roots of rice. Plant Cell Physiol.

Kobae, Y., Tamura, Y., Takai, S., Banba, M., and Hata, S. (2010). Localized expression of arbuscular mycorrhiza-inducible ammonium transporters in soybean. Plant Cell Physiol.

Kobayashi, Y., Maeda, T., Yamaguchi, K., Kameoka, H., Tanaka, S., Ezawa, T., Shigenobu, S., and Kawaguchi, M. (2018). The genome of Rhizophagus clarus HR1 reveals a common genetic basis for auxotrophy among arbuscular mycorrhizal fungi. BMC Genomics.

Koegel, S., Brulé, D., Wiemken, A., Boller, T., and Courty, P.E. (2015). The effect of different nitrogen sources on the symbiotic interaction between Sorghum bicolor and Glomus intraradices: Expression of plant and fungal genes involved in nitrogen assimilation. Soil Biol. Biochem.

Kohlen, W., Charnikhova, T., Liu, Q., Bours, R., Domagalska, M.A., Beguerie, S., Verstappen, F., Leyser, O., Bouwmeester, H., and Ruyter-Spira, C. (2011). Strigolactones are transported through the xylem and play a key role in shoot architectural response to phosphate deficiency in nonarbuscular mycorrhizal host arabidopsis. Plant Physiol.

Kokkoris, V., Chagnon, P., Yildirir, G., Clarke, K., Goh, D., MacLean, A.M., Dettman, J., Stefani, F., and Corradi, N. (2021). Host identity influences nuclear dynamics in arbuscular mycorrhizal fungi. Curr. Biol.: 1–8.

Kong, L. et al. (2017). A Phytophthora Effector Manipulates Host Histone Acetylation and Reprograms Defense Gene Expression to Promote Infection. Curr. Biol. **27**: 981–991.

Krajinski, F., Courty, P.E., Sieh, D., Franken, P., Zhang, H., Bucher, M., Gerlach, N., Kryvoruchko, I., Zoeller, D., Udvardi, M., and Hause, B. (2014). The H+-ATPase HA1 of Medicago truncatula is essential for phosphate transport and plant growth during arbuscular mycorrhizal symbiosis. Plant Cell **26**: 1808–1817.

Kubota, M., McGonigle, T.P., and Hyakumachi, M. (2005). Co-occurrence of Arum- and Paris-type morphologies of arbuscular mycorrhizae in cucumber and tomato. Mycorrhiza **15**: 73–77.

Kulikova, O., Franken, C., and Bisseling, T. (2018). In Situ Hybridization Method for Localization of mRNA Molecules in Medicago Tissue Sections. In Functional Genomics in Medicago truncatula: Methods and Protocols, L.A. Cañas and J.P. Beltrán, eds (Springer New York: New York, NY), pp. 145–159.

Lahrmann, U., Ding, Y., Banhara, A., Rath, M., Hajirezaei, M.R., Döhlemann, S., Von Wirén, N., Parniske, M., and Zuccaro, A. (2013). Host-related metabolic cues affect colonization strategies of a root endophyte. Proc. Natl. Acad. Sci. U. S. A. **110**: 13965–13970.

Lanfranco, L., Fiorilli, V., and Gutjahr, C. (2018). Partner communication and role of nutrients in the arbuscular mycorrhizal symbiosis. New Phytol. **220**: 1031–1046.

Larose, G., Chênevert, R., Moutoglis, P., Gagné, S., Piché, Y., and Vierheilig, H. (2002). Flavonoid levels in roots of Medicago sativa are modulated by the developmental stage of the symbiosis and the root colonizing arbuscular mycorrhizal fungus. J. Plant Physiol. **159**: 1329–1339.

Lee, S., Fu, F., Xu, S., Lee, S.Y., Yun, D.J., and Mengiste, T. (2016). Global regulation of plant immunity by histone lysine methyl transferases. Plant Cell **28**: 1640–1661.

Lee, S.J., Kelley, B.S., Damasceno, C.M.B., St. John, B., Kim, B.S., Kim, B.D., and Rose, J.K.C. (2006). A functional screen to characterize the secretomes of eukaryotic pathogens and their hosts in planta. Mol. Plant-Microbe Interact. **19**: 1368–1377.

Lefebvre, B., Klaus-Heisen, D., Pietraszewska-Bogiel, A., Hervé, C., Camut, S., Auri-

ac, M.C., Gasciolli, V., Nurisso, A., Gadella, T.W.J., and Cullimore, J. (2012). Role of N-glycosylation sites and CXC motifs in trafficking of Medicago truncatula Nod factor perception protein to plasma membrane. J. Biol. Chem. **287**: 10812–10823.

Li, H. et al. (2018). A phytophthora effector recruits a host cytoplasmic transacetylase into nuclear speckles to enhance plant susceptibility. Elife **7**: 1–23.

Li, J. (2019). Identification of host-specific effectors mediating pathogenicity of the vascular wilt pathogen Verticillium dahliae.

Li, X., Liu, Q., Feng, H., Deng, J., Zhang, R., Wen, J., Dong, J., and Wang, T. (2020). Dehydrin MtCAS31 promotes autophagic degradation under drought stress. Autophagy **16**: 862–877.

Liao, D., Sun, X., Wang, N., Song, F., and Liang, Y. (2018). Tomato LysM receptor-like kinase SlLYK12 is involved in arbuscular mycorrhizal symbiosis. Front. Plant Sci. **9**: 1–11.

Liebrand, T.W.H., Berg, G.C.M. van den, Zhao, Z., Smit, P., Cordewener, J.H.G., America, A.H.P., Sklenar, J., Jones, A.M.E., Tameling, W.I.L., Robatzek, S., Thomma, B.P.H.J., and Joosten, M.H.A.J. (2013). Receptor-like kinase SOBIR1/EVR interacts with receptor-like proteins in plant immunity against fungal infection. Proc. Natl. Acad. Sci. **110**: 13228–13228.

Limpens, E. (2019). Extracellular membranes in symbiosis. Nat. Plants **5**: 131–132.

Limpens, E., Franken, C., Smit, P., Willemse, J., Bisseling, T., and Geurts, R. (2003). LysM Domain Receptor Kinases Regulating Rhizobial Nod Factor-Induced Infection. Science (80-.). **302**: 630–633.

Limpens, E. and Geurts, R. (2014). Plant-driven genome selection of arbuscular mycorrhizal fungi. Mol. Plant Pathol. **15**: 531–534.

Limpens, E. and Geurts, R. (2018). Transcriptional Regulation of Nutrient Exchange in Arbuscular Mycorrhizal Symbiosis. Mol. Plant **11**: 1421–1423.

Limpens, E., Ramos, J., Franken, C., Raz, V., Compaan, B., Franssen, H., Bisseling, T., and Geurts, R. (2004). RNA interference in Agrobacterium rhizogenes-transformed roots of Arabidopsis and Medicago truncatula. J. Exp. Bot. **55**: 983–992.

Lin, K. et al. (2014). Single Nucleus Genome Sequencing Reveals High Similarity among Nuclei of an Endomycorrhizal Fungus. PLoS Genet. **10**.

Liu, W. et al. (2011). Strigolactone biosynthesis in Medicago truncatula and rice requires the symbiotic GRAS-type transcription factors NSP1 and NSP2. Plant Cell.

Liu, Y., Koornneef, M., and Soppe, W.J.J. (2007). The absence of histone H2B monoubiquitination in the Arabidopsis hub1 (rdo4) mutant reveals a role for chromatin remodeling in seed dormancy. Plant Cell **19**: 433–444.

Lobstein, J., Emrich, C.A., Jeans, C., Faulkner, M., Riggs, P., and Berkmen, M. (2012). SHuffle, a novel Escherichia coli protein expression strain capable of correctly folding disulfide bonded proteins in its cytoplasm. Microb. Cell Fact. **11**: 1.

Lohar, D.P., Sharopova, N., Endre, G., Peñuela, S., Samac, D., Town, C., Silverstein, K.A.T., and VandenBosch, K.A. (2006). Transcript analysis of early nodulation events in Medicago truncatula. Plant Physiol.

López-Ráez, J.A., Charnikhova, T., Gómez-Roldán, V., Matusova, R., Kohlen, W., De Vos, R., Verstappen, F., Puech-Pages, V., Bécard, G., Mulder, P., and Bouwmeester, H. (2008). Tomato strigolactones are derived from carotenoids and their biosynthesis is promoted by phosphate starvation. New Phytol. **178**: 863–874.

Lota, F., Wegmüller, S., Buer, B., Sato, S., Bräutigam, A., Hanf, B., and Bucher, M. (2013). The cis-acting CTTC-P1BS module is indicative for gene function of LjVTI12, a Qb-SNARE protein gene that is required for arbuscule formation in Lotus japonicus. Plant J. **74**: 280–293.

Lozano-Durán, R. and Zipfel, C. (2015). Trade-off between growth and immunity: Role of brassinosteroids. Trends Plant Sci. **20**: 12–19.

Lu, J., Boeren, S., de Vries, S.C., van Valenberg, H.J.F., Vervoort, J., and Hettinga, K. (2011). Filter-aided sample preparation with dimethyl labeling to identify and quantify milk fat globule membrane proteins. J. Proteomics **75**: 34–43.

Luginbuehl, L.H., Menard, G.N., Kurup, S., Van Erp, H., Radhakrishnan, G. V., Breakspear, A., Oldroyd, G.E.D., and Eastmond, P.J. (2017). Fatty acids in arbuscular mycorrhizal fungi are synthesized by the host plant. Science (80-.). **356**: 1175–1178.

Luginbuehl, L.H. and Oldroyd, G.E.D. (2017). Understanding the Arbuscule at the Heart of Endomycorrhizal Symbioses in Plants. Curr. Biol. **27**: R952–R963.

Ma, L., Lukasik, E., Gawehns, F., and Takken, F.L.W. (2012). The Use of Agroinfiltration for Transient Expression of Plant Resistance and Fungal Effector Proteins in Nicotiana benthamiana Leaves. In Plant Fungal Pathogens: Methods and Protocols, M.D. Bolton and B.P.H.J. Thomma, eds (Humana Press: Totowa, NJ), pp. 61–74.

Maclean, A.M., Bravo, A., and Harrison, M.J. (2017). Plant signaling and metabolic pathways enabling arbuscular mycorrhizal symbiosis. Plant Cell **29**: 2319–2335.

Madawala, H. M. S. P. (2021). Arbuscular mycorrhizal fungi as biofertilizers: Current trends, challenges, and future prospects. In Biofertilizers (pp. 83-93). Woodhead Publishing.

Madsen, E.B., Madsen, L.H., Radutoiu, S., Olbryt, M., Rakwalska, M., Szczyglowski, K., Sato, S., Kaneko, T., Tabata, S., Sandal, N., and Stougaard, J. (2003). A receptor kinase gene of the LysM type is involved in legume perception of rhizobial signals. Nature.

Maeda, T., Kobayashi, Y., Kameoka, H., Okuma, N., Takeda, N., Yamaguchi, K., Bino, T., Shigenobu, S., and Kawaguchi, M. (2018). Evidence of non-tandemly repeated rDNAs and their intragenomic heterogeneity in Rhizophagus irregularis. Commun. Biol. **1**.

Maillet, F. et al. (2011). Fungal lipochitooligosaccharide symbiotic signals in arbuscular mycorrhiza. Nature **469**: 58–64.

Maldonado-mendoza, I.E., Dewbre, G.R., Harrison, M.J., Samuel, T., Noble, R., and

Parkway, S.N. (2001). A Phosphate Transporter Gene from the Extra-Radical Mycelium of an Arbuscular Mycorrhizal Fungus Glomus intraradices Is Regulated in Response to Phosphate in the Environment. Mol. Plant-Microbe Interact. **14**: 1140–1148.

Manck-Götzenberger, J. and Requena, N. (2016). Arbuscular mycorrhiza symbiosis induces a major transcriptional reprogramming of the potato SWEET sugar transporter family. Front. Plant Sci.

Mao, Y.S., Zhang, B., and Spector, D.L. (2011). Biogenesis and function of nuclear bodies. Trends Genet. **27**: 295–306.

Martínez-García, L.B. and Pugnaire, F.I. (2011). Arbuscular mycorrhizal fungi host preference and site effects in two plant species in a semiarid environment. Appl. Soil Ecol. **48**: 313–317.

Martre, P., Morillon, R., Barrieu, F., North, G.B., Nobel, P.S., and Chrispeels, M.J. (2002). Plasma membrane aquaporins play a significant role during recovery from water deficit. Plant Physiol. **130**: 2101–2110.

Masclaux, F.G., Wyss, T., Pagni, M., Rosikiewicz, P., and Sanders, I.R. (2019). Investigating unexplained genetic variation and its expression in the arbuscular mycorrhizal fungus Rhizophagus irregularis: A comparison of whole genome and RAD sequencing data. PLoS One **14**: 1–20.

Mbodj, D., Effa-Effa, B., Kane, A., Manneh, B., Gantet, P., Laplaze, L., Diedhiou, A.G., and Grondin, A. (2018). Arbuscular mycorrhizal symbiosis in rice: Establishment, environmental control and impact on plant growth and resistance to abiotic stresses. Rhizosphere **8**: 12–26.

McGONIGLE, T.P., MILLER, M.H., EVANS, D.G., FAIRCHILD, G.L., and SWAN, J.A. (1990). A new method which gives an objective measure of colonization of roots by vesicular—arbuscular mycorrhizal fungi. New Phytol. **115**: 495–501.

McHaffie, M.B. and Maherali, H. (2020). Variation in mycorrhizal growth response influences competitive interactions and mechanisms of plant species coexistence. Oecologia **192**: 755–765.

Mélida, H., Sopeña-Torres, S., Bacete, L., Garrido-Arandia, M., Jordá, L., López, G., Muñoz-Barrios, A., Pacios, L.F., and Molina, A. (2018). Non-branched β-1,3-glucan oligosaccharides trigger immune responses in Arabidopsis. Plant J. **93**: 34–49.

Mikkelsen, B.L., Rosendahl, S., and Jakobsen, I. (2008). Underground resource allocation between individual networks of mycorrhizal fungi. New Phytol. **180**: 890–898.

Miyata, K. et al. (2014). The bifunctional plant receptor, OsCERK1, regulates both chitin-triggered immunity and arbuscular mycorrhizal symbiosis in rice. Plant Cell Physiol.

Monchgesang, S., Strehmel, N., Schmidt, S., Westphal, L., Taruttis, F., Muller, E., Herklotz, S., Neumann, S., and Scheel, D. (2016). Natural variation of root exudates in Arabidopsis thaliana-linking metabolomic and genomic data. Sci. Rep. **6**: 1–11.

Morin, E. et al. (2019). Comparative genomics of Rhizophagus irregularis, R. cerebriforme, R. diaphanus and Gigaspora rosea highlights specific genetic features in Glomeromycotina. New Phytol. **222**: 1584–1598.

Müller, L.M. and Harrison, M.J. (2019). Phytohormones, miRNAs, and peptide signals integrate plant phosphorus status with arbuscular mycorrhizal symbiosis. Curr. Opin. Plant Biol. **50**: 132–139.

Murray, J.D. et al. (2011). Vapyrin, a gene essential for intracellular progression of arbuscular mycorrhizal symbiosis, is also essential for infection by rhizobia in the nodule symbiosis of Medicago truncatula. Plant J. **65**: 244–252.

Musinova, Y.R., Lisitsyna, O.M., Golyshev, S.A., Tuzhikov, A.I., Polyakov, V.Y., and Sheval, E. V. (2011). Nucleolar localization/retention signal is responsible for transient accumulation of histone H2B in the nucleolus through electrostatic interactions. Biochim. Biophys. Acta - Mol. Cell Res. **1813**: 27–38.

Nadal, M. et al. (2017). An N-acetylglucosamine transporter required for arbuscular mycorrhizal symbioses in rice and maize. Nat. Plants **3**: 1–7.

Nagahashi, G. and Douds, D.D. (2011). The effects of hydroxy fatty acids on the hyphal branching of germinated spores of AM fungi. Fungal Biol.

Nars, A., Rey, T., Lafitte, C., Vergnes, S., Amatya, S., Jacquet, C., Dumas, B., Thibaudeau, C., Heux, L., Bottin, A., and Fliegmann, J. (2013). An experimental system to study responses of Medicago truncatula roots to chitin oligomers of high degree of polymerization and other microbial elicitors. Plant Cell Rep.

Nelson, D.C., Scaffidi, A., Dun, E.A., Waters, M.T., Flematti, G.R., Dixon, K.W., Beveridge, C.A., Ghisalberti, E.L., and Smith, S.M. (2011). F-box protein MAX2 has dual roles in karrikin and strigolactone signaling in Arabidopsis thaliana. Proc. Natl. Acad. Sci. U. S. A. **108**: 8897–8902.

Newman, M.A., Sundelin, T., Nielsen, J.T., and Erbs, G. (2013). MAMP (microbe-associated molecular pattern) triggered immunity in plants. Front. Plant Sci. **4**: 1–14.

Noë, R. and Kiers, E.T. (2018). Mycorrhizal Markets, Firms, and Co-ops. Trends Ecol. Evol. **33**: 777–789.

Nowara, D., Schweizer, P., Gay, A., Lacomme, C., Shaw, J., Ridout, C., Douchkov, D., Hensel, G., and Kumlehn, J. (2010). HIGS: Host-induced gene silencing in the obligate biotrophic fungal pathogen Blumeria graminis. Plant Cell **22**: 3130–3141.

Öpik, M., Vanatoa, A., Vanatoa, E., Moora, M., Davison, J., Kalwij, J.M., Reier, Ü., and Zobel, M. (2010). The online database MaarjAM reveals global and ecosystemic distribution patterns in arbuscular mycorrhizal fungi (Glomeromycota). New Phytol. **188**: 223–241.

Park, H.J., Floss, D.S., Levesque-Tremblay, V., Bravo, A., and Harrison, M.J. (2015). Hyphal branching during arbuscule development requires reduced arbuscular mycorrhiza. Plant Physiol. **169**: 2774–2788.

Parniske, M. (2008). Arbuscular mycorrhiza: The mother of plant root endosymbioses. Nat. Rev. Microbiol. **6**: 763–775.

Pérez-Tienda, J., Testillano, P.S., Balestrini, R., Fiorilli, V., Azcón-Aguilar, C., and Ferrol, N. (2011). GintAMT2, a new member of the ammonium transporter family in the arbuscular mycorrhizal fungus Glomus intraradices. Fungal Genet. Biol.

Pertea, M., Pertea, G.M., Antonescu, C.M., Chang, T.C., Mendell, J.T., and Salzberg, S.L. (2015). StringTie enables improved reconstruction of a transcriptome from RNA-seq reads. Nat. Biotechnol. **33**: 290–295.

Petre, B. and Kamoun, S. (2014). How Do Filamentous Pathogens Deliver Effector Proteins into Plant Cells? PLoS Biol. **12**.

Petutschnig, E.K., Jones, A.M.E., Serazetdinova, L., Lipka, U., and Lipka, V. (2010). The Lysin Motif Receptor-like Kinase (LysM-RLK) CERK1 is a major chitin-binding protein in Arabidopsis thaliana and subject to chitin-induced phosphorylation. J. Biol. Chem. **285**: 28902–28911.

Pfeffer, P.E., Douds, D.D., Bécard, G., and Shachar-Hill, Y. (1999). Carbon uptake and the metabolism and transport of lipids in an arbuscular mycorrhiza. Plant Physiol.

Pham, A.Q., Cho, S.H., Nguyen, C.T., and Stacey, G. (2020). Arabidopsis lectin receptor kinase P2K2 is a second plant receptor for extracellular atp and contributes to innate immunity. Plant Physiol. **183**: 1364–1375.

Pimprikar, P., Carbonnel, S., Paries, M., Katzer, K., Klingl, V., Bohmer, M.J., Karl, L., Floss, D.S., Harrison, M.J., Parniske, M., and Gutjahr, C. (2016). A CCaMK-CYCLOPS-DELLA complex activates transcription of RAM1 to regulate arbuscule branching. Curr. Biol. **26**: 987–998.

Plett, J.M., Daguerre, Y., Wittulsky, S., Vayssieres, A., Deveau, A., Melton, S.J., Kohler, A., Morrell-Falvey, J.L., Brun, A., Veneault-Fourrey, C., and Martin, F. (2014). Effector MiSSP7 of the mutualistic fungus Laccaria bicolor stabilizes the Populus JAZ6 protein and represses jasmonic acid (JA) responsive genes. Proc. Natl. Acad. Sci. U. S. A. **111**: 8299–8304.

Poncini, L., Wyrsch, I., Tendon, V.D., Vorley, T., Boller, T., Geldner, N., Métraux, J.P., and Lehmann, S. (2017). In roots of Arabidopsis thaliana, the damage-associated molecular pattern AtPep1 is a stronger elicitor of immune signalling than flg22 or the chitin heptamer. PLoS One **12**: 1–21.

Pozo, M.J., Azcón-Aguilar, C., Dumas-Gaudot, E., and Barea, J.M. (1999). β-1,3-glucanase activities in tomato roots inoculated with arbuscular mycorrhizal fungi and/or Phytophthora parasitica and their possible involvement in bioprotection. Plant Sci. **141**: 149–157.

Lo Presti, L., Lanver, D., Schweizer, G., Tanaka, S., Liang, L., Tollot, M., Zuccaro, A., Reissmann, S., and Kahmann, R. (2015). Fungal effectors and plant susceptibility. Annu. Rev. Plant Biol. **66**: 513–545.

Puga, M.I. et al. (2014). SPX1 is a phosphate-dependent inhibitor of Phosphate Starvation

Response 1 in Arabidopsis. Proc. Natl. Acad. Sci. U. S. A. **111**: 14947–14952.

Pumplin, N. and Harrison, M.J. (2009). Live-cell imaging reveals periarbuscular membrane domains and organelle location in Medicago truncatula roots during arbuscular mycorrhizal symbiosis. Plant Physiol. **151**: 809–819.

Pumplin, N., Mondo, S.J., Topp, S., Starker, C.G., Gantt, J.S., and Harrison, M.J. (2010). Medicago truncatula Vapyrin is a novel protein required for arbuscular mycorrhizal symbiosis. Plant J. **61**: 482–494.

Quiroga, G. (2019). Deciphering the contribution of maize aquaporins regulated by arbuscular mycorrhizae to the transport in planta of water andor solutes of physiological importance.

Quiroga, G., Erice, G., Ding, L., Chaumont, F., Aroca, R., and Ruiz-Lozano, J.M. (2019). The arbuscular mycorrhizal symbiosis regulates aquaporins activity and improves root cell water permeability in maize plants subjected to water stress. Plant Cell Environ. **42**: 2274–2290.

Radhakrishnan, G. V. et al. (2020). An ancestral signalling pathway is conserved in intracellular symbioses-forming plant lineages. Nat. Plants **6**: 280–289.

Radutoiu, S., Madsen, L.H., Madsen, E.B., Felle, H.H., Umehara, Y., Grønlund, M., Sato, S., Nakamura, Y., Tabata, S., Sandal, N., and Stougaard, J. (2003). Plant recognition of symbiotic bacteria requires two LysM receptor-like kinases. Nature.

Radutoiu, S., Madsen, L.H., Madsen, E.B., Jurkiewicz, A., Fukai, E., Quistgaard, E.M.H., Albrektsen, A.S., James, E.K., Thirup, S., and Stougaard, J. (2007). LysM domains mediate lipochitin-oligosaccharide recognition and Nfr genes extend the symbiotic host range. EMBO J. **26**: 3923–3935.

Ramirez-Prado, J.S., Abulfaraj, A.A., Rayapuram, N., Benhamed, M., and Hirt, H. (2018). Plant Immunity: From Signaling to Epigenetic Control of Defense. Trends Plant Sci. **23**: 833–844.

Ransom, R.F. and Walton, J.D. (1997). Histone hyperacetylation in maize in response to treatment with HC-toxin or infection by the filamentous fungus Cochliobolus carbonum. Plant Physiol. **115(3)**: 1021–1027.

Redecker, D., Kodner, R., and Graham, L.E. (2000). Glomalean fungi from the Ordovician. Science (80-.). **289**: 1920–1921.

Ropars, J., Toro, K.S., Noel, J., Pelin, A., Charron, P., Farinelli, L., Marton, T., Krüger, M., Fuchs, J., Brachmann, A., and Corradi, N. (2016). Evidence for the sexual origin of heterokaryosis in arbuscular mycorrhizal fungi. Nat. Microbiol. **1**: 1–9.

Roth, R., Hillmer, S., Funaya, C., Chiapello, M., Schumacher, K., Lo Presti, L., Kahmann, R., and Paszkowski, U. (2019). Arbuscular cell invasion coincides with extracellular vesicles and membrane tubules. Nat. Plants **5**: 204–211.

Roth, R. and Paszkowski, U. (2017). Plant carbon nourishment of arbuscular mycorrhizal

fungi. Curr. Opin. Plant Biol. **39**: 50–56.

Rouached, H., Arpat, A.B., and Poirier, Y. (2010). Regulation of phosphate starvation responses in plants: Signaling players and cross-talks. Mol. Plant **3**: 288–299.

Rovenich, H., Boshoven, J.C., and Thomma, B.P.H.J. (2014). Filamentous pathogen effector functions: Of pathogens, hosts and microbiomes. Curr. Opin. Plant Biol. **20**: 96–103.

Rubio, V., Linhares, F., Solano, R., Martín, A.C., Iglesias, J., Leyva, A., and Paz-Ares, J. (2001). A conserved MYB transcription factor involved in phosphate starvation signaling both in vascular plants and in unicellular algae. Genes Dev. **15**: 2122–2133.

Rudrappa, T., Czymmek, K.J., Paré, P.W., and Bais, H.P. (2008). Root-secreted malic acid recruits beneficial soil bacteria. Plant Physiol. **148**: 1547–1556.

Rush, T.A. et al. (2020). Lipo-chitooligosaccharides as regulatory signals of fungal growth and development. Nat. Commun. **11**.

Rutten, L., Miyata, K., Roswanjaya, Y.P., Huisman, R., Bu, F., Hartog, M., Linders, S., van Velzen, R., van Zeijl, A., Bisseling, T., Kohlen, W., and Geurts, R. (2020). Duplication of symbiotic lysin motif receptors predates the evolution of nitrogen-fixing nodule symbiosis. Plant Physiol. **184**: 1004–1023.

Sánchez-Vallet, A. et al. (2020). A secreted LysM effector protects fungal hyphae through chitin-dependent homodimer polymerization. PLoS Pathog. **16**: 1–21.

Sánchez-Vallet, A., Saleem-Batcha, R., Kombrink, A., Hansen, G., Valkenburg, D.J., Thomma, B.P.H.J., and Mesters, J.R. (2013). Fungal effector Ecp6 outcompetes host immune receptor for chitin binding through intrachain LysM dimerization. Elife **2013**: 1–16.

Sanders, I.R. and Croll, D. (2010). Arbuscular mycorrhiza: The challenge to understand the genetics of the fungal partner. Annu. Rev. Genet. **44**: 271–292.

Sasse, J., Martinoia, E., and Northen, T. (2018). Feed Your Friends: Do Plant Exudates Shape the Root Microbiome? Trends Plant Sci. **23**: 25–41.

Scervino, J.M., Ponce, M.A., Erra-Bassells, R., Vierheilig, H., Ocampo, J.A., and Godeas, A. (2005). Flavonoids exclusively present in mycorrhizal roots of white clover exhibit a different effect on arbuscular mycorrhizal fungi than flavonoids exclusively present in non-mycorrhizal roots of white clover. J. Plant Interact. **1**: 15–22.

Schliemann, W., Ammer, C., and Strack, D. (2008). Metabolite profiling of mycorrhizal roots of Medicago truncatula. Phytochemistry **69**: 112–146.

Schmitz, A.M. and Harrison, M.J. (2014). Signaling events during initiation of arbuscular mycorrhizal symbiosis. J. Integr. Plant Biol. **56**: 250–261.

Schmitz, A.M., Pawlowska, T.E., and Harrison, M.J. (2019). A short LysM protein with high molecular diversity from an arbuscular mycorrhizal fungus, Rhizophagus irregularis. Mycoscience **60**: 63–70.

Schultze, M. and Kondorosi, A. (1996). The role of Nod signal structures in the determi-

nation of host specificity in the Rhizobium-legume symbiosis. World J. Microbiol. Biotechnol. **12**: 137–149.

Schwechheimer, C. and Willige, B.C. (2009). Shedding light on gibberellic acid signalling. Curr. Opin. Plant Biol. **12**: 57–62.

Sędzielewska Toro, K. and Brachmann, A. (2016). The effector candidate repertoire of the arbuscular mycorrhizal fungus Rhizophagus clarus. BMC Genomics **17**.

Shachar-Hill, Y., Pfeffer, P.E., Douds, D., Osman, S.F., Doner, L.W., and Ratcliffe, R.G. (1995). Partitioning of intermediary carbon metabolism in vesicular-arbuscular mycorrhizal leek. Plant Physiol.

Shaw, P.J. and Brown, J.W. (2004). Plant nuclear bodies. Curr. Opin. Plant Biol. **7**: 614–620.

Shi, J., Hu, H., Zhang, K., Zhang, W., Yu, Y., Wu, Z., and Wu, P. (2014). The paralogous SPX3 and SPX5 genes redundantly modulate Pi homeostasis in rice. J. Exp. Bot. **65**: 859–870.

Shimizu, T., Nakano, T., Takamizawa, D., Desaki, Y., Ishii-Minami, N., Nishizawa, Y., Minami, E., Okada, K., Yamane, H., Kaku, H., and Shibuya, N. (2010). Two LysM receptor molecules, CEBiP and OsCERK1, cooperatively regulate chitin elicitor signaling in rice. Plant J.

Smaczniak, C., Li, N., Boeren, S., America, T., Van Dongen, W., Goerdayal, S.S., De Vries, S., Angenent, G.C., and Kaufmann, K. (2012). Proteomics-based identification of low-abundance signaling and regulatory protein complexes in native plant tissues. Nat. Protoc. **7**: 2144–2158.

Smit, P., Raedts, J., Portyanko, V., Debellé, F., Gough, C., Bisseling, T., and Geurts, R. (2005). NSP1 of the GRAS protein family is essential for rhizobial nod factor-induced transcription. Science (80-.). **308**: 1789–1791.

Smith, S. and Read, D. (2008). Mycorrhizal Symbiosis Third Edit. (Academic Press: Cambridge, UK).

Smith, S.E., Smith, F.A., and Jakobsen, I. (2004). Functional diversity in arbuscular mycorrhizal (AM) symbioses: The contribution of the mycorrhizal P uptake pathway is not correlated with mycorrhizal responses in growth or total P uptake. New Phytol.

Snelders, N.C., Rovenich, H., Petti, G.C., Rocafort, M., van den Berg, G.C.M., Vorholt, J.A., Mesters, J.R., Seidl, M.F., Nijland, R., and Thomma, B.P.H.J. (2020). Microbiome manipulation by a soil-borne fungal plant pathogen using effector proteins. Nat. Plants **6**: 1–10.

Snider, J., Kittanakom, S., Curak, J., and Stagljar, I. (2010). Split-ubiquitin based membrane yeast two-hybrid (MYTH) system: A powerful tool for identifying protein-protein interactions. J. Vis. Exp.: 1–7.

Spatafora, J.W. et al. (2016). A phylum-level phylogenetic classification of zygomycete

fungi based on genome-scale data. Mycologia **108**: 1028–1046.

Stanga, J.P., Smith, S.M., Briggs, W.R., and Nelson, D.C. (2013). SUPPRESSOR OF MORE AXILLARY GROWTH2 1 controls seed germination and seedling development in Arabidopsis. Plant Physiol. **163**: 318–330.

Stracke, S., Kistner, C., Yoshida, S., Mulder, L., Sato, S., Kaneko, T., Tabata, S., Sandal, N., Stougaard, J., Szczyglowski, K., and Parniske, M. (2002). A plant receptor-like kinase required for both bacterial and fungal symbiosis. Nature **417**: 959–962.

Streitwolf-engel, R., Boller, T., Wiemken, A., and Sanders, I.R. (1998). van der Heijden1998. **74**: 69–72.

Sugiura, Y., Akiyama, R., Tanaka, S., Yano, K., Kameoka, H., Marui, S., Saito, M., Kawaguchi, M., Akiyama, K., and Saito, K. (2020). Myristate can be used as a carbon and energy source for the asymbiotic growth of arbuscular mycorrhizal fungi. Proc. Natl. Acad. Sci. U. S. A. **117**: 25779–25788.

Sun, H., Tao, J., Liu, S., Huang, S., Chen, S., Xie, X., Yoneyama, K., Zhang, Y., and Xu, G. (2014). Strigolactones are involved in phosphate- and nitrate-deficiency-induced root development and auxin transport in rice. J. Exp. Bot.

Sun, L., Song, L., Zhang, Y., Zheng, Z., and Liu, D. (2016). Arabidopsis PHL2 and PHR1 act redundantly as the key components of the central regulatory system controlling transcriptional responses to phosphate starvation. Plant Physiol. **170**: 499–514.

Sun, Z.W. and Allis, C.D. (2002). Ubiquitination of histone H2B regulates H3 methylation and gene silencing in yeast. Nature **418**: 104–108.

Takeda, N., Maekawa, T., and Hayashi, M. (2012). Nuclear-localized and deregulated calcium- and calmodulin-dependent protein kinase activates rhizobial and mycorrhizal responses in Lotus japonicus. Plant Cell.

Terakura, S., Ueno, Y., Tagami, H., Kitakura, S., Machida, C., Wabiko, H., Aiba, H., Otten, L., Tsukagoshi, H., Nakamura, K., and Machida, Y. (2007). An oncoprotein from the plant pathogen Agrobacterium has histone chaperone-like activity. Plant Cell **19(9)**: 2855–2865.

Thines, M. (2019). An evolutionary framework for host shifts – jumping ships for survival. New Phytol. **224**: 605–617.

Thoms, D., Liang, Y., and Haney, C.H. (2021). Maintaining Symbiotic Homeostasis: How Do Plants Engage With Beneficial Microorganisms While at the Same Time Restricting Pathogens? Mol. Plant-Microbe Interact. **X**: MPMI-11-20-0318.

Thordal-Christensen, H., Birch, P.R.J., Spanu, P.D., and Panstruga, R. (2018). Why did filamentous plant pathogens evolve the potential to secrete hundreds of effectors to enable disease? Mol. Plant Pathol. **19**: 781–785.

Tian, C., Kasiborski, B., Koul, R., Lammers, P.J., Bucking, H., and Shachar-Hill, Y. (2010). Regulation of the nitrogen transfer pathway in the arbuscular mycorrhizal symbi-

osis: Gene characterization and the coordination of expression with nitrogen flux. Plant Physiol. **153**: 1175–1187.

Tian, T., Liu, Y., Yan, H., You, Q., Yi, X., Du, Z., Xu, W., and Su, Z. (2017). AgriGO v2.0: A GO analysis toolkit for the agricultural community, 2017 update. Nucleic Acids Res. **45**: W122–W129.

Tisserant, E. et al. (2013). Genome of an arbuscular mycorrhizal fungus provides insight into the oldest plant symbiosis. Proc. Natl. Acad. Sci. U. S. A.

Tisserant, E. et al. (2012). The transcriptome of the arbuscular mycorrhizal fungus Glomus intraradices (DAOM 197198) reveals functional tradeoffs in an obligate symbiont. New Phytol.

Torrecillas, E., Alguacil, M.M., and Roldán, A. (2012). Host preferences of arbuscular mycorrhizal fungi colonizing annual herbaceous plant species in semiarid mediterranean prairies. Appl. Environ. Microbiol. **78**: 6180–6186.

Tsuzuki, S., Handa, Y., Takeda, N., and Kawaguchi, M. (2016). Strigolactone-induced putative secreted protein 1 is required for the establishment of symbiosis by the arbuscular mycorrhizal fungus Rhizophagus irregularis. Mol. Plant-Microbe Interact. **29**: 277–286.

Tyerman, S.D., Niemietz, C.M., and Bramley, H. (2002). Plant aquaporins: Multifunctional water and solute channels with expanding roles. Plant, Cell Environ. **25**: 173–194.

Uehlein, N., Fileschi, K., Eckert, M., Bienert, G.P., Bertl, A., and Kaldenhoff, R. (2007). Arbuscular mycorrhizal symbiosis and plant aquaporin expression. Phytochemistry **68**: 122–129.

Uetake, Y., Kojima, T., Ezawa, T., and Saito, M. (2002). Extensive tubular vacuole system in an arbuscular mycorrhizal fungus, Gigaspora margarita. New Phytol.

Umehara, M. (2011). Strigolactone, a key regulator of nutrient allocation in plants. Plant Biotechnol. **28**: 429–437.

Umehara, M., Hanada, A., Magome, H., Takeda-Kamiya, N., and Yamaguchi, S. (2010). Contribution of strigolactones to the inhibition of tiller bud outgrowth under phosphate deficiency in rice. Plant Cell Physiol. **51**: 1118–1126.

Umehara, M., Hanada, A., Yoshida, S., Akiyama, K., Arite, T., Takeda-Kamiya, N., Magome, H., Kamiya, Y., Shirasu, K., Yoneyama, K., Kyozuka, J., and Yamaguchi, S. (2008). Inhibition of shoot branching by new terpenoid plant hormones. Nature **455**: 195–200.

Vaahtera, L., Schulz, J., and Hamann, T. (2019). Cell wall integrity maintenance during plant development and interaction with the environment. Nat. Plants **5**: 924–932.

van't Padje, A., Werner, G.D.A., and Kiers, E.T. (2021). Mycorrhizal fungi control phosphorus value in trade symbiosis with host roots when exposed to abrupt 'crashes' and 'booms' of resource availability. New Phytol. **229**: 2933–2944.

van't Padje, A., Werner, G.D.A., and Kiers, E.T. (2020). Mycorrhizal fungi control

phosphorus value in trade symbiosis with host roots when exposed to abrupt ‘crashes’ and ‘booms’ of resource availability. New Phytol.: 2933–2944.

Vandenkoornhuyse, P., Mahé, S., Ineson, P., Staddon, P., Ostle, N., Cliquet, J.B., Francez, A.J., Fitter, A.H., and Young, J.P.W. (2007). Active root-inhabiting microbes identified by rapid incorporation of plant-derived carbon into RNA. Proc. Natl. Acad. Sci. U. S. A. **104**: 16970–16975.

Vandenkoornhuyse, P., Ridgway, K.P., Watson, I.J., Fitter, A.H., and Young, J.P.W. (2003). Co-existing grass species have distinctive arbuscular mycorrhizal communities. Mol. Ecol. **12**: 3085–3095.

Vernié, T. et al. (2016). PUB1 interacts with the receptor kinase DMI2 and negatively regulates rhizobial and arbuscular mycorrhizal symbioses through its ubiquitination activity in medicago truncatula. Plant Physiol. **170**: 2312–2324.

Vogel, J.T., Walter, M.H., Giavalisco, P., Lytovchenko, A., Kohlen, W., Charnikhova, T., Simkin, A.J., Goulet, C., Strack, D., Bouwmeester, H.J., Fernie, A.R., and Klee, H.J. (2010). SlCCD7 controls strigolactone biosynthesis, shoot branching and mycorrhiza-induced apocarotenoid formation in tomato. Plant J. **61**: 300–311.

Volpin, H., Elkind, Y., Okon, Y., and Kapulnik, Y. (1994). A vesicular arbuscular mycorrhizal fungus (Glomus intraradix) induces a defense response in alfalfa roots. Plant Physiol. **104**: 683–689.

Voß, S., Betz, R., Heidt, S., Corradi, N., and Requena, N. (2018). RiCRN1, a crinkler effector from the arbuscular mycorrhizal fungus rhizophagus irregularis, functions in arbuscule development. Front. Microbiol. **9**: 1–18.

Walder, F., Niemann, H., Natarajan, M., Lehmann, M.F., Boller, T., and Wiemken, A. (2012). Mycorrhizal networks: Common goods of plants shared under unequal terms of trade. Plant Physiol. **159**: 789–797.

Walley, J.W., Rowe, H.C., Xiao, Y., Chehab, E.W., Kliebenstein, D.J., Wagner, D., and Dehesh, K. (2008). The chromatin remodeler SPLAYED regulates specific stress signaling pathways. PLoS Pathog. **4(12)**: e1000237.

Wang, E. et al. (2014a). A H+-ATPase that energizes nutrient uptake during mycorrhizal symbioses in rice and Medicago truncatula. Plant Cell **26**: 1818–1830.

Wang, P., Jiang, H., Boeren, S., Dings, H., Kulikova, O., Bisseling, T., and Limpens, E. (2021). A nuclear-targeted effector of Rhizophagus irregularis interferes with histone 2B mono-ubiquitination to promote arbuscular mycorrhisation. New Phytol.: 1142–1155.

Wang, S. et al. (2020). Functional analysis of the OsNPF4.5 nitrate transporter reveals a conserved mycorrhizal pathway of nitrogen acquisition in plants. Proc. Natl. Acad. Sci. U. S. A. **117**: 16649–16659.

Wang, W., Shi, J., Xie, Q., Jiang, Y., Yu, N., and Wang, E. (2017). Nutrient Exchange and Regulation in Arbuscular Mycorrhizal Symbiosis. Mol. Plant **10**: 1147–1158.

Wang, Y., Yang, L., Chen, X., Ye, T., Zhong, B., Liu, R., Wu, Y., and Chan, Z. (2016). Major latex protein-like protein 43 (MLP43) functions as a positive regulator during abscisic acid responses and confers drought tolerance in Arabidopsis thaliana. J. Exp. Bot. **67**: 421–434.

Wang, Z. et al. (2014b). Rice SPX1 and SPX2 inhibit phosphate starvation responses through interacting with PHR2 in a phosphate-dependent manner. Proc. Natl. Acad. Sci. U. S. A. **111**: 14953–14958.

Wanke, A., Rovenich, H., Schwanke, F., Velte, S., Becker, S., Hehemann, J.H., Wawra, S., and Zuccaro, A. (2020). Plant species-specific recognition of long and short β-1,3-linked glucans is mediated by different receptor systems. Plant J. **102**: 1142–1156.

Waters, M.T., Gutjahr, C., Bennett, T., and Nelson, D.C. (2017). Strigolactone Signaling and Evolution. Annu. Rev. Plant Biol. **68**: 291–322.

Wawra, S., Fesel, P., Widmer, H., Timm, M., Seibel, J., Leson, L., Kesseler, L., Nostadt, R., Hilbert, M., Langen, G., and Zuccaro, A. (2016). The fungal-specific β-glucan-binding lectin FGB1 alters cell-wall composition and suppresses glucan-triggered immunity in plants. Nat. Commun. 7.

Wendrich, J.R., Boeren, S., Möller, B.K., Weijers, D., and De Rybe L, B. (2017). In vivo identification of plant protein complexes using IP-MS/MS. In Methods in Molecular Biology, J. Kleine-Vehn and M. Sauer, eds (Springer New York: New York, NY), pp. 147–158.

Werner, G.D.A., Strassmann, J.E., Ivens, A.B.F., Engelmoer, D.J.P., Verbruggen, E., Queller, D.C., Noë, R., Johnson, N.C., Hammerstein, P., and Kiers, E.T. (2014). Evolution of microbial markets. Proc. Natl. Acad. Sci. U. S. A. **111**: 1237–1244.

Werner, G.D.A., Zhou, Y., Pieterse, C.M.J., and Kiers, E.T. (2018). Tracking plant preference for higher-quality mycorrhizal symbionts under varying CO2 conditions over multiple generations. Ecol. Evol. **8**: 78–87.

Wewer, V., Brands, M., and Dörmann, P. (2014). Fatty acid synthesis and lipid metabolism in the obligate biotrophic fungus Rhizophagus irregularis during mycorrhization of Lotus japonicus. Plant J. **79**: 398–412.

Wild, R., Gerasimaite, R., Jung, J.Y., Truffault, V., Pavlovic, I., Schmidt, A., Saiardi, A., Jacob Jessen, H., Poirier, Y., Hothorn, M., and Mayer, A. (2016). Control of eukaryotic phosphate homeostasis by inositol polyphosphate sensor domains. Science (80-.). **352**: 986–990.

Willmann, R. et al. (2011). Arabidopsis lysin-motif proteins LYM1 LYM3 CERK1 mediate bacterial peptidoglycan sensing and immunity to bacterial infection. Proc. Natl. Acad. Sci. U. S. A. **108**: 19824–19829.

Wipf, D., Krajinski, F., van Tuinen, D., Recorbet, G., and Courty, P.E. (2019). Trading on the arbuscular mycorrhiza market: from arbuscules to common mycorrhizal networks. New Phytol. **223**: 1127–1142.

Xie, X., Lin, H., Peng, X., Xu, C., Sun, Z., Jiang, K., Huang, A., Wu, X., Tang, N., Salv-

ioli, A., Bonfante, P., and Zhao, B. (2016). Arbuscular Mycorrhizal Symbiosis Requires a Phosphate Transceptor in the Gigaspora margarita Fungal Symbiont. Mol. Plant **9**: 1583–1608.

Xue, L., Klinnawee, L., Zhou, Y., Saridis, G., Vijayakumar, V., Brands, M., Dörmann, P., Gigolashvili, T., Turck, F., and Bucher, M. (2018). AP2 transcription factor CBX1 with a specific function in symbiotic exchange of nutrients in mycorrhizal Lotus japonicus. Proc. Natl. Acad. Sci. U. S. A. **115**: E9239–E9246.

Yamada, K., Saijo, Y., Nakagami, H., and Takano, Y. (2016). Regulation of sugar transporter activity for antibacterial defense in Arabidopsis. Science (80-.). **354**: 1427–1430.

Yang, S.Y. et al. (2012). Nonredundant regulation of rice arbuscular mycorrhizal symbiosis by two members of the PHOSPHATE TRANSPORTER1 gene family. Plant Cell.

Yano, K. et al. (2008). CYCLOPS, a mediator of symbiotic intracellular accommodation. Proc. Natl. Acad. Sci. U. S. A. **105**: 20540–20545.

Yao, R. et al. (2016). DWARF14 is a non-canonical hormone receptor for strigolactone. Nature **536**: 469–473.

Yoneyama, K., Xie, X., Kusumoto, D., Sekimoto, H., Sugimoto, Y., Takeuchi, Y., and Yoneyama, K. (2007a). Nitrogen deficiency as well as phosphorus deficiency in sorghum promotes the production and exudation of 5-deoxystrigol, the host recognition signal for arbuscular mycorrhizal fungi and root parasites. Planta.

Yoneyama, K., Xie, X., Nomura, T., and Yoneyama, K. (2020). Do Phosphate and Cytokinin Interact to Regulate Strigolactone Biosynthesis or Act Independently? Front. Plant Sci. **11**: 1–9.

Yoneyama, K., Xie, X., Sekimoto, H., Takeuchi, Y., Ogasawara, S., Akiyama, K., Hayashi, H., and Yoneyama, K. (2008). Strigolactones, host recognition signals for root parasitic plants and arbuscular mycorrhizal fungi, from Fabaceae plants (New Phytologist (2001) 179, (484-494)). New Phytol. **182**: 285.

Yoneyama, K., Yoneyama, K., Takeuchi, Y., and Sekimoto, H. (2007b). Phosphorus deficiency in red clover promotes exudation of orobanchol, the signal for mycorrhizal symbionts and germination stimulant for root parasites. Planta **225**: 1031–1038.

Yoshida, S., Kameoka, H., Tempo, M., Akiyama, K., Umehara, M., Yamaguchi, S., Hayashi, H., Kyozuka, J., and Shirasu, K. (2012). The D3 F-box protein is a key component in host strigolactone responses essential for arbuscular mycorrhizal symbiosis. New Phytol. **196**: 1208–1216.

Young, N.D., Debellé, F., Oldroyd, G.E.D., Geurts, R., Cannon, S.B., Udvardi, M.K., Benedito, V.A., Mayer, K.F.X., Gouzy, J., and Schoof, H. (2011). The Medicago genome provides insight into the evolution of rhizobial symbioses. Nature **480**: 520–524.

van Zeijl, A., Liu, W., Xiao, T.T., Kohlen, W., Yang, W.C., Bisseling, T., and Geurts, R. (2015). The strigolactone biosynthesis gene DWARF27 is co-opted in rhizobium symbiosis. BMC Plant Biol. **15**: 1–15.

Van Zeijl, A., Op Den Camp, R.H.M., Deinum, E.E., Charnikhova, T., Franssen, H., Op Den Camp, H.J.M., Bouwmeester, H., Kohlen, W., Bisseling, T., and Geurts, R. (2015). Rhizobium Lipo-chitooligosaccharide Signaling Triggers Accumulation of Cytokinins in Medicago truncatula Roots. Mol. Plant **8**: 1213–1226.

Zeng, T., Holmer, R., Hontelez, J., te Lintel-Hekkert, B., Marufu, L., de Zeeuw, T., Wu, F., Schijlen, E., Bisseling, T., and Limpens, E. (2018). Host- and stage-dependent secretome of the arbuscular mycorrhizal fungus Rhizophagus irregularis. Plant J. **94**: 411–425.

Zeng, T., Rodriguez-Moreno, L., Mansurkhodzaev, A., Wang, P., van den Berg, W., Gasciolli, V., Cottaz, S., Fort, S., Thomma, B.P.H.J., Bono, J.J., Bisseling, T., and Limpens, E. (2020). A lysin motif effector subverts chitin-triggered immunity to facilitate arbuscular mycorrhizal symbiosis. New Phytol. **225**: 448–460.

Zhang, C., He, J., Dai, H., Wang, G., Zhang, X., Wang, C., Shi, J., Chen, X., Wang, D., and Wang, E. (2021). Discriminating symbiosis and immunity signals by receptor competition in rice. Proc. Natl. Acad. Sci. **118**: e2023738118.

Zhang, Q., Blaylock, L.A., and Harrison, M.J. (2010). Two Medicago truncatula half-ABC transporters are essential for arbuscule development in arbuscular mycorrhizal symbiosis. Plant Cell **22**: 1483–1497.

Zhang, S., Feng, M., Chen, W., Zhou, X., Lu, J., Wang, Y., Li, Y., Jiang, C.Z., Gan, S.S., Ma, N., and Gao, J. (2019). In rose, transcription factor PTM balances growth and drought survival via PIP2;1 aquaporin. Nat. Plants **5**: 290–299.

Zhang, X., Pumplin, N., Ivanov, S., and Harrison, M.J. (2015a). EXO70I is required for development of a sub-domain of the periarbuscular membrane during arbuscular mycorrhizal symbiosis. Curr. Biol.

Zhang, Y. and Cremer, P.S. (2006). Interactions between macromolecules and ions: the Hofmeister series. Curr. Opin. Chem. Biol. **10**: 658–663.

Zhang, Y., Li, D., Zhang, H., Hong, Y., Huang, L., Liu, S., Li, X., Ouyang, Z., and Song, F. (2015b). Tomato histone H2B monoubiquitination enzymes SlHUB1 and SlHUB2 contribute to disease resistance against Botrytis cinerea through modulating the balance between SA- and JA/ET-mediated signaling pathways. BMC Plant Biol. **15**: 252 (2015).

Zhao, W., Neyt, P., Van Lijsebettens, M., Shen, W.H., and Berr, A. (2019). Interactive and noninteractive roles of histone H2B monoubiquitination and H3K36 methylation in the regulation of active gene transcription and control of plant growth and development. New Phytol. **221**: 1101–1116.

Zhong, Y., Wang, Y., Guo, J., Zhu, X., Shi, J., He, Q., Liu, Y., Wu, Y., Zhang, L., Lv, Q., and Mao, C. (2018). Rice SPX6 negatively regulates the phosphate starvation response through suppression of the transcription factor PHR2. New Phytol. **219**: 135–148.

Zhou, F., Emonet, A., Dénervaud Tendon, V., Marhavy, P., Wu, D., Lahaye, T., and Geldner, N. (2020). Co-incidence of Damage and Microbial Patterns Controls Localized Immune Responses in Roots. Cell **180**: 440-453.e18.

Zhou, J., Jiao, F.C., Wu, Z., Li, Y., Wang, X., He, X., Zhong, W., and Wu, P. (2008). OsPHR2 is involved in phosphate-starvation signaling and excessive phosphate accumulation in shoots of plants. Plant Physiol. **146**: 1673–1686.

Zhu, F.Y. et al. (2018). Comparative performance of the BGISEQ-500 and Illumina HiSeq4000 sequencing platforms for transcriptome analysis in plants. Plant Methods **14**: 1–14.

Ziegler, M.T., Thomas, S.R., and Danna, K.J. (2000). Accumulation of a thermostable endo-1,4-β-D-glucanase in the apoplast of Arabidopsis thaliana leaves. Mol. Breed.

Zipfel, C. (2009). Early molecular events in PAMP-triggered immunity. Curr. Opin. Plant Biol.

Zipfel, C., Kunze, G., Chinchilla, D., Caniard, A., Jones, J.D.G., Boller, T., and Felix, G. (2006). Perception of the Bacterial PAMP EF-Tu by the Receptor EFR Restricts Agrobacterium-Mediated Transformation. Cell.

Zou, B., Yang, D.L., Shi, Z., Dong, H., and Hua, J. (2014). Monoubiquitination of histone 2B at the disease resistance gene locus regulates its expression and impacts immune responses in Arabidopsis. Plant Physiol. **165**: 309–318.

List of publications

Wang, P., Snijders, R., Kohlen, W., Liu, J., Bisseling, T., & Limpens, E. (2021). Medicago SPX1 and SPX3 regulate phosphate homeostasis, mycorrhizal colonization and arbuscule degradation. *bioRxiv*.

Wang, P., Jiang, H., Boeren, S., Dings, H., Kulikova, O., Bisseling, T., & Limpens, E. (2021). A nuclear-targeted effector of Rhizophagus irregularis interferes with histone 2B mono-ubiquitination to promote arbuscular mycorrhization. *New Phytologist*, 230(3), 1142-1155.

van Creij, J., **Wang, P.**, & Limpens, E. (2020). Arbuscular mycorrhiza, a fungal perspective. *Molecular Aspects of Plant Beneficial Microbes in Agriculture*, 241-258.

Zeng, T., Rodriguez-Moreno, L., Mansurkhodzaev, A., **Wang, P.**, van den Berg, W., Gasciolli, V., ... & Limpens, E. (2020). A lysin motif effector subverts chitin-triggered immunity to facilitate arbuscular mycorrhizal symbiosis. *New Phytologist*, 225(1), 448-460.

Fu, H., **Wang, P.**, Wu, X., Zhou, X., Ji, G., Shen, Y., ... & Liang, J. (2019). Distinct genome-wide alternative polyadenylation during the response to silicon availability in the marine diatom Thalassiosira pseudonana. *The Plant Journal*, 99(1), 67-80.

Luo, C. S., Liang, J. R., Lin, Q., Li, C., Bowler, C., Anderson, D. M., **Wang, P.**, ... & Gao, Y. H. (2014). Cellular responses associated with ROS production and cell fate decision in early stress response to iron limitation in the diatom Thalassiosira pseudonana. *Journal of proteome research*, 13(12), 5510-5523.

About the author

Peng Wang (王 鹏) was born on the 12th of August 1990 in Yiyang, Hunan province, China. He started his bachelor study in Bioengineering at Hunan Institute of Science and Technology from 2009-2013. After graduation he continued academic education with an MSc in Biochemistry and Molecular Biology in Xiamen University from 2013-2016. There he studied the silicon enriched cell wall biosynthesis mechanisms of diatom. In 2016, he obtained a PhD fellowship from the China Scholarship Council (CSC) to join the laboratory of Molecular Biology at Wageningen University. Under the supervision of Prof. Ton Bisseling and Dr. Erik Limpens, he investigated the mechanisms of partner control in arbuscular mycorrhizal (AM) symbiosis, with focusing on the AM fungal effectors function study and arbuscule development regulation controled by phosphate status. The results of his research during PhD are presented in this thesis.

Acknowledgements

Finally, I come to this part with my PhD thesis! Looking back to my 5 years in MolBi as a PhD student, it was absolutely a remarkable journey and will be in my memory for my whole life. Upon the completion of this book, I am grateful to those people who have offered me encouragement and support during my research.

My deepest gratitude goes to my supervisors: Erik, your knowledge and critical thinking inspired me a lot. I really enjoyed working with you. whenever I got positive or negative results, I could immediately discuss them with you since you were always there. And also thanks for your patience in improving my scientific writing. Without your guidance and quick response in revisions of my manuscript, I could not complete this book in less than 5 years. Ton, many thanks for being my promoter and all the advices you provided during work discussion. I admire your passion for science and the ability to in charge of so many different projects smoothly.

I thank people who worked in the mycorrhiza team. Jelle, Tian, Rik, Jianyong, Fuxi. Thank you for creating such a great working environment. The protocols and detailed experimental skills shared by all of you helped me a lot, especially during my first year in the laboratory. I also thank master student Henan and Roxane for your help in the work described in chapter 2 and chapter 4. Special thanks to Tian for picking me up at the airport in my first time came to the Netherlands and helping me settle down in Wageningen. And Special thanks to Jelle for your friendship and introducing me the Dutch cultures when I was new to Wageningen. It is great to have you being my paranymph. I wish you graduate soon.

For the work in chapter 3, I would like to thank Nick, who helped me a lot with producing the difficult RiFGB1 effector protein in *E. coli*. I also owe gratitude to Sjef, who helped me with LC-MS/MS in chapter 2 and chapter 5.

I would like to thank my colleagues and friends from the Cluster Plant Developmental Biology. Maria and Marie-jose, Thanks for all your help in ordering, organization and other administrative work. Henk, Jan V, Jan H, Marijke, Caroline, Olga, Sidney, Thanks for all of your laboratory management work to make the laboratory works smoothly. Viola, thanks for your kind help in extending my contract and writing recommendation letters for me. Rene and Wouter, thanks for your help with my SPX manuscript. And all the other members, Joan, Renze, Titis, Kerstin, Robin, Rens, Joël, Arjan, Simon, Yuda, Luuk, Sultan, Kevin, Kana, Asma, Martinus, Lucas, Kavya, Anneke, Renan, Menno, Merijn, Vera, Jana, Jorge, Tijs, Alejandra, Hannie, Peter, Kiki, Michiel, Norbert, Henk K, Richard, Wilma, Amber, Andrea. I wish you all the best.

It is grateful to have many friends from home country when study abroad. I thank all my Chinese friends that I made in Wageningen. Defeng, Fengjiao, Huchen, Xu, Jieyu, Tingting, Guiling, Jing (special thanks for being my paranymph), Lili, Zhichun, Lu, Wenkun, Du, Yinshan, Mengmeng, Siqi, Jundi, Yueyang, Honglei, Zhuang, Jun, Qingqin, Haoling, Fang, Qian, Zhiyong, Qi, Yuanyuan Zhang, Jingling, Miao, Hui, Jie, Ling, Baojian, Xiaobing, Shan, Yuanyuan Yin. Thanks for all of your help and companion. I will never forget all the nice food and wine we enjoyed together.

Acknowledgements

最后，我要将此书献给我的家人。爸妈，姐姐，姐夫，奶奶，没有你们无尽的爱与关怀，我不可能从七家村小学一步步走到今天！

Peng Wang

Wageningen

5th July, 2021

Education Statement of the Graduate School

Experimental Plant Sciences

Issued to: **Peng Wang**
Date: **30 August 2021**
Group: **Laboratory of Molecular Biology**
University: **Wageningen University & Research**

1) Start-Up Phase	date	cp
► **First presentation of your project**		
Effectors in arbuscular mycorrhization	10-03-2017	1.5
► **Writing or rewriting a project proposal**		
Effectors in arbuscular mycorrhizal symbiosis	Sep - Nov 2016	3.0
► **MSc courses**		
Subtotal Start-Up Phase		4.5

2) Scientific Exposure	date	cp
► **EPS PhD student days**		
EPS Get2Gether 2017	09-02-2017 - 10-02-2017	0.6
EPS Get2Gether 2020	10-02-2020 - 11-02-2020	0.6
► **EPS theme symposia**		
EPS theme 1 'Developmental Biology of Plants'	30-01-2018	0.3
EPS theme 1 'Developmental Biology of Plants'	05-02-2020	0.3
EPS theme 1 'Developmental Biology of Plants'	28-01-2021	0.2
EPS theme 2 'Interactions between Plants and Biotic Agents' & Willie Commelin Scholten Day	23-01-2017	0.3
EPS theme 2 'Interactions between Plants and Biotic Agents' & Willie Commelin Scholten Day	24-01-2018	0.3
EPS theme 3 'Metabolism and Adaptation'	30-10-2020	0.2
EPS theme 4 'Genome biology'	03-12-2019	0.3
► **Lunteren Days and other national platforms**		
Annual Meeting 'Experimental Plant Sciences', Lunteren	10-04-2017 - 11-04-2017	0.6
Annual Meeting 'Experimental Plant Sciences', Lunteren	09-04-2018 - 10-04-2018	0.6
Annual Meeting 'Experimental Plant Sciences', Lunteren	08-04-2019 - 09-04-2019	0.6
Annual Meeting 'Experimental Plant Sciences', Lunteren	12-04-2021 - 13-04-2021	0.5
► **Seminars (series), workshops and symposia**		
Bregie Wertheim: 'Evolving immunity: Genomic basis of the evolution and variation in parasitoid resistence'	19-01-2017	0.1
Farewell Symposium Ton Bisseling	08-02-2017	0.2
Ford Denison: 'Improving cooperation among plants and microbes'	08-05-2017	0.1
KEYS symposium: 'Boosting crop productivity at KeyGene'	14-06-2017	0.1
Peter Linder: 'Why is the cape flora so species rich? Insight from the cape reeds'	06-10-2017	0.1

	Jean-Francois Arrighi: ‘Evolution of Nod factor-independent rhizobium symbiosis’	18-10-2017	0.1
	Giles Oldroyd: ‘Recognition of symbiotic microorganisms by plants’	18-10-2017	0.1
	Mary Wildemuth: ‘Salicylic acid and cell cycle control of plant-microbe interactions’	25-06-2018	0.1
	Michael Djordjevic: ‘CLE peptide dependent autoregulation of nodulation in Medicago truncatula’	15-08-2018	0.1
	Yan Wang: ‘A leucine-rich repeat receptor-like protein as PAMP receptor recognising XEG1, a Phytophthora glycoside hydrolase’	10-09-2018	0.1
	Diana Santelia: ‘Rewiring starch metabolism for plant environmental adaption’	01-11-2018	0.1
	Pilar Cubas: ‘To grow or not to grow- a bud’s question’	28-02-2019	0.1
	Brande Wulff: ‘Crumbs and Bread: understanding and exploiting immune receptor diversity in wild wheats’	04-04-2019	0.1
	Daniel Croll: ‘Parasites within parasites’	21-06-2019	0.1
	Public Lecture: Alga Zuccaro and Ikram Blilou (WUR)	09-09-2019	0.2
	Public Lecture: Jürgen Kleine-Vehn (WUR)	28-09-2019	0.1
	B-Wise Seminar – Eliana Papoutsoglou & Roeland Voorrips	01-10-2019	0.2
	Wageningen PhD Symposium: Science with Impact	25-10-2019	0.3
	Genetic and genomic analysis of polyploids	06-11-2019	0.2
	Jian Xu: ‘The root of single cell CAPability’	02-12-2019	0.1
	Pascal Ratet: ‘Suppression of defense during Medicago root nodule formation’	03-12-2019	0.1
	Daniel van Damme: ‘Is the endocytic TPLATE complex also an autophagic complex?’	24-01-2020	0.1
	Yoan Coudert: ‘Hormonal control and evolution of branching forms in mosses’	24-01-2020	0.1
	Duur Aanen: ‘Science and Myth in Evolution’	06-02-2020	0.1
	Vasilis Kokkoris: ‘Nuclear dynamics in the arbuscular mycorrhizal fungus Rhizophagus irregularis’	29-07-2020	0.1
	Seminar Research Unit ‘Plant growth and development’	20-11-2020	0.3
	Daniel Croll: ‘WEES Seminar: Drivers and brakes of pathogen emergence’	18-02-2021	0.1
	Michael Nodine: ‘RNA Biology of Plant Embryos’	26-02-2021	0.1
	Seminar: Virtual Seminars in Symbiosis (I) Uta Paszkowski and Martin Parniske	27-04-2020	0.2
	Seminar: Virtual Seminars in Symbiosis (II) Dugald Reid and Chao Su	25-05-2020	0.2
	Seminar: Virtual Seminars in Symbiosis (III) Lena Müller and Benoit Lefebvre	29-06-2020	0.2
►	**Seminar plus**		
►	**International symposia and congresses**		
	3rd International Molecular Mycorrhiza Meeting (iMMM 2017)	26-07-2017 - 28-07-2017	0.6
	4th International Molecular Mycorrhiza Meeting (iMMM 2019)	06-02-2019 - 08-02-2019	0.6
►	**Presentations**		
	Flash poster presentation iMMM 2019 ‘A nucleolar-targeted effector of Rhizophagus irregularis potentially affecting host translation’	06-02-2019 - 08-02-2019	1.0
	Poster Lunteren ‘A nucleolar-targeted effector of Rhizophagus irregularis potentially affecting host translation’	08-04-2019 - 09-04-2019	0.0
	Presentation EPS theme 4 ‘A nuclear-targeted effector of Rhizophagus irregularis suppresses host defense gene expression by interfering with H2B ubiquitination’	03-12-2019	1.0
	Presentation EPS theme 1 ‘Medicago SPX1 and SPX3 regulate phosphate homeostasis and arbuscule lifetime’	28-01-2021	1.0
►	**3rd year interview**		
►	**Excursions**		
		Subtotal Scientific Exposure	13.8

3) In-Depth Studies	date	cp
► **Advanced scientific courses & workshops**		
Course: Basic Statistics	10-05-2017 - 17-05-2017	1.5
Course: Microscopy and Spectroscopy in Food and Plant Science	14-05-2018 - 16-05-2018	1.0
Course: The Power of RNA-Seq	11-06-2018 - 13-06-2018	0.9
Course: Transcription Factors and Transcriptional Regulation	10-12-2018 - 12-12-2018	1.0
► **Journal club**		
Journal club Laboratory of Molecular Biology - WUR	2017-2021	3.0
► **Individual research training**		
Subtotal In-Depth Studies		7.4

4) Personal Development	date	cp
► **General skill training courses**		
Course: Bridging across Cultural Differences	24-11-2016 - 14-12-2016	0.6
Course: Information Literacy PhD including EndNote Introduction	06-12-2016 - 07-12-2016	0.6
Course: Scientific Writing	24-10-2017 - 16-01-2018	1.8
Workshop: Dr. Astrid Mars - Scientific Integrity	20-02-2020	0.1
► **Organisation of meetings, PhD courses or outreach activities**		
► **Membership of EPS PhD Council**		
Subtotal Personal Development		3.1

5) Teaching & Supervision Duties	date	cp
► **Courses**		
Gene Technology (MOB-20306)	Jun 2017	1.0
Gene Technology (MOB-20306)	Jun - Jul 2018	1.0
Gene Technology (MOB-20306)	Jun 2019	1.0
► **Supervision of BSc/MSc students**		
Henan Jiang: “A nuclear- and nucleolar-targeting effector of the arbuscular mycorrhizal fungus Rhizophagus irregularis interacts with host histone H2B and suppresses plant defense responses”	Oct 2018 - May 2019	1.0
Harm Dings: “The role of fungal effector protein RiNLE1 in arbuscular mycorrhization”	Oct 2019 - Feb 2020	1.0
Roxane Snijders: “Functional Analyses of SPX1 & SPX3 in M. truncatula”	Mar - Sep 2020	1.0
Subtotal Teaching & Supervision Duties		6.0

TOTAL NUMBER OF CREDIT POINTS*	**34.8**
Herewith the Graduate School declares that the PhD candidate has complied with the educational requirements set by the Educational Committee of EPS with a minimum total of 30 ECTS credits.	
** A credit represents a normative study load of 28 hours of study.*	

The research described in this thesis was conducted in the laboratory of Molecular Biology, Wageningen University, The Netherlands. With financial support by a PhD fellowship (201606310038) from the China Scholarship Council (CSC) and by the Dutch research school Experimental Plant Sciences (EPS).

Financial support from Wageningen University for printing this thesis is gratefully acknowledged.

Cover design: Peng Wang & Airan

Layout: Peng Wang

Printed by: proefschriftmaken.nl